Indian J. Chem. Vol. 27A No. 8 pp. 653-746
August 1988
CODEN: IJOCAP ISSN: 0019-5103
27A(8) 653-746 (1988)

Indian Journal of
CHEMISTRY

SECTION A
(Inorganic, Physical, Theoretical & Analytical)

Published by
PUBLICATIONS & INFORMATION DIRECTORATE, CSIR, NEW DELHI
in association with
THE INDIAN NATIONAL SCIENCE ACADEMY, NEW DELHI

A RANGE OF HIGH PRECISION, HIGH QUALITY RECORDING INSTRUMENTS FOR THE DISCRIMINATING RESEARCH SCIENTIST

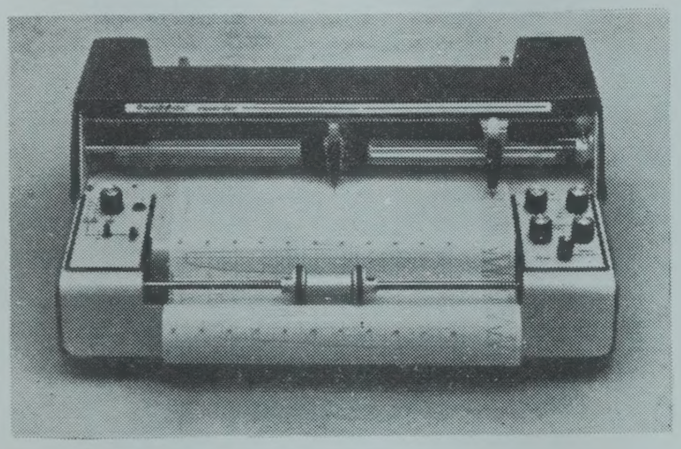

Series 5000 Strip Chart Recorder

The series 5000 Strip Chart Recorder and the series 2000 XY Recorder are well proven instruments incorporating State of the Art Circuitry. A wide range of models offer tremendous flexibility to the user. With over 5000 installations, these instruments are the preferred choice of discriminating users all over India.

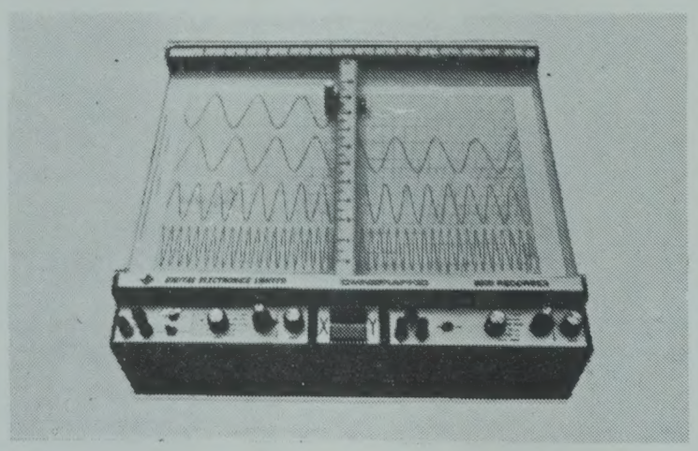

Series 2000 XY Recorder

Another quality product from

DIGITAL ELECTRONICS LIMITED

Reliability in Recording Instruments.

Digilog House 74/II, Marol Industrial Area MIDC, Andheri (East), Bombay- 400 093 Tel: 634 09 01, 632 86 76 Grams: 'DIGILOG'

A Company in collaboration with houston instrument

Special Effects/DE/25/86

INDIAN JOURNAL OF CHEMISTRY

Section A: Inorganic, Physical, Theoretical & Analytical Chemistry

Published by the Publications & Information Directorate (CSIR), Hillside Road, New Delhi 110 012

Editor-in-Chief: S.P. Ambasta

The Indian Journal of Chemistry is issued monthly in two sections: A and B. Communications regarding contributions for publication in the journal should be addressed to the Editor, Indian Journal of Chemistry, Publications & Information Directorate, Hillside Road, New Delhi 110 012.

Correspondence regarding subscriptions and advertisements should be addressed to the Sales & Distribution Officer, Publications & Information Directorate, hillside Road, New Delhi 110 012.

The Publications & Information Directorate (CSIR) assumes no responsibility for the statements and opinions advanced by contributors. The Editorial Board in its work of examining papers received for publication is assisted, in an honorary capacity by a large number of distinguished scientists, working in various parts of India.

Annual Subscription: Rs. 300.00 £ 70.00 $ 100.00; 50% discount admissible to research workers and students and 25% discount to non-research individuals on annual subscription.

Single Copy: Rs. 30.00 £ 7.00 $ 10.00

Payments in respect of subscriptions and advertisements may be sent by cheque, bank draft, money order or postal order marked payable to Publications & Information Directorate, Hillside Road, New Delhi 110 012.

Claims for missing numbers will be allowed only if received within 3 months of the date of issue of the journal plus the time normally required for postal delivery of the journal and the claim.

Indian Journal of Chemistry

Sect A: Inorganic, Physical, Theoretical & Analytical

VOLUME 27A NUMBER 8 AUGUST 1988

CONTENTS

Continued overleaf

CONTENTS

Authors for correspondence are indicated by (*)

Author Index

Indian Journal of Chemistry
Vol. 27A, August 1988, pp. 653-656

On the Stability of Azacyclobutadienes: A Graph Theoretical Analysis

S SINGH, R K MISHRA & B K MISHRA*
Chemical Physics Group, Department of Chemistry, Sambalpur University, Jyoti Vihar 768019

Received 21 *September* 1987; *accepted* 31 *December* 1987

The effect of replacement of a carbon core by a nitrogen core in the cyclobutadiene ring system on the stability of the resultant monoazacyclobutadiene has been studied by a graph theoretical analysis. The topological resonance energy (TRE) values of the azacyclobutadienes have been calculated employing Sachs theorem. The electron density and pi-mobile bond order values of azacyclobutadienes and their dissected counterparts are reported. A rectangular structure for 1,2-diazacyclobutadiene is proposed from the quantum chemical parameters.

Cyclobutadiene is antiaromatic and highly unstable, though there is a report of its existence at very low temperature[1]. The theoretical aspect of this molecule is vividly studied, but still there is a debate whether it has a rectangular structure or square structure[2]. The aza derivatives of cyclobutadiene are very well studied both from theoretical and experimental standpoints. The β-lactam, the monoazacyclobutadiene (azete) derivative is the essential unit in the penicillin antibiotics. Among the fully saturated aza derivatives of cyclobutadiene the synthesis of a few substituted compounds of monoaza derivatives have been reported. The stability of these derivatives was theoretically predicted before these were finally synthesised. Wagner[3] calculated the resonance energy of monoazacyclobutadiene and showed that incorporation of nitrogen, which acted as an acceptor, in the cyclobutadiene ring increased the stability of the resultant monoazacyclobutadiene. In this paper we have made an attempt to calculate the topological resonance energy (TRE), mobile bond order and electron density of the azacyclobutadienes and their acyclic derivatives by graph theoretical techniques.

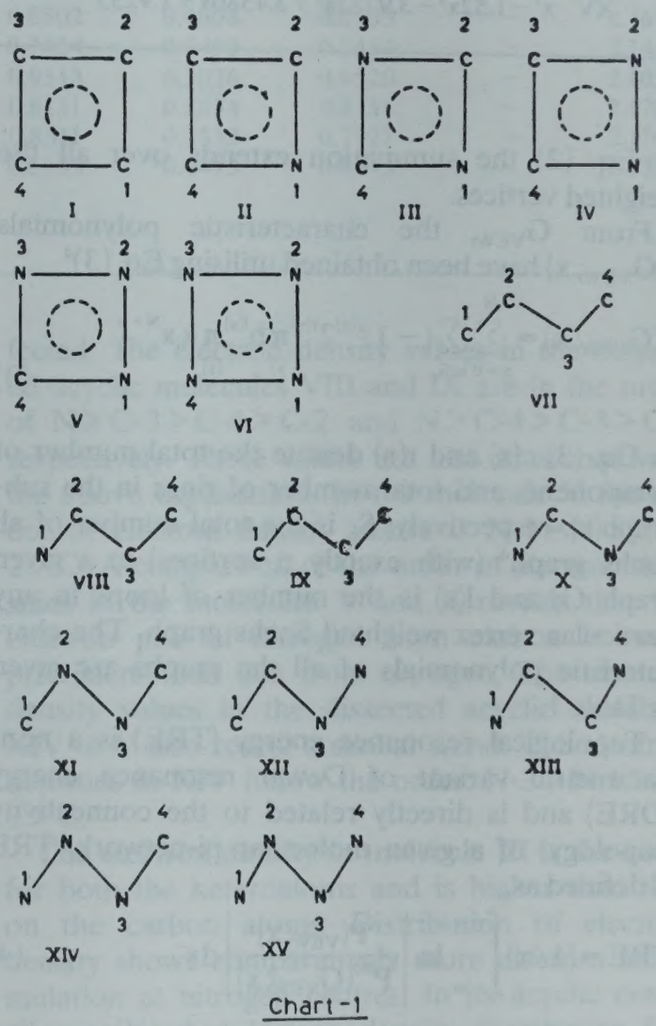

Chart-1

Method of Calculation

The molecules under study (Chart 1) can be represented as a graph with four vertices and three (for acyclic) or four (for cyclic) edges. For cyclobutadiene the vertices and edges are normal but for aza derivatives the graph is defined as vertex and edge-weighted graph, G_{VEW}[4]. The weight of the vertices and edges are identified with Hückel parameters h (for vertex) and k (for edge) for nitrogen and C−N bond respectively[5]. The weight can be well reflected on the diagonal and off-diagonal elements of the adjacency matrix, represented as A for the normal molecule, i.e. cyclobutadiene (Eq. 1) and W for the weighted matrix, i.e. aza cyclobutadiene (Eq. 2)

$$\mathrm{Tr}\, A(G) = 0 \qquad \ldots (1)$$

$$\mathrm{Tr}\, W(G_{VEW}; x) = \sum_i h_i \qquad \ldots (2)$$

Table 1 – Characteristic Polynomial of Vertex-Edge Weighted Graph

Graph	$P(G_{VEW}; x)$
I	$x^4 - 4x^2$
II	$x^4 - 0.38x^3 - 2.98x^2 + 0.76x$
III	$x^4 - 0.76x^3 - 1.8156x^2 + 0.7448x$
IV	$x^4 - 0.76x^3 - 3.4485x^2 + 1.1324x + 0.4640$
V	$x^4 - 1.14x^3 - 3.9726x^2 + 1.9157x - 0.1415$
VI	$x^4 - 1.52x^3 - 5.5852x^2 + 4.6877x - 0.9107$
VII	$x^4 - 3x^2 + 1.00$
VIII	$x^4 - 0.38x^3 - 2.49x^2 + 0.76x + 0.4900$
IX	$x^4 - 0.38x^3 - 1.98x^2 + 0.38x + 0.4900$
X	$x^4 - 0.76x^3 - 1.3256x^2 + 0.5586x + 0.2401$
XI	$x^4 - 0.76x^3 - 2.4485x^2 + 0.3724x + 0.2401$
XII	$x^4 - 0.76x^3 - 2.9585x^2 + 0.9462x + 1.4685$
XIII	$x^4 - 0.76x^3 - 1.8356x^2 + 1.1324x + 0.0957$
XIV	$x^4 - 1.14x^3 - 3.2826x^2 + 1.5433x + 0.7195$
XV	$x^4 - 1.52x^3 - 3.9723x^2 + 3.4580x + 1.9235$

In Eq. (2) the summation extends over all the weighted vertices.

From G_{VEW}, the characteristic polynomials $P(G_{VEW}; x)$ have been obtained utilising Eq. (3)[4]

$$P(G_{VEW}; x) = \sum_{n=0}^{N} \sum_{s \in S_n} (-1)^{c(s)} 2^{r(s)} \pi h_i^{l(s)} \pi k_j x^{N-n} \quad \ldots (3)$$

In Eq. (3) c(s) and r(s) denote the total number of components and total number of rings in the subgraph(s), respectively; S_n is the total number of all Sachs graph[4] (with exactly n vertices) in a given graph G; and l(s) is the number of loops in any particular vertex weighted Sachs graph. The characteristic polynomials of all the graphs are given in Table 1.

Topological resonance energy (TRE) is a non-parametric variant of Dewar resonance energy (DRE) and is directly related to the connectivity (topology) of a given molecular pi-network. TRE is defined as,

$$TRE = (1/\pi) \int_{-\infty}^{+\infty} \ln \left| \frac{P(_{VEW}; x)}{P^{ac}(G_{VEW}; x)} \right| dx \quad \ldots (4)$$

where $P^{ac}(G_{VEW}; x)$ represents the corresponding acyclic polynomial of the vertex-edge weighted graph. TRE values can be normalized to produce the intrinsic topological resonance quantity. TRE(PE) index can be obtained by dividing the TRE with the number of pi-electrons (N) and is given by Eq. (5)

$$TRE(PE) = TRE/N \quad \ldots (5)$$

Rouvray[6] has proved the commutation of topological and Hückel matrices. The quantum chemical parameters such as mobile bond order and electron density are calculated by the graph theoretical techniques as proposed by Rouvray[6]. The TRE, pi-mobile bond order and electron density of all the molecules have been calculated and given in Table 2.

The corresponding acyclic graphs generated by dissecting the edges of the cyclic graphs at different places have also put to a similar approach and their aforesaid parameters have been calculated and are given in Table 2.

Interpretation of Data

Topological resonance energy (TRE) of a cyclic graph is well defined by Gutman *et al*[5]. In their work they have shown the TRE of acyclic graph to be zero. Hess and Schaad[7] have evaluated the TRE values of substituted cyclobutadiene and monoazacyclobutadiene and predicted the stability of the corresponding compounds. The TRE values given in Table 2 reveal that incorporation of nitrogen (which acts as an acceptor) in the cyclobutadiene system increases the TRE values thereby decreasing the antiaromaticity and increasing the stability of the molecules. It is obvious that (to satisfy Hückel's theory) for aromaticity cyclobutadiene needs electrons and this has been achieved by incorporating electron-rich atoms (e.g. N) in the ring leading to stabilization of the molecule[3]. The TRE values of these molecules are in the order of VI < I < II < III < V < IV. The introduction of the second nitrogen in the ring system as in III, further increases the TRE value. But 1,2-diazacyclobutadiene (IV) is found to be more stable than the 1,3-diazacyclobutadiene (III). Hess and Schaad[7] have reported the RE values (calculated by HMO) of 2-amino- and 3-amino-monoazacyclobutadienes to be -0.40β and -0.76β respectively and the TRE values as -0.043β and -0.145β respectively. These values also support our findings. The TRE – value of 0.0831β for IV reveals that the molecule bears some non-aromatic character (threshold value of nonaroamticity is $-10^{-2}\beta$ to $10^{-2}\beta$). This gets further support from the mobile bond order and electron density calculation from this work (Table 2). The introduction of third nitrogen in the ring as in V unexpectedly reduces the TRE value as compared to that of IV. With the incorporation of the fourth nitrogen atom in the ring as in tetraazacyclobutadiene (VI) the TRE value is found to be less than that of the cyclobutadiene indicating more destabilization in the system.

As the lone pair electrons of the nitrogen is not

Table 2 – TRE, Electron Density and Mobile Bond Order of Azacyclobutadienes and Their Dissected Derivatives.

Graph	TRE (PE) in β unit	q_1	q_2	q_3	q_4	P_{12}	P_{23}	P_{34}	P_{14}	P_{rs}
I	−0.3065	1.0000	1.0000	1.0000	1.0000	0.50000 (1.0000)‡	0.50000 (0.0000)‡	0.50000 (1.0000)‡	0.50000 (0.0000)‡	2.0000
II	−0.1936 (−0.2503)	1.7610	0.4862	1.2653	0.4862	0.3504	0.6138	0.6138	0.3504	1.9284
III	−0.1356 (−0.2145)	1.5670	0.4328	1.5670	0.4328	0.4954	0.4954	0.4954	0.4954	1.9816
IV	−0.0831 (−0.1215)	1.0000	1.0000	1.0000	1.0000	1.0000	0.0000	1.0000	0.0000	2.0000
V	−0.1833 (−0.2707)	1.5080	0.8095	1.5080	0.1739	0.6413	0.6413	0.2972	0.2972	1.8770
VI	−0.3332 (−0.3893)	1.0000	1.0000	1.0000	1.0000	0.5000	0.5000	0.50000	0.50000	2.0000
VII	–	1.0000	1.0000	1.0000	1.0000	0.8942	0.4473	0.8942	–	2.2357
VIII	–	1.3334	0.8039	1.0158	0.8466	0.8134	0.5207	0.8514	–	2.1855
IX	–	0.7704	1.2235	0.9852	1.0205	0.8995	0.3717	0.9275	–	2.1987
X	–	1.3362	0.7693	1.2308	0.6631	0.8502	0.4608	0.8503	–	2.1613
XI	–	0.8867	1.1131	1.1131	0.8867	0.7454	0.6493	0.7454	–	2.1441
XII	–	0.9663	1.0011	1.0020	1.0302	0.9513	0.3026	0.9520	–	2.1059
XIII	–	1.1485	0.8513	0.8513	1.1485	0.8131	0.5534	0.8131	–	2.1796
XIV	–	1.1606	0.9879	1.1910	0.6602	0.8311	0.5532	0.7921	–	2.1764
XV	–	1.0000	1.0000	1.0000	1.0000	0.8943	0.4473	0.8943	–	2.2359

‡Mobile bond order of the rectangular structure.

considered for delocalization, an attempt has been made to calculate the TRE values of the azacyclobutadienes by deleting the loops from the graphs (values given in parentheses in Table 2). These values are found to be of high magnitude than the former indicating less stable structure for the compounds.

These findings, however, have not been supported by the synthesis of fully unsaturated system. The saturated derivatives of II, III and IV have been synthesised[8,9]. But there is no report on the synthesis of fully unsaturated derivatives of these compounds except for I and II. Synthesis of these molecules would be of considerable interest.

To complete the specification of the topological characterisation of these molecules the quantum chemical parameters such as electron density and pi-mobile bond order have been calculated. The mobile bond order value reflects the bond length of the molecule and the electron density values can predict the types of substitution reactions at different centres (electrophilic substitution at higher electron density and nucleophilic substitution at lower electron density) in the molecule.

The electron density values of II are in the order of N > C-3 > C-2 = C-4. It is obvious that C-2 and C-4 will acquire less electron density due to the adjacent more electronegative nitrogen, whereas the electron density at C-3 remains unaffected. The electron density values in the dissected acyclic molecules VIII and IX are in the order of N > C-3 > C-4 > C-2 and N > C-4 > C-3 > C-1 respectively. These values are also in accord with the above explanation. In the molecule V the order of electron density values is N-1 = N-3 > N-2 > C. A comparison of the order of electron densities in the molecules V and II reveals that the electron pull of nitrogen from carbon is more prominent than that from nitrogen. The electron density values in the dissected acyclic molecule XIV of V also reveal a similar trend. The electron densities in XIV follow the order: N-3 > N-1 > N-2 > C.

The electron density in molecule III is the same for both the heteroatoms and is higher than that on the carbon atoms. Distribution of electron density shows comparatively more electron accumulation at nitrogen centres. In its acyclic counterpart (X) the electron density distribution follows the order: N-1 > N-3 > C-2 > C-4. A lower value of electron density at C-4 than at C-2 is due to the pulling of electrons from C-4 by two nitrogen atoms through bond delocalization. The distribution of electron density in IV provides an interesting result. No change in electron density is observed though there are two electronegative atoms present in the ring. The molecule behaves as if either there is no delocalization or cent per cent

delocalization with equal distribution on each atom. The electron density values are similar to those of cyclobutadiene or tetraazacyclobutadiene. But the pi-mobile bond order data reveal that there is no delocalisation of the pi-bonds. This molecule can give three different acyclic derivatives (XI, XII, XIII) by dissecting at three different edges. In all the cases the electron density values are higher at the nitrogen centres and the distribution of electron density are as expected. The electron density and pi-mobile bond order distributions in tetraazacyclobutadiene (VI) and its acyclic counterpart (XV) are same as those of cyclobutadiene and butadiene respectively.

Since the bond orders give a measure of bond strength arising from pi-electron system, it has been established that the mobile bond order has some kind of inverse correlation with the bond length. Such a correlation can never be absolute in this case because the σ-bond order is not included in the calculation.

In the molecule II the value of the bond order P_{CN} is found to be smaller than P_{CC} which suggests a longer bond length of C−N than C−C and this is ridiculous. In the case of the acyclic counterpart, VIII, similar trend is observed. But for the molecule VIII Samchez and Malrieu[10] have reported the order of bond length to be $P_{C-C} > P_{C=C} > P_{C=N}$. The values calculated in our case need the σ-bond order of C−N bond to explain the bond length. A decrease of the total pi-bond order ΣPrs, from the value 2.000 (the bond order for localised II from VB theory) may be due to distirbution of some mobile bond order at the loop of the nitrogen. On the contrary increase of ΣPrs in the molecules VIII and IX may be attributed to the excess bonding due to the delocalisation which comes around 0.24 for butadiene[11].

In the molecule III, all the bonds have same pi-bond orders indicating same bond length for all the four bonds with a very little decrease in the total bond order from the value of 2.00. The bond orders of the acyclic derivative X, clearly suggest a shorter bond length for C=N than that for C−N. The bond order values of IV reveal that the molecule does not experience any delocalisation of the mobile pi-bond order and hence a rectangular structure for the molecule can be suggested. Interestingly no deviation of the original electron density of the molecule has been observed supported the rectangular structure for the molecule IV. Considering the rectangular structure of cyclobutadiene the bond orders have been calculated and found to match with those of IV. The bond orders of the other molecules are in accord with the expected and reported bond length values of the same type of molecule[10].

References

1 Chapman O L, McIntosh C L & Pacamsky J, *J Am chem Soc*, **95** (1973) 614.

2 Shaik S S, Hiberty P C, Lefour J M & Ohamessia G, *J Am chem Soc*, **109** (1987) 363.

3 Wagner H U, *Angew Chem*, (Int. Ed), **12** (1973) 848.

4 Trinajstic N, *Croat Chem Acta*, **49** (1977) 593.

5 (a) Aihara J, *J Am chem Soc*, **98** (1976) 2750.
(b) Gutman I, Milun M & Trinajstic N, *J Am chem Soc*, **99** (1977) 1692.

6 Rouvray D H, *Chemical application of graph theory* edited by A T Balaban (Academic Press, London) 1976 204.

7 Hess (Jr) H A & Schaad L J, *J org Chem*, **41** (1976) 3058.

8 Moody C J, Pearson C J & Lawton G, *Tetrahedron Lett*, **26** (1985) 3172.

9 Al Talib M, Tibril I, Jochims J C & Huttner G, *Tetrahedron Lett*, **41** (1985) 527.

10 Marin J S & Malrieu J P, *J phys Chem*, **89** (1985) 978.

11 Yates K, *Hückel molecular orbital theory* (Academic Press, London) 1978 pp. 72.

Indian Journal of Chemistry
Vol. 27A, August 1988, pp. 657-660

Theoretical Evaluation of HOMO Energies, Heats of Formation & Resonance Energies of Non-alternant Hydrocarbons

V P TEWARI* & A K SRIVASTAVA
Department of Chemistry, University of Allahabad, Allahabad

Received 8 *June* 1987; *revised and accepted* 21 *January* 1988

A new version of IOC-ω-technique to calculate HOMO energies and heats of formation of non-alternant hydrocarbons, is described. The calculated values compare well with the experimental and some previously calculated values. Mulliken-Parr or empirical resonance energies have also been calculated for a number of non-alternant hydrocarbons and it has been shown that the results are qualitatively in excellent agreement with the concept of aromaticity.

In our previous papers[1-4] a new version of IOC-ω-technique was used to calculate the various molecular properties of a number of alternant hydrocarbons and heteromolecules containing nitrogen and oxygen. This technique has now been applied to some non-alternant hydrocarbons and values of HOMO energies, heats of formation and resonance energies have been evaluated.

With systematic approximation to Roothaan equation Gupta and Krishna[5] have been able to deduce the IOC-ω technique and suggested Eq. (1) for the diagonal matrix element.

$$F_{\mu\mu} = \alpha + \omega\left[1 - \frac{1}{2}\sum_{\sigma}(p_{\mu\sigma} S_{\mu\sigma} + p_{\sigma\mu} S_{\sigma\mu})\right] \quad \ldots (1)$$

The ω-technique, which has been put to successful use by Aihara-Junichi[6], can be said to be a simplified version of PPP method[7] which is based on zero differential overlap (ZDO) approximations and since these approximations are valid only over orthogonal atomic orbitals (OAOs) and not over usual non-orthogonal Slater-type atomic orbitals (STAOs), the use of OAOs is essentially warranted in it. It has been shown by Gupta[8] that this necessity in ω-technique is fulfilled by inclusion of overlap charges. This is arrived at by deducing the IOC-ω technique in the framework of Lowdin's OAOs. For the first time in the framework of IOC-ω technique, Eq. (2) of the off diagonal matrix element has been used,

$$F_{\mu\nu} = K\, S_{\mu\nu}\,(F_{\mu\mu} \times F_{\nu\nu})^{1/2} \quad \ldots (2)$$

where K is a dimensionless constant and $S_{\mu\nu}$ represents the overlap integrals. Since $F_{\mu\nu}$ represents the energy of interaction between atomic orbitals μ and ν, the geometric mean formula[9] incorporates all the possible interactions between different atomic orbitals. It is thought that the neglect of difference between nuclear and electronic repulsion energies in resonance integral has been compensated up to some extent by the use of geometric mean formula[10].

Method of Calculation

Relative matrix was formed and diagonalized using Jacobi method to give eigen vectors and eigen values. These were used to form a modified matrix using the Eqs (1) and (2) for diagonal elements $F_{\mu\mu}$ and off-diagonal elements $F_{\mu\nu}$, respectively. It was further diagonalized to give eigen vectors and eigen values obtained by IOC-ω technique. One iteration was capable of giving good results. The calculations were performed on a mini-computer with a precision of tenth place of decimal.

HOMO energy

In the realm of MO theory the energy of HOMO is an approximation to one of the ionization potentials[11]. If ψ_N is the HOMO,

$$-I = \sum_{\mu}\sum_{\nu} C_{N\mu}\, C_{N\nu}\, F_{\mu\nu} \quad \ldots (3)$$

Using $F_{\mu\mu}$ and $F_{\mu\nu}$ as given by Eqs (1) and (2), HOMO energy can be calculated with the help of Eq. (3).

π-Bond energy

In the MO theory the π-electronic energy is given by Eq. (4).

E_π = Total MO energy

$$= \sum_{\mu}\sum_{\nu} p_{\mu\nu} F_{\mu\nu} \quad \ldots (4)$$

Substituting the values of $F_{\mu\mu}$ and $F_{\mu\nu}$ into Eq. (4), we get expression (5) for the total π-electronic energy,

$$E_\pi = \sum_{\mu} q_\mu \alpha + \omega \sum_{\mu} q_\mu (1 - q_\mu) - \omega S \sum_{\mu}\sum_{\sigma \neq \mu} q_\mu\, p_{\mu\sigma}$$
$$+ KS \sum_{\mu}\sum_{\nu} p_{\mu\nu}[(\alpha + \omega(1 - q_\mu) - \omega S \sum_{\sigma} p_{\mu\sigma})$$
$$\times (\alpha + \omega(1 - q_\nu) - \omega S \sum_{\sigma} p_{\nu\sigma})]^{1/2} \quad \ldots (5)$$

Now, consider the energy liberated when n carbon atoms with *p*-electrons combine to form π-bonds, i.e. energy, $E_{\pi b}$. Total π-electronic energy of a molecule is given by the algebraic sum of the energy of electrons in *p*-orbitals of widely separated carbon atoms and the π-bond energy, $E_{\pi b}$. The energy of electrons in *p*-orbitals of widely separated atoms may be equated to $\sum_{\mu} q_\mu \alpha$ since whole of the lattice is made up of carbon atoms. Hence, π-bond energy may be expressed by Eq. (6).

$$E_{\pi b} = \omega \sum_{\mu} q_\mu (1 - q_\mu) - \omega S \sum_{\mu} \sum_{\sigma \neq \mu} q_\mu p_{\mu\sigma} + K S \sum_{\mu} \sum_{\nu} p_{\mu\nu} \times [(\alpha + \omega (1 - q_\mu) - \omega S \sum_{\sigma} p_{\mu\sigma}) \times (\alpha + \omega (1 - q_\nu) - \omega S \sum_{\sigma} p_{\nu\sigma})]^{1/2} \quad \ldots (6)$$

Heat of formation or atomisation

The heat of formation of a molecule in its equilibrium configuration is the additive sum of the bond energies. The total bond energy of the molecule is given by the sum of the total σ-bond energy, $E_{\sigma b}$ and the total π-bond energy, $E_{\pi b}$. Thus,

$$\Delta H_f = E_{\sigma b} + E_{\pi b} \quad \ldots (7)$$

If E_{C-C} and E_{C-H} be the bond energies of C − C and C − H bonds respectively, the expression for $E_{\sigma b}$ is,

$$E_{\sigma b} = N_C E_{CC} + N_C E_{CH} \quad \ldots (8)$$

Therefore,

$$\Delta H_f = N_C E_{CC} + N_H E_{CH} + E_{\pi b} \quad \ldots (9)$$

where, N_C and N_H are the respective numbers of C − C and C − H bonds respectively.

Resonance energy

Amongst the many possible definitions for the term resonance energy, that due to mulliken-Parr[12] is the one that is most commonly used. The Mulliken-Parr or empirical resonance energy is taken to be the difference between the bond energies of (I) and (II) (see Eq. 10)

$$E_R = E_{b(I)} - E_{b(II)} \quad \ldots (10)$$

where, (I) represents an aromatic structure with all bonds equal to 1.40 Å and (II) represents a structure with alternating C − C bond-lengths and C = C bond-lengths, respectively. The bond energies may be calculated with the help of Eqs (11) and (12),

$$E_{b(I)} = N E_C + N_H E_H + E_{\pi b(I)} \quad \ldots (11)$$

$$E_{b(II)} = N_1 E_1 + N_2 E_2 + N_H E_H \quad \ldots (12)$$

In Eqs (11) and (12) $E_{\pi b(I)}$ is the π-bond energy of (I) and $N = N_1 + N_2$. E_1 and E_2 are the energies of C − C bond of length 1.48 Å and C = C bond of length 1.34 Å respectively. N_1, N_2, N_H, E_H represent respectively the number of single and double bonds, number of C − H bonds and energy of carbonhydrogen bonds.

On combining Eqs (11), (12) with Eq (10), Eq (12a) is obtained for E_R

$$E_R = NE_C - N_1 E_1 - N_2 E_2 + E_{\pi b(I)} \quad \ldots (12a)$$

Now, since the values of E_1 and E_2 are very uncertain, we have used Eq. (13) for obtaining E_R instead of using E_1 and E_2 directly,

$$E_R = N A_0 + (N_1 - N_2) A_1 + E_{\pi b(I)} \quad \ldots (13)$$

In Eq. (13)

$$A_0 = E_C - \frac{E_1 + E_2}{2} \quad \ldots (14)$$

and

$$A_1 = \frac{E_2 - E_1}{1} \quad \ldots (15)$$

A_0 and A_1 are obviously related to various bond energies and are to be treated as empirical parameters in this communication.

Choice of parameters

In the present communication, it has been assumed that the overlap integral, $S_{\mu\nu}$, vanishes for non-neighbour μ, ν and it has a constant value S for μ, ν directly bonded. S has been assigned a value of 0.25. ω has been taken to be 1.4. Both the values have been extensively used by several workers[13,14]. K has been assigned a value of 1.634 which is quoted in literature[15]. A_0 and A_1 have been assigned values as − 1.22 and 0.64 respectively. Mostly non-alternant hydrocarbons have a five-membered ring. It is known and is also evident from bond matrix that there is a pronounced bond alternation in five-membered ring as compared to six-membered ring. Therefore, in such cases different values of E_{C-C} should be used for the formal single and double bonds. Hence a value of 3.64 eV for C − C and 3.99 eV for C = C bond has been used. A-value of 4.43 eV has been used for C − H bond as suggested by Dewar and Gleicher[16]. The values of C − C and C = C are slightly different from Dewar and Gleicher's average value 3.812 eV for C − C bond. α has been taken as 7.00.

Results and Discussion

Table 1 lists the values of HOMO energy of non-alternant hydrocarbons calculated by present method as well as the values obtained by some previous workers[17-19] along with the available experimental

Table 1—HOMO Energies of Non-alternant Hydrocarbons

Compound	HOMO energies (in eV)				
	Present work	Ref. (17)	Ref. (18)	Ref. (19)	Experimental (20)
Azulene	7.59	6.96	7.47	8.32	7.43
Fulvene	8.07	7.48	8.54	9.07	—
Methylenecyclopropene	7.09	—	—	—	—
Fluoranthene	8.19	8.37	8.14	8.54	7.80
Pentalene	6.85	—	—	—	—
Fulvalene	7.20	—	—	—	—
Acenaphthylene	8.17	7.65	8.24	8.73	8.02
Fulvadiene	7.12	—	—	—	—
S-Indacene	7.96	—	—	—	—
AS-Indacene	7.26	—	—	—	—
Pyracylene	7.57	—	—	—	—
Heptafulvene	7.04	6.64	7.31	—	—
Heptalene	9.24	—	—	—	—
Heptafulvalene	9.26	—	—	—	—
Heptafulvadiene	8.41	—	—	—	—
6-Vinylfulvene	8.02	7.08	—	—	—
2,3-Benzfulvene	7.24	6.73	—	—	—
Sesquifulvalene	7.90	7.00	7.43	—	—
Pleiadiene	7.16	—	—	—	—
Benzopleiadiene	6.87	6.12	—	—	—
Dibenzfulvene	8.35	8.44	—	—	—
Vinyl-Dibenzfulvene	7.90	7.77	—	—	—
Acepleiadylene	7.68	7.53	—	—	—
Dibiphenyleneethylene	7.90	—	—	—	—
Dibiphenylenebutadiene	7.67	—	—	—	—

Table 2—π-Bond Energies and Heats of Formation of Non-alternant Hydrocarbons

Compound	$E_{\pi b}$ (in eV)	Heats of formation (in eV)			
		Present work	Ref. (21)	Ref. (22)	Experimental Ref. (23)
Azulene	12.97	90.20	80.458	89.500	89.19
Fulvene	7.00	56.47	56.335	56.648	—
Methylcyclopropene	4.63	37.61	—	37.352	—
Fluoranthene	21.99	138.25	138.668	137.414	138.11
Pentalene	9.78	70.52	70.532	70.266	—
Fulvalene	12.59	89.82	—	88.348	—
Acenaphthylene	16.19	104.69	104.861	103.916	104.32
Fulvadiene	15.07	108.80	—	108.400	—
S-Indacene	15.96	104.46	—	103.309	—
As-Indacene	15.45	103.95	—	102.889	—
Pyracylene	18.93	118.70	—	122.097	—
Heptafulvene	9.54	75.50	—	75.108	—
Heptalene	15.14	108.86	108.145	107.650	—
Heptafulvalene	17.44	127.65	—	126.716	—
Heptafulvadiene	19.63	146.33	—	—	—
6-Vinylfulvene	9.57	75.53	—	75.127	—
2,3-Benzfulvene	12.30	89.53	—	89.063	—
Sesquifulvalene	15.37	109.11	—	108.260	—
Pleiadiene	18.72	123.71	—	—	—
Benz-pleiadiene	24.23	157.33	—	—	—
Dibenzfulvene	18.76	123.75	—	122.835	—
Vinyl-dibenzfulvene	21.35	142.83	—	141.710	—
Acepleiadylene	21.69	137.95	—	137.274	—
Dibephenyleneethylene	35.74	224.01	—	222.269	—
Dibiphenylenebutadiene	38.26	243.02	—	—	—

Table 3—Empirical Resonance Energies of Non-alternant Hydrocarbons

Compound	Empirical resonance energy (in eV)	Compound	Empirical resonance energy (in eV)
Azulene	+0.19	Heptafulvalene	−0.22
Fulvene	−0.32	Heptafulvadiene	−0.47
Methylcyclopropene	−0.25	6-Vinylfulvene	−0.19
Fluoranthene	+0.73	2,3-Benzfulvene	−0.48
Pentalene	−0.56	Sesquifulvalene	+0.15
Fulvalene	−0.19	Pleiadiene	+0.48
Acenaphthylene	+0.39	Benzpleiadiene	−0.75
Fulvadiene	−0.15	Dibenzfulvene	+0.92
S-Indacene	+0.16	Vinyl-dibenzfulvene	+1.07
As-Indacene	−0.35	Acepleiadylene	+0.43
Pyracylene	+0.11	Dibiphenyleneethylene	+1.12
Heptafulvene	−0.23	Dibiphenylenebutadiene	+1.20
Heptalene	−0.08		

data[20]. The values calculated by us are in good agreement with the literature values.

Table 2 reports the values of heats of formation of non-alternant hydrocarbons calculated by present method and some previously calculated values[21,22] along with experimental values[23], wherever available. The results obtained by present method are in good agreement with the literature results.

The resonance energies of non-alternant hydrocarbons are given in Table 3. Unfortunately no experimental values of resonance energies are available in literature except that for azulene (0.00 eV)[23], but the success of the present method lies in the fact that it assigns negative resonance energies to some known *anti*-aromatic non-alternants and positive resonance energies to some known aromatic compounds, while most of the previous methods e.g. Huckel[24], Pople[24] and SPO method[24] incorrectly predict that the non-benzenoid hydrocarbons should all be aromatic. Only recent calculations by Hess (Jr)[25] have been able to predict the differences somewhat correctly.

The presently calculated resonance energy values are qualitatively in excellent agreement with observed facts.

Acknowledgement

One of the authors (VPT) is highly thankful to the CSIR, New Delhi for providing financial assistance (RA).

References

1 Tewari V P, Lal K B & Srivastava AK, *Indian J Chem*, **22** (1983) 893.
2 Tewari V P, Lal K B & Srivastava A K, *Bull Chem Soc Japan*, **57** (1984) 1401.
3 Tewari V P, Lal K B & Srivastava A K, *Indian J Phys*, **58** (1984) 161.
4 Tewari V P & Srivastava A K, *Indian J Chem*, **26A** (1987) 449.
5 Gupta S P & Krishna B, *J Phys B*, **5** (1972) 1101.
6 Aihara Junichi, *Bull Chem Soc Japan*, **53** (1980) 2689.
7 Doggett G, *Molec Phys*, **10** (1966) 225.
8 Gupta S P, *Indian J Chem*, **13** (1975) 717.
9 Ballhausen C J & Gray H B, *Inorg Chem*, **1** (1962) 111.
10 Hastie J W & Morgrava J L, *J Phys Chem*, **73** (1969) 1105.
11 Koopmanns T, *Physica*, **1** (1933) 104.
12 Mulliken R S & Parr R G, *J chem Phys*, **19** (1951) 1271.
13 Mullar N & Mulliken R S, *J Am chem Soc*, **80** (1958) 3489.
14 Streitwieser (Jr) A & Nair P M, *Tetrahedron*, **5** (1959) 149.
15 Ros P & Schmit C C A, *Theor Chim Acta*, **4** (1966) 1.
16 Dewar M J S & Gleicher G J, *J chem Phys*, **44** (1966) 759.
17 Srivastava A K & Krishna B, *Indian J pure appl Phys*, **11** (1973) 246.
18 Warren K D & Yandle J L, *Theor Chim Acta*, **12** (1968) 279.
19 Streitwieser (Jr) A, *J Am chem Soc*, **82** (1960) 4123.
20 Dewar M J S, Haselbach E & Warley S D, *Proc Roy Soc London*, **A-135** (1970) 413.
21 Dewar M J S & Dillano C R, *J Am chem Soc*, **91** (1969) 789.
22 Srivastava A K, D Phil Thesis, University of Allahabad, Allahabad (India) 1973, pp. 76, 89.
23 Dewar M J S, *The molecular theory of organic chemistry* (Mc-Graw Hills, New York) 1969.
24 Dewar M J S & Chung A L, *J chem Phys*, **42** (1965) 756.
25 Hess (Jr) B A & Schaad L J, *J Am chem Soc*, **93** (1971) 305, 2413; *J org Chem*, **36** (1971) 3418.

Indian Journal of Chemistry
Vol. 27A, August 1988, pp. 661-665

A Comparative Study of Role of Both Anionic & Cationic Dopants (Al^{3+} & PO_4^{3-}) & Irradiation on the Solid Phase Thermal Decomposition of Barium Bromate

D BHATTA*, B JENA & (Late) S R MOHANTY
Nuclear Chemistry Laboratory, Utkal University, Bhubaneswar 751004

Received 28 *July* 1987; *revised* 16 *December* 1987; *accepted* 11 *January* 1988

The influence of cation (Al^{3+}) and anion (PO_4^{3-}) dopings as well as γ-irradiation on the isothermal decomposition of barium bromate has been investigated at 553K. It is soon that both the dopants shorten the induction period and enhance the rate constants in the linear, acceleratory and decay stages. Irradiation (2.0 MGy) enhances the rates of linear and acceleratory stages but decreases the decay period.

Though many workers[1-6] have reported the role of dopants as well as γ-irradiation on the isothermal decomposition of alkali and alkaline earth metal halates, a comparative study of the kinetics of these processes has not been discussed in detail. Also the role of anion doping has not received much attention. It is of interest therefore, to investigate the influence of both cationic and anionic dopants and irradiation on the kinetics of isothermal decomposition of barium bromate.

Experimental

Barium bromate was prepared from AR grade chemicals and was purified by repeated crystallization. Crystals of barium bromade doped with Al^{3+} (0.1 mol%) and PO_4^{3-} (0.1×10^{-1} mol%) ions were obtained by slow crystallization from aqueous solutions of the corresponding salts. A sample of barium bromate from the preparation was also subjected to the same treatment. Pure and doped samples of barium bromate were dried at 443 K to constant weight and the uniformity of the doped crystals was checked by X-ray diffraction.

Barium bromate of AR grade was sealed *in vacuo* in pyrex glass ampoules and was irradiated with a dose of 2.0 MGy of ^{60}Co γ-rays at a dose rate of 0.12×10^{-2} MGy h^{-1} and the decomposition of pure, doped and irradiated crystals was studied adopting the procedure described earlier[5]. The fraction decomposed (α) was calculated from the ratio p/p_f, where p is the pressure of oxygen evolved at different time intervals and P_f, the final pressure on completion of the reaction.

Results and Discussion

The solid phase decomposition of barium bromate occurs[7] as shown in Eq.(1).

$$Ba(BrO_3)_2 \rightarrow BaBr_2 + 3O_2 \quad \ldots (1)$$

Various unstable intermediates formed during decomposition are as follows:

$$BrO_3^- \rightarrow BrO_2^- + O$$
$$BrO_2^- \rightarrow BrO^- + O$$
$$BrO^- \rightarrow Br^- + O$$
$$O + O + Br^- \rightarrow O_2 + Br^-$$

Upon exposure[8] of crystalline barium bromate to γ-irradiation the BrO_3^- ion undergoes excitation and ionization leading to rupture of the bromine-oxygen bonds. Under the present experimental conditions i.e. room temperature irradiation and moderate doses of irradiation the species generated are Br^-, BrO^-, BrO_2^-, O_3^-, O_2, O and BrO_4^-. These damaged entities play a significant role both in nucleation as well as in nucleus growth. Pre-irradiated crystals when subjected to thermal decomposition, the bromine bearing fragments undergo decomposition to afford bromide and O_2 in the manner discussed earlier.

The decomposition isotherms at 553 K (Fig. 1) exhibit different stages: (i) initial rapid gas evolution; (ii) a short induction period; and (iii) a slow linear reaction followed by a sigmoidal regime consisting of (iv) acceleratory and (v) decay.

Initial gas evolution

The initial gas evolution ($\alpha \sim 0.04$) in pure barium bromate is completed within the first a few minutes of heating and is not affected either by cation or anion doping but is enhanced a little ($\alpha \sim 0.06$) by irradiation, which may arise due to release of radiolytic damage oxygen trapped in

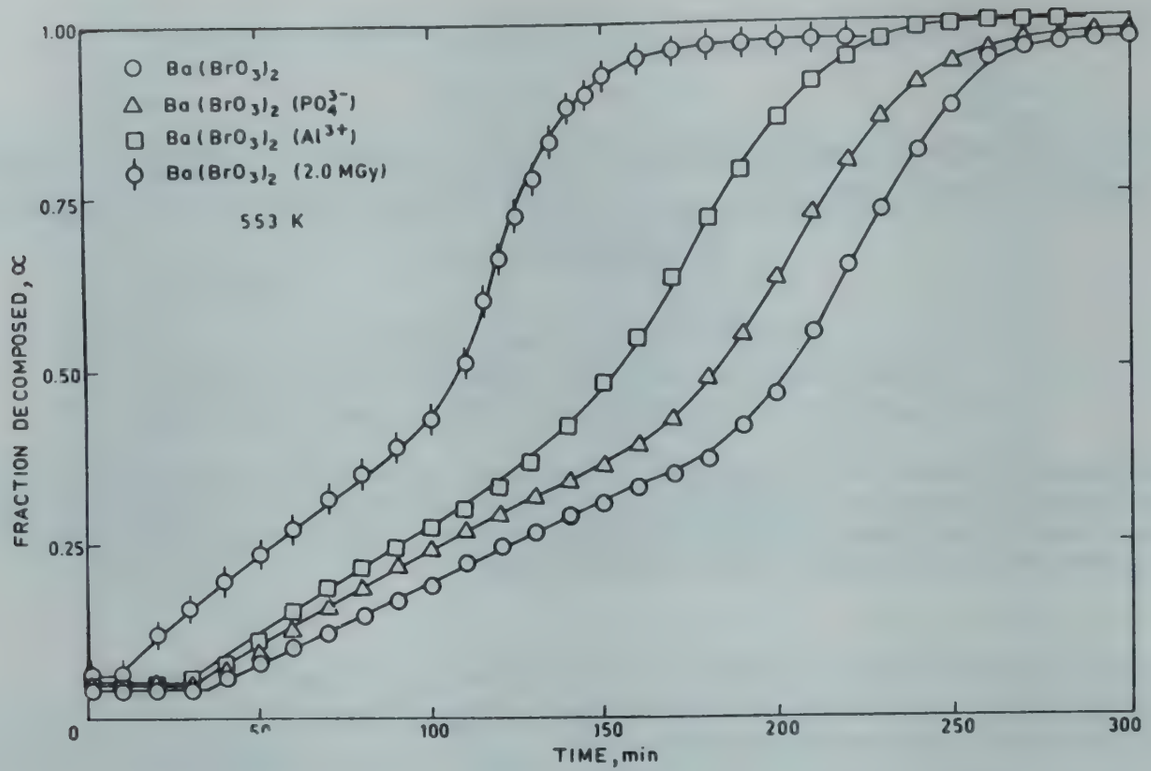

Fig. 1 – Role of doping and irradiation on isothermal decomposition of barium bromate at 553 K.

Table 1 – Effect of Doping (Al^{3+} and PO_4^{3-}) and γ-Irradiation on Solid Phase Thermal Decomposition of Barium Bromate at 553 K

Substance	Initial gas evolution (α)	Induction period (min)	Linear rate constant ($k_1 \times 10^2 min^{-1}$)	Acceleratory rate constant ($k_2 \times 10^2 min^{-1}$)	Decay rate constant ($k_3 \times 10^2 min^{-1}$)
Pure $Ba(BrO_3)_2$	0.04	34.0	0.22	0.40	1.70
Doped (PO_4^{3-})	0.04	30.0	0.30	0.47	1.86
Doped (Al^{3+})	0.04	25.0	0.32	1.67	2.82
Irrd. 2.0 MGy	0.06	4.0	0.49	2.46	0.34

the crystal lattice[3,6,8] and also due to the evolution of trapped gases from the defect-induced crystal lattice. Kinetic informations are not obtained for this stage as the process is an abrupt one.

Induction period

The data (Table 1) show that induction period I (min) is shortened by doping as well as upon irradiation. Crystals of barium bromate prior to γ-irradiation, are supposed to have initially 'n_0' number of nuclei. The radiolytic damage entities; Br^-, BrO^-, BrO_2^-, O_3^-, O_2, O and BrO_4^-, generated within the crystal lattice constitute decomposition nuclei themselves and may be termed irradiation nuclei which upon subsequent heating grow in size or in number and the induction period continues till a critical value of nuclei 'n_c' is attained. Thus the density of nucleation centres within the crystal lattice is increased resulting reduction in the time required to attain 'n_c', shortening the value of the induction period I. Doping (both cationic and anionic) generates vacancies in the lattice, thereby creating space and local strain[2,8,9]. As a result the linear stage starts earlier, consequently lowering the induction period I. The magnitude of shortening of the induction period I is higher in Al^{3+} doped crystals than that in PO_4^{3-} doped crystals. This may be attributed to presence of more defects in the crystal lattice of the former.

Linear stage

The induction period I is followed by the linear stages, expressed by the relationship

$$\alpha = k_1 t + C_1 \qquad \ldots (2)$$

where k_1 is the rate constant and C_1 is another

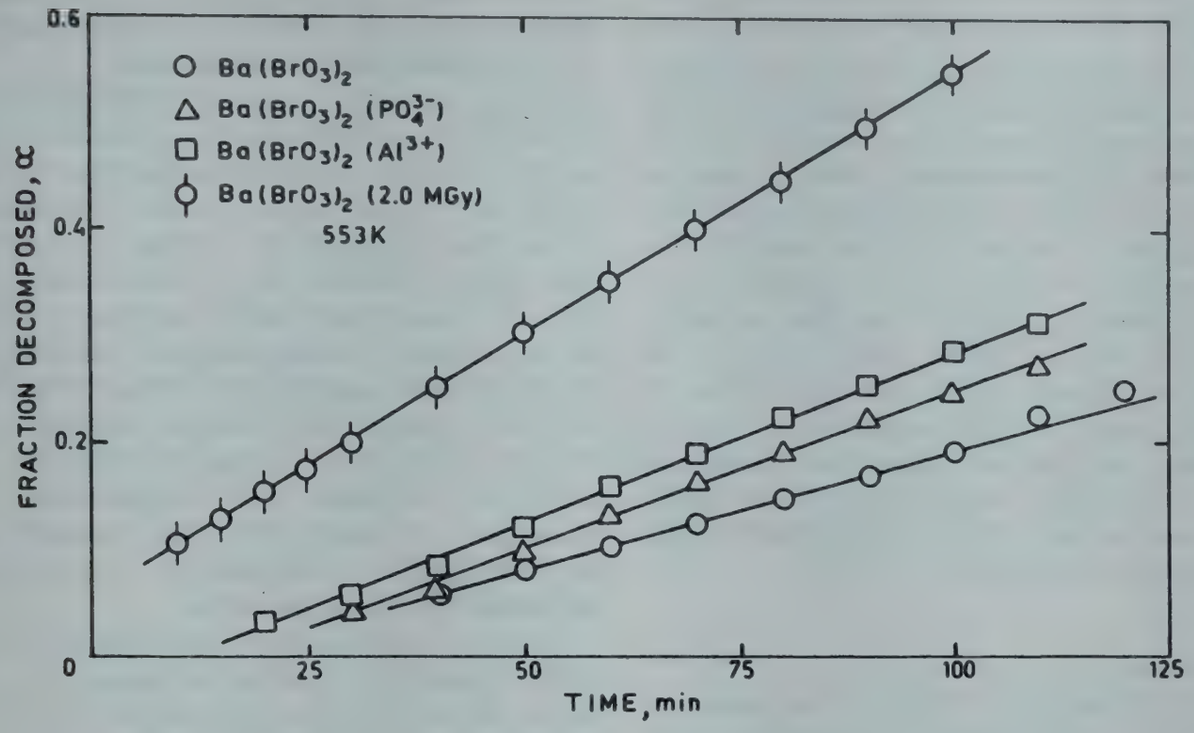

Fig. 2 – The linear stage reaction of pure, doped and irradiated barium bromate at 553 K.

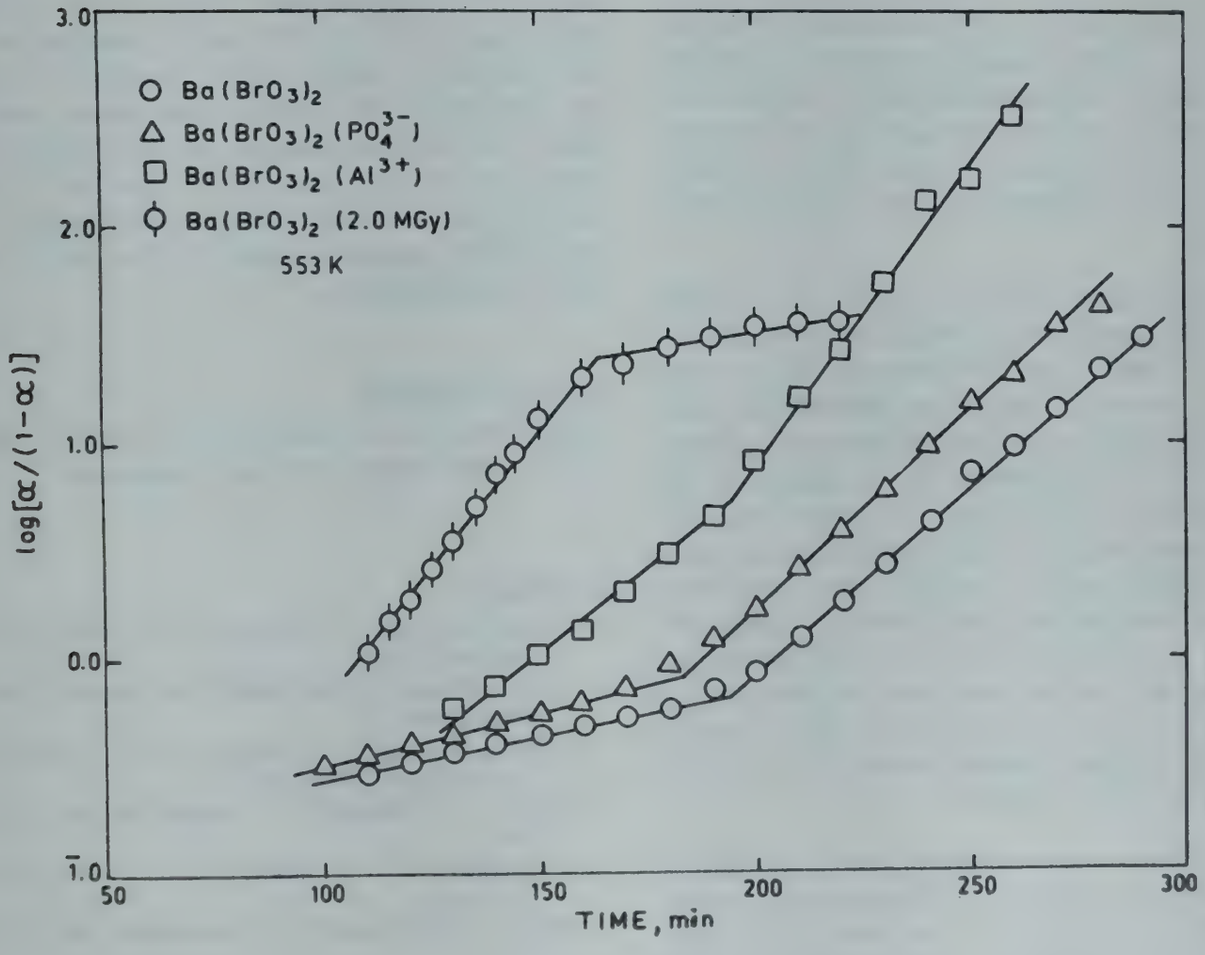

Fig. 3 – Prout-Tompkins relationship in pure, doped and irradiated barium bromate at 553 K.

constant; the former increases with increase in temperature. The data (Table 1) show that both cation and anion dopings as well as γ-irradiation enhance the rate of the linear stage (Fig. 2), the effect being more prominent on γ-irradiation. The rate of linear stage reaction is a function of concentration of potential nuclei forming sites present on the surface of the lattice[3]. The density of the reactive nucleation centres of the crystal lattice is higher in irradiated material[10] than that in the unirradiated as well as doped samples and is responsible for enhancement in the rate. Values of linear rate constant are approximately the same in both cationic and anionic doped crystals suggesting that same effect takes place at this stage though cation dopant (Al^{3+}) is of higher concentration than that of anion (PO_4^{3-}).

Sigmoidal regime

Data for the sigmoidal regimes was analysed following the Prout-Tompkins relationship[11] (see Fig. 3).

$$\log [\alpha/(1-\alpha)] = k_{2,3}t + C_{2,3} \quad \ldots (3)$$

where k_2 and k_3 are the rate constants for the acceleratory and decay stages respectively. It is seen that both cation and anion dopings as well as irradiation enhance the rate constant k_2, the value being higher with the latter crystals. But k_3 is accelerated in doped crystals and is reduced by γ-irradiation.

The acceleratory stage occurs as the reaction thereafter proceeds down the reactant-product interface or cracks and dislocations in a chain branching manner[3,12]. But from acceleratory period onwards, the rate of decomposition is proportional to the concentration of the molecules left undecomposed. The higher k_2-value for the doped crystals may arise due to rapid progression of the reactant-product interface along the lattice distortation and defects, introduced by doping[3,8,9]. It is seen that cation (Al^{3+}, 0.1 mol %) has got more influence on the rate process than that of anion (PO_4^{3-}, 0.1×10^{-1} mol %). This may be ascribed to higher concentrations of the defects present in the former crystals.

The significant increase in the Prout-Tompkins[11] rate constant, k_2 (Table 1) in the case of irradiated salt may be attributed to increase in the density of potential nucleation centres and the catalytic effect of damage entities, generated[13] upon irradiation. These damage fragments constitute point defects and act as potential nucleation centres for the thermal decomposition process.

During the decay stage, the nuclei generated[14,15] in the crystal lattice have overlapped as a result of which the whole surface has undergone decomposition and further nucleation does not occur. But the central regions of the crystal still contain undecomposed material. As a result of which further reaction causes progressive decrease in the area of the reactant product interface resulting in the deceleration of reaction rate. Present data indicate that both cationic and anionic dopings enhance the rate of the decay stage, the influence being higher for the former. This phenomenon may be ascribed to presence of higher concentration of the undecomposed bromate ions, left at the commencement of the decay period.

As pre-irradiation of barium bromate has introduced[8] radiolytic damage bromide, Br^- in the crystal lattice, the concentration of this ion in the decomposing irradiated solid at the end of the acceleratory period is higher than that in the doped crystals. When the decomposition crosses over to deceleratory stage, the rate of the reaction depends upon the amount of bromate left undecomposed[14,15] at a given time. It is seen that rate k_3 of the decay stage is retarded by irradiation. This may be due to the fact that irradiation enhances the decomposition process, and consequently reduces the concentration of undecomposed molecules. So the reactant-product interface contain[15] less number of reactive molecules (barium bromate) at the commencement of the decay period causing deceleration.

Acknowledgement

The authors are grateful to Dr (Ms) N Bohidar for her keen interest and encouragement.

References

1 Bhattamishra S D & Mohanty S R, *J inorg nucle Chem*, **39** ((1977) 2103.

2 Jena B, Mohanty S R & Satpathy M, *Indian J Chem*, **19A** (1980) 1939.

3 Bohidar N, Jena B & Mohanty S R, *J radioanal nucl Chem Lett*, **95** (1985) 291.

4 Bohidar N & Mohanty S R, *Radiochim Acta*, **27** (1980) 19.

5 Bhattamishra S D & Mohanty S R, *Radiat Effects*, **29** (1976) 41.

6 Nair S M K & James C, *Thermochim Acta*, **96** (1985) 27.

7 Bancroft G M & Gesser H D, *J inorg nucl Chem*, **27** (1965) 1545.

8 Bhatta D, Mohanty S R & Samantaray K C, *Radiochim Acta*, **28** (1981) 13.
9 Mohapatra B M & Bhatta D, *Radiat Phys Chem*, **27** (1986) 339.
10 Devlin D J & Herley P J, *Thermochim Acta*, **104** (1986) 159.
11 Prout E G & Tompkins F C, *Trans Faraday Soc*, **40** (1944) 468.
12 Levy P W & Herley P J, *J phys Chem*, **75** (1971) 191.
13 Boldyrev V V & Oblivantsev A N, *Kinet Katal*, **3** (1962) 887.
14 Jacobs P W M & Tompkins F C in *Chemistry of the solid state*, edited W E Garner (Butterworths, London) 1955 pp. 184.
15 Galwey A K, in *Chemistry of solids*, (Chapman Hall, London) 1967, pp. 166.

Indian Journal of Chemistry
Vol. 27A, August 1988, pp. 666-668

Normal Coordinate Analysis of MoF_5 & $MoCl_5$

E M NOUR*† & H M KILLA
Department of Chemistry, Faculty of Science, Zagazig University, Zagazig, Egypt

Received 12 *December* 1986; *revised and accepted* 30 *December* 1987

The vibrational spectra of MoF_5 and $MoCl_5$ have been interpreted in terms of the normal coordinate treatment based on D_{3h} symmetry of the molecules employing a valence force field . The good fit between the observed and calculated frequencies as well as the potential energy distribution values has made it possible to assign all vibrations. Force constant values indicate the weakness of the axial Mo-X' bonds compared with the equatorial Mo-X bonds for both the molecules. The effect of change in the coordinated halide from F^- to Cl^- in term of the force constant values of MoF_5 and $MoCl_5$ is discussed.

The assignments of the vibrational spectra of some monomeric pentahalide metal complexes (MX_5), is still a matter of dispute. Acquista and Abramowitz[1] studied the infrared spectrum of NbF_5 and concluded that this species belongs to the square pyramidal structures (C_{4v} symmetry), while some other workers[2,3] assigned the spectrum on the basis of the trigonal bipyramidal (D_{3h}) structure. X-ray studies on MoF_5 single crystal[4,5] indicated that the species crystallizes to form square tetramers in which the four Mo atoms are joined through fluorine bridges and that it is isostructural with NbF_5. However, Acquista and Abramowitz[6] reported on the basis of their infrared matrix isolation study that the MoF_5 monomer has the D_{3h} symmetry. The same conclusion was also drawn by some other workers[7,8]. Despite the fact that these studies agree on the D_{3h} symmetry for the MoF_5 monomer, there are wide differences in their reported band assignments. Similar D_{3h} symmetry was reported for the analogous $MoCl_5$ monomer on the basis of the gas-phase Raman study by Beattie and Ozin[9]. The crystal structure of $MoCl_5$ is reported[10] to consist of dimers with chlorine atoms forming two octahedra which share a common edge.

The pentachlorides of phosphorous, antimony and niobium have been shown to have the D_{3h} symmetry[11,12] as well as the pentafluorides of antimony, phosphorous, vanadium and arsenic[11-14]. However, other species such as SF_5^-,, SeF_5^- and TeF_5^- belong to the C_{4v} symmetry[14]. The bonding and structures for both the D_{3h} and C_{4v} models are discussed by Rossi and Hoffmann[15]. Normal coordinate analyses have been reported for some pentahalide complexes[11,14,16,17], but no such analysis is reported for MoF_5 and $MoCl_5$.

The main aim of this study is to present the normal coordinate analysis for MoF_5 and $MoCl_5$ molecules in order to make a full assignments of vibrational modes for each molecule based on the calculated potential energy distribution values and to clarify the ambiguity regarding the assignments, particularly for MoF_5.

Method of Calculation

The eight fundamental vibrations associated with each of the pentahalide molybdenum complex are distributed over the D_{3h} symmetry species $2A_1' + 2A_2'' + 3E' + E''$.

The normal coordinate analysis was carried out for both MoF_5 and $MoCl_5$ using the GF matrix method based on a general quadratic force field utilizing no non-bonded interactions. The internal coordinates in these compounds are shown in Fig.1. The symmetry coordinates for the 12 vibrations were constructed as previously explained[11,16]. The average Mo-F and Mo-Cl bond lengths were taken equal to 185 and 224

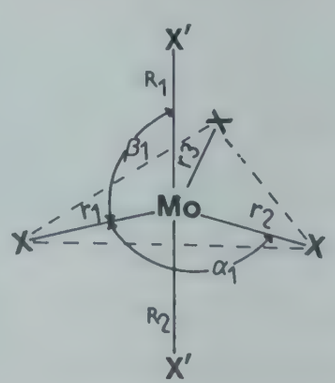

Fig. 1—Definition of internal coordinates in MoX_5 (X = Cl or F)

†Present Address: Department of Chemistry, Qatar University, Doha P.O. Box 2713, Qatar (Arabian Gulf)

ppm, respectively[5,10]. The computer calculations were done using modified versions of the programs of Schachtschneider[19]. The initial force constants were introduced and perturbed untill the best fit between the observed and calculated frequencies was obtained; then the off-diagonal constants were added one by one to improve the calculations. Finally, the diagonal and off-diagonal elements were refined simultaneously to obtain the best set of force constants as a whole for both MoF_5 and $MoCl_5$ as shown in Table 1. The observed and calculated frequencies and their assignments based on the calculated potential energy distribution values are given in Table 2.

Table 1—Force Constants* for MoF_5 and $MoCl_5$

Symbol	Description	Value*	
		MoF_5	$MoCl_5$
f_R	Mo-X′	391.0	196.0
f_r	Mo-X	485.0	258.0
f_α	X-Mo-X	51.4	81.1
f_β	X-Mo-X′	41.0	79.3
$f_{\alpha\beta}$	X-Mo-X,X-Mo-X′	12.2	12.5
f_{RR}	Mo-X′, Mo-X′	15.0	12.0
f_{Rr}	Mo-X′, Mo-X	3.0	8.0
f_{rr}	Mo-X, Mo-X	29.4	21.0
$f_{\beta\beta}$	X-Mo-X′, X-Mo-X′	—	-4.0
$f_{r\beta}$	Mo-X, X-Mo-X′	19.3	16.2

*Stretching constants in Nm^{-1}, bending constants in Nm^{-1} Rad^2

Results and Discussion

Interestingly, the trends in the distribution values in both MoF_5 and $MoCl_5$ are similar and lead to quantitative assignments for each compound. Moreover, the assignments show almost the same order of frequencies for both compounds. Similar order was also observed in our previous studies on $NbCl_5$ and $NbBr_5$[16]. Our assignments, for $MoCl_5$ (Table 2) agree with those reported by Beattie and Ozin[9] based on their gas-phase Raman study. The two bands associated with A_2'' species related to ν_3 and ν_4, which are Raman-inactive, are calculated to be at 401 and 149 cm^{-1}, respectively. On the other hand, our assignments for MoF_5 (Table 2) agree with those reported by Acquista and Abramowitz[6] based on their infrared matrix study, and disagree with the assignments reported by Bates[7] and by Quellette *et al.*[8]. Such disagreement could arise from mistaken assignment of some bands of the tetramers to the MoF_5 monomer by Bates[7] and Quellette *et al.*[8]. It should be noted that the solid MoF_5 consists mainly of the tetramer[4,5] and hence the Raman spectra of the solid reported by Bates[7] should not be associated with the monomer. In the liquid phase, it seems that both the monomer and tetramer of MoF_5 co-exist. The spectra of the liquid reported by Quellette *et al.*[8] show that beside the bands of the monomer, there are a number of bands at 747, 500 and 440 cm^{-1} which should

Table 2—Observed and Calculated Frequencies (cm^{-1}), Potential Energy Distribution (PED) and Vibrational Assignments for MoF_5 and $MoCl_5$

Compound	Frequency		PED‡				Assignments
	Obs.†	Calc.	f_R	f_r	f_α	f_β	
MoF_5	703	699	1	99	0	0	A_1' : ν(Mo-F)
	—	602	99	1	0	0	ν(Mo-F′)
	683	686	98	0	0	2	A_2'' : ν(Mo-F′)
	—	181	1	0	0	99	δ(FMoF′)
	713	719	0	97	2	1	E'*: ν(Mo-F)
	261	259	0	1	87	12	δ(FMoF)
	112	115	0	3	28	69	δ(FMoF′)
	201	201	0	0	0	100	E'' : δ(FMoF′)
$MoCl_5$	390	387	5	95	0	0	A_1' : ν(Mo-Cl)
	313	311	93	7	0	0	ν(Mo-Cl′)
	—	401	94	0	0	6	A_2'' : ν(Mo-Cl′)
	—	149	6	0	0	94	δ(ClMoCl′)
	418	421	0	94	4	2	E'*: νMo-Cl)
	200	198	0	5	77	18	δ(ClMoCl)
	100	104	0	2	27	71	δ(ClMoCl′)
	175	173	0	0	0	100	E'': δ(ClMoCl′)

*Coupled motions

†Observed values for MoF_5 are taken from refs 6 and 8 and for $MoCl_5$ from ref.9.

‡Normalized to total 100 for the diagonal force constant distributions.

be associated with the tetramer. This was judged by comparing the liquid spectrum reported by Quellette *et al.*[8] with the solid tetramer spectrum of Bates[7]. However, the monomer may be generated in higher ratio in the gas phase as in the case of $MoCl_5$ (ref. 9), or may be isolated in a low temperature matrix as in MoF_5 (ref. 6). The two bands reported by Quellette *et at.*[8] at 703 and 201 cm^{-1} and assigned by them to ν_2 (A_1') and $\nu_7(E')$ modes, respectively, should be on the basis of our work assigned to $\nu_1(A_1')$ and $\nu_8(E'')$ modes, respectively. The latter two modes are infrared-inactive and, therefore, were not reported in the matrix spectrum of Acquista and Abramowitz[6].

Table 1 shows hat the axial Mo-F′and Mo-Cl′ bond stretching force constants (f_R) are 391 and 196 Nm^{-1}, respectively. The corresponding values for the equatorial Mo-F and Mo-Cl bonds (f_r) are 485 and 258 Nm^{-1}. Since the force constant value is an approximate measure of the relative bond strength, the above f_R and f_r values indicate that the bonds in MoF_5 are much stronger compared with those of $MoCl_5$, as also expected from the smaller size of F^-. Secondly, the equatorial Mo-X bonds are 1.24 and 1.32 times stronger than the axial Mo-X′ bonds in MoF_5 and $MoCl_5$, respectively. In general, these values may indicate a higher covalent character for the equatorial bonds since force constant value reflects only the covalent properties of the bond. This conclusion agrees with that derived from the M.O. treatment of the pentacoordinate species[15,20].

References

1 Acquista N & Abramowitz S, *J chem Phys*, **56** (1972) 5221.

2 Alexander L E, Beattie I R & Jones P J, *J chem Soc*, (1972) 210.

3 Selig H, Reis A & Gasner E, *J inorg nucl Chem*, **30** (1968) 2087.

4 Peacock R D, *Proc chem Soc (Lond)*, (1957) 59.

5 Edwards A, Peacock R D & Small R W H, *J chem Soc*, (1962) 4486.

6 Acquista N & Abramowitz S, *J chem Phys*, **58** (1973) 5484.

7 Bates J B, *Spectrochim Acta*, **27A** (1971) 1255.

8 Quellette T J, Ratcliffe C T & Sharp D W A, *J chem Soc, A* (1969) 2351.

9 Beattie I R & Ozin G A, *J chem Soc, A* (1969) 1691.

10 Sands D E & Zalkin A, *Acta Crystallogr*, **12** (1959) 723.

11 Condrate R A & Nakamoto K, *Bull chem Soc Japan*, **29** (1966) 1108.

12 Nunziante-Cesaro S, Maltese M, Spoliti M & Janis B, *Spectrochim Acta*, **40A** (1984) 579.

13 Hoskins L C & Perng C N, *J chem Phys*, **55** (1971) 5063.

14 Christe K O, Curtis E C, Schack C J & Pilipovich D, *Inorg Chem*, **11** (1972) 1679.

15 Rossi A R & Hoffmann R, *Inorg Chem*, **14** (1975) 365.

16 Nour E M, *Spectrochim Acta*, **42A** (1986) 1411.

17 Selig H, Holloway J H, Tyson J & Claassen H H, *J chem Phys*, **53** (1970) 2559.

18 Wilson E G, Decius J C & Cross P C, *Molecular vibrations* McGraw-Hill, New York) 1955.

19 Schachtschneider J H, *Vibrational analysis of polyatomic molecules, V and VI, Technical report* (Shell Co., California) 1964.

20 Bader R F W & Westland A D, *Can J Chem*, **39** (1961) 2306.

Indian Journal of Chemistry
Vol. 27A, August 1988, pp. 669-673

Spectroscopic & Kinetic Studies on Electron Donor-Acceptor Interaction between Thiomorpholine & Chloranil

MANNAM KRISHNAMURTHY, K SURENDRA BABU & U MURALIKRISHNA*
Department of Chemistry, Andhra University P.G. Extension Centre, Nuzvid 521 201.

Received 20 *August* 1987; *revised* 28 *October, accepted* 4 *January* 1988

The 1:1 charge transfer complex formation between thiomorpholine as electron donor and chloranil (2,3,5,6-tetrachloro-1,4-benzoquinone) as electron acceptor in chloroform medium has been studied spectrophotometrically. In the presence of excess donor, the 1:1 complex is transformed into a final product, which has been isolated and characterised as 2,5-dichloro-3,6-dithiomorpholino-1,4-benzoquinone by IR, PMR and elemental analyses. Based on the kinetic results a plausible mechanism for the formation of the complex and its transformation into the product in solution is presented and discussed. In the presence of excess chloranil, the complex is sufficiently stable and this property is used in the direct photometric determination of thiomorpholine.

We have recently reported our results on electron donor-acceptor (EDA) interactions involving quinones as acceptors[1-6]. As an extension, the results of the interaction of thiomorpholine, a twin site *n*-donor with chloranil are reported in the present paper. Such studies, particularly involving multisite *n*-electron donors, such as organic bases are interesting[2] and provide information on the nature and reactivity of organic bases. Chloranil, a well known electron acceptor, is known to form charge transfer (CT) complexes with a variety of electron donors[7,8].

Materials and Methods

Chloranil (Merck) was recrystallised twice from acetone, while thiomorpholine (Aldrich, USA) was purified by distillation over KOH. Chloroform (Glaxo, India) of spectroscopy grade was used as solvent after further purification by standard methods[9]. All other chemicals and solvents used were sufficiently pure.

Isolation of final product

Chloranil (~0.2 g) was mixed with four-fold excess of thiomorpholine in chloroform. The reaction mixture was refluxed for 45 min and fractionated over a silica gel column, using chloroform as the eluent. The solution containing the final product was evaporated and the residual solid was dried at 70°C.

Instruments

Systronics UV-VIS spectrophotometer 108 with matched and stoppered 1 cm cells was used for absorption measurements. Shimadzu IR spectrophotometer and Varian XL-100 A NMR spectrometer were used for characterisation of final product.

Kinetics

The reaction kinetics for the transformation of CT Complex into the final product in solution was followed at 298 ± 1 K, keeping the [donor] sufficiently in excess over the [acceptor]. The increase in absorbance (i) of the CT complex at 570 nm and (ii) that of the product at 446 nm was followed by varying concentration of acceptor as well as donor. The decrease in absorbance (iii) of acceptor at 293 nm and (iv) that of the CT complex at 570 nm was also followed spectrophotometrically. The first order rate constants were calculated from the gradients of log $(A_\infty - A_t)$ against time plots for (i) and (ii), where A_∞ and A_t represent the absorbances at infinity and time t respectively. The gradients of log A_t were used for the evaluation of the rate constants of (iii) and (iv).

The effect of varying dielectric constant (ε) was studied by mixing chloroform with carbon tetrachloride (for lower ε) and dichloromethane (for higher ε).

Photometric determination of thiomorpholine

An aliquot of thiomorpholine (1 to 4 ml of 2×10^{-3} mol dm^{-3}) was added to saturated chloranil solution (2 ml) in chloroform and the volume made upto 10 ml. The absorbance of the blue coloured solution was measured after 30 min at 570 nm against a reagent blank. Thiomorpholine was then estimated from the standard Beer's law plot.

Results and Discussion

Spectral characteristics of CT complex

Thiomorpholine, a twin site *n*-donor (through N and S atoms) on mixing with excess of chlora-

nil, a π-acceptor in chloroform, imparts a blue colour to the final solution, which exhibits maximum absorption at 570 nm. The absorption spectrum is relatively broad with a half band width of 5030 cm^{-1}. These results suggest that the colouration is due to an outer sphere complex formed[10] between thiomorpholine and chloranil, the binding force being a probable CT from the electron rich thiomorpholine to the electron acceptor, chloranil.

The composition of the complex, as revealed by the Job's continuous variation[11] and the mol ratio[12] methods, is 1:1. Further, single absorbing species around the absorption maximum of the complex is verified using the plots due to Coleman *et al*[13]. Although thiomorpholine is a twin site *n*-donor, the CT transition observed in the 1:1 complex is only from one site. More electronegative nitrogen atom of the donor, may probably be involved in the formation of the outer sphere complex.

Stability parameters

The position and results of the equilibrium between the CT complex and its components, viz. acceptor and donor were obtained as suggested by Seal *et al*[14]. The values of the oscillator strength and the transition dipolemoment of the CT complex were also derived as reported earlier[3]. The results on electronic absorption as well as those on the equilibrium of CT complex of chloranil with thiomorpholine are presented in Table 1. The results reported earlier for those of piperazine and morpholine with the same acceptor[1,4] are also listed in Table 1 for comparison.

The results indicate that CT complexes between chloranil and twin site *n*-donors are relatively strong. Further, amongst the twin site organic bases, viz. piperazine, morpholine and thiomorpholine, piperazine is relatively a stronger donor. While the secondary nitrogen is the donor site in all the three donors, the effect of other heteroatoms instead of favouring donation, inhibits their donating strengths. This may be due to steric repulsion to the lone pair of the donation site by the second heteroatom. In the case of thiomorpholine and morpholine, each of the second heteroatom itself has two line pairs, thereby the magnitude of the repulsive forces is enhanced. Between thiomorpholine and morpholine, the spectrophotometric results indicate that the former is relatively a stronger donor. This could be ascribed to the low electronegativity of the sulphur donor atom of thiomorpholine than the oxygen donor atom of morpholine and in the latter case there may be more perturbation of the lone pair of the nitrogen atom.

Transformation of CT complex

In the presence of excess of acceptor, the complex formation is rapid and the complex formed is sufficiently stable. However, with slight excess of donor, the blue coloured CT complex slowly transforms into a yellow coloured species in solution. The time dependent absorption pattern is indicated in Fig. 1. The yellow coloured species in solution shows absorption maximum at 446 nm. No further transformation is observed even with a large excess of donor.

Characterisation of the final product

The absorption maxima of yellow coloured species in solution and that of the final product in chloroform are the same, indicating that the isolated product and the product in solution are one and the same. Due to the aliphatic nature of the donor, it will be highly basic and its strong driving force may favour a substitution reaction as observed in the case of similar interactions[3]. If the reaction leads to substitution, HCl will be one of the products, the presence of which was confirmed by the silver nitrate test with an aqueous extract of the reaction mixture.

The IR spectrum of the final product in KBr exhibited a peak at 1660 cm^{-1}, assignable to the quinonoid carbonyl group of the product. The substitution of the >NH group of the donor moiety of the product was confirmed by the absence of ν_{NH} mode (at ~3200 cm^{-1}) in the IR spectrum. The PMR spectrum of the final product

Table 1 – Spectral and Stability Data for Charge Transfer Complexes of Chloranil with Heteroalicyclic Bases

Donor	λ_{CT} (nm)	Excitation energy of CT complex (eV)	Half band width of CT complex (cm^{-1})	ε_{max} ($dm^3mol^{-1}cm^{-1}$)	Equilibrium constant (K) (dm^3mol^{-1})	Oscilator strength (f)	Transition dipolemoment (debye)	$\lambda_{product}$ (nm)
Piperazine	578	2.143	5020	1820	37400	0.059	2.69	448
Morpholine	572	2.168	5030	1260	8500	0.041	2.23	442
Thiomorpholine	570	2.175	5030	1350	11100	0.045	2.29	446

in $CDCl_3$ (TMS as internal standard) was devoid of the signal at δ 1.6 assignable to NH proton of the donor moiety. Further, the resonance signals at δ 3.01 and 3.46 were of equal integration ratio and could be assigned to the protons of the donor moiety, adjacent to sulphur and nitrogen atoms respectively, thus supporting the substitution reaction. The degree of substitution was found to be 2, by elemental analyses and the final product may be characterised as 2,5-dichloro-3,6-dithiomorpholino-1,4-benzoquinone.

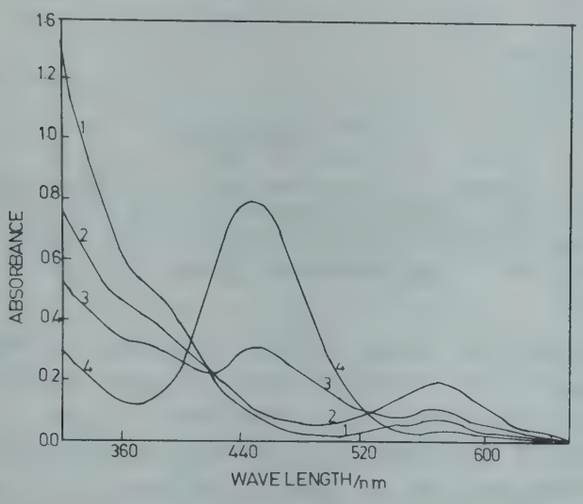

Fig. 1 – Time dependent absorption spectra (1, 2, 3 and 4 are recorded 2, 11, 30 and 75 min, respectively after mixing the components in chloroform. [chloranil] = 1×10^{-4}, [thiomorpholine] = 0.1 mol dm^{-3}).

Kinetic results

The kinetic results are summarised as follows:

(i) The pseudo-first order rate constants for the CT formation are almost constant (Table 2) at different initial [chloranil], indicating first order dependence in [acceptor]. A model kinetic run is represented diagramatically in Fig. 2.

(ii) The log-log plot of k'_s versus [thiomorpholine] is linear with a slope of unity, indicating unit dependence in [donor].

The results obey the rate law (1)

$$d(\mathrm{CT})/dt = k_{CT}[\text{chloranil}]_0[\text{thiomorpholine}]_0 \quad \ldots (1)$$

As 1:1 CT complex has the equilibrium constant (K) of the order of 10^4 dm^3 mol^{-1}, the CT formation may be approximated to Eq. (2).

$$\text{Chloranil} + \text{thiomorpholine} \xrightarrow{K} \text{CT complex} \quad \ldots (2)$$

The rate law for Eq. (2) will be the same as the experimentally observed one (Eq. 1).

(iii) The kinetic results for the product formation follow the trend similar to that observed in

Table 2 – Kinetic Results of EDA Interaction: Effect of Varying [Chloranil], [Thiomorpholine] and Dielectric Constant on Reaction Rate*

10^5[Chloranil] (mol dm^{-3})	10^3[Thiomorpholine] (mol dm^{-3})	Dielectric constant	10^5 k (s^{-1})	$10^3 k_{CT}$ (or k_p) ($dm^3 mol^{-1} s^{-1}$)
		Formation of CT complex		
20.2	12.0	4.8	34.4	
30.3	12.0	4.8	34.4	
40.4	12.0	4.8	33.4	27.3
60.6	12.0	4.8	33.4	
40.4	4.9	4.8	13.7	27.9
40.4	18.0	4.8	51.2	28.4
40.4	25.0	4.8	71.4	28.5
40.4	18.0	3.5		23.6
40.4	18.0	6.3		46.9
40.4	18.0	7.0		72.5
		Formation of Product		
4.02	4.00	4.8	1.25	
6.03	4.00	4.8	1.26	
8.04	4.00	4.8	1.25	3.12
9.94	4.00	4.8	1.26	
8.04	1.56	4.8	0.49	3.13
8.04	7.01	4.8	2.21	3.16
8.04	10.51	4.8	3.27	3.13
8.04	7.01	3.5		2.74
8.04	7.01	6.3		6.87
8.04	7.01	7.0		7.52

*k' = Pseudo-first order rate constant and k_{CT} and k_p = specific rate constants for formation of CT and product respectively.

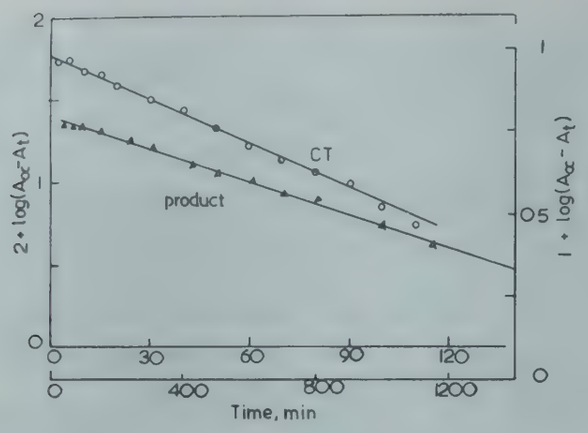

Fig. 2 – Plot of absorbance of product versus time ([chloranil] = 7×10^{-5}, [thiomorpholine] = 4×10^{-3} mol dm^{-3}).

the CT formation (Fig. 2 and Table 2). The experimental rate law, may be given by Eq. (3).

$$d(\text{product})/dt = k_p[\text{CT complex}][\text{thiomorpholine}] \quad \ldots (3)$$

Under the experimental condition, the concentration of CT complex can be taken as equal to the initial [chloranil]. The rate law, hence, can be expressed as Eq. (4).

$$d(\text{product})/dt = k_p[\text{chloranil}]_0[\text{thiomorpholine}]_0 \quad \ldots (4)$$

(iv) The kinetic results for the decrease in the absorbance of the acceptor are observed to be similar to those of the formation of CT complex and obey the rate law (5).

$$d(\text{CT})/dt = k_{CT}[\text{CT}] = -k_a[\text{chloranil}]_0 \quad \ldots (5)$$

Further, the specific rate constant obtained for the CT formation from the kinetic study of decrease in $[\text{chloranil}]_0$ comes out to be 0.0298 dm^{3}mol^{-1}s^{-1}, which is in good agreement with that obtained from the study of increase in CT complex concentration (Table 2).

(v) The kinetic results for the decrease in absorbance of the CT complex, follow the trend similar to that of the product formation and obey the rate law similar to that represented by Eq. (5). However, the specific rate constant obtained from the decrease in concentration of CT complex (2.25×10^{-3}dm^{3}mol^{-1}s^{-1}), differs from that obtained for the product formation (Table 2). This indicates that the product results from a path involving an intermediate between the CT complex and the product.

The plot of absorbance of the product versus time shows initial non-linearity (Fig. 3). This supports the postulation of an intermediate between the CT complex and the product[15]. However, the

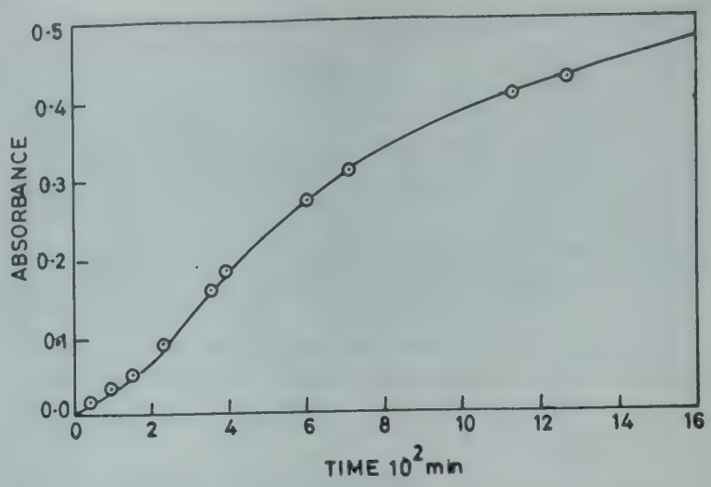

Fig. 3 – Kinetics of formation of CT complex ([chloranil] = 4×10^{-4}, [thiomorpholine] = 1.2×10^{-2} mol dm^{-3}) and product formed ([chloranil] = 8×10^{-5} and [chlomorpholine] = 4×10^{-3} mol dm^{-3})

intermediate could not be detected spectrophotometrically, probably due to the nature of the intermediate, which may be of an inner sphere complex type with a partial ionic character. Similar observations in the EDA interactions are not uncommon[3,15,16].

Effect of ε on the reaction rate

With varying dielectric constant (ε) values, the rate of the formation of CT complex as well as the product are found to be affected much. At low ε, the specific rate constants (k_{CT} and k_p) are decreased and while at high ε they are increased (Table 2).

Mechanism

Based on the characteristics of the CT complex, product and based on the kinetic results obtained, the mechanism of the EDA interaction between thiomorpholine and chloranil can be represented by Eqs (6) and (7).

(a) In the presence of excess acceptor

$$A + D \overset{\text{fast}}{\rightleftharpoons} \text{CT complex} \quad \ldots (6)$$

(b) In the presence of excess donor

$$A + D \overset{\text{fast}}{\rightleftharpoons} \text{CT complex} \xrightarrow[D]{\text{slow}} \text{Inner complex} \xrightarrow[-2\,HCl]{\text{fast}} \text{Final product} \quad \ldots (7)$$

Photometric determination of thiomorpholine

The higher stability of 1:1 complex in the presence of excess of chloranil is utilised for the spectrophotometric determination of thiomorpholine using chloranil as the reagent. Variation in [chloranil] suggests that 5 to 100 fold excess of chloranil does not affect the absorption of the complex.

Table 3 – Results of Spectrophotometric Determination of Thiomorpholine using Chloranil as Reagent

Thiomorpholine, μg ml^{-1}		Error* %	Coefficient of variance*
Taken	Found		
12.1	12.1	—	0.32
36.3	36.2	0.28	0.26
60.7	60.5	0.33	0.42
84.5	84.7	0.24	0.58

*For six determinations.

However, chloranil should always be kept sufficiently in excess. The time-stability study of the complex indicates that CT complex is very stable and reproducible absorbances are obtained even after a day. The Beer's law is obeyed in the donor concentration range of 10 to 90 μg ml^{-1} with a Sandell's sensitivity of 0.108 μg cm^{-2} per 0.001 absorbance unit. The results are listed in Table 3.

The method is simple, direct and convenient and advantageous like the other methods reported by us[17,18]. Piperidine, piperazine and morpholine are found to interfere at all concentrations, but pyridine, pyrazine and diphenylamine upto 5-fold excess and N-methylpiperidine and N-methylmorpholine upto 10-fold excess do not interfere in the determination of thiomorpholine.

Acknowledgement

One of the authors (KSB) thanks the UGC, New Delhi, for the award of a fellowship under FIP programme.

References

1 Muralikrishna U, Seshasayi Y V S K & Krishnamurthy M, *J Indian chem Soc*, **60** (1983) 447.
2 Muralikrishna U, *J Indian chem Soc*, **62** (1985) 1052.
3 Muralikrishna U & Krishnamurthy, *Indian J Chem*, **21A** (1982) 1018; **22A** (1983) 512, 858; **25A** (1986) 949; *Spectrocs Lett*, **16** (1983) 711; *Spectrochim Acta*, **40A** (1984) 65.
4 Muralikrishna U, Seshasayi Y V S K & Krishnamurthy M, *J Indian Chem Soc*, **60** (1983) 1048; *Natl Acad Sci Lett*, **6** (1983) 383.
5 Muralikrishna U, Seshasayi Y V S K & Krishnamurthy M, *Indian J Chem*, **22A** (1983) 409; *React Kinet Catal Lett*, **24** (1984) 193.
6 Muralikrishna U, Krishnamurthy M & Rao N S, *Indian J Chem*, **23A** (1984) 77; *Analyst*, **109** (1984) 1277.
7 Foster R & Foreman M I, *The chemistry of quinonoid compounds* **Part 1**, edited by S Patai (John Wiley, London) 1974, pp 257.
8 Butufei O, *Rev chim Buch*, **31** (1980) 140.
9 Riddick J A & Bunger W B, *Techniques of chemistry*, **Part 2** (Wiley, New York) 1970, pp 771.
10 Mulliken R S & Person W B, *Molecular complexes* (Wiley, New York) 1969.
11 Job P, *Ann Chim (Paris)*, **9** (1928) 113.
12 Yoe J H & Jones A L, *Ind engng Chem (Anal Edn)*, **16** (1944) 111.
13 Coleman L S, Varga L P & Mastin S H, *Inorg Chem*, **9** (1970) 1015.
14 Seal B K, Mukharjee A K & Mukharjee D C, *Bull chem Soc Japan*, **52** (1979) 2088.
15 Nogami T, Yamoka T, Yoshihara K & Nagakura S, *Bull chem Soc Japan*, **44** (1971) 380.
16 Rappoport Z, *J chem Soc*, (1963) 4498.
17 Muralikrishna U, Krishnamurthy M & Seshasayi Y V S K, *Indian J Chem*, **22A** (1983) 904.
18 Krishnamurthy M & Muralikrishna U, *Indian Drugs*, **22** (1985) 171; *Microchem J*, **31** (1985) 210.

Indian Journal of Chemistry
Vol. 27A, August 1988, pp. 674-676

Catalytic Properties of Heteropolyacids—Conversion of Isopropyl Alcohol into Saturated Hydrocarbons

B VISWANATHAN*, M J OMANA & T K VARADARAJAN
Department of Chemistry, Indian Institute of Technology, Madras 600 036

Received 29 *September* 1987; *revised and accepted* 9 *November* 1987

The conversion of isopropyl alcohol into propane on heteropoly tungstic acid catalyst occurs mostly by disproportionation of the olefin formed as well as from H transfer carbonization route.

The catalytic properties of heteropolyacids (HPA) of tungsten ($H_3PW_{12}O_{40}$; HPW) and molybdenum ($H_3PMo_{12}O_{40}$; HPMo) and their salts have been examined in detail in recent times with a view to finding out alternatives for zeolites for the conversion of methanol and other alcohols into hydrocarbons. In these studies, HPAs are considered to function similar to zeolites for the production of higher hydrocarbons[1]. Highfield and Moffat[2] observed the formation of C_3— and C_4—hydrocarbons in the sustained catalysis of isopropyl alcohol (IPA) on HPW at 523 and 623 K. Ohukara *et al.*[3] observed only propene and water together with a small quantity of ether on copper salts of HPW at 373 K. However, it is expected that saturated hydrocarbons especially propane can be formed on these catalysts as has been observed with methanol[4]. Propane from IPA could be formed by either of the following reactions: (i) hydrogenation of the olefin formed by dehydration; (ii) nucleophilic substitution of OH^- by H^- originating from water[5]; and (iii) disproportionation of propene[6]. The purpose of the title investigation is to examine which one of these three routes (i-iii) is probable on HPW in the conversion of IPA into saturated hydrocarbons.

The surface acidic properties of these systems especially those of HPW and HSiW and their salts have been examined by a number of workers[7]. The acidic properties of these systems are dependent on the temperature of pretreatment as well as the environment employed for calcination[8]. In methanol conversion, heating in air is known to reduce the activity possibly due to extraction of acidic sites by oxygen, while heating in hydrogen/helium is known to enhance the yield of hydrocarbons due to alteration in the distribution of acid sites[7]. In the present work, therefore, the acidity of HPW has been examined using indicator method with a view to (a) evaluating the effect of pretreatment temperature and environments (air, vacuum, flowing argon or hydrogen) on the acidity of the catalyst, (b) correlating acidity with activity for saturated hydrocarbon formation from IPA; and (c) gaining information on the probable route for propane formation.

Materials and Methods

12-Tungstophosphoric acid was prepared from sodium tungstate and disodium phosphate following the literature procedure[9]. The acid was calcined at 573 K and 673 K for 4 hr under various atmospheres like air, vacuum, argon and hydrogen.

Acid strength distribution of the catalyst pretreated under different conditions was determined following the procedure of Benesi[10] using Hammett indicators.

The catalytic reactions of IPA were carried out in a fixed bed flow-type reactor working at atmospheric pressure. The products were analysed either gas chromatographically or using Orsat apparatus. The carbon contents on the catalysts were estimated by conversion to carbon dioxide and using baryta solution for estimation.

Results and Discussion

The products of decomposition of IPA in the temperature range of 383-423 K are propene, water, diisopropyl ether and propane. No dehydrogenation product, namely acetone or hydrogen was formed. Direct hydrogenation of propene by hydrogen formed by dehydrogenation, though may be thermodynamically favourable is likely to be kinetically controlled in the above reaction, since dehydrogenation is feasible only at higher temperatures[5] (> 623 K). The hydrogen transfer and carbonization reaction is predominant only around 523K though it is observable even at 423K (ref. 2). In the light of the observations reported in literature we have carried out the decomposition of IPA at 383 K on the catalyst calcined at 573K in the presence of various substrates like hydrogen, water, ether and nitrogen. The variation in the amounts of propene and propane formed as a function of partial pressure of IPA is shown in Fig.

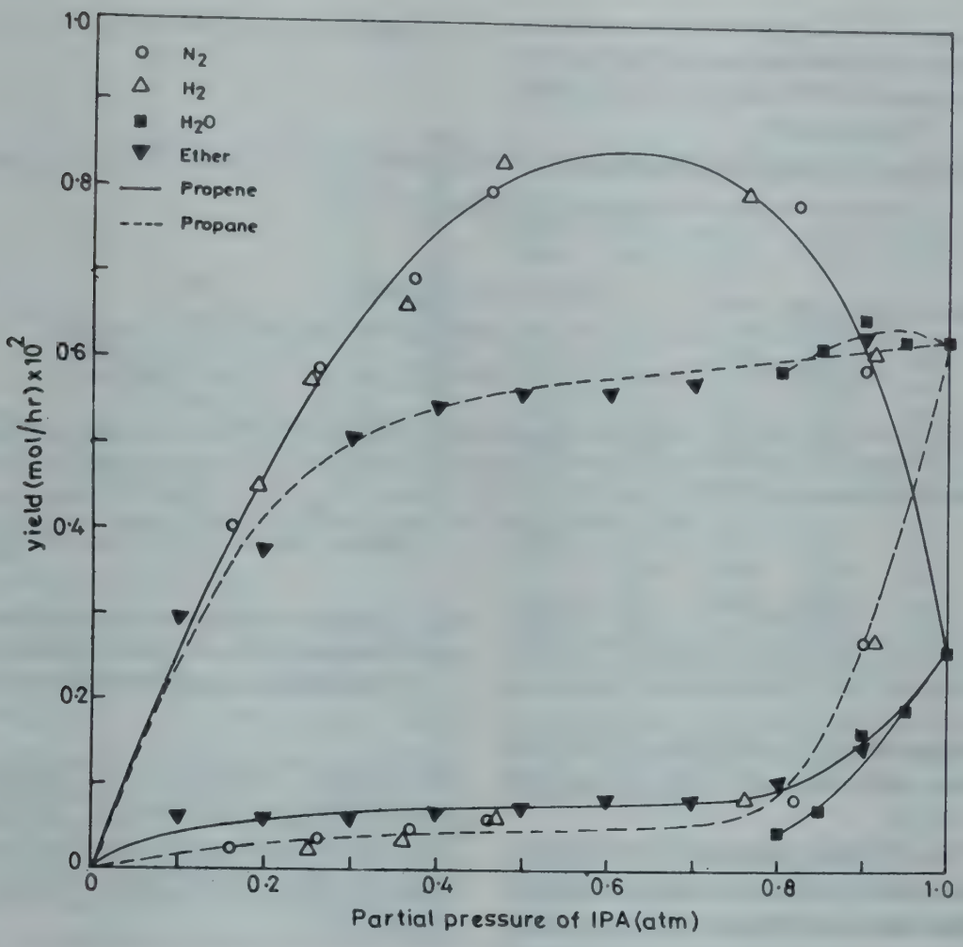

Fig. 1—Effect of partial pressure of IPA on hydrocarbon yield in the presence of various substrates [Reaction temperature 383 K; contact time 1.33 sec]

1. The following points emerge from the results presented in Fig. 1.

(i) Similar results obtained for the formation of propane and propene in the presence of nitrogen and hydrogen ruled out direct hydrogenation of olefin by molecular or adsorbed hydrogen.

(ii) In the presence of water, the amount of olefin formed was small while considerable amount of propane was formed indicating that either the olefin formed was converted into propane or the olefin formation was suppressed in presence of water in the feed.

(iii) In the presence of diisopropyl ether propane formation was a favoured reaction.

The extent of carbon formation during IPA decomposition was separately estimated. Propane to carbon ratio was found to be around 1.5 at all temperatures studied. Propene formed disproportionates in accordance with the reaction[6].

$$4CH_3{-}CH=CH_2 \rightarrow 3CH_3{-}CH_2{-}CH_3 + 3C,$$

and if this were to be the only route for propane formation then the propane to carbon ratio should have been one instead of 1.5 observed presently. It is therefore considered that propane could also be formed by another route on HPW. The alternate route could involve the nucleophilic attack of thehydride ion on the dehydration product or the alcohol itself.

The acid strength distribution obtained for the catalysts calcined at 573 and 673 K in various atmospheres are given inTable 1. The following points emerge from these results:

(i) In air and argon atmospheres, pretreatment at higher temperatures (673 K) increases the number of highly acidic sites ($H_o \leqslant -3.0$) while moderate acid sites ($-3.0 < H_o < +3.3$) predominate in the sample pretreated at 573 K.

(ii) The influence of temperature of pretreatment on the acidity of the catalyst when treated in vacuum or in hydrogen is not significant.

(iii) Samples pretreated in vacuum contain only strong acidic sites ($H_o < -3.0$) while samples pretreated in other atmospheres do contain sites with moderate acid strength.

XRD patterns obtained for HPW after pretreatment at various temperatures and atmospheres show that Keggin unit is stable upto 673K.

In earlier reports on HPAs attempts were made to correlate the surface properties with catalytic activities. Moffat and coworkers[7] have generated data to

Table 1—Surface Acidity Distribution on Heteropolytungstic Acids Pretreated at 573 and 673 K in Various Atmospheres

Pretreatment	*H*-Butylamine titer (mmol/g) in the H_o range					
	+6.8 to +5.0	+5.0 to +3.3	+3.3 to +1.5	+1.5 to −3.0	−3.0 to −5.6	−5.6 to −8.2
Sample pretreated at 573 K						
Vacuum	0.7	0.2	0.2	0.2	0.2	2.0
Air	0.5	0.4	0.2	1.2	0.2	1.0
Argon	0.5	0.4	0.2	1.8	0.2	0.4
Hydrogen	0.7	0.2	0.2	1.6	0.2	0.6
Sample pretreated at 673 K						
Vacuum	1.2	0.2	0.2	0.2	0.2	2.0
Air	0.5	0.2	0.2	0.2	0.2	2.2
Argon	1.0	0.4	0.2	0.6	0.2	1.6
Hydrogen	1.0	0.6	0.2	1.6	0.2	0.4

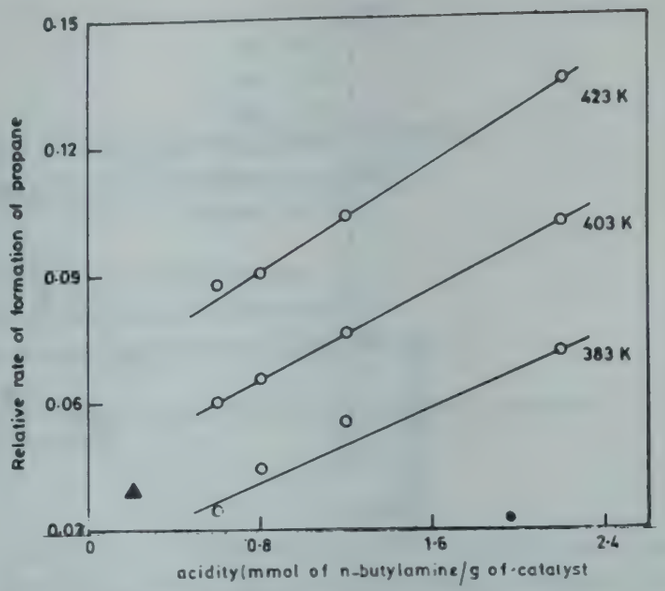

Fig. 2—Variation of relative rate of propane formation with respect to acidity (H_o = −3.0 to −8.2) [▲, value corresponding to the ammonium salt of the heteropoly acid at 423 K]

show that the formation of C_4-hydrocarbons from methanol correlates with the acidic sites of strength $H_o < +3.3$ or $< +1.5$.

Highfield and Moffat have postulated that the activity may be promoted by judicious control of the acid strength distribution, i.e. weaker sites favouring olefin formation while stronger sites may be involved in carbonization route. In order to substantiate the postulate that formation of propane from IPA may involve such a H transfer-carbonization route, we have attempted to correlate the initial slope of the plot of the ratio of propane/propane + propene versus contact time with acidity. The dependent parameter chosen can be considered to be related to the rate of propane formation relative to propene formed. The correlation plots obtained at 383, 403 and 423 K are shown in Fig. 2. It is seen that the acitivity for propane formation is related to the strong acid sites present on the surface favouring a H transfer-carbonization route for propane formation. The relative variation of these plots with temperature may be indicative of the number of such sites participating in the carbonization route.

References

1 Ono Y. & Mori T, *J chem Soc Faraday Trans*, I 77 (1981) 2209.
2 Highfield J G & Moffat J B, *J Catal*, **98** (1986) 245.
3 Okuhara T, Hashimoto T, Hibi T & Misono M, *J Catal*, **93** (1985) 224.
4 Hayashi H & Moffat J B, *J Catal*, **81** (1983) 61.
5 McMonagle J B & Moffat J B, *J Catal*, **91** (1985) 132.
6 Thomas C L & Barmby D S, *J Catal*, **12** (1968) 341.
7 Ghosh A K & Moffat J B, *J Catal*, **101** (1986) 238.
8 Hayashi H & Moffat J B, *J Catal*, **77** (1982) 473.
9 Bailor J C, *Inorganic synthesis*, Vol 1 edited by H C Booth (McGraw Hill, New York) 1939 pp 132.
10 Benesi H A, *J Am chem Soc*, **61** (1957) 970.

Indian Journal of Chemistry
Vol. 27A, August 1988, pp. 677-679

Synthesis & Characterisation of a Triosmium Cluster Containing Thiocyanate Ligand

SHARIFF E KABIR
Department of Chemistry, Jahangirnagar University, Savar, Dhaka, Bangladesh

Received 22 *July* 1987; *revised* 29 *October* 1987; *accepted* 21 *December* 1987

The cationic clusters $[Os_3H(CO)_{11}(CH_3CN)]$ BF_4(I) and $[Os_3H(CO)_{10}(CH_3CN)_2]BF_4$(II) react with $(Bu_4N)SCN$ to give the new hydridothiocyanato cluster $[Os_3H(SCN)(CO)_{10}]$ (III). Reactions of I with ROH (R = Me or Et) lead to the known clusters $[Os_3H(COR)(CO)_{10}]$ (IV). The cluster $[Os_3H(Cl)(CO)_{10}]$ (V) also reacts with $(Bu_4N)SCN$ to give $[Os_3H(SCN)(CO)_{10}]$(III) whereas with $(Et_4N)CN$ it gives only intractable residue.

The synthesis of cationic clusters such as $[Os_3H(CO)_{11}(CH_3CN)]$ BF_4 and $[Os_3H(CO)_{10}(CH_3CN)_2]$ BF_4 by the reactions of $[Os_3(CO)_{11}(CH_3CN)]$ and $[Os_3(CO)_{10}(CH_3CN)_2]$ with acids HX(X = PF_6 or BF_4) has recently been reported[1]. With a view to synthesising neutral compounds of the type $[Os_3H(X)(CO)_{10}]$ by displacement of CH_3CN from the above cationic clusters, we have presently studied the reactions of these cationic clusters with a variety of ligands such as tetrabutylammonium thiocyanate, MeOH, EtOH or tetraethylammonium cyanide and the results of this investigation are described in this paper.

Materials and Methods

IR spectra were recorded on a Perkin-Elmer PE 983 spectrophotometer and PMR spectra on a XL 200 instrument (University College, London). The starting clusters $[Os_3(CO)_{11}(CH_3CN)]$ (ref. 2), $[Os_3(CO)_{10}(CH_3CN)_2]$ (ref. 2) and $[Os_3H(Cl)(CO)_{10}]$ (ref. 3) were prepared by published methods. Tetrabutylammonium thiocyanate (Bu_4NSCN) was prepared by the reaction of tetrabutylammonium hydroxide (1 mol dm^{-3} in MeOH) with ammonium thiocyanate (Found: C, 67.1; H, 11.5; N, 9.6; S, 10.4. $C_{17}H_{36}N_2S$ requires C, 67.9; H, 12.1; S, 10.7; N, 9.3%).

Preparation of $[Os_3H(CO)_{11}(CH_3CN)]BF_4$*(I)*

$HBF_4.Et_2O$ (0.022 ml, 5 mol/mol Os_3) was added to a $CDCl_3$ (0.5 ml) solution of $[Os_3(CO)_{11}(CH_3CN)]$ (0.025 g) and the reaction monitored by PMR which indicated complete formation of $[Os_3H(CO)_{11}(CH_3CN)]^+$. Recrystallisation from ether gave I (0.022 g, 82%) as pale yellow crystals, fully characterised by comparing IR and PMR spectra with those reported[1].

Preparation of $[Os_3H(CO)_{10}(CH_3CN)_2]BF_4$*(II)*

The PMR spectrum of a solution of $HBF_4.Et_2O$ (0.022 ml, 5 mol/mol Os_3) and $[Os_3(CO)_{10}(CH_3CN)_2]$ (0.025 g) in $CDCl_3$ (0.5 ml) showed that complete protonation had occurred. The solvent was removed *in vacuo* and the residue recrystallised from CH_2Cl_2/ether to give II (0.021 g, 78%) as pale yellow crystals.

Reaction of I with $(Bu_4N)SCN$

Tetrabutylammonium thiocyanate (0.015 g) was added to a CH_2Cl_2 (20 ml) solution of I (0.01 g). After 30 min the solvent was removed *in vacuo*. TLC of the residue over silica gel and elution with light pet (b.p. 30-40°)/dichloromethane (10:2, v/v) gave $[Os_3H(SCN)(CO)_{10}]$ (III) (0.005 g, 56%) as yellow crystals (Found: C, 15.1; H, 0.5; N, 1.8; S, 4.0. $C_{11}HNO_{10}Os_3S$ requires C, 14.5; H, 0.1; N, 1.6; S, 3.5%); IR (cyclohexane): νCO at 2115 m, 2079 vs, 2068 s, 2030 vs, 2019 vs, 1995 cm^{-1}; PMR ($CDCl_3$): δ −16.85 (*s*, Os*H*).

Reaction of II with $(Bu_4N)SCN$

Treatment of cluster II (0.01 g) and $(Bu_4N)SCN$ (0.014 g, 5 mol/mol Os_3) as above for 3 hr followed by similar work-up gave the cluster III (0.004 g, 44%) and a small quantity of an uncharacterised compound.

Reaction of $[Os_3H(Cl)(CO)_{10}]$ *(V) with* $(Bu_4N)SCN$

$(Bu_4N)SCN$ (0.027 g, 2 mol/mol Os_3) was added to an acetone (50 ml) solution of V (0.075 g) and allowed to stand at room temperature in the dark for 2 hr. Removal of the solvent left a residue which was subjected to TLC over silica gel. Elution with light pet (b.p. 30-40°)/dichloromethane (10:2, v/v) afforded V (0.010 g), III (0.009 g, 11%) and another uncharacterised compound (0.004 g).

Reactions of V: (i) with KCN in MeOH; (ii) with MeOH; and (iii) with $(Et_4N)CN$

KCN (0.008 g, 20% excess) was added to a metha-

nol (15 ml) solution of V (0.075 g). After removal of the solvent *in vacuo* the residue was chromatographed on silica TLC plates. Elution with pentane gave $[Os_3H(OMe)(CO)_{10}]$ (ref. 4) (VI) (0.042 g, 56%). V did not react with MeOH even when the mixture of V and MeOH was left for 4 hr. The reaction of V with $(Et_4N)CN$ in dichloromethane afforded an intractable mixture.

Reaction of I with KCN in MeOH

KCN (0.019 g, 2 mol/mol Os_3) was added to a solution of I (0.04 g) in methanol and allowed to stand at room temperature under nitrogen for 1 hr. The solvent was removed under reduced pressure and the residue was chromatographed over silica TLC plates. Elution with pentane gave $[Os_3H(OMe)(CO)_{10}]$ (ref. 4) (0.007 g, 8%) and $[Os_3H(COMe)(CO)_{10}]$ (ref. 5) (0.028 g, 30%), characterised by comparing their IR and PMR spectra with those previously reported.

Reaction of I with MeOH or EtOH: Formation of $[Os_3H(COMe)(CO)_{10}]$ *or* $[Os_3H(COEt)(CO)_{10}]$

Cluster I (0.02 g) was dissolved slowly in methanol or ethanol (15 ml) and the solution was allowed to stand at room temperature for 24 hr. The solvent was removed under reduced pressure and the residue subjected to TLC over silica gel. Elution with light pet (b.p. 30-40°) gave $[Os_3H(COMe)(CO)_{10}]$ (0.01 g, 46%) or $[Os_3H(COEt)(CO)_{10}]$ (ref. 6) (0.01 g, 37%) as yellow crystals.

Results and Discussion

The cationic cluster $[Os_3H(CO)_{11}(CH_3CN)]BF_4$ reacts with $(Bu_4N)SCN$ at ambient temperature to give $[Os_3H(SCN)(CO)_{10}]$ (III) (Scheme 1) by the loss of acetonitrile and CO. This new hydridothiocyanato cluster (III) has been characterised by spectral data. Its PMR spectrum exhibits a singlet at $\delta - 16.85$ attributable to the hydrido ligand, while its IR spectrum in the νCO region is consistent with the structure shown. The mass spectrum gave the parent molecular ion corresponding to its elemental analysis thus supporting the proposed formulation. The reaction of $(Bu_4N)SCN$ with $[Os_3H(CO)_{10}(MeCN)_2]BF_4$ also gives the cluster $[Os_3H(SCN)(CO)_{10}]$ (III). In an alternative approach towards III, $(Bu_4N)SCN$ was reacted with $[Os_3H(Cl)(CO)_{10}]$ and a low yield of III was obtained. This behaviour is very similar to that observed for $[Os_3H(OH)(CO)_{10}]$ which gave derivatives of type $[Os_3H(X)(CO)_{10}]$ on reaction with strongly coordinating anions $X(X = Cl^-$ or $MeCO_2^-)$ (ref. 6). The reactions of $[Os_3H(CO)_{11}(CH_3CN)]BF_4$ with ROH (R = Me or Et) give the known clusters $[Os_3H(CO)_{10}(COR)]$ (ref. 5) which have previously been obtained by the reaction of $[Os_3H(CO)_{11}]Et_4N$ with $MeSO_3F$ or $Et_3O\,BF_4$.

The SCN^- group may coordinate to the metal through the sulphur or the nitrogen or both[7] and accordingly the cluster $[Os_3H(SCN)(CO)_{10}]$ may have structure IIIa or IIIb or IIIc differing in the way the SCN^- ligand is bonded to the triosmium cluster.

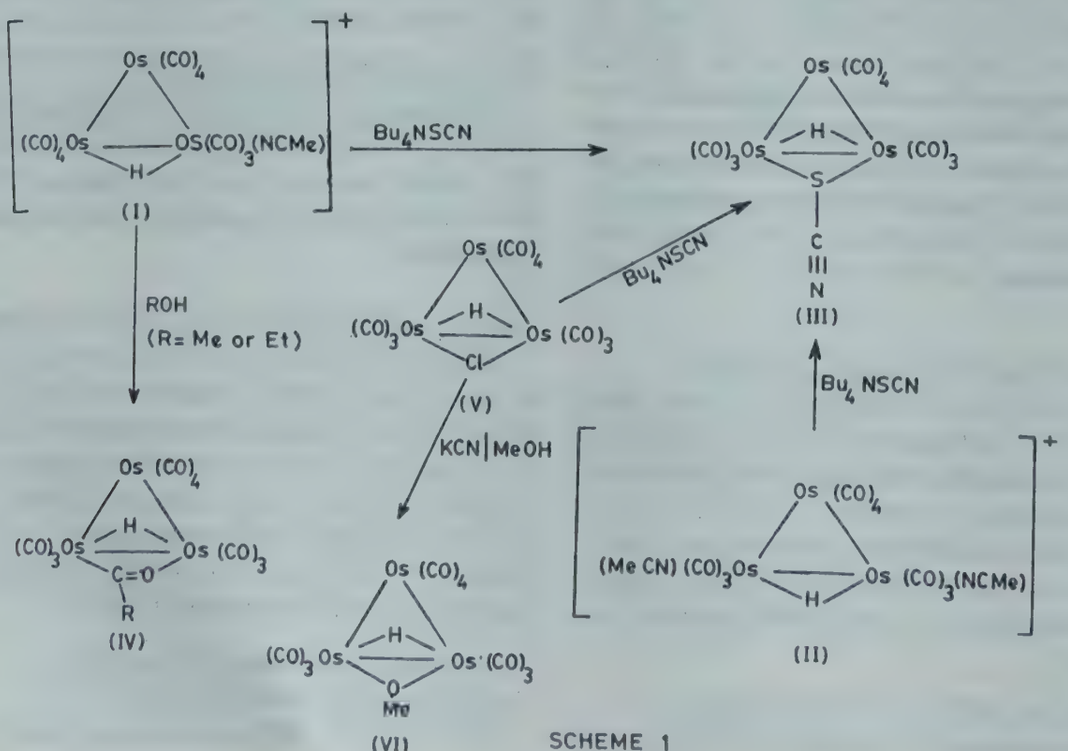

SCHEME 1

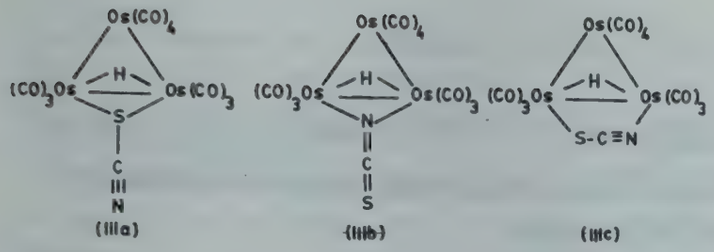

The above proposed modes of ligand coordination have been found for other related systems. For example, in $[Os_3H(SCHNPh)(CO)_{10}]$ there is a single sulphur atom bridging[8] but in the OCN analogue the bridge is through the nitrogen atom[9]. In $[Os_3H(SCHNPh)(CO)_9]$ the bridge is both through sulphur and nitrogen atoms[8]. The IR spectra of thiocyanate complexes can in most cases differentiate between sulphur and nitrogen bridging. For example the νCN modes are generally higher in sulphur-bridged complexes of the ligand. The appearance of νCN at 2161 cm^{-1} suggests that SCN group in cluster III is most probably bridging through S atom but without X-ray analyses it is not possible to establish the structure.

The synthesis of $[Os_3H(SCN)(CO)_{10}]$ by the reactions of $(Bu_4N)SCN$ with $[Os_3H(Cl)(CO)_{10}]$ or $[Os_3H(CH_3CN)(CO)_{11}]BF_4$ led us to believe that the corresponding reaction of KCN with $[Os_3H(Cl)(CO)_{10}]$ or $[Os_3H(CH_3CN)(CO)_{11}]^+$ should give the μ-CN compound, $[Os_3H(\mu\text{-}CN)(CO)_{10}]$. However chromatographic work-up of the reaction product gave an intractable residue. In another attempt to synthesise the cyanide compound, KCN was reacted with $[Os_3H(Cl)(CO)_{10}]$ but the product obtained was $[Os_3H(OMe)(CO)_{10}]$. $[Os_3H(Cl)(CO)_{10}]$ did not react with MeOH or EtOH alone under exactly the same experimental conditions as that with KCN in MeOH. It is, therefore, believed that the reaction of $[Os_3H(Cl)(CO)_{10}]$ with KCN forms the expected cyanide compound which readily undergoes reaction with methanol to give $[Os_3H(OMe)(CO)_{10}]$. In another attempt $(NEt_4)CN$ was reacted with $[Os_3H(Cl)(CO)_{10}]$ in CH_2Cl_2. Chromatographic work-up gave an intractable residue.

Acknowledgement

The author thanks Dr A J Deeming, Department of Chemistry, University College, London, for helpful discussions and providing the PMR and IR spectra and elemental analyses.

References

1 Anson C E, Ditzel E J, Fajardo M, Holden H D, Johnson B F G, Lewis J, Puga J & Raithby P R, *J chem Soc Dalton*, (1984) 2723.
2 Johnson B F G, Lewis J & Pippard D A, *J chem Soc Dalton*, (1981) 407.
3 Arce A J, Deeming A J, Donovan-Mtunzi S & Kabir S E, *J chem Soc Dalton*, (1985) 2479; Deeming A J & Hasso S E, *J organometal Chem*, **114** (1976) 313.
4 Johnson B F G, Lewis J & Kilty O A, *J chem Soc (A)*, (1968) 2859.
5 Gavens P D & Mays M J, *J organometal Chem*, **162** (1978) 389.
6 Kamiets E D, Maksakov V A, Kedrova L K, Shakot'ko N I & Gupin S P, *Izv Akad Nauk SSR, Ser Khim*, **2** (1983) 435.
7 Nakamoto K, *Infrared & Raman spectra of inorganic and coordination compounds* (Wiley Inter-Science, New York) 1978, P270.
8 Adams R D, Golembeski N M & Selegue J P, *Organometallics*, **2** (1983) 315.
9 Deeming A J, Ghatak I, Owen D W & Peters R, *Chem Commun*, (1982) 392.

Indian Journal of Chemistry
Vol. 27A, August 1988, pp. 680-686

Macrocyclic Complexes: Part XII – Complexes of Ni(II) with Fluoro-boro Bridged Macrocyclic Ligands, Dimethyl, Diacetyl Cyclopean & Dimethyl, Dicarbethoxy Cyclopean

BHAGIRATHI SAHOO, N C PATRA, A K ROUT & B SAHOO*
Indian Institute of Technology, Kharagpur 721 302

Received 3 *August* 1987; *revised and accepted* 4 *January* 1988

A new series of tetraaza, pentaaza and hexaaza fluoro-boro-bridged macrocyclic nickel(II) complexes, containing methyl and $-CH_3CO$ or $-COOC_2H_5$ as pendants on the macro-ring, have been synthesized. The precursor nitroso complexes are remarkably different in spectral, magnetic and electrochemical behaviour from the respective macrocyclic complexes. The macrocyclic ligands provide a facile electron delocalization, resulting in a weaker ligand field corresponding to the spin crossover region. The precursors and macrocycles undergo two-step one-electron reduction and the redox behaviour depends on macrocyclic effect, ring size and substitutents on the macro-ring apart from the electrostatic interaction of the donor nitrogen atoms.

Syntheses, structures and electrochemical redox properties of macrocyclic metal complexes of tetraaza, pentaaza and hexaaza Me_4cyclopean and Ph_4cyclopean ligands have been described earlier[1,2]. Spectrochemical and electrochemical behaviour of these two cyclopean series of complexes show distinct effect of the substituents on the macro-ring and are remarkably different from the FBOX series of complexes[3].

Though works on adducts appear to be wide-ranging with fluoroboro-bridged macrocyclic complexes[4-10], the study of the effect of substituents on the macro-ring on the physicochemical properties of the cyclops has been limited. The substituents on the tetraaza macrocycles, with rings varying from 12 to 16, and even substituents on naturally occurring macrocycles such as chlorophylls and porphyrins have remarkable effect on their physicochemical properties. The behaviour of the Me_4cyclopeans and Ph_4cyclopeans systems reported earlier from this laboratory has prompted us to study the effect of new substituents in the ring on the physicochemical properties of cyclopean macrocycles. During the course of this study, we have succeeded in isolating two new series of cyclopean ligands and the results of these investigations are reported here.

Intermolecular condensation of nitrite ions with 2,4-pentanedione in the presence of nickel(II) and ammonium acetate was found to give a diamagnetic bright red compound, $Ni(C_5H_7O_2N_2)_2$[11]. The investigations were extended later using diamines and several other metal ions[12,13]. When the reaction was carried out with ethylenediamine, nickel(II) ion, acetylacetone, sodium nitrite, acetic acid and sodium acetate, compound (1) was isolated. Use of propylenediamine in place of ethylenediamine gave a similar quadratically bonded complex. A capped pentacoordinated (structure 2) and an octahedral hexa-coordinated complex (structure 3) have been prepared by us using diethylenetriamine and triethylenetetramine respectively. A new series of nitroso complexes has been isolated following similar reactions involving the amines, ethylacetoacetate, sodium nitrite, acetic acid, sodium acetate and nickel(II) ions, where the carbethoxy groups are introduced as the pendant substituents (4). The nitroso ligands are versatile enough to react with the lewis acid BF_3 producing a new series of

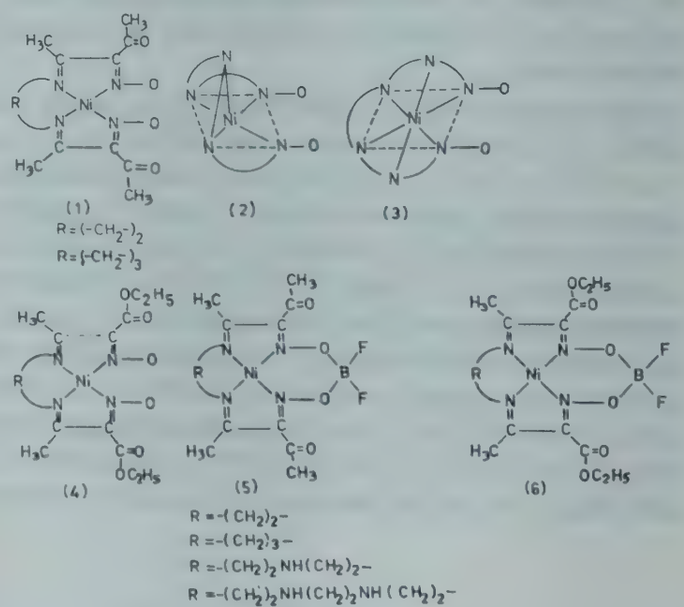

cyclopean macrocyclic complexes. Reactions with silane derivatives are currently being investigated and the results will be communicated in due course to this journal.

The structures of cyclopean nickel(II) complexes prepared now are presented in (5) and (6). The tetraaza Cy^1, Cy^2, Cy^5 and Cy^6 systems are: Cy^1 = 1,1-difluoro-5,10-dimethyl-4,11-diacetyl-1-bora-3,6,9,12-tetraaza-2,13-dioxocyclotrideca-3,5,9,11-tetraene, abbr. $\{Me_2Ac_2[13]N_4O_2BF_2\}^-$, Cy^2 = 1,1-difluoro-5,11-dimethyl-4,12-diacetyl-1-bora-3,6,10,13-tetraaza-2,14-dioxocyclotetradeca-3,5,10,13-tetraene, abbr. $\{Me_2Ac_2[14]N_4O_2BF_2\}^-$, Cy^5 = 1,1-difluoro-5,10-dimethyl-4,11-dicarbethoxy-1-bora-3,6,9,12-tetraaza-2,13-dioxocyclotrideca-3,5,9,11-tetraene, abbr. $\{Me_2(carbethoxy)_2[13]N_4O_2BF_2\}^-$, Cy^6 = 1,1-difluoro-5,11-dimethyl-4,12-dicarbethoxy-1-bora-3,6,10,13-tetraaza-2,14-dioxocyclotetradeca-3,5,10,13-tetraene, abbr. $\{Me_2(carbethoxy)_2[14]N_4O_2BF_2\}^-$. The pentaaza systems are Cy^3 and Cy^7: Cy^3 = 1,1-difluoro-5,13-dimethyl-4,14-diacetyl-1-bora-3,6,9,12,15-pentaaza-2,16-dioxocyclohexadeca-3,5,12,14-tetraene, abbr. $\{Me_2Ac_2[16]N_5O_2BF_2\}^-$, Cy^7 = 1,1-difluoro-5,13-dimethyl-4,14-carbethoxy-1-bora-3,6,9,12,15-pentaaza-2,16-dioxocyclohexadeca-3,5,12,14-tetraene, abbr. $\{Me_2(carbethoxy)_2[16]N_5O_2BF_2\}^-$. The hexaaza systems are Cy^4 and Cy^8: Cy^4 = 1,1-difluoro-5,16-dimethyl-4,17-diacetyl-1-bora-3,6,9,12,15,18-hexaaza-2,19-dioxocyclononandeca-3,5,15,17-tetraene, abbr. $\{Me_2Ac_2[19]N_6O_2BF_2\}^-$, Cy^8 = 1,1-difluoro-5,16-dimethyl-4,17-dicarbethoxy-1-bora-3,6,9,12,15,18-hexaaza-2,19-dioxocyclononandeca-3,5,15,17-tetraene, abbr. $\{Me_2(carbethoxy)_2$-[19]-$N_6O_2BF_2\}^-$. They can act as donors through nitrogen lone pairs with metal ions. They have varying degree of unsaturation and electrophilic character on account of substituents like $-C(=O)-CH_3$ and $-C(=O)-OC_2H_5$ apart from a couple of α-diimine groups, a common feature in the backbone of the cyclopean ligands.

Materials and Methods

Ethylenediamine, propylenediamine, acetylacetone, ethyl acetoacetate, diethylenetriamine, sodium nitrite and boron trifluoride were BDH reagents while triethylenetetramine was a Riedel reagent.

The complexes NiL^{1-8}, where L^1 = N,N′-ethylene-bis-(isonitrosoacetylacetoneimino)nickel(II), L^2 = N,N′-propylene-bis-(isonitrosoacetylacetoneimino)-nickel(II), L^3 = N,N′-diethylenetriamine-bis-(isonitrosoacetylacetoneimino)nickel(II), L^4 = triethylenetetramine-bis-(isonitrosoacetylacetoneimino)nickel (II), L^5 = N,N′-ethylene-bis-(isonitrosoethylacetoacetateimino)nickel(II), L^6 = N,N′-propylene-bis-(isonitrosoethylacetoacetateimino)nickel(II), L^7 = N,N′-diethylenetriamine-bis-(isonitrosoethylacetoacetateimino)nickel(II) and L^8 = N,N′-triethylenetetramine-bis-(isonitrosoethylacetoacetateimino)nickel(II) were prepared following similar procedures. The method adopted for NiL^1 is given below.

N,N′-Ethylene-bis-(isonitrosoacetylacetoneimino)-nickel(II) $Ni(C_{12}H_{16}N_4O_4)$

$Ni(CH_3COO)_2.4H_2O$ (2.5 g, 0.01 mol) dissolved in ethanol was treated with acetylacetone (2.0 g, 0.02 mol), ethylenediamine (0.6 g, 0.01 mol), sodium nitrite (5.0 g) and acetic acid (4 ml) and the mixture was continuously stirred for one hour when fine red crystals were separated. They were filtered, washed with ethanol and ether and dried.

The $(CH_3)_2(CH_3CO)_2$cyclopean complexes were isolated by action of freshly distilled boron trifluoride on the above precursor complexes in the acetonitrile medium. The preparation of $(NiCy^1)BF_4$ is given below.

1,1-*Difluoro*-5,10-*dimethyl*-4,11-*diacetyl*-1-*bora*-3,6,9,12-*tetraaza*-2,13-*dioxocyclotrideca*-3,5,9,11-*tetraenenickel(II)* $Ni[Me_2Ac_2[13]N_4O_2BF_2]BF_4$:

NiL^1 (3.40 g, 0.01 mol) was suspended in acetonitrile; one drop of dilute fluoroboric acid was added to catalyze and enhance the reaction rate. Then boron trifluoride (freshly distilled, 3 ml) was added dropwise while stirring till the red colour transformed to orange. On allowing the solution to stand for three hours, an orange crystalline product was obtained. It was filtered, washed with acetonitrile and dried *in vacuo*.

Me_2(carbethoxy)$_2$cyclopean complexes were prepared by following similar procedures; a typical preparation for one such compound is given here.

1,1-*Difluoro*-5,10-*dimethyl*-4,11-*dicarbethoxy*-1-*bora*-3,6,9,12-*tetraaza*-2,13-*dioxocyclotrideca*-3,5,9,11-*tetraenenickel(II)* $[Ni(Me_2(carbethoxy)_2$-$[13]N_4O_2BF_2]BF_4$:

NiL^5 (4.0 g, 0.01 mol) was suspended in 30 ml of acetonitrile and about 4 ml of boron trifluoride etherate was slowly added while stirring. The stirring was continued for about six hours when the colour of the compound changed from red to yellow. It was left overnight and finally filtered, washed with acetonitrile and dried *in vacuo*.

The analytical data are given in Tables 1 and 2.

Results and Discussion

The nitroso complexes have been obtained by the traditional method using 2,4-pentanedione, a diamine/triamine/tetramine, nickel(II) ion, sodium

Table 1—Analytical Data and Colour of Complexes NiL^{1-8}

Sl. No.	Complexes	Colour	Found (Calc.) %			
			Metal	N	C	H
1	NiL^1 $Ni(C_{12}H_{16}N_4O_4)$	Red	17.32 (17.40)	16.35 (16.51)	42.32 (42.47)	4.54 (4.71)
2	NiL^2 $Ni(C_{13}H_{18}N_4O_4)$	Red	16.62 (16.71)	15.71 (15.86)	44.05 (44.19)	4.98 (5.09)
3	NiL^3 $Ni(C_{14}H_{21}N_5O_4)$	Red	15.36 (15.44)	18.22 (18.32)	43.80 (43.97)	5.34 (5.49)
4	NiL^4 $Ni(C_{16}H_{26}N_6O_4)$	Reddish brown	13.82 (13.88)	19.62 (19.76)	44.98 (45.17)	5.96 (6.11)
5	NiL^5 $Ni(C_{14}H_{20}N_4O_6)$	Red	14.70 (14.78)	13.85 (14.03)	41.98 (42.10)	4.91 (5.01)
6	NiL^6 $Ni(C_{15}H_{22}N_4O_6)$	Red	14.20 (14.28)	13.48 (13.55)	43.36 (43.58)	5.18 (5.32)
7	NiL^7 $Ni(C_{16}H_{25}N_5O_6)$	Orange red	13.26 (13.36)	15.65 (15.83)	43.24 (43.42)	5.48 (5.65)
8	NiL^8 $Ni(C_{18}H_{30}N_6O_6)$	Red	12.02 (12.16)	17.21 (17.31)	44.25 (44.53)	6.05 (6.18)

Table 2—Analytical Data and Colours of the Complexes $[NiCy^{1-8}]BF_4$

Sl No.	Complexes	Colour	Found (Calc.) %			
			Metal	N	C	H
1	$[NiCy^1]BF_4$ $Ni(C_{12}H_{16}N_4O_4B_2F_6)$	Orange	12.30 (12.42)	11.62 (11.78)	30.12 (30.31)	3.22 (3.36)
2	$[NiCy^2]BF_4$ $Ni(C_{13}H_{18}N_4O_4B_2F_6)$	Yellow	11.98 (12.06)	11.34 (11.45)	31.74 (31.90)	3.52 (3.68)
3	$[NiCy^3]BF_4$ $Ni(C_{14}H_{21}N_5O_4B_2F_6)$	Orange yellow	11.30 (11.38)	13.36 (13.51)	32.28 (32.43)	3.92 (4.05)
4	$[NiCy^4]BF_4$ $Ni(C_{16}H_{26}N_6O_4B_2F_6)$	Orange yellow	10.42 (10.51)	14.78 (14.97)	34.08 (34.22)	4.48 (4.63)
5	$[NiCy^5]BF_4$ $Ni(C_{14}H_{20}N_4O_6B_2F_6)$	Yellow	10.86 (11.02)	10.30 (10.46)	31.20 (31.40)	3.52 (3.73)
6	$[NiCy^6]BF_4$ $Ni(C_{15}H_{22}N_4O_6B_2F_6)$	Yellow	10.64 (10.74)	10.02 (10.20)	32.52 (32.78)	3.86 (4.00)
7	$[NiCy^7]BF_4$ $Ni(C_{16}H_{25}N_5O_6B_2F_6)$	Yellow	10.12 (10.20)	11.96 (12.11)	33.10 (33.21)	4.28 (4.32)
8	$[NiCy^8]BF_4$ $Ni(C_{18}H_{30}N_6O_6B_2F_6)$	Orange yellow	9.48 (9.50)	13.44 (13.52)	34.56 (34.78)	4.78 (4.83)

nitrite and acetic acid. As the reaction proceeds, the green colour of the solution gradually changes and a bright red precipitate progressively appears. The reaction is almost complete in about an hour in the case of diamines; however, in the case of tri- and tetramines it takes about 10-12 hr. The complexes are obtained in about 60-80% yield and are diamagnetic.

The diamagnetic red complexes react with boron trifluoride in methyl cyanide medium. Gradual change in colour occurs and finally an yellow or orange yellow product is obtained. From analytical and physical data it is seen that the reaction is consistent with equation 1.

$$NiL + 2BF_3 \rightarrow [NiCyBF_2]^+BF_4^- \quad \ldots (1)$$

The complexes possess anomalous magnetic properties, but the ligand field spectra correspond to those expected for such behaviour.

IR Spectra

We have recorded the spectral and magnetic data for the complexes N,N′-ethylene-bis-(isonitrosoacetylacetoneimino)nickel(II) [1] and our results closely resemble the results reported by earlier workers[12,14]. The structurally important IR bands pertain to $\nu C=O$, $\nu C=N$, and $\nu N-O$ vibrations. The dimethyl, diacetyl cyclopean complexes show a strong band at ~1700 cm^{-1} and the dimethyl, dicarbethoxy cyclopeans at ~1750 cm^{-1} which has been assigned to the free carbonyl groups. The $\nu C=N$ band in N,N′-ethylene-bis-(isonitroso-

acetylacetoneimino)nickel(II) and N,N′-propylene-bis-(isonitrosoacetylacetoneimino)nickel(II) is observed below 1600 cm^{-1} (ref. 15).

Bands near 1160 cm^{-1} have been attributed to N–O stretching vibrations. Coordination of isonitroso groups through nitrogen is considered to increase the N–O frequency and in many nitrogen coordinated multidentate isonitroso complexes, the N–O frequency occurs around 1250-1150 cm^{-1} (refs. 16-18).

The IR spectra of N,N′-diethylenetriamine-bis-(isonitrosoacetylacetoneimino)nickel(II) and N,N′-triethylenetetramine-bis-(isonitrosoacetylacetoneimino) nickel(II) complexes and the corresponding bis-(isonitrosoethylacetoacetateimino)nickel(II) complexes possess a few additional bands which are observed near 3315 and 1320 cm^{-1}, the former band is attributed to the stretching vibrations of secondary NH groups and the latter band has been assigned to νC–N vibrations.

The dimethyl, diacetyl cyclopean complexes and the dimethyl, dicarbethoxy cyclopean complexes, the products of interàction of boron trifluoride with the parent metal complexes of the nitroso ligands, NiL^{1-8} in methyl cyanide medium, show several new bands apart from the νC=O, νC=N and νN–O frequencies in their respective regions. The bands occurring at 1020 and 795 cm^{-1} have been identified from their characteristic features to be ν(B–F) and ν(B–O) vibrations, respectively. These spectral features unambiguously manifest that the oximato oxygen atoms act as nucleophilic groups and react with boron trifluoride according to the Scheme 1, finally yielding the macrocyclic structures presented in [5 and 6]. In the reaction process the oximato group is first bonded on account of donor-acceptor bond formation with the lewis acid BF_3, forming an intermediate product which is subsequently subjected to another nucleophilic attack from the adjacent oximato group displacing a halogen atom as the halide ion and completing the cyclization. The displaced halide ion reacts with boron trifluoride to form fluoroborate ion and is accommodated in the outer sphere.

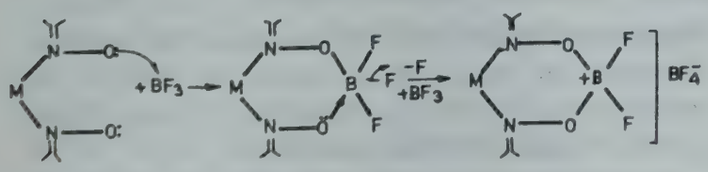

Scheme 1

These observations lead us to suggest the structure and mode of bonding in these complexes as presented in [5 and 6] which show that the

$(O=\overset{\downarrow}{C}-CH_3)$ and carbethoxy $(-COOC_2H_5)$ groups are pendants on the macrocyclic rings.

Electronic spectra

The diamagnetic isonitroso complexes show a ligand field band around 22,000 cm^{-1} which would normally suggest that the coordination environment around the metal ion is square-planar. However, the polarographic data which are discussed below exhibit two-step one-electron reduction processes. The mode of reduction from tetraaza to hexaaza series of ligands follows a parallel pattern as has been observed for Me_4cyclopeans and Ph_4cyclopeans, i.e., going from tetraaza to pentaaza and hexaaza the reduction wave becomes more cathodic in character. This picture is consistent with the capped five-coordinated structure for N,N′-diethylene-triamine-bis-(isonitrosoacetylacetoneimino)nickel(II) complex and N,N′-diethylenetrimine-bis-(isonitrosoethylacetoacetateimino)nickel(II) complex and octahedral hexacoordinated structure for N,N′-triethylenetetramine-bis-(isonitrosoethylacetoacetateimino)nickel(II) complexes. However, the axial nitrogen coordination is not strong enough for spin cross-over to occur for the penta- and hexa-coordinated complexes from spin singlet to lower energy triplet states.

In contrast to parent nitroso complexes, the dimethyl, diacetyl cyclopean and dimethyl, dicarbethoxy cyclopean ligands of nickel(II) are magnetically subnormal and the magnetic moments at the ambient temperatures have been observed in the range 1.8 to 2.4 B.M. The electronic spectra of these complexes show distinct features which can be satisfactorily explained on the basis of structures where nickel(II) ions occur in spin-singlet and spin-triplet equilibrium[19].

The present series of complexes show ligand field transitions at 9000, 17000, 22000 and 27000 cm^{-1} respectively. The new features in lower frequency and high frequency regions, in sharp contrast to a single ligand field band at 22,000 cm^{-1} for isonitroso complexes, are attributes of nickel(II) ions in spin-singlet and spin-triplet ground terms coexisting together. The first two bands at 9,000 and 17,000 cm^{-1} are attributed to transitions $^3A_{2g} \rightarrow {}^3T_{1g}(F)$ and $^3A_{2g} \rightarrow {}^3T_{2g}(F)$ under octahedral ligand field of the nickel ion. The highest frequency band at 27,000 cm^{-1} is attributed to the transition $^3A_{2g} \rightarrow {}^3T_{1g}(P)$ while the band at 22,000 cm^{-1} originates from the spin-singlet to singlet transition $^1A_{1g} \rightarrow {}^1A_{2g}$ under

square planar field. The results manifest that cyclization with BF_3 of the oxygen atoms of nitroso groups leads to creation of ligand fields around the metal ion that are in the spin cross-over region and the singlet-triplet equilibrium occurs.

Electrochemical studies

Majority of the tetraaza nickel(II) macrocyclic complexes undergo one electron reduction; however, the products obtained occur in different states. An examination of the results shows two extreme cases. Ligands with α-diimine groups, on electrochemical reduction, give nickel(II)-ligand radical anion species as shown by EPR studies. On the other hand, with nonconjugated ligands, the reduced products contain Ni(I) complexes. In a recent report[20], a fluoro-boro cyclopean complex has been reported to give one electron reduction product; EPR spectrum has two signals, one attributable to Ni(I) at $g=2.133$ and second at $g=2.048$ assignable to a nickel(II)-ligand radical anion species.

There are examples of nickel(II) macrocyclic complexes[21] which show two reversible one-electron reduction waves near $E_{\frac{1}{2}}^1 = -1.0$ V and $E_{\frac{1}{2}}^2 = -1.55$ V. From ESR studies the reduced species have been found to correspond to the formation of $[Ni^{II}(L^{\cdot -})]^+$ and $[Ni^{I}(L^{\cdot -})]^0$, respectively. Such macrocycles possess structures with diimino groups, behaving as good π-acceptors and possess energetically favourable low-lying π-orbitals.

The electrochemical data for the present series of cyclopean ligands together with those for the open chain precursor molecules are reported in Table 3. The macrocyclic complexes undergo two reversible or quasireversible reductions in DMF:water medium (80:20) at $\mu = 0.1$ *M* (sodium perchlorate), and, as in the earlier cases, the redox processes are diffusion-controlled and each of the redox step corresponds to transfer of one electron. It has been reported earlier that the Me_4- and Ph_4-cyclopeans and their precursors are characterised by a one electron redox wave[1,2].

The effect of ligand structure on the thermodynamic parameters $E_{\frac{1}{2}}$ for the redox processes of the macrocycles and their open chain analogues is shown in Figs 1 and 2 and for the Me_4- and Ph_4-cyclops in Fig. 3. The $E_{\frac{1}{2}}$ values are plotted against ligand atomicity (i.e., the number of C,N,O and B atoms present in the chain of the precursors and in the macrocycles) and coordination number (given in parentheses). The plots clearly indicate the effect of cyclisation, role of electron donating and withdrawing ability of the substituents on the ligands as well as on the macro-rings,

Table 3—Polarographic Data of the Complexes NiL^{1-8} in Aqueous DMF

Complexes	$-E_{\frac{1}{2}}^1$(V)	Slope^{-1} (mV)	$-E_{\frac{1}{2}}^2$(V)	Slope^{-1} (mV)
NiL^1	0.820	80	1.350	88
NiL^2	0.88	86	1.50	76
NiL^3	0.905	78	1.55	88
NiL^4	0.935	85	1.62	76
NiL^5	0.850	86	1.420	70
NiL^6	0.895	88	1.525	86
NiL^7	0.920	75	1.60	84
NiL^8	0.955	70	1.63	86
$[NiCy^1]BF_4$	0.785	75	1.10	88
$[NiCy^2]BF_4$	0.840	80	1.150	86
$[NiCy^3]BF_4$	0.875	90	1.300	90
$[NiCy^4]BF_4$	0.880	84	1.366	90
$[NiCy^5]BF_4$	0.795	96	1.320	94
$[NiCy^6]BF_4$	0.855	92	1.350	98
$[NiCy^7]BF_4$	0.892	95	1.56	96
$[NiCy^8]BF_4$	0.90	98	1.60	96

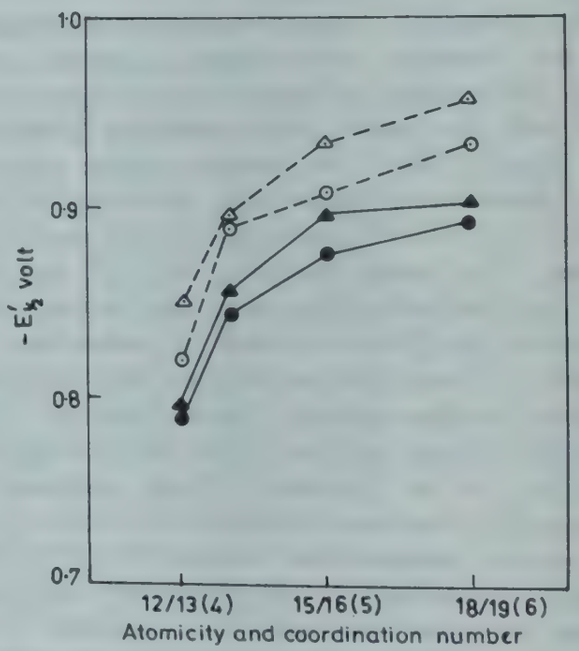

Fig. 1—Plot of $E_{\frac{1}{2}}$[$NiMe_2(CH_3CO)_2$cyclopean and $NiMe_2(O-C-C_2H_5)_2$cyclopean] values for the open chain and macrocyclic complexes vs. ligand atomicity (number of carbon, nitrogen, oxygen and boron atoms in the chain or ring) [$Me_2(CH_3CO)_2$cyclopean: open chain $-\odot-\odot-\odot-$; macrocycle $-\bullet-\bullet-\bullet-$; $Me_2(O-C-C_2H_5)_2$cyclopean: open chain $-\triangle-\triangle-\triangle-$, macrocycle $-\blacktriangle-\blacktriangle-\blacktriangle-$]

electrostatic interaction of the donor nitrogen atoms with the metal ion, coordination number and the electron delocalizing influence of the α-diimine groups coupled with the substituents.

An increase in coordination number of the metal ion though coordination with strong nucleophilic secondary amine groups shifts the $E_{\frac{1}{2}}$ values towards a higher cathodic region. The $E_{\frac{1}{2}}$ values manifest the propensity of the macrocyclic effect.

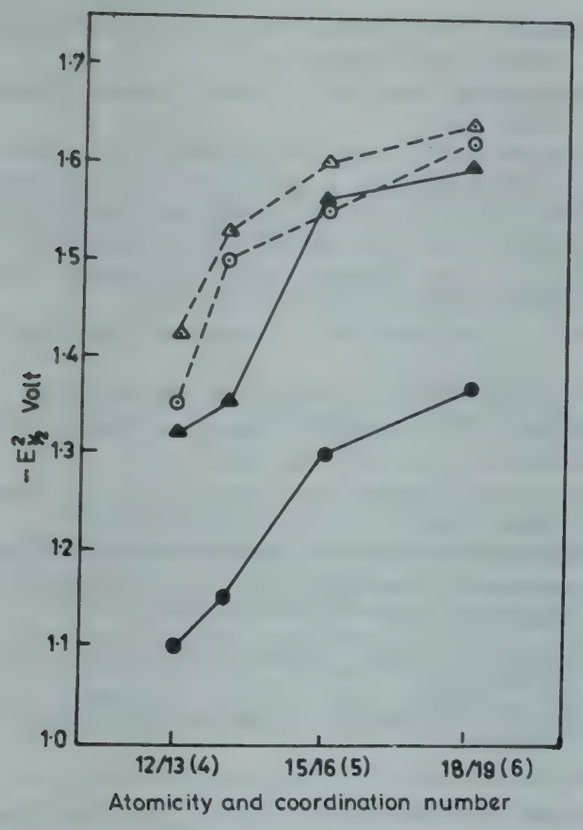

Fig. 2—Plot of $E^{2}_{\frac{1}{2}}$[$NiMe_2(CH_3CO)_2$cyclopean and $NiMe_2(O-\overset{O}{\overset{\|}{C}}-C_2H_5)_2$cyclopean] values for the open chain and macrocyclic complexes vs. ligand atomicity (number of carbon, nitrogen, oxygen and boron atom in the chain or ring) [$Me_2(CH_3CO)_2$cyclopean: open chain $-\odot-\odot-\odot-$, macrocycle $-\bullet-\bullet-\bullet-$; $Me_2(O-\overset{O}{\overset{\|}{C}}-C_2H_5)_2$cyclopean: open chain $-\triangle-\triangle-\triangle-$, macrocycle $-\blacktriangle-\blacktriangle-\blacktriangle-$]

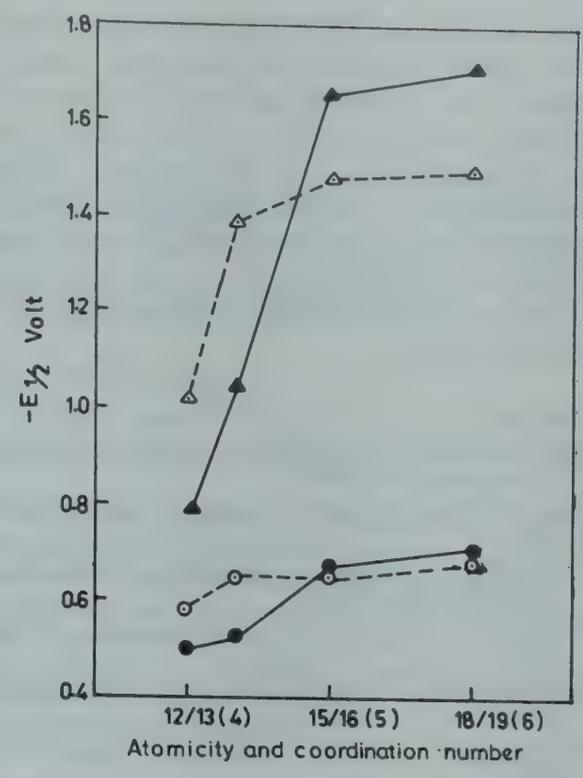

Fig. 3—Plot of $E_{\frac{1}{2}}$ ($NiMe_4$cyclopean & $NiPh_4$cyclopean) values for the open chain and macrocyclic complexes vs. ligand atomicity (number of carbon, nitrogen, oxygen and boron atoms in the chain or ring) [Me_4cyclopean: open chain $-\triangle-\triangle-\triangle-$, macrocycle $-\blacktriangle-\blacktriangle-\blacktriangle-$; Ph_4cyclopean: open chain $-\odot-\odot-\odot-$, macrocycle $-\bullet-\bullet-\bullet-$]

The reduction processes for the macrocyclic complexes with BF_2 bridgeheads are more facile and occur at more anodic potentials than those for the respective noncyclic parent complexes, with the exceptions of pentaaza and hexaaza Me_4- and Ph_4-cyclopeans. However, these distinctive features of the ligand field effect, are influenced by the substituents on the ligand systems to some degree, on account of their electrophilic character that directly affects the electron density on the metal atom.

For the complexes (either open chain or macrocycles) with constant atomicity and coordination number, the $E_{\frac{1}{2}}$ values for the first redox wave are in the order: $-(CH_3)_4 > (CH_3)_2\ (C_2H_5-O-\overset{O}{\overset{\|}{C}}-)_2 > (CH_3)_2(CH_3-\overset{O}{\overset{\|}{C}}-)_2 > (-C_6H_5)_4$ cyclops. The positions of methyl, carbethoxy and acetyl substituents are consistent with their relative electrophilic character and are in the order of their respective Taft constants or Hammett substitution constants[22-24], but the position of phenyl group is rather atypical. This atypical behaviour of Ph_4cyclops seems to arise on account of the presence of a quartet of phenyl groups in conjugation with α-diimines that enhance the charge delocalization over a wider ligand frame.

The polarographic results can be interpreted in terms of two pathways. According to path 1 the first wave in the range -0.82 to -0.95 V and -0.78 to -0.90 V for the precursors and macrocyclic complexes, respectively, gives the metal-stabilized ligand radical species.

Path I: $[Ni^{II}L]^+ + e \rightleftharpoons [Ni^{I}(L^{\cdot -})]^0$

A nickel(I) species is formed in the second step of the redox process,

$[Ni^{II}(L^{\cdot -})]^0 + e \rightleftharpoons [Ni^{I}(L^{\cdot})]^0$

The latter step might be associated with the formation of a ligand dianion radical followed by intramolecular ligand to metal electron transfer. In the second pathway, we attribute the successive waves to be due to metal centred reduction processes,

Path II: $[Ni^{II}L]^+ + e \rightleftharpoons [Ni^{I}L]^+ + e \rightleftharpoons [Ni^{O}L]^+$

From a careful comparison of the electrochemical data of several macrocyclic complexes containing α-diimine and β-diimine groups, it appears that the redox mechanism may be depicted by path I rather than path II. In the first step of reduction the electron resides on the unsaturated part of the macrocyclic ligand. This conclusion is pronounced from the observations that $\Delta E_{\frac{1}{2}} (= E^1_{\frac{1}{2}} - E^2_{\frac{1}{2}})$ values for different complex species are variable and are ligand-dependent.

References

1 Sahoo Bhagirathi, Chakrabarty J & Sahoo B, *Indian J Chem*, **23A** (1984) 209.

2 Sahoo Bhagirathi & Sahoo B, *Indian J Chem*, **22A** (1983) 560.

3 Chakrabarty J, Naik Kunja B, Singh K L & Sahoo B, *Indian J Chem*, **22A** (1983) 35.

4 Anderson O P & Marshall J C, *Inrog Chem*, **17** (1978) 1258.

5 Anderson O P & Packard A B, *Inorg Chem*, **18** (1979) 1940.

6 Anderson O P & Packard A B, *Inorg Chem*, **18** (1979) 3064.

7 Anderson O P & Packard A B, *Inorg Chem*, **19** (1980) 2123.

8 Anderson O P & Packard A B, *Inorg Chem*, **19** (1980) 2941.

9 Addison A W, Carpenter M, Lau L K M & Wicholas M, *Inorg Chem*, **17** (1978) 1545.

10 Shankar Ravi, Rout A K & Sahoo B, *Indian J Chem*, **26A** (1987) 156.

11 Djordjevic C D, Lewis J & Nyholm R S, *J chem .Soc*, (1962) 4778.

12 Bose K .S & Patel C C, *J inorg nucl Chem*, **33** (1971) 2947.

13 Ablov A V & Zubarev V N, *Russ J inorg Chem*, **13** (1968) 1563.

14 Patel N J & Halder B C, *J inorg nucl Chem*, **29** (1967) 1037.

15 Ueno K & Martell A E, *J phys Chem*, **59** (1955) 998.

16 Burger K, Ruff I & Ruff F, *J inorg nucl Chem*, **27** (1965) 179.

17 Krause R A, Colthup N B & Busch D H, *J phys Chem*, **65** (1961) 2216.

18 Kalia K C & Chakravorty A, *Inorg Chem*, **7** (1978) 2016.

19 Chakrabarty J, Naik Kunja B & Sahoo B, *Indian J Chem*, **21A** (1982) 370.

20 Gagne R R & Spiro Clifford L, *J Am chem Soc*, **102** (1980) 1444.

21 Lewis J & Schröder M, *J chem Soc Dalton Trans*, (1982) 1085.

22 Riley D P & Busch D H, *Inorg Synth*, **VIII** (1978) 36.

23 Streeky J A, Pillsbury D G & Busch D H, *Inorg Chem*, **19** (1980) 3148.

24 Hine J, *Physical Organic Chemistry* 2nd edition (McGraw Hill Book Company Inc., New York), 1962, 92-102.

Indian Journal of Chemistry
Vol. 27A, August 1988, pp. 687-690

Studies on Potential Antibacterial & Chelating Agents: Part IV—Synthesis, Formation Constants & Biological Activity of Co(II), Ni(II), Cu(II) & Zn(II) Metal Chelates with Some Sulphonamidobenzimidazoles†

M M NANDI*, (Smt) R RAY & (Smt) J CHOUDHURY
Inorganic Chemistry Laboratory, Tripura University, Agartala 799 004

Received 25 *May* 1987; *revised* 29 *September* 1987; *rerevised and accepted* 21 *December* 1987

Complex formation of Co(II), Ni(II), Cu(II) and Zn(II) with 2-benzenesulphonamidomethylbenzimidazole ($R_m^{bs}H$), 2-(α-benzenesulphonamido)ethylbenzimidazole ($R_{e\alpha}^{bs}H$) and 2-(β-benzenesulphonamido)ethylbenzimidazole ($R_{e\beta}^{bs}H$) in water-acetone (1:1) at $\mu = 0.25$ and at the temperature 20° ± 0.5° has been studied potentiometrically. Formation of 1:1 and 1:2 complexes has been indicated. The successive formation constants K_1 and K_2 have been determined by Irving and Rossotti method. The stabilities follow Irving-Williams order. The basicities of the ligands follow the order $R_m^{bs}H_2^+ < R_{e\alpha}^{bs}H_2^+ < R_{e\beta}^{bs}H_2^+$. However, $R_{e\alpha}^{bs}H_2^+$ forms weakest complexes probably due to steric effect of methyl group. All 1:2 chelates and some mixed ligand complexes using 1-benzenesulphonamido-1,2-bis(2′-benzimidazolyl)ethane have been synthesised and characterised. Biological activity of the metal chelates has been also studied.

In continuation of our work on synthesis[1-4], complexation behaviour[5-9] and biological activity[3,4,9] of some benzimidazole derivatives, we have now studied the complexation behaviour of 2-benzenesulphonamidomethylbenzimidazole ($R_m^{bs}H$), 2-(α-benzenesulphonamido)ethylbenzimidazole ($R_{e\alpha}^{bs}H$), 2-(β-benzenesulphonamido)ethylbenzimidazole ($R_{e\beta}^{bs}H$) and 1-benzenesulphonamido-1,2-bis(2′-benzimidazolyl) ethane ($R_{pb}^{bs}H$). Co(II), Ni(II) and Cu(II) complexes of $R_m^{bs}H$ and $R_{e\beta}^{bs}H$ have been reported[10,11]. But their biological activity has not been studied. Recently, we have reported[9] the synthesis, physicochemical properties and biological activity of Co(II), Ni(II) and Cu(II) complexes of the corresponding benzamidobenzimidazoles.

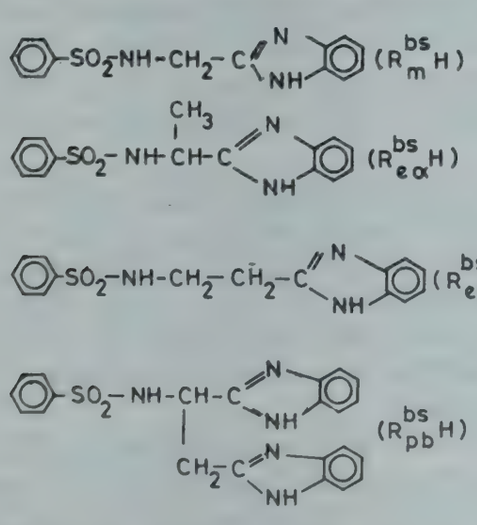

†Abstracted in the proceedings of the Third International Conference on Bioinorganic Chemistry held at Noordwjkerhout, Netherlands, July 1987.

Materials and Methods

The ligands $R_m^{bs}H$, $R_{e\beta}^{bs}H$ and $R_{pb}^{bs}H$ were prepared by condensing benzenesulphonyl derivatives of glycine, β-alanine and L-(−)-aspartic acid with *o*-phenylenediamine following Phillips[13] and fusion[14] methods as described earlier[1,15]. $R_{e\alpha}^{bs}H$ was also synthesised following similar procedure by the fusion method. The compounds were recrystallised from aqueous ethanol and used after drying at 110°. Sodium salts of the ligands were prepared by mixing their ethanol solutions with one equivalent of NaOH followed by evaporation. All other reagents were either of AR quality or were properly purified. The solutions were made in doubly distilled CO_2-free water and purified acetone[16].

The *p*H measurements were made with a Systronics *p*H meter having a glass electrode (1-13 *p*H range) in conjunction with a saturated calomel electrode connected by means of an agar-2*M* $NaNO_3$ bridge. The *p*H meter was calibrated with sodium hydrogen phthalate and borax-buffer solutions in water taking due temperature correction. The following solutions (volume 50 ml) were titrated potentiometrically in water-acetone (1:1) at 20° ± 0.5° and $\mu = 0.25$ ($NaClO_4$) against 0.150 *M* NaOH solution:

(a) 0.01 *M* $HClO_4$, (b) 0.01 *M* $HClO_4$ + 0.02 *M* RH_2ClO_4, (c) 0.01 *M* $HClO_4$ + 0.005 *M* $M(ClO_4)_2$ + 0.02 *M* RH_2ClO_4, (d) 0.01 *M* $HClO_4$ + 0.003 *M* $M(ClO_4)_2$ + 0.02 *M* RH_2ClO_4.

The ligand perchlorates were obtained *in situ* by mixing quantitatively RH and $HClO_4$ in molar ratio 1:1. IR spectra were recorded on a Perkin-Elmer spectrophotometer model 577 in the range 4000-

200 cm^{-1} using KBr pellets. The diffuse reflectance spectra were recorded on a Beckman 5270 spectrophotometer. Magnetic measurements were carried out at 302 K using a standard Gouy balance. Satisfactory analytical data were obtained for the metal chelates.

Preparation of Co(II) complexes

$Co(R^{bs}_{e\alpha})_2.H_2O$—A mixture of cobalt(II) chloride hexahydrate (0.003 mol) and ligand (0.006 mol) in 50 ml aqueous ethanol was warmed on a water bath. Dilute ammonia was added to adjust the *p*H to ~ 7. A violet coloured compound separated, which was filtered and washed with ethanol and air-dried.

$Co(R^{bs}_m)_2$ and $Co(R^{bs}_{e\beta})_2$—These were prepared as reported earlier[10,11].

Preparation of Ni(II) complexes

$Ni(R^{bs}_{e\alpha})_2.2H_2O$—Nickel(II) chloride hexahydrate (0.003 mol) and ligand (0.006 mol) were dissolved in 75 ml hot aqueous ethanol and *p*H was adjusted to ~ 7 by dilute ammonia. On keeping overnight, a dull red coloured compound separated. It was filtered, washed with ethanol and air-dried.

$Ni(R^{bs}_m)_2$ and $Ni(R^{bs}_{e\beta})_2$—These were prepared as reported earlier[10,11].

Preparation of Cu(II) complexes

$Cu(R^{bs}_{e\alpha})_2.3H_2O$—Cupric chloride dihydrate (0.003 mol) and ligand (0.006 mol) were dissolved in 70 ml warm acetone. Diluted ammonia was added to raise the *p*H to ~ 7 and contents were kept overnight. Blue crystals separated, which were filtered, washed with acetone and air-dried.

$Cu(R^{bs}_m)_2.H_2O$ and $Cu(R^{bs}_{e\beta})_2$—These were prepared as reported earlier[10,11].

Preparation of Zn(II) complexes

$Zn(R^{bs}_m)_2.2H_2O$, $Zn(R^{bs}_{e\alpha})_2.2H_2O$ and $Zn(R^{bs}_{e\beta})_2.H_2O$

Zinc(II) perchlorate (0.003 mol) and ligand (0.006 mol) were dissolved in 50 ml aqueous acetone. Dilute ammonia was added to raise the *p*H to ~ 7 and contents were kept overnight. White crystals separated. These were filtered, washed with acetone and air-dried.

Preparation of mixed ligand chelates:

$Cu(R^{bs}_{pb})(R^{bs}_m).3H_2O$, $Cu(R^{bs}_{pb})((R^{bs}_{e\alpha}).H_2O$ and $Cu(R^{bs}_{pb})(R^{bs}_{e\beta}).3H_2O$

$Cu(R^{bs}_{pb})Cl.H_2O$[17] (0.002 mol) and calculated amount of $R^{bs}_m H$, $R^{bs}_{e\alpha} H$ or $R^{bs}_{e\beta} H$ were mixed in 30 ml ethanol and refluxed on a water bath for 1 hr when a deep green solution was obtained. *p*H of the solution was adjusted to ~ 7 by adding a few drops of dilute ammonia solution in warm condition. $Cu(R^{bs}_{pb})(R^{bs}_{e\alpha}).3H_2O$ separated as green crystalline solid immediately whereas the other two green compounds were obtained on keeping the solution overnight. These were filtered, washed with ethanol and air-dried.

$Co(R^{bs}_{pb})(R^{bs}_m).2H_2O$, $Co(R^{bs}_{pb})(R^{bs}_{e\alpha}).2H_2O$ and $Co(R^{bs}_{pb})(R^{bs}_{e\beta}).3H_2O$

$Co(R^{bs}_{pb})(OH)$[9] (0.001 mol) and calculated amount of ligand were mixed in 30 ml ethanol and refluxed on a water-bath for 1 hr when a violet solution was obtained. It was filtered and violet complexes were obtained on slow evaporation. These were recrystallised from ethanol and collected.

Results and Discussion

The stepwise formation of the complexes of $R^{bs}_m H_2^+$, $R^{bs}_{e\alpha} H_2^+$ and $R^{bs}_{e\beta} H_2^+$ (RH_2^+) with Co(II), Ni(II), Cu(II), and Zn(II) ions may be represented as,

$$M^{2+} + RH_2^+ \rightleftharpoons M(R)^+ + 2H^+ \quad \ldots (1)$$

$$M(R^+) + RH_2^+ \rightleftharpoons M(R)_2 + 2H^+ \quad \ldots (2)$$

The stepwise formation constants have been evaluated following Irving-Williams technique[12] (Table 1). Formation of 1:1 and 1:2 complexes is indicated. The 1:2 complexes have been isolated in the solid state and characterised. The overall stability of the complexes has been found to follow Irving-Williams order, i.e., Co(II) < Ni(II) < Cu(II) > Zn(II). The basicities of the ligands follow the order: $R^{bs}_m H_2^+ < R^{bs}_{e\alpha} H_2^+ < R^{bs}_{e\beta} H_2^+$. However, the stability order of the complexes with respect to ligands is: $R^{bs}_{e\alpha} H_2^+ < R^{bs}_m H_2^+ < R^{bs}_{e\beta} H_2^+$. The formation of weak complexes by $R^{bs}_{e\alpha} H_2^+$ than those formed by $R^{bs}_m H_2^+$ is due to steric effect in the former. Similar studies with corresponding benzamidobenzimidazoles suggest very weak interaction with the metals and precipitation occurs at the early stages of titration. There was no indication of deprotonation of $-CO-NH-$ hydrogen atom up to *p*H ~ 11.0 in the absence of metal ion.

Benzamidobenzimidazoles are more basic than sulphonamidobenzimidazoles due to more electron-attracting inductive effect of C_6H_5-SO_2-group.

All 1:2 complexes of Co(II), Ni(II), Cu(II) and Zn(II) have been isolated and characterised on the basis of magnetic data, elemental analysis, IR and electronic spectra.

Co(II), Ni(II) and Cu(II) complexes of $R^{bs}_m H$ and $R^{bs}_{e\beta} H$ have already been characterised[10,11]. Magnetic moments of Cu(II) complexes (1.91-2.2 BM) are in the expected region[18]. Reflectance spectra show bands in the region 600-690 nm indicating distorted octahedral geometry[19].

Table 1—Formation Constants of Metal(II) Chelates

Metal ion	$R_m^{bs}H_2^+$		$R_{e\alpha}^{bs}H_2^+$		$R_{e\beta}^{bs}H_2^+$	
	log K_1	log K_2	log K_1	log K_2	log K_1	log K_2
Co(II)	6.57 ± 0.04	5.55 ± 0.04	6.05 ± 0.04	4.75 ± 0.04	7.72 ± 0.04	5.75 ± 0.04
	*± 0.015		*± 0.022		*± 0.022	
	†0.05 < $\bar{n}$ < 1.65		†0.05 < $\bar{n}$ < 1.65		†0.10 < $\bar{n}$ < 1.72	
Ni(II)	6.80 ± 0.04	5.62 ± 0.04	6.22 ± 0.03	4.95 ± 0.03	8.25 ± 0.04	6.01 ± 0.04
	*± 0.026		*± 0.016		*± 0.024	
	†0.15 < $\bar{n}$ < 1.71		†0.05 < $\bar{n}$ < 1.80		†0.10 < $\bar{n}$ < 1.80	
Cu(II)	9.25 ± 0.03	—	8.82 ± 0.03	—	9.87 ± 0.03	6.62 ± 0.03
	*± 0.019		*± 0.014		*± 0.019	
	†0.10 < $\bar{n}$ < 0.90		†0.05 < $\bar{n}$ < 0.9		†0.10 < $\bar{n}$ < 1.75	
Zn(II)	8.12 ± 0.04	—	7.71 ± 0.04	6.31 ± 0.04	9.41 ± 0.04	6.50 ± 0.04
	*± 0.017		*± 0.019		*± 0.023	
	†0.05 < $\bar{n}$ < 0.90		†0.10 < $\bar{n}$ < 1.65		†0.05 < $\bar{n}$ < 1.70	
	pK_1^*	pK_2^*	pK_1^*	pK_2^*	pK_1^*	pK_2^*
	11.60 ± 0.01	4.72 ± 0.01	11.81 ± 0.03	4.78 ± 0.03	12.55 ± 0.02	5.60 ± 0.02
	*± 0.004		*± 0.007		*± 0.006	
	†0.10 < $\bar{n}_H$ < 1.90		†0.10 < $\bar{n}_H$ < 1.94		†0.10 < $\bar{n}_H$ < 1.94	
	—	4.75 ± 0.03	—	4.87 ± 0.02	—	5.65 ± 0.02
	*± 0.012		*± 0.010		*± 0.010	
	†1.0 < $\bar{n}_H$ < 1.99		†1.0 < $\bar{n}_H$ < 1.99		†1.0 < $\bar{n}_H$ < 1.99	

Values in the last set are due to corresponding benzamidobenzimidazoles.
*Standard deviation.
†Range

$Ni(R_m^{bs})_2$ and $Ni(R_{e\beta}^{bs})_2$ possess octahedral stereochemistry[10,11] in which benzimidazole nucleus may act as a bidentate ligand by intermolecular interaction[20]. Magnetic moment value of $Ni(R_{e\alpha}^{bs})_2.H_2O$ (2.8 BM) suggests octahedral stereochemistry. Reflectance spectrum of $Ni(R_{e\alpha}^{bs})_2.H_2O$ shows bands at 400, 490, 560 nm; and 740 and 835 nm. These bands in an octahedral field may be assigned to $^3A_{2g}(F) \rightarrow {}^3T_{1g}(P)$; $^3A_{2g}(F) \rightarrow {}^3T_{1g}(F)$ (split) and $^3A_{2g} \rightarrow {}^3T_{2g}(F)$ (split) transitions respectively.

$Co(R_m^{bs})_2$ and $Co(R_{e\beta}^{bs})_2$ possess octahedral stereochemistry[10,11]. Magnetic moments of $Co(R_{e\alpha}^{bs})_2.H_2O$ and other mixed ligand Co(II) complexes (4.23-4.33 BM) are slightly lower than those usually observed for spin-free octahedral complexes which may be due to the presence of some Co(III) complexes[6,21]. Reflectance spectra give three bands in the regions 1110-1160, 560-580, and 470-505 nm due to $^4T_{1g}(F) \rightarrow {}^4T_{2g}(F)$, $^4T_{1g}(F) \rightarrow {}^4A_{2g}(F)$ and $^4T_{1g}(F) \rightarrow {}^4T_{1g}(P)$ transitions respectively, characteristic of octahedral geometry[22].

Deprotonation of $-SO_2-NH-$ proton has been assumed while representing the interaction of the RH_2^+ with metal ions. The IR spectral data show shift in $-SO_2-N\langle$ stretching frequency (band II) from 1338-1380 cm^{-1} in the ligands to 1250-1280 cm^{-1} in the complexes due to deprotonation of $-SO_2-NH-$ proton. Sodium salts of these ligands show the corresponding band in the intermediate region (1300-1330 cm^{-1}) confirming the deprotonation during complexation. Greater shift in the complexes is due to coordination of the nitrogen with the metals. A slight shift in $-SO_2-N\langle$ stretching frequency (band I) from 1160-1164 cm^{-1} in the ligands to 1150-1160 in the sodium salts and to 1130-1150 cm^{-1} in the complexes is also observed. Shift of $\nu C=N$ is also observed on complex formation along with that in heterocyclic breathing modes. These may be regarded as evidences of bonding of nitrogen of $-SO_2-N\langle$ as well as basic nitrogen (tertiary one) in the imidazole ring to metal[6,10,11]. All Co(II), Ni(II) and Cu(II) complexes are octahedral in nature but there is a possibility of intermolecular interaction through O atom of $-SO_2-N\langle$ group[10] or bidentate mode of bonding of benzimidazole nucleus[20].

Biological activity

Antibacterial screening of these ligands and their metal chelates against three microorganisms, viz., *Escherichia coli, Staphylococcus aureus* and *Bacillus megaterium*, was carried out employing agar-

Table 2—Antibacterial Screening of the Metal Chelates

Species	Inhibition zone (in mm)		
	E. coli	*S. aureus*	*B. megaterium*
$Co(R^{bs}_{m})_2$	18.5	16.5	18.5
$Co(R^{bs}_{e\alpha})_2.H_2O$	17.0	14.5	17.5
$Co(R^{bs}_{e\beta})_2$	22.5	17.0	16.5
$Ni(R^{bs}_{m})_2$	18.5	10.5	18.5
$Ni(R^{bs}_{e\alpha})_2H_2O$	15.0	—	15.5
$Ni(R^{bs}_{e\beta})_2$	14.5	—	14.5
$Cu(R^{bs}_{m})_2.H_2O$	14.0	—	18.0
$Cu(R^{bs}_{e\alpha})_2.3H_2O$	12.0	—	13.0
$Cu(R^{bs}_{e\beta})_2$	18.0	10.5	17.0
$Zn(R^{bs}_{m})_2.2H_2O$	13.5	—	17.5
$Zn(R^{bs}_{e\alpha})_2.2H_2O$	—	10.0	17.0
$Zn(R^{bs}_{e\beta})_2.H_2O$	14.5	—	15.5
$Cu(R^{bs}_{pb})(R^{bs}_{m}).3H_2O$	13.0	17.0	12.5
$Cu(R^{bs}_{pb})(R^{bs}_{e\alpha}).H_2O$	12.0	16.0	11.5
$Cu(R^{bs}_{pb})(R^{bs}_{e\beta}).3H_2O$	15.5	16.5	12.5
$Co(R^{bs}_{pb})(R^{bs}_{m}).2H_2O$	17.5	16.5	13.0
$Co(R^{bs}_{pb})(R^{bs}_{e\alpha}).2H_2O$	15.5	15.5	13.0
$Co(R^{bs}_{pb})(R^{bs}_{e\beta}).3H_2O$	18.0	16.6	16.5
Co^{2+}	13.0	13.0	13.0
Ni^{2+}	12.5	—	11.0
Cu^{2+}	—	—	11.5
Zn^{2+}	—	—	—
DMSO	—	—	—
$R^{bs}_{m}H$	—	—	17.0
$R^{bs}_{e\alpha}H$	14.0	—	18.0
$R^{bs}_{e\beta}H$	—	—	14.0

cup-plate diffusion method[4] (Table 2). All Co(II) chelates are active against these microorganisms. The activities of these chelates are more than those of free metal ions. These chelates are obviously more stable than the non-chelated complexes of the corresponding benzamidobenzimidazoles. But comparable biological activity of these chelates may be due to intermolecular interaction in the Co(II), Ni(II) and Cu(II) complexes leading to the rapid interaction of these complexes with DNA base to satisfy coordination number. All Co(II) complexes are not always more active than other complexes. Only tetrahedral Co(II) complexes of benzamidobenzimidazoles were found to be more active than Ni(II) and Cu(II) complexes[9].

Acknowledgement

Thanks are due to the Director, CDRI, Lucknow for providing facilities to record IR spectra and to the UGC, New Delhi for some financial assistance.

References

1 Ghosh N N & Nandi M M, *J Indian chem Soc*, **53** (1976) 274, 331.
2 Nandi M M, *Curr Sci*, **44** (1977) 698.
3 Nandi M M & Mishra A K, *Trans Bose Res Inst*, **44** (1981) 19.
4 Nandi M M & Ray Ruma, *Indian J Chem*, **25B** (1986) 222.
5 Ghosh N N & Nandi M M, *Indian J Chem*, **14A** (1978) 778.
6 Ghosh N N & Nandi M M, *J Indian chem Soc*, **53** (1976) 643; **54** (1977) 139; **55** (1978) 749.
7 Nandi M M, *Indian J Chem*, **15A** (1977) 809.
8 Nandi M M, *Indian J Chem*, **19A** (1978) 493.
9 Nandi M M, Ray Ruma & Mishra A K, *Indian J Chem*, **26A** (1987) 345.
10 Ghosh N N & Bhattacharya A, *J inorg nucl Chem*, **35** (1973) 517.
11 Ghosh N N, *J inorg nucl Chem*, **36** (1974) 1909.
12 Irving H M & Rossotti H S, *J chem Soc*, (1954) 2904.
13 Phillips M A, *J chem Soc*, (1928) 2393.
14 Hughes J K & Lions F, *J Proc Soc NSW*, **71** (1938) 209.
15 Ghosh N N, *Indian J Chem*, **15A** (1977) 568.
16 Vogel A I, *A text book of practical organic chemistry*, (E L B S, London) 1961, 177.
17 Nandi M M, *PRS Dissertation*, University of Calcutta, 1978.
18 Figgis B N & Lewis J, *Prog inorg Chem*, **6** (1964) 37.
19 Sacconi L & Chiampolini M, *J chem Soc*, (1964) 276.
20 Goodgame M & Haines L I B, *J chem Soc*, **A** (1966) 174.
21 Cotton F A & Wilkinson G, *Advanced inorganic chemistry* (John Wiley, New York) 1980.
22 Sacconi L, *Trans Met Chem*, **4** (1968) 199.

Indian Journal of Chemistry
Vol. 27A, August 1988, pp. 691-694

Metal(II) Complexes of 4-X-Benzenesulphinic Acids: Structures & Substituent Effects on Their Infrared Spectra

C NATARAJAN* & P R ATHAPPAN
Department of Inorganic Chemistry, Madurai Kamaraj University, Madurai 625 021

Received 31 *August* 1987; *revised and accepted* 16 *November* 1987

Complexes of Mn(II), Fe(II), Co(II), Ni(II), Cu(II), Zn(II), Cd(II) and Hg(II) with 4-X-benzenesulphinic acids (X = Cl; Br; OCH_3) have been prepared and characterized on the basis of their elemental analysis, conductivity measurements, magnetic moments, UV and IR spectra. It is observed that the ligand is bonded through both of its oxygens except in bis(*p*-methoxybenzene sulphinato)mercury(II) where S-coordination is observed. The effects of *p*-substituents in the phenyl ring and changing of metal ion on ν(SOO) and stability of metal(II) complexes have been studied. The positions of the sulphinic acids in the spectrochemical and nephelauxetic series have been determined on the basis of the crystal field parameters of the complexes.

Sulphinic acids undergo autoxidation and disproportionation and are generally known to be unstable. However, their metal salts are stable. Metal(II) complexes of benzene-, *p*-toluene-[1,2] and naphthalenesulphinic acids[3] are known. Sulphinic acids, being ambidentate, can coordinate as monodentate ligands through O or S and as bidentate ligands through two oxygen atoms. Although sulphinato metal(II) complexes are known, the effects of *p*-substituents in the phenyl ring and change of metal ion on ν(SOO) have not been studied. Hence, an attempt has been made to investigate the above aspects.

In this paper we present the synthesis and characterisation of Mn(II), Fe(II), Co(II), Ni(II), Cu(II), Zn(II), Cd(II) and Hg(II) complexes of *p*-chloro-(CBSOOH), *p*-bromo-(BBSOOH), and *p*-methoxybenzenesulphinic acids (MBSOOH). The positions of sulphinic acids in the spectrochemical series have been determined from the crystal field parameters.

Materials and Methods

Analar grade (BDH) chemicals were used. 4-X-Benzenesulphinic acids were prepared adopting the procedure reported in the literature[4]. Bis(4-X-benzene-sulphinato-O, O')diaquometal(II) complexes were prepared as reported elsewhere[3].

The IR spectra were recorded in nujol mull on a Perkin Elmer 577 grating IR spectrophotometer in the 4000-200 cm^{-1} region. The visible spectra were measured in nujol on a Carl-Zeiss-DMR 21 UV-Vis spectrophotometer. The magnetic susceptibilities were determined at room temperature on a Gouy balance, and diamagnetic corrections were calculated using Pascal's constants. Thermogravimetric curves were obtained on a Stanton-Redcraft recording thermo-balance. Molar conductivities of the complexes in DMF were measured using a Toshniwal conductivity bridge (CL01/02A). Metals were estimated by EDTA titrations after decomposing the complexes with a mixture of concentrated HNO_3 and H_2O_2. Elemental analyses were carried out at the Central Drug Research Institute (CDRI), Lucknow.

Results and Discussion

All these 4-X-benzenesulphinatometal(II) complexes are obtained as crystalline substances and their elemental analyses conform to the general formula $M(RSOO)_2.2H_2O$, except in the case of cadmium(II) complex (Table 1). Manganese(II), zinc(II), cadmium(II) and mercury(II) complexes are colourless while rest of the complexes are coloured (Table 1). These complexes are extremely insoluble in all polar and non-polar solvents except DMSO and DMF, which may be due to their polymeric nature. Conductivity measurements reveal the non-ionic nature of these complexes.

All these diaquometal(II) sulphinates are stable upto 120°, above which they lose water to form anhydrous complexes. These anhydrous compounds which are stable upto ~240° decompose finally to their respective metal oxides. The decomposition of anhydrous compounds to metal oxides is fast proceeding in single, double or even in multiple stages. It is tentatively concluded that decomposition of $(RSO_2)_2M$ proceeds probably through the formation of sulphates and finally the oxides[5,6]. In the case of copper complexes the decomposition to oxides proceeds in two stages as in copper(II) sulphate[7].

Zinc(II), cadmium(II) and mercury(II) sulphinates are diamagnetic as expected. Manganese(II), iron(II), cobalt(II), nickel(II) and copper(II) complexes are paramagnetic and their magnetic moments (Table 1) correspond to the spin-only value of a high-spin octahedral configuration.

Table 1—Analytical, Magnetic Moment and Selected IR Spectral Data* of Metal(II) Complexes of 4-X-Benzenesulphinic Acids

Complex (Colour)	Found (calc.)%			IR bands (cm^{-1})		$\mu_{eff.}$ (B.M.)
	M	C	H	ν_{as}(SOO)	ν_s(SOO)	
CBSOONa	—	—	—	1041	1010	—
BBSOONa	—	—	—	1042	1005	—
MBSOONa	—	—	—	1045	1002	—
$Mn(CBSOO)_2.2H_2O$	12.56	32.10	2.86	998	955	5.98
(Colourless)	(12.42)	(32.59)	(2.78)			
$Mn(BBSOO)_2.2H_2O$	10.10	27.01	2.01	993	952	5.34
(Colourless)	(10.34)	(27.13)	(2.28)			
$Mn(MBSOO)_2.2H_2O$	12.31	37.92	4.82	985	944	6.04
(Colourless)	(12.67)	(38.80)	(4.18)			
$Fe(CBSOO)_2.2H_2O$	12.52	32.02	2.92	983	938	5.52
(Cream)	(12.60)	(32.52)	(2.73)			
$Fe(BBSOO)_2.2H_2O$	10.21	26.82	2.42	990	940	5.38
(Light brown)	(10.49)	(27.09)	(2.27)			
$Fe(MBSOO)_2.2H_2O$	12.42	37.82	4.61	982	936	5.42
(Light brown)	(12.86)	(38.72)	(4.17)			
$Co(CBSOO)_2.2H_2O$	13.24	32.06	2.81	982	939	4.83
(Rose)	(13.20)	(32.30)	(2.71)			
$Co(BBSOO)_2.2H_2O$	10.82	26.43	2.81	982	938	4.65
(Rose)	(11.01)	(26.93)	(2.26)			
$Co(MBSOO)_2.2H_2O$	13.40	38.01	4.26	978	930	4.86
(Rose)	(13.49)	(38.44)	(4.15)			
$Ni(CBSOO)_2.2H_2O$	13.18	32.16	2.96	986	940	3.13
(Pale green)	(13.16)	(32.32)	(2.71)			
$Ni(BBSOO)_2.2H_2O$	10.52	26.41	2.42	975	936	3.08
(Pale green)	(10.97)	(26.94)	(2.26)			
$Ni(MBSOO)_2.2H_2O$	13.42	38.20	4.44	982	941	3.12
(Pale green)	(13.43)	(38.46)	(4.15)			
$Cu(CBSOO)_2.2H_2O$	14.21	32.03	2.72	955	908	1.81
(Light green)	(14.09)	(31.97)	(2.68)			
$Cu(BBSOO)_2.2H_2O$	11.51	26.62	2.23	949	931	2.02
(Light green)	(11.77)	(26.70)	(2.24)			
$Cu(MBSOO)_2.2H_2O$	13.20	37.26	4.20	942	928	1.89
(Light green)	(13.37)	(38.04)	(4.10)	1000		
$Zn(CBSOO)_2.2H_2O$	14.24	31.58	2.52	987	940	—
(Colourless)	(14.44)	(31.84)	(2.69)			
$Zn(BBSOO)_2.2H_2O$	12.10	26.52	2.41	985	940	—
(Colourless)	(12.07)	(26.61)	(2.23)			
$Zn(MBSOO)_2.2H_2O$	14.52	37.46	4.31	985	938	—
(Colourless)	(14.73)	(37.88)	(4.08)			
$Cd(CBSOO)_2.2H_2O$	22.20	28.52	2.56	982	940	—
(Colourless)	(22.49)	(28.84)	(2.42)			
$Cd(BBSOO)_2.2H_2O$	18.92	24.02	2.21	983	940	—
(Colourless)	(19.09)	(24.48)	(2.05)			
$Cd(MBSOO)_2$	24.34	36.02	4.86	960	945	—
(Colourless)	(24.71)	(36.97)	(3.10)			
$Hg(CBSOO)_2.2H_2O$	33.02	24.46	2.12	1000	980	—
(Colourless)	(34.12)	(24.52)	(2.06)		960	
$Hg(BBSOO)_2.2H_2O$	29.24	20.92	2.62	1000	980	—
(Colourless)	(29.64)	(21.29)	(2.78)	1010	965	
$Hg(MBSOO)_2.2H_2O$	36.42	30.02	2.61	1242	1026	—
(Colourless)	(36.94)	(30.96)	(2.59)			

* Spectra in KBr disc; all peaks are strong

In sodium salts of 4-X-benzenesulphinic acids, where the metal-ligand interaction is considered to be negligible, the ν_{as}(SOO) and ν_s(SOO) appear in the regions 1040 and 1005 cm^{-1} respectively. The bands observed near 1600 and 1500 cm^{-1} are assigned to $\nu C=C$ of the phenyl ring[8]. In all these sulphinates there appears a strong absorption in the region 830 cm^{-1} which is assigned to the C—H out-of-plane

bending vibrations[8]. The C—S stretching frequency is observed as a medium strong band around 750 cm^{-1}.

In all these sulphinato complexes a strong but broad absorption is observed in the region 3385-3000 cm^{-1} which is assigned to the ν(OH) mode of the coordinated water[9]. The out-of-plane C—H vibrations and the νC—S vibrations are not affected on coordination. Compared to sodium sulphinate, the ν_{as}(SOO) (~ 985 cm^{-1}) and ν_s(SOO) (~ 935 cm^{-1}) occur at lower frequencies almost in all the metal complexes. The frequency difference (Δν) between the ν_{as}(SOO) and ν_s(SOO) is 31-47 cm^{-1} in CBSOOH complexes, 37-50 cm^{-1} in BBSOOH complexes and 15-62 cm^{-1} in MBSOOH complexes. These observations are indicative of double oxygen coordination[2] and the complexes are of the sulphinato-O, O′ type.

$Cd(MBSOO)_2$ has got no coordinated or crystal-held water. As indicated by the Δν value (15 cm^{-1}), $MBSOO^-$ acts as a bidentate ligand and the complex may be formulated as bis(*p*-methoxybenzenesulphinato-O,O′)cadmium(II), the configuration most probably being tetrahedral.

In the case of mercury(II) complex of MBSOOH, the ν_{as}(SOO) and ν_s(SOO) modes are shifted to higher frequencies and occur respectively at 1242 and 1026 cm^{-1}. The Δν value (216 cm^{-1}) is indicative of monodentate S-coordination. The S-coordination in the bis(*p*-methoxybenzenesulphinato-S)mercury(II) is attributed to the presence of electron releasing methoxyl group which makes the sulphur more polarised and it preferentially bonds with soft acid, mercury(II).

Effect of metal ion substitution

When the sulphinate ion is bonded through both of its oxygen atoms, the ν_{as}(SOO) and ν_s(SOO) are expected to undergo characteristic change depending on M—O bond strength. When the M—O bond becomes stronger the S—O bond is weakened resulting in a decrease in the ν_{as}(SOO) and ν_s(SOO) frequencies; the magnitude of their decrease is correlated to the stability of metal(II) sulphinates. It is obvious that the ν_{as}(SOO) and ν_s(SOO) decrease as follows: Mn > Fe > Co ≤ Ni > Cu < Zn. This corresponds to an increase in the M—O bond strength in the order: Mn < Fe < Co ≥ Ni < Cu > Zn, which is consistent with the Irving-Williams order of stabilities.

Effect of ligand substitution

The presence of electron releasing substituents like Me and OMe in the 4-position in the substituted benzenesulphinato complexes will increase the electron density on sulphur which may be transmitted to the oxygen atom due to its higher electronegativity. Thus,

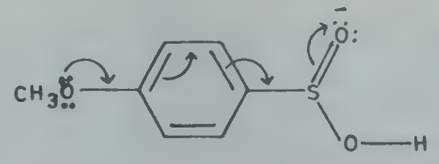

(I)

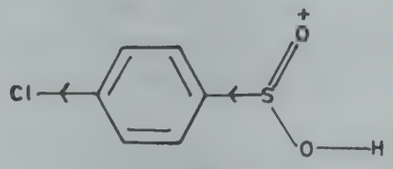

(II)

the σ-donor property of oxygen increases indirectly (I). On the other hand, the σ-donor property of oxygen will be decreased by the presence of electron attracting groups like Cl and Br in the 4 position (II). Accordingly, ν_{as}(SOO) and ν_s(SOO) will be lower in the former than in the latter.

In Mn(II), Fe(II) and Co(II) complexes, the ν(SOO) mode registers lower values for Me and OMe substituents and higher values for chloro and bromo substituents than that in the parent benzene derivatives[2]. Thus, the stability of these metal sulphinates decreases in the expected order, $OCH_3 > CH_3 > H > Cl$ ~ Br. However, this order is reversed in Zn(II) complexes, which may be due to the presence of completely filled 3*d* orbitals. The correlation between the Hammett substituent constant, σ, and ν(SOO) is not much pronounced as expected because of the interposition of sulphur atom which can expand its valency shell.

Ligand field spectra

Bis(4-X-benzenesulphinato)diaquomanganese(II) complexes show a series of very weak, and rather narrow combination bands, and it is not possible to assign transitions with certainty. The bands observed in the region 10750-11100 cm^{-1} for iron(II) complexes have been assigned to $^5T_{2g} \rightarrow {}^5E_g$ transition in an octahedral environment[10]. The bands have doublet structure and this may be due to a low symmetry ligand field which lifts the two-fold orbital degeneracy of the ^5E_g level[11]. All the sulphinato cobalt(II) complexes give rise to absorptions in the region 8100 and a doublet around 19000 and 21000 cm^{-1}. The 8100 cm^{-1} band is assigned to the transition $^4T_{1g}(F) \rightarrow {}^4T_{2g}$ (ν_1) in an octahedral environment. The splitting of ν_3 band around 20000 cm^{-1} represents $^4T_{1g}(F) \rightarrow {}^4T_{1g}(P)$ transition in admixture with spin-forbidden transitions to doublet states derived principally from the free ion terms[12,2] *G* and ^2H. The ν_2, being a two electron transition, is not observed. Nickel(II) sulphinato complexes show three bands around 8200, 13300 and 24000 cm^{-1} and are assigned re-

spectively to the transitions $^3A_{2g}(F) \rightarrow {}^3T_{2g}(\nu_1)$, $^3A_{2g} \rightarrow {}^3T_{1g}(\nu_2)$ and $^3A_{2g} \rightarrow {}^3T_{1g}(P)$ (ν_3) in an octahedral field[12]. Further, the ν_2/ν_1 ratio of 1.60-1.63 may be taken as a clear indication of octahedral environment[11]. Copper(II) complexes exhibit a single broad absorption around 12500 cm^{-1} which is assigned to the combination of the transitions $^2B_{1g} \rightarrow {}^2A_{1g}$, $\rightarrow {}^2B_{2g}$ and $\rightarrow {}^2E_g$ in a tetragonal field[11].

In cobalt(II) and nickel(II) sulphinato complexes the interelectron repulsion has been reduced to about 80% of the free ion value and the percentage covalency is about 17 and 20 respectively for nickel(II) and cobalt(II) complexes. The departure of the ratio $B'/B = \beta$, from unity is used to place the ligand in the nephelauxetic series. The β value is around 0.81 and these sulphinic acids find a place near ethylenediamine in the nephelauxetic series[11].

Assuming a tris(sulphinato) complex and using the average environment method[13], we have calculated values of $10Dq$ and hence the 'f' factor of these sulphinic acids[14]. The value of 'f' thus obtained is around 1.03 and these sulphinic acids may be placed between NCS^-(N-coordinated, $f = 1.02$) and p-$CH_3-C_6H_4NH_2$ ($f = 1.15$) in the spectrochemical series[15]. Sulphinic acids being weak field ligands, there should be some configuration interaction and these interaction energies (X) are found to be around 700 and 1200 cm^{-1} respectively for cobalt(II) and nickel(II) complexes.

Acknowledgement

We thank USIC, Madurai Kamaraj University and RSIC, IIT, Madras for instrumental facilities.

References

1 Deacon G B & Cookeson P G, *Inorg nucl chem Lett*, **5** (1970) 607.
2 Lindner E, Vitzthum G & Weber H, *Z anorg allg Chem*, **373** (1970) 122.
3 Natarajan C & Athappan P R, *Indian J Chem*, **15A** (1977) 1102.
4 (a) Vogel A I, *Practical organic chemistry* (Longmans, London) 1959; (b) Kulka M, *J Am chem Soc*, **72** (1950) 1216; (c) Nerdel F, Goetz H & Fabienke E, *Ann*, **643** (1961) 6; *Chem Abstr*, **55** (1961) 2341.
5 Hartman F A & Wokcicki, *Inorg Chem*, **7** (1968) 1504.
6 Mays M J & Simpson R N F, *J chem Soc(A)*, (1967) 1936.
7 Borchardt H J & Daniels F, *J phys Chem*, **61** (1957) 917.
8 Nakanishi, *Infrared absorption spectroscopy* (Holden-Day, San Francisco) 1962.
9 Gamo I, *Bull chem Soc (Japan)*, **34** (1961) 1430.
10 Dunn T M, *Modern coordination chemistry*, edited by J Lewis & R G Wilkins (Interscience, New York) 1960.
11 Sutton D, *Electronic spectra of transition metal complexes* (McGraw-Hill, London) 1968.
12 Lever A B P, *Inorganic electronic spectroscopy* (Elsevier, Amsterdam) 1968.
13 Figgis B N, *Introduction to ligand fields* (Interscience, New York) 1967.
14 Jorgensen C K, *Absorption spectra and chemical bonding in complexes* (Pergaman, Elmsford, New York) 1962 & *Oxidation numbers and oxidation states* (Springer, New York) 1969.
15 Huheey J E, *Inorganic chemistry* (Harper International Edition, New York) 1978.

Indian Journal of Chemistry
Vol. 27A, August 1988, pp. 695-697

Unsymmetrical Distortion in Piperidine Ring: Evidence from Rates of N-Methylation of Piperidines & Piperidin-4-ones

R JEYARAMAN† & L CHANDRASEKARAN
Department of Chemistry, The American College, Madurai 625 002
K GANAPATHY* & V GOPALAKRISHNAN
Department of Chemistry, Annamalai University, Annamalainagar 608 002

Received 8 *April* 1987; *revised* 10 *August* 1987; *accepted* 18 *September* 1987

The rates of N-methylation of several 2,6-diphenylpiperidin-4-ones (**1a-e**) and the corresponding piperidines (**2a-e**) with methyl iodide under second order conditions, show that a large distortion occurs at the site of methylation, i.e. the nitrogen atom as substituents at C-3 and C-5 are changed from H to alkyl groups. The greatest distortion is observed in the case of 3,3-dimethyl derivatives which react about 3 to 5 times faster than the 3-methyl derivatives which show the lowest rate constants among the series studied. Thus an axial 3-methyl substituent enhances the rate of N-methylation indicating unsymmetrical distortion in the ring with possible flattening around C(2)-N-C(6) atoms.

The chemistry of 2,6-diphenylpiperidin-4-ones (**1**) and 2,6-diphenylpiperidines (**2**) has recently gained considerable importance in view of the occurrence of simple piperidines with alkyl and aryl substituents at C-2 and C-6 in various alkaloids, ant venoms, frog toxins, pheromones, etc[1].

Stereochemical studies on **1**[2] have been performed mainly with systems where the reaction center is the C-4. Some interesting qualitative and quantitative kinetic works so far carried out include catalytic reduction and reduction with various reducing agents[3], acetylation of piperidin-4-ols[4], alkaline hydrolysis of 4-acetoxypiperidines[5], chromic acid oxidation of piperidin-4-ols[6], semicarbazone formation[7], and equilibrium studies on cyanohydrins[8].

In almost all the cases reported conformation of piperidine ring has been equated to that of similarly substituted cyclohexanes. However, the region of C(2)-N-C(6) atoms is influenced by polar, steric, electronic and field effects while that around C(3)-C(4)-C(5) atoms is controlled chiefly by steric effects of the substituents at C-3 and C-5 positions, except where H-bonding also plays a role when there are protic substituents at C-4.

In a systematic analysis of the results obtained from the earlier work on piperidines it was suspected that any reaction at the ring nitrogen would be influenced by the steric requirements of the alkyl substituents at C-3 and C-5 also. The reactions conceived suitable for testing the validity of this speculation were N-acetylation and N-methylation of the piperidin-4-ones and piperidines.

Though it was already known that treatment of 2,6-diphenylpiperidin-4-ones (**1**) with acetic anhydride in pyridine did not yield the N-acetyl derivative[1], the reaction was tried under various kinetic conditions employing titrimetric and spectroscopic techniques. In all the cases there was no N-acetylation and those cases where consumption of acetic anhydride occurred were traced to other reactions.

This paper describes the results of N-methylation studies on piperidines.

Materials and Methods

The 2,6-diphenylpiperidin-4-ones (**1a-e**) were prepared by standard procedures[2] and purified by two or three recrystallizations and dried *in vacuo* at 50-80° before use. 2,6-Diphenylpiperidines (**2a-e**) were prepared by Wolf-Kishner reduction of **1a-e**. The melting points were compared with those reported[2] and found agreeable.

The product analysis revealed the formation of only N-methyl derivative in each case. For the determination of the products formed the solvent from the reaction mixture after complete reaction was evaporated and the residual material analysed by co-TLC with authentic samples. After recrystallization the melting point of each of the product formed also confirmed the formation of N-methyl derivative.

The solvent acetone was purified as follows: A solution of silver nitrate (2.5 g) in water (15 ml)

†Present address: Department of Chemistry, Bharathidasan University, Tiruchirapalli 620 024

was added to acetone (500 ml) followed by aqueous sodium hydroxide (1*N*, 15 ml) and the mixture was shaken well for 10 min. The acetone-water mixture was filtered, dried ($CaSO_4$), filtered and acetone fractionally distilled over dry potassium carbonate and the fraction boiling at 56-57° was collected[9].

Kinetic measurements

The reaction mixture consisting of two parts of piperidine and one part of methyl iodide in acetone was take in a boiling tube (length 15 cm) with a ground glass joint. A suitably modifed conductivity cell (with air-tight ground glass connections) was placed in it. Care was taken to tightly wrap the joints with polythene film, so that the solvents and methyl iodide did not escape. The resistance was measured with Philips GM-4249 resistance bridge as soon as the reactants were mixed and at different time intervals. The temperature was maintained at 30.0 ± 0.1°C.

Under the second order reaction conditions there may not be any possibility for the presence of free hydrogen iodide in solution during the course of the reaction. Since the piperidine concentration was maintained twice that of methyl iodide, as soon as hydrogen iodide was formed it could be trapped by excess piperidine. The reaction tube was covered with black cloth in order to minimize side reactions. However, in the absence of the piperidine no noticeable increase in conductivity was observed even when the methyl iodide solution was kept exposed to diffused light for a day.

A plot of $(x_t\text{-}x_0)/(x_{inf}\text{-}x_t)$ (*where* x_0 is the initial conductance, x_{inf} is the conductance after complete reaction, and x_t is the conductance at time t), against time was linear showing that the rection followed second order kinetics. The conductance at the completion of the reaction was measured by (i) keeping the reaction mixture for several days and considering the constant conductance reading obtained after 18-36 hr as the final conductance and (ii) by mixing a solution of the corresponding N-methylpiperidine and hydriodic acid of the appropriate concentration and measuring the conductivity of the resulting solution. The two values generally agreed very well and the difference was within 2% in all the cases.

The rate constant k_2 was calculated by Eq.(1).

$$k_2 = \frac{1}{\text{slope} \times 2b} \qquad \ldots(1)$$

where b is the initial concentration of methyl iodide[10].

Results and Discussion

Table 1 gives the rate constants for the rection of methyl iodide with various alkyl substituted 2,6-diphenylpiperidin-4-ones (**1a-e**) and 2,6-diphenylpiperidines (**2a-e**) at 30.0 °C in acetone solution. The products formed exclusively are the respective *N*-methyl derivatives, viz., **3** from **1** and **4** from **2**.

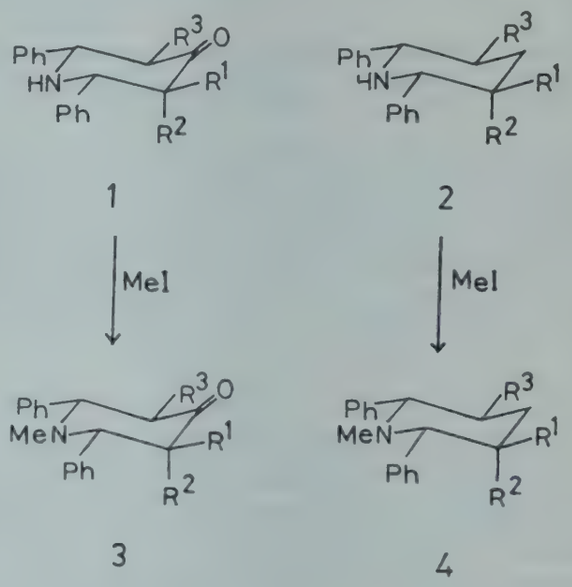

1-4: (a) $R^1 = R^2 = R^3 = H$; (b) $R^1 = Me$, $R^2 = R^3 = H$; (c) $R^1 = R^3 = H$, $R^2 = H$; (d) $R^1 = Et$, $R^2 = R^3 = H$; (e) $R^1 = R^2 = Me$, $R^3 = H$

The compound 1,3,3-trimethyl-2,6-diphenylpiperidin-4-one (**3c**) has been shown to exist in a flexible conformation[11]. In the chair conformation of the piperidine two kinds of rotational isomers (for Ph) have been considered. If the phenyl group is oriented perpendicular to the average plane of the heterocyclic ring there will be severe non-bonded interaction between the phenyl group at C-2 and the axial methyl group at C-3. If the phenyl group is in the same plane of the heterocyclic ring then there will be severe interaction from C_3-methyl (equatorial) and N-methyl groups.

Table 1—Rate Constants for Reaction of Methyl Iodide with 2,6-Diphenylpiperidin-4-ones (**1a-e**) and 2,6-diphenylpiperidin-4-ones (**2a-e**)

Temp. 30°C

	$10^4 \times k_1$ ($dm^3\ mol^{-1}\ s^{-1}$)		$10^3 \times k_2$ ($dm^3\ mol^{-1}\ s^{-1}$)	k_1/k_2
1a	5.0	**2a**	4.1	8.2
1b	3.0	**2b**	2.2	7.3
1c	6.6	**2c**	3.6	5.4
1d	4.6	**2d**	3.6	8.0
1e	19.0	**2e**	10.0	5.2

The puckered structure may be operative in the NH compound also.

The observed reactivity order in the N-methylation of both piperidin-4-ones and piperidines supports the distorted chair conformation with unsymmetrical distortion around C(3)-C(4)-C(5) carbons with flattening around C(2)-N-C(6) atoms in the case of 3,3-dimethyl derivatives during N-alkylation (e.g. as shown in structure **5**). This conformation may be responsible for the greater reaction rates at the nitrogen site of the piperidin-4-one (**1e**) and piperidine (**2e**) having 3,3-dimethyl substituents.

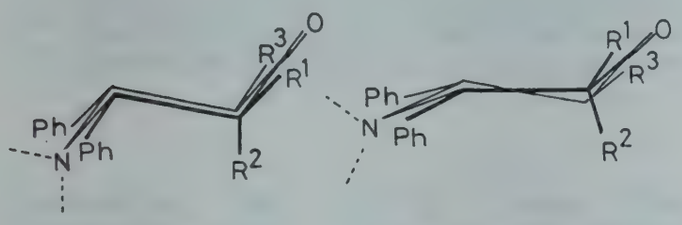

normal chair distorted chair

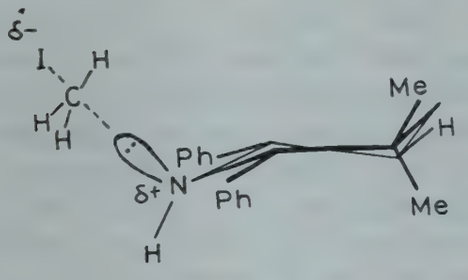

5

The rates of N-chlorination reactions[12] have been found to be too fast for one to follow under the conditions employed. Thus a comparison between N-methylation, N-acylation and N-chlorination could not be made.

An axial course of substitution, followed by nitrogen inversion, would show a slower rate since the axial methyl group at C-3 will reduce the probability of approach of methyl iodide from the axial side. On the other hand, reaction from the equatorial side will not be influenced by the steric hindrance of C_3-methyl (axial) substituent. However, if unsymmetrical distortion of the ring occurs the steric hindrance due to phenyl groups is expected to decrease. Thus the enhanced rates in the case of the 3,3-dimethyl-2,6-diphenylpiperidines suggests that the rection also proceeds from the equatorial position of the piperidine ring.

The ratio of the rate constants between the piperidin-4-one and the corresponding piperidine was calculated for each case. Though the results are not to be taken as highly significant there is some hint to show that the methyl substituents at C-3 and C-5 have nearly the same influence on the distortion of the piperidin-4-ones and piperidines.

Thus, the present study not only supports the established fact that an axial alkyl substitution at C-3 or C-5 causes an unsymmetrical distortion in the piperidine ring but also suggests that there is a stretching (flattening) effect on the piperidine ring on the side of the C(2)-N-C(6) atoms.

Acknowledgement

The financial support from the UGC and the R&D Committee of the American College is gratefully acknowledged.

References

1 Baliah V, Jeyaraman R & Chandrasekaran L, *Chem Rev*, **83** (1983) 379.
2 Baliah V & Ekambaram A, *J Indian chem Soc*, **33** (1955) 274 and references therein.
3 Balasubramanian N & Padma N, *Tetrahedron*, **19** (1963) 2135; **24** (1968) 5395.
4 Radhakrishnan T R, Balasubramanian M & Baliah V, *Indian J Chem*, **11** (1973) 562.
5 Dharmaraj C R, Sivakumar R, Devarajan V & Ramalingam K, *Indian J Chem*, **14B** (1976) 140.
6 Baliah V & Chandrasekaran J, *Indian J Chem*, **15B** (1977) 1035.
7 Baliah V, Chandrasekaran J & Natarajan A, *Indian J Chem*, **15B** (1977) 829.
8 Baliah V & Chandrasekaran J, *Indian J Chem*, **15B** (1977) 826.
9 Vogel A I, *Practical organic chemistry* (ELBS & Longmans) 1980, pp 273.
10 Guggenheim E A & Prue J E, *Physicochemical calculations*, (North-Holland, Amsterdam) 1956, p 443.
11 Radhakrishnan T R, Balasubramanian M & Baliah V, *Indian J Chem*, **11** (1973) 318.
12 Ganapathy K & Vijayan B, *J Indian chem Soc*, **60** (1983) 572.

Indian Journal of Chemistry
Vol. 27A, August 1988, pp. 698-701

Kinetics of Complexation of Ni(II) & Cu(II) with L-α-Amino-β-indolepropionic Acid

H C MALHOTRA* & GIAN CHAND SHARMA
Department of Chemistry, University of Delhi, Delhi 110 007

Received 22 *June* 1987; *revised* 17 *November* 1987; *accepted* 18 *December* 1987

The kinetics of complexation of Ni(II) and Cu(II) by L-α-amino-β-indolepropionic acid have been investigated at 25, 30, 35 and 40 ± 0.05°C and at $I = 0.1$ mol dm^{-3} KNO_3 in the *p*H range 6.08-7.43 in the case of Ni(II) and 2.50-3.31 in the case of Cu(II). Only one reaction has been observed in the case of Ni(II) whereas two reactions take place in the case of Cu(II). The anionic form of the ligand is found to be reactive whereas protonated form is found to be slightly reactive in case of Ni(II) but appreciably reactive in case of Cu(II). For the fast reaction, k_{12} and k_{43} corresponding to the interaction of protonated and deprotonated forms of the ligand with metal ions respectively and the corresponding activation parameters have been calculated.

The rates of complexation reactions of metal ions with a large variety of ligands[1-4] depend to a large extent on the charge of the reacting ligand. Generally the rates of substitution on metal ion is controlled by the rate of water exchange, and the rate determining step is the loss of water molecule from inner coordination sphere of the metal ion.

$$M^{2+}_{aq.} + L^{n-}_{aq} \underset{fast}{\overset{K_{os}}{\rightleftharpoons}} M^{2+}_{aq} L^{n-} \xrightarrow[slow]{k_0} ML^{(2-n)+} + H_2O \quad \ldots (1)$$

L-α-Amino-β-indolepropionic acid (L-tryptophan) is found in human blood plasma. Ultracentrifugation study[5] using ^{64}Cu shows that Cu(II) interacts more rapidly with amino acids than albumin in blood serum. In view of this it was thought of interest to determine the binding steps, rate constants corresponding to the binding steps (see Eq. 1) and activation parameters corresponding to the interaction of protonated and deprotonated forms of the ligand.

Materials and Methods

L-α-Amino-β-indolepropionic acid (L-tryptophan, Loba), 2,6-lutidine (Merck-Schuchardt) and bromothymol blue (BDH) were used as such. Other chemicals used were of AR quality. Solutions of Ni(II) (~ 10^{-2} mol dm^{-3}) and Cu(II) (~ 10^{-2} mol dm^{-3}) were prepared from $Ni(NO_3)_2.6H_2O$ (Merck) and $Cu(NO_3)_2.3H_2O$ (Merck) and standardised by EDTA titration. Doubly distilled water was used for preparing all the solutions. The ionic strength was kept constant at 0.1 mol dm^{-3} (KNO_3). Freshly prepared solutions 1.26×10^{-3} and 3.80×10^{-3} mol dm^{-3} of L-α-amino-β-indolepropionic acid were used for Ni(II) and Cu(II) respectively.

In the case of Ni(II)-L-α-amino-β-indolepropionic acid reaction, Ni(II) and L-α-amino-β-indolepropionic acid were buffered with 2,6-lutidine (0.052 mol dm^{-3}). Bromothymol blue (~ 10^{-5} mol dm^{-3}) was added to L-α-amino-β-indolepropionic acid. The initial *p*H's of the metal and ligand solutions were made the same. There was, however, slight change in the *p*H (of the order of 0.05 *p*H unit) after mixing. The *p*H's reported in the case of Ni(II) are those of the reaction mixtures. But in the case of Cu(II)-L-α-amino-β-indolepropionic acid, the *p*H was adjusted by dropwise addition of KOH/or HNO_3. The final *p*H was adjusted with an accuracy of ± 0.01 unit. Radiometer *p*H meter (model *p*H M 26) was used for *p*H measurements. Kinetic measurements were made on Aminco-Morrow stopped flow spectrophotometer. The driving syringes and reaction chamber were thermostated at 25, 30, 35 and 40 ± 0.05°C. In the stopped flow reaction chamber, the solution of Ni(II)/Cu(II) ion having ionic strength $I = 0.1$ mol dm − 3 and at the desired *p*H (6.08-7.43 for Ni and 2.50-3.31 for Cu) was mixed with a solution of L-α-amino-β-indole propionic acid at the same *p*H and ionic strength. Changes in transmittance brought about by Ni(II)-L-α-amino-β-indolepropionic acid reaction were monitored at 620 nm using bromothymol blue as an indicator. In case of Cu(II)-L-α-amino-β-indolepropionic acid reaction changes in transmittance were monitored at 600 nm without using any *p*H indicator since in this case transmittance changes were large enough to be monitored directly.

Blank experiments in which Ni(II) ions were mixed with buffer (2,6-lutidine) and indicator showed no change in the transmittance on mixing. Transmittance changes for each run were traced out

from the oscilloscope. The k'_{obs} were calculated from the semilogarithmic plots of logΔV (change in voltage) versus time.

Results and Discussion

The structure of the protonated form of L-α-amino-β-indolepropionic acid (I) should be able to form three fused rings[6], viz five-membered, seven-membered and eight-membered on reaction with Ni(II) and Cu(II). But seven- and eight-membered rings are unstable due to large steric strain and this is in conformity with the literature[7] that indole nitrogen does not take part in complexation. Therefore, it is obvious that reaction of Ni(II) and Cu(II) should lead to the formation of a five-membered ring through α-amino acid moiety.

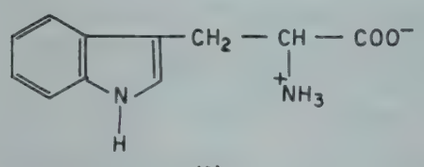

(I)

Ni(II)-L-α-amino-β-indolepropionic acid reaction

The dissociation of L-α-amino-β-indolepropionic acid can be written as:

$$NH^+-OH \overset{K_1}{\rightleftharpoons} NH^+-O^- \overset{K_2}{\rightleftharpoons} N-O^-$$

where HN^+-OH, HN^+-O^- and $N-O^-$ are diprotonated, monoprotonated and deprotonated forms of the ligand. The overall rate equation for Ni(II)-L-α-amino-β-indolepropionic acid can be represented by Eq. (2).

$$\text{Rate} = k'_{obs}\{[HN^+-OH]+[HN^+-O^-]+[N-O^-]\} \quad \ldots (2)$$

where $k'_{obs} = k_{obs}[Ni^{2+}]$. Values of k_{obs} are given in Table 1.

The three forms of amino acid can react with Ni(II) in a stepwise manner as shown in Scheme 1.

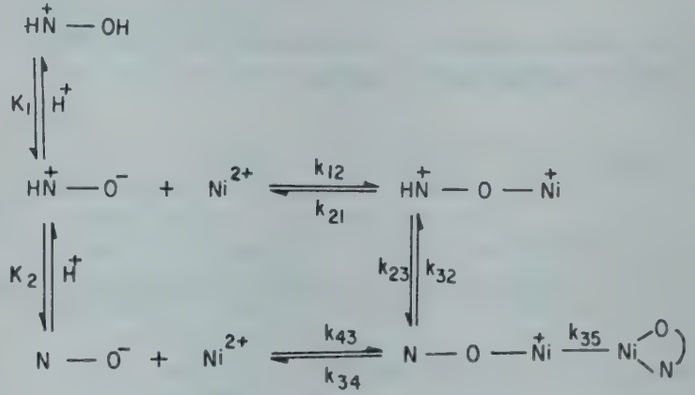

SCHEME 1

Table 1—Second Order Rate Constants (k_{obs}) for the Reaction of Ni(II) and Cu(II) with L-α-Amino-β-indolepropionic Acid

[L-α-Amino-β-indolepropionic acid] = 1.26×10^{-3} mol dm^{-3} for Ni(II) and 3.80×10^{-3} mol dm^{-3} for Cu(II); I = 0.1 (KNO_3) mol dm^{-3}

Ni(II)-L-α-Amino-β-indolepropionic acid				Cu(II)-L-α-Amino-β-indolepropionic acid			
$[Ni^{2+}]$ (mol dm^{-3})	Temp. (°C)	*p*H	$k_{obs} \times 10^{-1}$ (dm^3 mol^{-1} s^{-1})	$[Cu^{2+}]$ (mol dm^{-3})	Temp. (°C)	*p*H	$k_{obs} \times 10^{-3}$ (dm^3 mol^{-1} s^{-1})
0.012	25	6.21	0.339 ± 0.02	0.0200	25	2.50	0.495 ± 0.05
0.012	25	6.61	0.577 ± 0.04	0.0200	25	2.60	0.577 ± 0.05
0.012	25	6.72	0.825 ± 0.03	0.0200	25	2.78	0.866 ± 0.03
0.012	25	6.89	1.25 ± 0.04	0.0185	25	2.90	1.15 ± 0.06
0.012	25	7.14	2.06 ± 0.04	0.0185	25	2.98	1.39 ± 0.08
0.012	25	7.43	4.12 ± 0.06	0.0220	25	3.00	1.39 ± 0.05
0.012	30	6.16	0.950 ± 0.01	0.0220	25	3.10	1.86 ± 0.04
0.012	30	6.54	1.44 ± 0.03	0.0200	25	3.20	2.37 ± 0.06
0.012	30	6.63	1.99 ± 0.02	0.0200	25	3.31	3.07 ± 0.02
0.015	30	6.81	2.22 ± 0.02	0.0200	30	2.51	0.657 ± 0.03
0.015	30	7.04	3.40 ± 0.04	0.0200	30	2.60	0.820 ± 0.02
0.015	30	7.37	6.42 ± 0.07	0.0200	30	2.84	1.49 ± 0.04
0.012	35	6.10	2.05 ± 0.05	0.0200	30	3.00	2.20 ± 0.07
0.012	35	6.46	2.80 ± 0.03	0.0200	30	3.09	2.65 ± 0.08
0.012	35	6.59	3.61 ± 0.05	0.0200	30	3.19	3.48 ± 0.06
0.015	35	6.79	4.44 ± 0.05	0.0200	35	2.54	1.05 ± 0.04
0.015	35	7.32	11.0 ± 0.06	0.0200	35	2.72	1.65 ± 0.03
0.012	40	6.08	4.25 ± 0.05	0.0200	35	2.87	2.44 ± 0.07
0.012	40	6.54	6.50 ± 0.06	0.0250	35	3.00	3.12 ± 0.08
0.012	40	6.90	9.10 ± 0.03				
0.015	40	7.22	15.4 ± 0.04				
0.015	40	6.44	5.35 ± 0.05				

Scheme 1 is different from the scheme given by Cassatt[4], Voss and Jordan[8], who did not take into account the dissociation of $HN^+ - OH$. In accordance with Scheme1, the rate is given by Eq. (3).

$$\text{Rate} = k_{35}[N-O-Ni^+] \quad \ldots (3)$$

Using the steady state approximation for $[\overset{+}{H}N-O-Ni]$ and $[N-O-Ni]$ and applying the approximation $k_{23} > k_{21}$ it can be shown that:

$$\text{Rate} = \frac{k_{12}k_{35}K_1[H^+] + k_{43}k_{35}K_1K_2}{k_{34}+k_{35}} \cdot \frac{[\overset{+}{H}N-OH][Ni^{2+}]}{[H^+]^2} \quad \ldots (4)$$

By substituting $[\overset{+}{H}N-\bar{O}]$ and $[N-O^-]$ in terms of $[\overset{+}{H}N-OH]$ in Eq. (2) we get

$$\text{Rate} = \frac{k_{obs}[Ni^{2+}][\overset{+}{H}N-OH]}{[H^+]^2}\{[H^+]^2 + K_1[H^+] + K_1K_2\} \quad \ldots (5)$$

On comparing Eqs (4) and (5) it can be shown that:

$$k_{obs} \cdot \frac{[H^+]^2 + K_1[H^+] + K_1K_2}{K_1[H^+]} = \frac{k_{12}k_{35}}{k_{34}+k_{35}} + \frac{k_{43}k_{35}}{k_{34}+k_{35}}\frac{K_2}{[H^+]} \quad \ldots (6)$$

Since in Scheme 1 the first bond formed will be strong, i.e. $k_{43} > k_{34}$ if reasonable assumption (i.e. $k_{35} \sim k_{43}$) is made, then $k_{35} > k_{34}$ which is the case for normal substitution as reported by Letter and Jordan[9]. Therefore, Eq. (6) becomes Eq. (7).

$$k_{obs} \cdot \frac{[H^+]^2 + K_1[H^+] + K_1K_2}{K_1[H^+]} = k_{12} + \frac{k_{43}K_2}{[H^+]} \quad \ldots (7)$$

Plots of $k_{obs}\cdot\{[H^+]^2 + K_1[H^+] + K_1K_2\}/K_1[H^+]$ versus $[H^+]^{-1}$ were linear at temperatures 25, 30, 35 and 40°C. (The values of K_2 at 25°C was taken from the literature[10] and corrected for temperatures of our investigation). The values of k_{12} and k_{43} obtained from these linear plots are presented in Table 2. The values of activation parameters corresponding to k_{12} and k_{43} were calculated from the linear plots of log k and log k/T versus 1/T and these values are given in Table 3.

Finally the rate law in terms of outer sphere complex formation constant (K_{os}) and rate constant of water loss (k_o) (see Eq. 1) is given by

$$\text{Rate} = \frac{d}{dt}[NiL^+] = K_{os}k_o[Ni^{2+}][L^-] \quad \ldots (8)$$

By taking k_{12} and k_{43} steps in Scheme 1, it can be written that

$$\text{Rate} = k_{12}[\overset{+}{H}N-O^-][Ni^{2+}] + k_{43}[N-O^-][Ni^{2+}] \quad \ldots (9)$$

Because $k_{12} \ll k_{43}$, Eq. (9) reduces to

$$\text{Rate} = k_{43}[N-O^-][Ni^{2+}] \quad \ldots (10)$$

From Eqs (8) and (10) we get

$$k_{43} = K_{os}k_o \quad \ldots (11)$$

The value of K_{os} at 25°C was calculated to be 2.17 $dm^3\ mol^{-1}$. Using these, the value of k_o at 25°C was calculated to be $1.43 \times 10^3\ s^{-1}$. Swift and Connick[13] have reported a value of $2.7 \times 10^4\ s^{-1}$ for the water exchange rate constant of Ni(II). This difference is due to the formation of stabler outer sphere complex in our case.

Cu(II)-L-α-Amino-β-indolepropionic acid reaction

An oscilloscope trace of voltage versus time

Table 3—Values of Activation Parameters for the Reaction of Ni(II) and Cu(II) with L-α-Amino-β-indolepropionic Acid

	Ni(II)-L-α-Amino-β-indole propionic acid	Cu(II)-L-α-Amino-β-indole propionic acid
$\Delta H^{\ddagger}_{12}$ (kJ mol^{-1}) $\times 10^{-2}$	1.32 ± 0.20	0.456 ± 0.30
$\Delta E^{\ddagger}_{12}$ (kJ mol^{-1}) $\times 10^{-2}$	1.36 ± 0.24	0.479 ± 0.25
$\Delta S^{\ddagger}_{12}$ ($JK^{-1}\ mol^{-1}$) $\times 10^{-2}$	1.90 ± 0.43	0.425 ± 0.10
$\Delta H^{\ddagger}_{43}$ (kJ mol^{-1}) $\times 10^{-1}$	3.59 ± 0.50	1.40 ± 0.25
$\Delta E^{\ddagger}_{43}$ (kJ mol^{-1}) $\times 10^{-1}$	3.82 ± 0.65	1.64 ± 0.40
$\Delta S^{\ddagger}_{43}$ ($JK^{-1}\ mol^{-1}$) $\times 10^{-1}$	− 7.43 ± 0.55	− 1.36 ± 0.35

Table 2—Values of k_{12} and k_{43} for the Reaction of Ni(II) and Cu(II) with L-α-Amino-β-indolepropionic Acid

Temp. (°C)	Ni(II)-L-α-Amino-β-indolepropionic acid		Cu(II)-L-α-Amino-β-indolepropionic acid	
	$k_{12} \times 10^{-1}$ ($dm^3\ mol^{-1}\ s^{-1}$)	$k_{43} \times 10^{-3}$ ($dm^3\ mol^{-1}\ s^{-1}$)	$k_{12} \times 10^{-3}$ ($dm^3\ mol^{-1}\ s^{-1}$)	$k_{43} \times 10^{-10}$ ($dm^3\ mol^{-1}\ s^{-1}$)
25	0.150 ± 0.02	3.08 ± 0.05	2.90 ± 0.08	3.14 ± 0.15
30	0.600 ± 0.02	3.96 ± 0.04	3.95 ± 0.05	3.49 ± 0.15
35	1.50 ± 0.15	5.30 ± 0.05	5.40 ± 0.14	3.90 ± 0.12
40	3.35 ± 0.25	6.54 ± 0.15		

shows that two consecutive reactions are taking place. The fast reaction corresponds to the formation of the mono complex (CuL) and second slow step corresponds to the formation of hydroxy complex. Values of pseudo-first order rate constants (k'_{obs}) were calculated using the usual Guggenheim's method. The values of $k_{obs} = k'_{obs}/[Cu^{2+}]$ are given in Table 1.

To avoid hydrolysis, we restricted our investigation to the *p*H range 2.50-3.31. Rate of the reaction can be given by same equation as described in Ni(II)-L-amino-β-indolepropionic acid reaction.

Plots of $k_{obs}.\{[H^+]^2 + K_1[H^+] + K_1K_2\}/K_1[H^+]$ versus $[H^+]^{-1}$ were linear and the values of k_{12} and k_{43} and the activation parameters were obtained in a similar way as in the case of Ni(II). These values are given in Tables 2 and 3 respectively. Similarly the value of k_o was obtained from Eq. (11) as 1.45×10^{10} s^{-1}. Value reported by Swift and Connick[13] is 2×10^8 s^{-1}. The higher value of k_o in our case is the direct result of John Teller distortion of Cu(II) ion (i.e. d^9 ion).

The values of k_{43} in the case of Cu(II) is very large as compared to those for Ni(II) (Table 2). This can be explained on the basis of crystal field stabilization energy difference (CFSE). The loss of water molecule from the metal ion changes the geometry from octahedral (O_h) to trigonal bipyramidal (TBP). The CFSE[14] of the Ni(II) and Cu(II) for the octahedral geometry can be calculated as 12 Dq (high spin) and 6 Dq (high spin) respectively. For TBP geometry the value of CFSE can be calculated as 6.27 Dq (high spin) and 7.09 Dq (high spin) for Ni(II) and Cu(II) respectively. Therefore, the difference in CFSE (O_h-TBP) in the case of Ni(II) is 5.73 Dq and for Cu(II) it is 1.09 Dq. The lower value in the case of Cu(II) is responsible for the larger value of k_{43}.

Since the fast reaction was found to be second order and was accompanied by release of a proton, the slower reaction was of little importance. Moreover, the slower reaction has no dependence on [Cu(II)]. This was confirmed by using [Cu(II)] = 0.02, 0.04, 0.06 and 0.08 mol dm^{-3}. In every case $t_{1/2} = 0.15$ s was observed. The slow reaction was also found to be independent of *p*H (k'_{obs} was found to be ~ 4.6 s^{-1} in the *p*H range 2.50-3.31).

Therefore, it could be assumed that the formation of a small amount of hydroxy complex of the type Cu(L-α-amino-β-indolepropionic acid). $(H_2O)_3OH^+$ takes place. This type of hydroxy complex for Ni(II) has been reported in literature[4].

Acknowledgement

One of the authors (GCS) is thankful to the CSIR, New Delhi for the award of senior research fellowship.

References

1 Wilkins R G, *Acc chem Res*, **3** (1970) 408.
2 Kustin K & Swinehart J, *Prog inorg Chem*, **13** (1970) 107.
3 Cassatt J C & Wilkins R G, *J Am chem Soc*, **90** (1968) 6045.
4 Cassatt J C, Johnson A W, Smith L M & Wilkins R G, *J Am chem Soc*, **94** (1972) 8399.
5 Sigel H, *Metal ions in biological systems*, Vol 2 (Marcel Dekker, New York) 1973.
6 Weber O A & Simeon V L, *Biochim Biophys Acta*, **244** (1971) 94.
7 William D R, *J chem Soc* (1970) 1550.
8 Voss R H & Jordan R B, *J Am chem Soc*, **98** (1976) 2173.
9 Letter J E & Jordan R B, *J Am chem Soc*, **97** (1975) 2381.
10 Martell E & Smith R M, *Critical stability constants* Vol 1: *Amino acids* (Plenum Press, London) 1974.
11 Fuoss R M, *J Am chem Soc*, **80** (1958) 5059.
12 Burgess J, *Metal ions in solution* (Ellis Horwood, England) 1978.
13 Swift T J & Connick R E, *J chem Phys*, **37** (1962) 307.
14 Basolo F & Pearson R G, *Mechanism of inorganic reactions*, (Wiley Interscience) (1967).

Indian Journal of Chemistry
Vol. 27A, August 1988, pp. 702-705

Kinetics & Mechanism of Oxidation of Aliphatic Ketones by Bromamine-B in Alkaline Buffer Medium

K MOHAN & D S MAHADEVAPPA*

Department of Post-graduate Studies & Research in Chemistry, University of Mysore, Manasagangothri, Mysore 570006

Received 7 *July* 1987; *revised* 8 *December* 1987; *accepted* 21 *December* 1987

The title reaction in buffer medium (*p*H 9-11) at 303.15 K shows first order dependence in $[oxidant]_0$ but variable dependence (one to zero) in $[ketone]_0$. The rate increases with increase in *p*H. The reaction product, benzenesulphonamide retards the rate. Variation of ionic strength of medium or the addition of halide ions has no effect on the rate. Kinetic and thermodynamic parameters have been calculated and the isokinetic temperature, 350 K is much above the temperature employed (303.15 K). The rate increases in the order: pentan-3-one < 4-methylpentan-2-one < pentan-2-one < butan-2-one < propan-2-one. A suitable mechanism is proposed.

A variety of compounds can be oxidized by bromamine-B (BAB)[1] both in acidic and alkaline media, but only a few of these reactions have been kinetically investigated. As a part of our broad programme[1] on mechanistic studies of oxidation of substrates with N-metallo-N-bromoarylsulphonamides, we report the kinetics of oxidation of propan-2-one, butan-2-one, pentan-2-one, pentan-3-one, 4-methylpentan-2-one by BAB in alkaline buffer medium (*p*H 9-11) at 30°C.

Materials and Methods

Bromamine-B was prepared in the laboratory[2] and its purity was checked iodometrically and by ^{13}C NMR. All solutions were prepared in triply distilled water.

Aqueous solution of BAB was standardized iodometrically and was preserved in brown bottles. Propan-2-one (AR, IDPL) was used after distillation. The other ketones (SDS, India) were redistilled before use. All other chemicals used were of AR grade. The ionic strength of reaction mixture was maintained at a constant high value by adding concentrated solution of $NaClO_4$. Standard buffer systems (borax + NaOH) were employed.

Kinetic measurements

Requisite amounts of oxidant, $NaClO_4$ and buffer (to keep the total volume constant for all runs) were taken in the pyrex tube blackened from outside and equilibrated at 30°C. A measured amount of aqueous solution of ketone of known concentration (≈ 0.2 mol dm^{-3}) also thermostated at the same temperature was rapidly added to the above mixture. The progress of reaction was monitored at different intervals of time by a double excess back titration of unreacted BAB in a measured aliquot of reaction mixture against standard BAB solution after adding a known excess of ascorbic acid (5×10^{-4} mol dm^{-3}). The course of the reaction was studied for more than two half-lives. The rate constants calculated were reproducible within ± 3%.

Regression analysis of experimental data was carried out on a TDC-316 computer and a EC-72 statistical calculator.

Stoichiometry

Reaction mixtures containing varying proportions of BAB and ketones were kept at room temperature in the presence of buffer of *p*H 9.9 for 24 hr. Estimation of the unreacted BAB showed that propan-2-one consumes 3 mol of oxidant per mol (Eq. 1) while a 1:2 stoichiometry (Eqs 2 and 3) prevailed for other ketones:

$$\begin{matrix} CH_3 \\ CH_3 \end{matrix}\!\!\rangle CO + 3PhSO_2NNaBr + 3H_2O \rightarrow HCOOH + CH_3COOH + 3PhSO_2NH_2 + 3NaBr \quad \ldots(1)$$

$$\begin{matrix} C_2H_5 \\ C_2H_5 \end{matrix}\!\!\rangle CO + 2PhSO_2NNaBr + H_2O \rightarrow CH_3COCOC_2H_5 + 2PhSO_2NH_2 + 2NaBr \quad \ldots(2)$$

$$\begin{matrix} CH_3 \\ R'CH_2 \end{matrix}\!\!\rangle CO + 2PhSO_2NNaBr + H_2O \rightarrow R'COCOCH_3 + 2PhSO_2NH_2 + 2NaBr \quad \ldots(3)$$

where R′ = $-CH_3$ for butan-2-one, $-CH_2.CH_3$ for pentan-2-one and $-CH(CH_3)_2$ for 4-methyl pentan-2-one.

The reaction product, $PhSO_2NH_2$ was detected by paper chromatography[2]. The end products formate and acetate ions formed during oxidation of propan-2-one were detected by spot tests[3a]. Diketones obtained in the oxidation of other ketones were quantitatively estimated through their 2,4-dinitrophenylhydrazone derivatives[3b].

Results

With $[ketone]_0$ in large excess, plots of log [BAB] versus time are linear ($r > 0.9904$, $S \leqslant 0.07$) indicating first order dependence on $[oxidant]_0$. The rate increases with increase in $[ketone]_0$ and a plot of log k' versus log $[ketone]_0$ is linear ($r > 0.9978$, $S \leqslant 0.07$) with unit slope. At higher $[ketone]_0$ the order is fractional and the rate becomes independent of $[ketone]_0$ (Table 1). The rate also increases with increase in pH and a plot of log k' versus pH is linear ($r > 0.9991$, $S \leqslant 0.03$) with a slope of unity showing a first order dependence on $[OH^-]$.

Addition of the reaction product, benzenesulphonamide ($PhSO_2NH_2$) retards the rate. Addition of Cl^-, Br^- or ClO_4^- ion had no effect on the rate. The solvent composition was varied by adding methanol (0-30%), but no significant change in the rate was noticed with increase in methanol content of the reaction medium. Addition of reaction mixture to aqueous acrylamide solution did not initiate polymerization ruling out the possibility of a radical mechanism.

The reaction was studied at different temperatures (298-313 K). From the linear plot of log k' versus $1/T$ ($r > 0.9946$) activation parameters were computed (Table 2).

Solvent isotope studies were made in D_2O medium (0-100%) with propan-2-one as a probe ($k'_{H_2O}/k'_{D_2O} = 0.55$). The results of proton inventory studies obtained with $H_2O - D_2O$ mixtures containing different atom fractions of deuterium (n) are presented in Table 3.

Discussion

In the present investigation, retardation of rate by added $PhSO_2NH_2$ and absence of a primary salt effect exclude the traditional mechanism[4,5] involving formation of an enolate ion. The initial enol content (in terms of $pK_{enol} = -\log K_{enol}$) was estimated[6]. For aliphatic ketones, $pK_{enol} > 7$, indicating that the initial

Table 1—Effect of Varying $[ketone]_0$ on Rate of Reaction.

($[BAB]_0 = 2.0 \times 10^{-4}$ mol dm^{-3}; $\mu = 0.5$ mol dm^{-3}; pH 9.9; temp: 303.15 K.)

10^2 $[ketone]_0$ (mol dm^{-3})	10^4 k' (s^{-1})				
	Propan-2-one	Butan-2-one	Pentan-2-one	Pentan-3-one	4-Methylpentan-2-one
0.5	3.72	2.41	2.03	0.94	1.24
1.0	6.87	4.75	4.32	1.96	2.48
1.5	10.80	7.40	7.38	2.78	3.72
2.0	13.31	9.54	9.02	3.81	5.14
3.0	20.10	14.80	12.95	5.63	7.43
4.0	25.90	18.70	17.49	7.55	9.40
5.0	30.50	24.60	23.58	9.36	13.00
6.0	33.30	28.50	26.40	10.46	15.20
8.0	35.20	33.50	31.10	13.50	19.20
10.0	38.60	36.50	34.10	16.10	21.70
15.0	40.10	39.10	37.20	17.60	23.00
17.0	40.20	39.20	37.20	17.70	23.20
20.0	40.30	39.40	37.40	17.80	—
25.0	—	39.40	37.50	18.10	—

Table 2—Kinetic and Thermodynamic Parameters for Oxidation of Aliphatic Ketones by BAB in a Buffer Medium (pH 9.9)

Ketone	E_a (kJ mol^{-1})	$\Delta H\ddagger$ (kJ mol^{-1})	$\Delta S\ddagger$ (JK^{-1}mol^{-1})	$\Delta G\ddagger$ (kJ mol^{-1})	log A
Propan-2-one	32.5	30.0 ± 0.1	−206.8 ± 0.3	93.2 ± 1.3	7.5
Butan-2-one	41.7	39.2 ± 0.1	−179.6 ± 0.0	94.1 ± 1.1	9.0
Pentan-2-one	45.1	42.6 ± 0.1	−169.2 ± 0.2	94.3 ± 0.9	9.5
Pentan-3-one	59.4	57.0 ± 0.1	−129.0 ± 0.6	96.3 ± 0.8	11.6
4-Methylpentan-2-one	50.2	47.8 ± 0.1	−157.4 ± 0.5	95.8 ± 1.0	10.1

Table 3—Results of Proton Inventory Studies for propan-2-one in $H_2O - D_2O$ mixtures at 303.15 K

([BAB] = 2×10^{-4} mol dm^{-3}; [ketone]$_0$ = 1.0×10^{-2} mol dm^{-3}; pH = 9,9; μ = 0.5 mol dm^{-3}).

n	$10^4\ k'_n$ (s^{-1})	$(k'_0/k'_n)^{1/2}$
0.000	6.87	1.0000
0.248	7.68	0.9458
0.496	8.84	0.8816
0.744	10.00	0.8289
0.932	12.43	0.7434

Table 4—Values of k_1 and k_{-1}/k_2 from double reciprocal plots

Ketone	k_1 (dm^{3}mol^{-1}s^{-1})	$10^{-2}(k_{-1}/k_2)$
Propan-2-one	71.0	2.3
Butan-2-one	75.3	3.5
Pentan-2-one	69.4	3.3
Pentan-3-one	72.7	13.3
4-Methyl pentan-2-one	66.1	7.5

enol content of these ketones is very small. Hence in the present studies at the pH employed it may be assumed that the substrate interacts through the keto form. In moderately alkaline BAB solutions the dominant oxidant species are $PhSO_2NHBr$ and HOBr and OBr^- ion becomes important at pH > 12. Hence Scheme 1 can be proposed to account for the observed kinetics. In Scheme 1 steps (i) and (ii) are slow steps, but step (ii) is rate limiting. Step (iii) is fast.

$$PhSO_2NHBr + OH^- \underset{k_{-1}}{\overset{k_1}{\rightleftharpoons}} PhSO_2NH^- + HOBr \quad \ldots(i)$$

$$HOBr + \text{ketone} \xrightarrow{k_2} X \quad \ldots(ii)$$

$$X + n\ HOBr \rightarrow \text{Products} \quad \ldots(iii)$$

(n = 2 for propan-2-one and 1 for other ketones)

Scheme 1

Scheme 1 leads to rate law (6)

$$-\frac{d[BAB]}{dt} = \frac{k_2 k_1 [BAB]_0 [\text{ketone}]_0 [OH^-]}{k_{-1}[PhSO_2NH^-] + k_2 [\text{ketone}]_0} \quad \ldots(6)$$

Equation (6) can be transformed into Eq. (7):

$$\frac{1}{k'} = \frac{k_{-1}[PhSO_2NH^-]}{k_2 k_1 [\text{ketone}]_0 [OH^-]} + \frac{1}{k_1 [OH^-]} \quad \ldots(7)$$

From the double reciprocal plot involving [ketone]$_0$ in the fractional range (Table 1), values of k_1 and k_{-1}/k_2 were calculated and are presented in Table 4.

The large negative entropy of activation values indicate a rigid activated state and the near constancy of $\Delta G^{\ddagger}$ values indicates the operation of a similar mechanism in the oxidation of all ketones.

Proton inventory studies

Solvent isotope studies in D_2O medium (Table 3) show an increase in rate, since OD^- is a stronger base[7] than OH^- ion. The proton inventory plot is expected to throw light on the nature of transition state[8,9]. The dependence of rate constant k'_n on atom fraction of deuterium (n) in a solvent mixture containing H_2O and D_2O is given by Eq. (8):

$$\frac{k'_n}{k'_0} = \frac{\prod_{TS}(1 - n + n\phi_i)}{\prod_{RS}(1 - n + n\phi_j)} \quad \ldots(8)$$

Here ϕ_i and ϕ_j are isotopic fraction factors for isotopically exchangable hydrogen sites in the transition state (TS) and reactant site (RS) respectively. If it is assumed that the reaction proceeds through a single transition state[9], Eq. (8) takes the forms shown in (9) and (10):

$$k'_n = k'_0 (1 - n + n\phi_j)^{-2} \quad \ldots(9)$$

$$(k'_0/k'_n)^{1/2} = [1 + n(\phi_j - 1)] \quad \ldots(10)$$

A plot of $(k'_0/k'_n)^{1/2}$ versus n should be linear. Such a plot is found to be linear (r = 0.9907, Fig. 1) with slope $(\phi_j - 1) = -0.27$ from which ϕ_j comes out to be 0.73. This value of ϕ_j agrees with the value of 0.8 suggested for the fractionation factor of OH^- ion by Kresge and Allred[10] and Gold and Crist[11].

Attempts were also made to arrive at a linear free energy relation[12] for the oxidation of ketones by BAB. Tests of the complete Taft equation and the single parameter correlations with polar substitution constant σ^* and steric substitution constant E_s have been made and the following regression equations (11-13) are obtained:

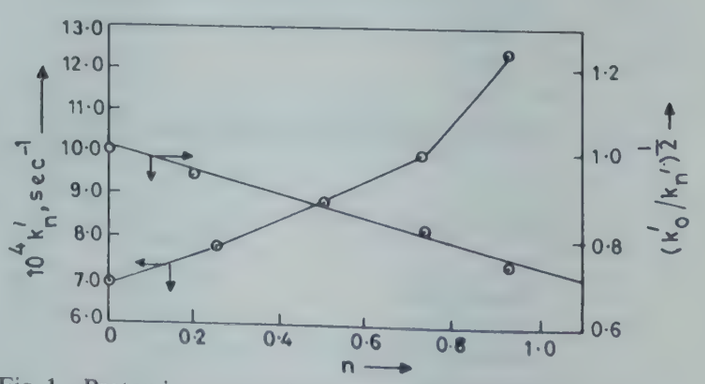

Fig. 1—Proton inventory plot for the oxidation of propan-2-one by BAB at 303.15 K ([BAB]$_0$ = 2.0×10^{-4} mol dm^{-3}; [ketone]$_0$ = 1.0×10^{-2} mol dm^{-3}; pH 9.9; μ = 0.5 mol dm^{-3}).

$$(\log k' - E_s) = -2.30\,\sigma^* + 0.78;\ (r = 0.5216) \quad \ldots(11)$$

$$\log k' = 2.63\,\sigma^* + 0.86;\ (r = 0.8274) \quad \ldots(12)$$

$$\log k' = 0.41\,E_s + 0.78;\ (r = 0.9554) \quad \ldots(13)$$

The poor correlation of k' values with the polar substitutent constant σ^* in Eq. (12) indicates that steric effects are important. A positive value of ρ^* (2.63) in Eq. (12) shows that elecron donating centres decrease the rate of reaction. Increase in inductive effect possibly decreases the acidic character of $-CH_2$ group α to the carbonyl, which is the site of attack. Attempts to use Pavelich-Taft equation[13] in the four-parameter form gave $\rho^* = 1.07$ and $\delta = 0.31$. It is observed that the rates of oxidation of ketones with BAB increases in the order: pentan-3-one < 4-methyl pentan-2-one < pentan-2-one < butan-2-one < propan-2-one.

The activation energy is highest for the slowest reaction and *vice versa*, indicating that it is enthalpy-controlled. This is verified by calculating the isokinetic temperature (β), which is much higher (350 K) than the temperature range employed (303 K) in the present work. The genuine nature of isokinetic relationship was also tested through the Exner criterion[14] by plotting log k' (35°C) versus log k' (25°C) ($r = 0.9984$) from which β was found to be 354 K.

Acknowledgement

One of the authors (K M) thanks the UGC, New Delhi, for the award of a research fellowship under the Faculty Improvement Programme. He is grateful to the Management of A V K College for Women, Hassan, for deputing him to University of Mysore.

References

1a Mahadevappa D S, Ananda S, Murthy A S A & Rangappa K S, *Tetrahedron*, **40** (1984) 1673.
b Mahadevappa D S & Ananda S, *Indian J Chem*, **24A** (1985) 589.
c Mahadevappa D S, Mohan K & Ananda S, *Tetrahedron*, **42** (1986) 4857.
2 Ahmed M S & Mahadevappa D S, *Talanta*, **27** (1980) 669.
3a Feigl F, *Spot tests in organic analysis*, (Elsevier, New York) 1956, pp. 462.
b Vogel A I, *Text-book of practical organic chemistry*, (ELBS Longman, London) 1973, p. 344.
4 Mushran S P, Sanehi R & Bose A K, *Acta Chim Acad Sci* (Hungary) **84** (1975) 135.
5a Bell R P & Archer G, *J chem Soc*, (1959) 3228.
b Bell R P & Yates K, *J chem Soc*, (1962) 1927.
6a Guthrie J P & Cullimore P A, *Can J Chem*, **57** (1979) 240.
b Guthrie J P, *Can J chem*, **57** (1979) 787.
7 *Isotope effect in chemical reactions*, edited by C J Collins & N S Bowman (Van-Nostrand-Reinhold, New York) 1970, p. 267.
8 Albery W J & Davies M H, *J chem Soc Faraday Trans*, (1972) 167.
9 Gopalakrishnan G & Hogg J L, *J org Chem*, **50** (1985) 1206.
10 Kresge A J & Allred A L, *J Am chem Soc*, **85** (1963) 1541.
11 Gold V & Crist S, *J chem Soc, Perkin Trans II*, (1972) 89.
12 Gilliom R D, *Introduction to physical organic chemistry*, (Addison-Wesley, London) 1970, pp. (a) 264, (b) 156-160.
13 Pavelich W A & Taft R W, *J Am chem Soc*, **79** (1957) 4935.
14 Exner O, *Coll Czech chem Commun*, **29** (1964) 1094.

Indian Journal of Chemistry
Vol. 27A, August 1988, pp. 706-707

Notes

Photochemical Reduction of Uranyl Ion with Ditertiary Phosphines

S S SANDHU* & M S SIDHU

Department of Chemistry, Guru Nanak Dev Univesity, Amritsar 143 005

and

A S BRAR

Department of Chemistry, Indian Institute of Technology, New Delhi

Received 21 *September* 1987; *revised and accepted* 23 *November* 1987

Photochemical reduction of uranyl ion with ditertiary phosphines, $Ph_2P(CH_2)_nPPh_2$ (where $n = 1$ to 4) leads to the formation of ditertiary phosphine oxides and uranium(IV). Decrease in quantum yield for U(IV) formation and increase in the Stern-Volmer constants(K_{sv}) with increase in the number of bridging methylene groups of ditertiary phosphines have been observed. This is attributed to an increase in vibrational degrees of freedom, leading to enhanced physical rather than chemical quenching of uranyl ion luminescence.

Inter- and intra-molecular hydrogen atom abstraction mechanisms have been suggested for photochemical reduction of uranyl ion with organic substrates. On the other hand, inorganic ions or molecules quench optically excited uranyl ion via inter- or intra-molecular electron transfer process[1,2]. In photochemical reduction of uranyl ion with triphenyl-phosphine/arsine/antimony/bismuthine[3], tri-*p*-tolylphosphine[4] and dialkyl sulphides[5], an oxygen atom transfer from uranyl ion to substrates has ben suggested. In the present investigation, ditertiary phosphines are oxidized to their respective oxides and the effect of increase in number of bridging methylene groups in ditertiary phosphines on efficiency of uranyl ion to photochemically oxidise these substrates has been investigated.

Substrates used were: 1,1-methylene-bis(diphenylphosphine) (MDP), 1,2-ethylene-bis(diphenylphosphine) (EDP), 1,3-propylene-bis(diphenylphosphine) (PDP) and 1,4-butylene-bis(diphenylphosphine) (BDP). The purity of MDP and PDP (Pressure Chem Co, Pittsburg) was checked before use. EDP and BDP were prepared from AR grade triphenylphosphine and purified by the literature method[6]. Experimental details are given elsewhere[4]. Fluorescence quenching was measured with a Perkin-Elmer MPF-448 fluorescence spectrophotometer and quantum yield of U(IV) formation was determined using potassium ferrioxalate as an actinometer[7].

Ditertiary phosphines absorb in the UV region ($n \rightarrow \pi^*$ and $\pi \rightarrow \pi^*$) whereas uranyl ion absorbs both in the UV and visible regions[1,2,8]. Pyrex glass photochemical reactor cuts off radiations below 350nm and prevents simultaneous excitation of ditertiary phosphines and uranyl ion. Protonation of uranyl ion with sulphuric acid is attended by a blue shift from 430nm ($\varepsilon_{max} = 45$ dm^3 mol^{-1} cm^{-1}) to 420 nm ($\varepsilon_{max} = 14.5$ dm^3 mol^{-1} cm^{-1}). However, addition of MDP (0.005 mol dm^{-3})/EDP (0.0050 mol dm^{-3})/PDP (0.0025 mol dm^{-3})/BDP(0.0025 mol dm^{-3}) to uranyl ion (0.010 mol dm^{-3}) in acidic solution does not affect the absorption spectra (shape and intensity) of uranyl ion in the visible region due to lack of ground state interaction between the two species.

It is likely that U(IV) formed may absorb radiation to get reoxidized to U(VI). In the presence of oxygen, tetra(acetylacetonato)uranium(IV) was shown to be photooxygenated to dioxouranium(VI)[9]. However, in the kinetic study of photo-accelerated uranium(IV)-uranium(VI) electron exchange reaction, it has been observed that light of wavelength 540-550 nm and > 600 nm which is absorbed by U(IV) is inefficient for photoexchange reactions[10]. Moreover, in an inert atmosphere (nitrogen), oxidation of U(IV) and ditertiary phosphines is not possible.

Upon irradiation all the solutions show decrease in absorbance at 420 nm for U(VI) and increase in absorbance at 660 nm for U(IV). This was used to monitor the progress of the reaction. Quantum yields for U(IV) formation are given in Table 1. The band at 636 nm or 770 nm or at higher wavelength was not observed, ruling out the possibility of U(V) formation[11,12]. On irradiating the solutions for a longer time under N_2 atmosphere, green crystals consisting of a mixture of U(IV) and U(VI) complexed with tertiary phosphines and/or tertiary phosphine oxides were obtained. Infrared spectra of the green crystals exhibited bands at 1040-1035 cm^{-1} due to coordinated phosphoryl group corresponding to oxides of MDP, EDP, PDP and BDP. The ESR spectrum (1450, 3100 and 8600G) of the green crystals also supported that it was mixture of U(IV) and U(VI).

During irradiation of uranyl ion, an electron jumps from HOMO (mainly consisting of oxygen $2p$ and uranium $5f/6d$ atomic orbitals) to LUMO (mainly consisting of non-bonding uranium $5f$ atomic orbital), thereby weakening and elongating the (U = O) double bond and reducing the extent of positive charge on uranium atom[8]. On the other hand $d\pi$-$p\pi$ interaction between phosphorus (phosphine) and oxygen (uranyl ion) facilitates oxygen atom transfer[13].

Table 1—Quantum Yield for Uranium(IV) Formation ($\phi_{U(IV)}$) and Stern-Volmer Constants (K_{sv}) for Photochemical Reduction of Uranyl Ion with Ditertiary Phosphines $[UO_2^{2+}] = 0.010$ mol dm^{-3}, $[H^+] = 0.40$ mol dm^{-3}

[Substrate] mol dm^{-3}	$\phi_{U(IV)}$	K_{sv} dm^3 mol^{-1}
	MDP	
0.0025	0.20	126.61
0.0050	0.32	
0.0075	0.39	
0.0100	0.49	
	EDP	
0.0025	0.19	317.24
0.0050	0.30	
0.0075	0.37	
0.0100	0.44	
	PDP	
0.0050	0.19	159.85
0.0075	0.23	
0.0100	0.27	
0.0125	0.30	
	BDP	
0.0050	0.10	207.25
0.0075	0.14	
0.0100	0.16	
0.0125	0.18	

Donor-acceptor interaction between excited uranyl ion and aromatic π-electrons[14,15] plays an important role in uranyl ion luminescence quenching and reduces the efficiency of photochemical reaction. Thus, aromatic π-electrons quench the luminescence due to uranyl ion to the same extent in the case of each phosphine. Solvent molecules also quench uranyl ion luminescence via energy transfer to higher overtones of the solvent molecules to the same extent in each reaction[1,16,17].

Photochemical reductions of uranyl ion with all the ditertiary phosphines obey Stern-Volmer equation (Eq. 1) in aqueous acidic medium.

$$\frac{I_f^o}{I_f} = 1 + K_{sv}[Q] \qquad \ldots (1)$$

The K_{sv} values (Table 1) increase with an increase in the number of bridging methylene groups, except for EDP which shows an abnormal behaviour. In the case of EDP decrease in quantum yield for U(IV) formation and increase in K_{sv} value are observed, though the electronic environment around phosphorus component remains almost constant.

Thus increase in physical quenching of excited uranyl ion through exciplex formation with ditertiary phosphines is due to an increase in the number of vibrational degrees of freedom ($3n$—6). However, the exceptional behaviour of EDP in this series of compounds is intriguing and is under investigation.

The authors are thankful to Prof P Natarajan, Madras University, Madras for providing luminescence measurement facilities and one of the authors (MSS) is grateful to Department of Atomic Energy, Government of India for financial assistance.

References

1 Burrows H D & Kemp T J, *Chem Soc Rev*, **3** (1974) 139.
2 Balzani V, Bolletta F, Gandolfi M T & Maestri M, *Topics in current chemistry*, Vol 75 (Springer-Verlag Berlin) 1978.
3 Sandhu S S, Sarpal A S & Brar A S, *Indian J Chem*, **19A** (1980) 413; **16A** (1978) 587; **18A** (1979) 19; **19A** (1980) 902.
4 Sandhu S S, Sidhu M S & Brar A S, *J Indian chem Soc*, **59** (1982) 173.
5 Sandhu S S, Kohli K B & Brar A S, *Inorg Chem*, **23** (1984) 3609.
6 Aguiar A M & Beisler J, *J org Chem*, **29** (1964) 1660.
7 Calvert J G & Pitts J N, *Photochemistry* (John Wiley, New York) 1966.
8 McGlynn S P & Smith J K, *J mol Spectro*, **6** (1961) 164.
9 Sostero S, Traverso O, Magon L, Zanella P & Scibona G, *J chem soc Dalton*, (1980) 1324.
10 Kato V & Fukutomi H, *J inorg nucl Chem*, **38** (1976) 1323.
11 Cauzzo G, Gennari G, Giacometti G, Agostini G C & Gambaro A, *Inorg chim Acta*, **32** (1979) 45.
12 Rofer DePoorter C K & DePoorter G L, *J inorg nucl Chem*, **41** (1979) 215.
13 Kosolapoff G M & Mair L, *Organic phosphorus compounds*, Vol 1 (John Wiley, New York) 1972.
14 Matsushima R & Sakuraba S, *J Am chem Soc*, **93** (1971) 7143.
15 Matsushima R, *J Am chem Soc*, **94** (1972) 6010.
16 Kuhn K, Wasgestlan F & Kubka H, *J phys Chem*, **85** (1961) 665.
17 Pant D D & Pant H C, *Indian J pure appl Phys*, **6** (1968) 219.

Indian Journal of Chemistry
Vol. 27A, August 1988, pp. 708-709

Gamma Radiolysis of Anhydrous & Hydrated Thorium Nitrates

D G GARWAY, D V PARWATE & A N GARG*
Department of Chemistry,
Nagpur University, Nagpur 440010

Received 17 *July* 1987; *revised* 27 *November* 1987;
accepted 21 *December* 1987

The γ-ray induced decomposition of anhydrous and hexahydrated thorium nitrates has been studied using ^{60}Co γ-source in the dose range of 38-550 kGy. The $G(NO_2^-)$ values decrease somewhat exponentially with the dose. Gamma-radiolysis of 0.05 and 0.1 *M* aqueous solutions has also been studied at 45 kGy.

Decomposition of alkali metal and many other nitrates induced by γ-radiation has been investigated by several workers[1-8]. Baberkin and Proskurnin[9] have observed that $G(NO_2^-)$ are higher in some hydrated nitrates than those in the corresponding anhydrous crystals. Previous works[1,4-6] from our laboratory on the γ-radiolysis of mono-, bi-, and trivalent metal nitrates have shown that the nature of outer cation and water of crystallisation affect the $G(NO_2^-)$ values considerably. Herein we report the results of γ-radiolysis of both anhydrous and hexahydrated thorium nitrates at an absorbed dose of 38-550 kGy. Preliminary results of γ-radiolysis of 0.05 and 0.1 *M* aqueous solutions of thorium nitrate are also reported.

All chemicals used were of AR grade and solutions were prepared in doubly distilled water. Samples in dried Corning glassware were irradiated at room temperature in cobalt-60 gamma chamber at a dose rate of 1.90 kGy hr^{-1}. Gamma dose was measured with Fricke dosimeter using $G(Fe^{3+}) = 15.6$. The damage product, nitrite was estimated spectrophotometrically at 540 nm employing a Beckman model DU-2 spectrophotometer and following the diazo colour reaction of Shin[10] as modified by Kershaw and Chamberlin[11]. The *G*-values were calculated on the basis of the total dose absorbed without any further correction. Blank correction was found to be quite significant in both the cases.

The plots of growth of damage nitrite, $[NO_2^-]$ with dose (in the range of 38 to 550 kGy) for both anhydrous and hexahydrated thorium nitrate samples are linear and pass through the origin at low doses (<0.1 MGy). At higher doses such plots, though linear, show sharp breaks and the rate of production of $[NO_2^-]$ becomes slow. It follows a first order rate equation (1)

$$[NO_2^-] = kD + C \quad \ldots (1)$$

where D is the absorbed dose and k and C are constants. At low doses (<0.1 MGy) C vanishes and the rate of decomposition is very fast. The $G(NO_2^-)$ values for both the samples decrease almost exponentially with increase in dose. Yields of NO_2^- and $G(NO_2^-)$ at an absorbed dose of 4.5 Mrads for both the samples as well as in aqueous solutions (0.05 *M* and 0.1 *M*) of thorium nitrate are given in Table 1.

Chen and Johnson[12] have postulated the mechanism, shown in Scheme 1, for nitrate decomposition.

$$MNO_3 \rightarrow MNO_2 + O \quad \ldots (i)$$
$$O + NO_3^- \rightarrow NO_2^- + O_2 \quad (ii)$$
$$O + NO_2^- \rightarrow NO_3^- \quad \ldots (iii)$$
$$O + O \rightarrow O_2 \quad \ldots (iv)$$

Scheme 1

However, recent studies have indicated that the reaction mechanism is complex and the formation of NO, NO_2, NO_3^{2-} and NO_2^{2-} including some excited species has been also proposed[13,14]. The decomposition of nitrates has been shown to be complex with dependence on lattice parameters, linear energy transfer, temperature and pressure[15].

The predominance of either of reactions, (ii), (iii) and (iv) may make the decomposition a fast or slow process. Probably at higher doses when all the water molecules have been consumed, recombination processes (iii) and (iv) may be taking place, or the whole lattice may be getting disturbed so that the production of NO_2^- becomes slow. It is further observed that the rate of production of NO_2^- is higher for hydrated form as

Table 1 – Yield of NO_2^- and $G(NO_2^-)$ Values for Thorium Nitrate at an Absorbed Dose of 45 kGy.

Sample	Conc. of NO_2^- (ppm)	$G(NO_2^-)$
$Th(NO_3)_4$ (solid)	356 ± 10	1.55 ± 0.04
$Th(NO_3)_4.6H_2O$ (solid)	457 ± 9	2.10 ± 0.07
$Th(NO_3)_4.6H_2O$, (0.05 *M* aq soln)	63.0 ± 0.1	0.22 ± 0.01
$Th(NO_3)_4.6H_2O$, (0.1 *M* aq. soln)	77.8 ± 0.2	0.36 ± 0.01

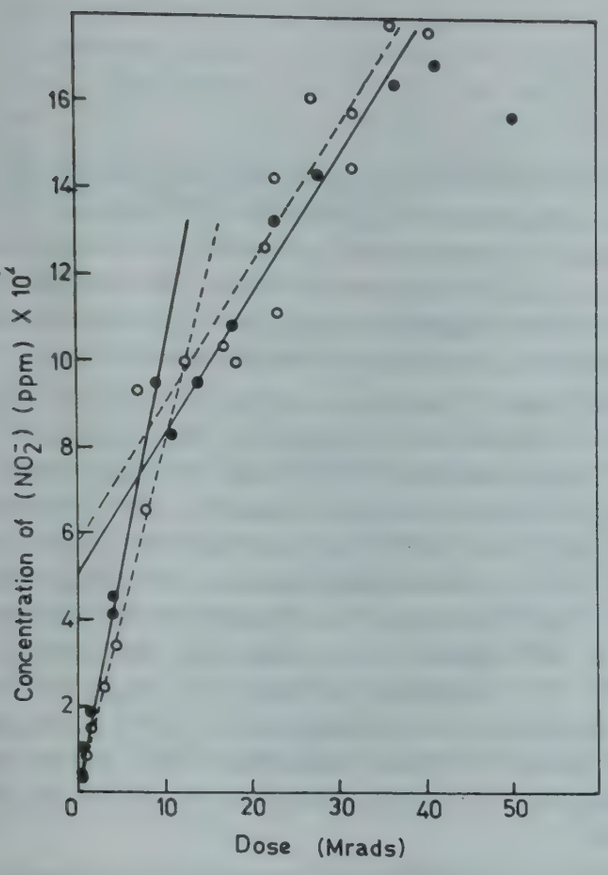

Fig. 1 – Yield of nitrite ion formation with absorbed dose in hydrated (●) and anhydrous (○) thorium nitrate samples.

compared to that for the anhydrous compound. It is expected that only one NO_3^- is available in the case of nitrates of monovalent cations while increasing number of nitrate ions are available for the decomposition of nitrates of multivalent cations. Thus $G(NO_2^-)$ is bound to be higher for nitrates of higher valent cations. The presence of six water molecules in $Th(NO_3)_4.6H_2O$ may facilitate the decomposition as was observed in the case of mercuric nitrate[6]. In both the cases $G(NO_2^-)$ values decrease with dose almost in an exponential manner, though slowly in the case of anhydrous salt. In case of anhydrous form variation of $G(NO_2^-)$ versus dose is not smooth but several breaks are observed. This type of behaviour may possibily be due to phase transformation or some other microcrystalline changes taking place in the crystals. Baberkin and Proskurnin[9] have postulated a reverse reaction of the type (iii) for anhydrous calcium nitrate. In hydrated salt, either the rate of this reaction is slowed down or the reaction is completely stopped presumably due to structural interferences from water molecules. The presence of water molecules of crystallisation might accelerate the process of radiolytic decomposition because of species such as H_3O^+ and OH^- which are likely to be formed in the lattice itself[1].

It may also be noted from Fig. 1 that the role of water of crystallization in the radiolysis is only at the initial doses up to about 0.1 MGy. Beyond this dose, $G(NO_2^-)$ values are almost similar for anhydrous and hydrated thorium nitrate samples. It implies that all the water molecules of crystallization get radiolysed at <0.1 MGy upto which production of NO_2^- is accelerated. After this, however, the production of NO_2^- becomes slower because of non-availability of other participating species.

In aqueous solution of $Th(NO_3)_4.6H_2O$, the rate of production of NO_2^- is considerably slowed down (Table 1) and resultant $G(NO_2^-)$ values are also low. With increase in thorium nitrate concentration, the yield of (NO_2^-) and $G(NO_2^-)$ both increase but not in the same proportion. In this case, major part of energy is likely to be shared by the solvent molecules and only a fraction is available for radiolytic decomposition of the nitrate salt. Also the large number of oxidising species so formed may be combining to retard the formation of NO_2^-.

Further investigations are in progress to pinpoint the role of water of crystallization or of solvent.

References

1 Batra R J & Garg A N, *Radiochem Radioanal Lett*, **53** (1982) 177.
2 Doigan P & Davis T W, *J phys Chem*, **56** (1952) 764.
3 Hochandel P J & Davis T W, *J chem Phys*, **27** (1957) 333.
4 Kulkarni S P & Garg A N, *Indian J Chem*, **23A** (1984) 712.
5 Kulkarni S P & Garg A N, *J radioanal nucl chem Articles*, **98** (1986) 65.
6 Parwate D V & Garg A N, *J radioanal nucl chem Lett*, **85** (1984) 203.
7 Patil S F & Nalawade C G, *Radiochem Radioanal Lett*, **45** (1980) 133; **46** (1981) 343.
8 Shrivastava S B, Sarpotdar A S & Shankar J, *Indian J Chem*, **8** (1970) 426; **9** (1971) 144.
9 Baberkin A S & Proskurnin M A, *Dokl Akad Nauk SSSR*, **121** (1958) 492; Baberkin A S, *Dokl Akad Nauk SSSR*, **126** (1959) 591.
10 Shinn M B, *Ind. engng Chem (anal edn)*, **13** (1941) 33.
11 Kershaw N F & Chamberlin N S, *Ind engng Chem (anal edn)*, **14** (1942) 312.
12 Chen T H & Johnson E R, *J phys Chem*, **66** (1962) 2249.
13 Muhammad D & Maddock A G, *J chem Soc Faraday Trans I*, **74** (1978) 919.
14 Fuller A M & Torr C E, *J chem Phys*, **56** (1971) 438.
15 Johnson E R, *The radiation induced decomposition of inorganic molecular ions* (Gordon and Breach, New York), 1970.

Indian Journal of Chemistry
Vol. 27A, August 1988, pp. 710-711

Effect of Substituents on Thermal Stability of Some Vinyl Polymers

H L GIRDHAR & G M PEERZADA*
Department of Chemistry, University of Kashmir, Srinagar 190 006

Received 26 *October* 1987; *revised and accepted* 21 *December* 1987

Thermal decomposition of polyacrylic acid, polyacrylamide, polyacrylonitrile, polymethylacrylate and polystyrene has been studied by thermogravimetry. The order of thermal stabilities of these polymers is in accordance with the relative order of the electron-withdrawing power of the side groups on the hydrocarbon backbone of repeat unit, i.e. the thermal stabilities of these polymers follow the order : CN > COOH > COOR > Ar > $CONH_2$

Thermal degradation of polymers is mainly caused by chemical bond cleavage at elevated temperatures and therefore, it is expected to be largely dependent on the chemical structure of the polymer. So far the discussion of the structural effects on the thermal behaviour of polymers is of qualitative nature in most cases[1,2]. Numerous data have been published[3] on thermal and oxidative degradation of vinyl polymers. However, the data could not be correlated because of the differences in the temperature range, the experimental conditions and the methods of preparing the polymeric samples. Presently we have studied the thermal behaviour of five vinyl polymers containing acid, ester, nitrile, amide and phenyl substituent groups prepared under similar conditions.

Polyacrylic acid (PAA), polyacrylamide (PAM) and polyacrylonitrile (PAN) were prepared by solution polymerization using benzoyl peroxide (2% by wt of monomer) as initiator. However, polymethylacrylate (PMA) and polystyrene (PS) were prepared by bulk polymerization using the above mentioned concentration of the initiator. The details of the purification and drying of polymeric samples are similar to those reported earlier[4]. The average molecular weights of PAA, PAM, PAN, PMA and PS were 27×10^4, 11.5×10^4, 5.3×10^4, 20.1×10^4 and 1.1×10^4 respectively.

Thermal decomposition of powdered polymeric samples of particle size in the range of 151-195 μm was studied by TG technique at two different heating rates under nitrogen at a flow rate of 40ml/min. The sample holder was a small pyrex crucible. However, in certain cases where the temperature employed was > 700°C a stainless steel crucible was used. The desired linear heating rate was obtained using a solid state temperature programmer-cum-indicator. The maximum fluctuation in the linearity of heating rate was ± 1°C. For each run 100mg of the sample was used and the weight of the sample as a function of temperature was recorded with an accuracy of 1 mg.

The plots of fraction decomposed, α versus temperature for the five polymers at a heating rate of ~ 10°C/min, show that PAM, PS and PMA decompose very little before the sharp mass loss that occurs at 250°, 400° and 425°C respectively. But both PAA and PAN show some mass loss steps prior to the sharp fall in their TG curves. PAA decomposes with a mass loss of 80% prior to the sharp fall that occurs at 530°C. PAN degrades with only 65% mass loss before the occurrence of sharp fall at 710°C. Although PAN shows 30% mass loss upto 400°C, above this temperature, it is more stable than the other four polymers.

The order of stability of the polymers examined on the basis of the temperatures corresponding to the occurrence of the sharp fall in mass loss is found to be : PAN > PAA > PMA > PS > PAM. Experiments were also repeated at a heating rate of 5°C/min. The general trend of TG curves and the order of relative stabilities were found to be the same as discussed above. However, a decrease in heating rate shifted the mass loss curves towards lower temperature which is expected since mass loss is a function of both time and temperature.

These results reveal that the stability of vinyl polymers is affected by the type of substituent groups. In view of the complexity of degradation processes, an attempt is made to arrive at some correlation concerning the stability and the field effect of the substituent group. If it is assumed that the side groups are relatively stable to heat and the principal reaction sites are the main chains, then a free radical mechanism is operative because C-C bonds are scarcely polarized. In that case the role of side group in weakening the adjacent C-C bonds in the hydrocarbon backbone of the polymer will depend upon its electron-donating power. The electron withdrawing nature of CN, COOH, COOR and aryl(Ar) groups follow the order: CN > COOH > COOR > Ar. Due to the presence of lone pair of electrons on nitrogen in $CONH_2$, the electron-withdrawing power of $-CO-$ is nullified and the $CONH_2$ group has practically no field effect. Therefore, the position of $CONH_2$ should be below Ar, It is interesting to note that the relative order of the

thermal stabilities of vinyl polymers observed from TG experiments is in accordance with the order of the electron-withdrawing power of the substituent groups, viz CN > COOH > COOR > Ar > $CONH_2$.

The authors are indebted to the Ministry of Defence, New Delhi for financial aid.

References

1 Stivala S S & Reich L, *Polym Engg &Sci*, **20** (1980) 654.
2 *Aspects of degradation and stabilization of polymers*, edited by H H G Jellinek (Elsevier, New York) 1978.
3 *Thermal stability of polymers*, Vol 1, edited by R T Conley (Marcel Dekker, New York) 1970.
4 Girdhar H L, Peerzada G M & Handoo D, *Fuel*, **64** (1985) 1011.

Indian Journal of Chemistry
Vol. 27A, August 1988, pp. 712-713

A Novel Synthetic Route for Preparation of Ammonium, Alkali Metal & Monoalkylammonium Hexafluorosilicates

K SYED MOHAMED† & D K PADMA*
Department of Inorganic and Physical Chemistry, Indian Institute of Science, Bangalore 560 012

Received 24 *August* 1987; *revised* 15 *December* 1987; *accepted* 7 *January* 1987

A one-pot method has been developed for the synthesis of ammonium, alkali metal and monoalkylammonium hexafluorosilicates. The chlorides of ammonium, sodium and potassium, bromides of rubidium and cesium and monoalkylamines react with pyridinium hexafluorosilicate at room temperature to form the corresponding hexafluorosilicates in high yields (~90%). The products obtained have been characterised by elemental analyses, IR, PMR spectra, and X-ray powder diffraction data.

Hexafluorosilicates are widely used in industry[1,2] and research, from water fluoridation to photovoltaic applications[3]. Despite several methods[4-9] available for their preparation, very few methods give pure salts in good yields. Herein we report a general, one-pot method for obtaining these salts at room temperature in a pure state and high yields.

All the chemicals used were of either AR(BDH) or GR(Merck) grade. Solvents were purified by standard procedure. Pyridine and alkylamines were purified by distillation over potassium hydroxide.

Preparation of ammonium and alkali metal hexafluorosilicates

To a solution of pyridinium hexafluorosilicate[10] (5g) in water (10 ml) was added a solution of ammonium chloride (1.9 g)/sodium chloride (2.29g)/potassium chloride (2.9 g)/rubidium bromide (3.4 g)/cesium bromide (4.38 g), in water (10 ml). In the case of the ammonium salt, a clear solution resulted whereas with alkali metal salts, immediate precipitation occurred. The clear solution containing the ammonium salt when treated with 95% ethanol (50 ml) afforded a precipitate which was filtered, washed and dried in a vacuum desicator. The yield of ammonium hexafluorosilicate was 86% and that of sodium, potassium, rubidium, and cesium hexafluorosilicates the yields were 95-96%. The salts were analysed for their SiF_6^{2-} content[11] (see Table 1). The IR spectra[12] of these hexafluorosilicates exhibited the ν(Si-F) and δ(Si-F) modes respectively as follows (cm^{-1}): Na_2SiF_6, 725 vs, 480 s; K_2SiF_6, 740 vs, 480s; Rb_2SiF_6, 740 vs, 480 s; and Cs_2SiF_6, 740s, 480s; $(NH_4)_2SiF_6$ 725 vs, 480s (this salt exhibited νNH and δN—H modes at 3300 and 1410 cm^{-1} respectively). The *d*-spacings in the X-ray powder patterns of these salts were in agreement with the values reported in literature[13].

Table 1—Analytical Data of Hexafluorosilicates (M_2SiF_6)

M_2SiF_6 (M =)	SiF_6(%) Found (calc)	N(%) Found(calc)
Ammonium	78.85(79.78)	15.61(15.72)
Sodium	74.80(75.54)	—
Potassium	64.05(64.56)	—
Rubidium	45.60(45.59)	—
Cesium	34.59(34.84)	—
n-$C_3H_7NH_3$	53.63(54.21)	10.60(10.68)
i-$C_3H_7NH_3$	54.55(54.21)	10.62(10.68)
n-$C_4H_9NH_3$	48.76(48.98)	9.60 (9.65)
t-$C_4H_9NH_3$	48.67(48.98)	9.59 (9.65)
$C_6H_{11}NH_3$	41.58(41.54)	8.15 (8.18)
$C_6H_5CH_2NH_3$	40.02(39.68)	7.80 (7.82)

Table 2—^1H NMR Chemical Shifts (δ, ppm) of Monoalkylammonium Hexafluorosilicates

Compound	(ppm)
1. $(n\text{-}C_3H_7NH_3)_2SiF_6$	0.93t(-CH_3) 1.6 m(β—CH_2) 2.9 t(α—CH_2)
2. $(i\text{-}C_3H_7NH_3)_2SiF_6$	1.3 d (—C $\langle$ CH_2 / CH_2 3.5 m (—CH$\rangle$)
3. $(n-C_4H_9NH_3)_2SiF_6$	0.93 t (CH_3-) 1.47 m (β and γ CH_2) 3.0 t (α − CH_2)
4. $(t-C_4H_9NH_3)_2S_iF_6$	1.33 s(—C − C $\langle$ CH_3 / CH_3 / CH_3
5. $(C_6H_{11}NH_3)_2SiF_6$	1.57 m (10 ring protons except α-proton) 3.10 s (α-proton)
6. $(C_6H_5CH_2NH_3)_2SiF_6$	4.02 s (−CH_2—) 7.40 s (C_6H_5—)

S = singlet, d = doublet, t = triplet, M = multiplet.

Preparation of monoalkylammonium hexafluorosilicates

Pyridinium hexafluorosilicate when treated with the more basic amines (compared to pyridine) displaced pyridine to form alkyl substituted ammonium hexafluorosilicates.

† Dept. of Chemistry, Govt. Arts & Science College, Krishnagiri, Tamil Nadu

To pyridinium hexafluorosilicate (5 g) was added *n*-propylamine (4 ml) dropwise with cooling and stirring. A pasty mass was formed. After 1 hr at room temperature, the contents were stirred with ether when a white precipitate was thrown out. The precipitate was filtered, washed with ether till free from pyridine, dried and stored in a vacuum dessicator over phosphorus pentoxide. The yield of *n*-propylammonium hexafluorosilicate was 90% (3.91 g). Five other monoalkylammonium hexafluorosilicates were prepared in a similar manner using the primary amines, viz. isopropylamine, *n*-butylamine, *t*-butylamine, cyclohexylamine and benzylamine. The yields varied in the range of 90-93%. These products were characterised by elemental analyses (see Table 1).

The results indicate that both ammonium and alkali metal hexafluorosilicates have been obtained in high yields. The analytical data, IR spectral analysis and X-ray powder diffraction data clearly indicate that the salts are pure. In the case of monoalkylammonium hexafluorosilicates, the IR spectra exhibit bands characteristic of the octahedrally symmetric (O_h) hexafluorosilicate anion, in the regions 720-740 and 470-480 cm^{-1} corresponding to the ν(Si-F) and δ(Si-F) modes, respectively of the alkali metal hexafluorosilicates indicating that the cation does not have a major influence on the anion. For the cation, the ν(N—H) and ν(C—H) show characteristic strong vibrations which merge due to overlap of the spectral regions (2800-3240 cm^{-1}). In addition to these vibrations, there are a number of bands in the region 2800-2300 cm^{-1} which might be due to the amine salt combination bands. Similar, observations have been made by Harris and Rudner[14]. All other vibrations are due to organic moieties. The δ(N—H) occurs in the region 1560-1590 cm^{-1}.

The ^1H NMR spectra (D_2O as solvent: DSS-internal standard) of all the alkylammonium hexafluorosilicates identify the organic moieties (see Table 2).

References

1 Lange W in *Fluorine chemistry*, Vol 1, edited by J H Simons (Academic Press, New York) 1050 p, 125.

2 Ryss I C, *The chemistry of fluorine and its inorganic compounds* (State Publishing House for Scientific, Technical and Chemical Literature, Moscow) 1956; AEC (tr) 3292 (Part 1) pp 123.

3 Carleton K L, Olson J M & Kibbler A, *J electrochemc Soc*, **130** (1983) 782.

4 Schnell E, *Mh Chem*, **93** (1962) 65.

5 Guertin J P & Onyzchuk M, *Can J Chem*, **47** (1969) 1275.

6 Enan A A, Kats B M, Petrosyan U P & Chekirda T N, *Zh neorg Khim*, **20** (1975) 382.

7 Petrosyan V P & Ennan A A, *Zh neorg Khim*, **24** (1979) 1562.

8 Ennan A A, Garrilova L A & Gorina M V, *Zh Obschch Khim*, **46** (1976) 1656.

9 Harris J J & Rudner B, *J inorg nucl chem*, **34** (1972) 75.

10 Kalbandkeri R G, Syed Mohamed K, Padma D K & Vasudeva Murthy A R, *Polyhedron*, **4** (1985) 787.

11 Jacobson C A, *J phys Chem*, **28** (1924) 506.

12 Brown D H, Dixon K R, Livingston C M, Nuttal R H & Sharp D W A, *J chem Soc A*, (1967) 100.

13 *X-ray powder diffraction file*, published by the Joint Committee on Powder Diffraction Standard, Pennsylvania, 19103, 1967, 7-13, 8-36, 7-217, 7-207, 7-6.

14 Harris J J & Rudner B, *J inorg nucl chem*, **34** (1972) 75.

Indian Journal of Chemistry
Vol. 27A, August 1988, pp. 714-715

Alternative Routes to the Synthesis of Chevreul's Salt, $Cu^{II}[Cu^{I}(SO_3)]_2.2H_2O$

MANABENDRA N BHATTACHARJEE, MIHIR K CHAUDHURI* & MINAKSHI DEVI

Department of Chemistry, North-Eastern Hill University, Shillong 793 003

Received 9 *November* 1987; *revised and accepted* 16 *December* 1987

Yellow Etard's salt ($Cu^{I}_2SO_3.1/2H_2O$) and red Chevreul's salt ($Cu^{II}[Cu^{I}SO_3]_2.2H_2O$) have been synthesised by the reaction of cupric acetate or freshly prepared $Cu(OH)_2$ with SO_2(g) in aqueous medium. Characterisation of the compounds is based on the results of elemental analyses, IR spectral and magnetic moment studies and chemical reactions.

The literature[1-3] methods of preparation of Chevreul's salt (cupric cuprososulphite, $Cu^{II}[Cu^{I}-SO_3]_2.2H_2O$) involves either the use of $KHSO_3$ in a considerably high amount or the prior synthesis of Etard's salt ($Cu^{I}SO_3.1/2H_2O$). The latter method always yields impure product containing an equimolar mixture of metallic copper and $Cu[CuSO_3]_2.2H_2O$. In view of the current interest[4] in mixed valence metal complexes, we have reinvestigated the sulphito-chemistry of copper and have developed two new straight-forward methods for the synthesis of the title compound. The chosen reaction strategies also enabled us to obtain Etard's salt in a pure form, as an intermediate product.

Reagent grade chemicals were used. Copper(II) hydroxide was precipitated from $CuCl_2.2H_2O$, centrifuged and washed several times to make it free from chloride and alkali. IR spectra were recorded on a Perkin-Elmer model 983 spectrophotometer. Magnetic susceptibility measurements were made by Guoy method using $Hg[Co(NCS)_4]$ as the calibrant.

Total copper content in the compounds was estimated iodometrically[5] after oxidation with H_2O_2 and removal of excess peroxide. In Chevreul's salt, $Cu[CuSO_3]_2.2H_2O$, the percentage of cupric copper was determined by direct iodometric titration. The difference between the total copper content and that of cupric ion, directly afforded the percentage of cuprous ion in the compound. Sulphur was estimated[6] as $BaSO_4$ after conversion of sulphite to sulphate by boiling with H_2O_2.

Synthesis of Chevreul's salt ($Cu^{II}[Cu^{I}SO_3]_2.2H_2O$)

Method I: Through an aqueous suspension of freshly prepared copper(II) hydroxide was bubbled SO_2 gas for ~10 min. The suspended hydroxide slowly went into solution, the colour of which gradually turned to light blue with simultaneous appearance of some yellow precipitate. On bubbling the gas for further 5 min, the precipitate redissolved resulting in a clear, transparent light blue solution. The bubbling of SO_2 was stopped at this stage, and the solution was heated on a steam-bath for 15 min whereupon a red crystalline compound which analysed for $Cu^{II}[Cu^{I}SO_3]_2.2H_2O$ separated out. The compound was washed thrice with acetone and dried *in vacuo*.

Method II: Through an aqueous solution of hydrated cupric acetate [$Cu(CH_3COO)_2.H_2O$], SO_2 gas was bubbled for ~20 min to obtain a clear light blue solution. The rest of the procedure, including isolation of the compound was similar to that described under method-I.

(Found: Cu, 49.1; S, 16.2. Calc for $Cu_3S_2O_8H_4$; Cu, 49.3; S, 16.6%); μ_{eff} (298 K), 1.82 B.M.; IR (cm^{-1}): 1030 m, 995s, 980m, 915m, 860w, 638m, 580m and 485 (SO modes).

Isolation of intermediate yellow product: Etard's salt ($Cu_2SO_3.1/2H_2O$)

The yellow precipitate obtained in the preparation of $Cu[CuSO_3]_2.2H_2O$ (vide method-I) was filtered off, and the filtrate was treated with ethanol taken in an amount equal to half the volume of the filtrate. The mixture was allowed to stand for 5 min in a deep freeze when an additional amount of yellow precipitate was obtained. Both the lots of the yellow products were purified by separately washing with ethanol and finally dried *in vacuo*. Each of the products analysed for $Cu_2SO_3.1/2H_2O$ (Found: 58.6; S, 14.4. Calcd. for $Cu_2SO_{3.5}H$: Cu, 58.8; S, 14.8%); IR (cm^{-1}): 980m, 892m, 661s, 490sh and 480s (SO modes).

In the course of our studies on fluoro(sulphato)cuprates(II)[7], attempts were made to synthesise the aforesaid compounds from a reaction mixture containing $Cu(OH)_2$, alkali metal fluoride, SO_2(g) and H_2O_2. However all attempts led to a red compound, which analysed for $Cu[CuSO_3]_2.2H_2O$. This prompted us to study the behaviour of copper(II) ion in the presence of SO_2 under different experimental conditions. Accordingly, reactions of copper(II) with SO_2 gas in aqueous as well as organic media were carried out. Reaction of either an acidified (dil. H_2SO_4) aqueous solution of cupric sulphate or that of a suspension of it in acetonitrile, with SO_2 gas resulted in the total reduction of copper(II) to copper(I). Similar observation was also made when cupric acetate or freshly prepared cupric hydroxide was treated with SO_2 gas in

acetonitrile. On the contrary, when the reaction of cupric acetate or a suspension of freshly prepared cupric hydroxide with SO_2 gas was performed in an aqueous medium (see preparation of Chevreul's salt) the colour of the solution was still observed to be blue although partial conversion of copper(II) to copper(I) was not discounted. The reduction in the intensity of the blue colour of the solution supported this contention. The resultant solution obtained at this stage, on being warmed on a steam-bath, afforded Chevreul's salt. It is to be noted that if bubbling of SO_2 gas is stopped at a stage when the yellow product just begins to appear and the mother liquor is treated with ethanol to obtain another crop of the yellow product, the compound obtained under this condition is identified as similar to that of Etard's salt ($Cu_2SO_3.1/2H_2O$). This, therefore, provides evidence that reaction proceeds through the formation of Etard's salt as an intermediate.

Thus it is imperative to emphasise, in accord with our experimental conditions and findings, that the reaction of copper(II) with SO_2 should not be conducted with a pre-acidified solution. From the course of reactions, as monitored by the isolation of products at different stages (Etard's salt and Chevreul's salt, respectively), it may be concluded that SO_2 only partly reduces copper(II) to copper(I). Thus SO_2 plays at least two important roles, viz. as a controlled reducing agent for copper(II) and also to produce SO_3^{2-} in the reaction medium which coordinates with copper centre permitting isolation of the products. Another significant aspect of the present methods of synthesis is that the mixed valence cupric cuprososulphite compound prepared by either method is obtained in a very pure form, which is evident from the results of chemical analyses, IR spectrum, magnetic moment and chemical reactions.

For example, treatment of the red $Cu[CuSO_3]_2.2H_2O$ with aqueous ammonia dissolves the copper compound completely in the form of soluble ammine complexes producing a clear transparent blue solution and leaves no residue of metallic copper. This implies that no impurity of metallic copper is present in the compound, as opposed to that of Rogojski's salt[3]. The above mentioned chemical reaction is considered crucial for checking the purity of the product. Further, the results of direct iodometric titration of the mixed valence compound showed electron-transfer corresponding to one-third of the total copper content in the compound, which is in accord witht the formulation.

The analytical data and physical properties of both the compounds, reported herein, are in conformity with those reported earlier[3,8]. $Cu[CuSO_3]_2.2H_2O$ is only sparingly soluble in water. $Cu_2SO_3.1/2H_2O$, as expected, showed diamagnetic behaviour[3]. The room temperature (298 K) magnetic moment of the mixed-valence $Cu[CuSO_3]_2.2H_2O$ is found to be 1.82 B.M. This value, of course, is slightly higher than that of Rogojski's salt (1.76 B.M.)[3], which, however, is an equimolar mixture of $Cu[CuSO_3]_2.2H_2O$ and copper powder. The appearance of νSO modes at higher wave number regions as compared to those of the free SO_3^{2-} ion as well as the strong band at 995 cm^{-1} in the IR spectrum of Chevreul's salt imply that the pyramidal sulphite group is bonded to metal centre through sulphur[9,10]. Moreover, the appearance of a moderate intensity band at 915 cm^{-1} causes[10,11] us to infer that there also exists an appreciable interaction between an oxygen atom of SO_3^{2-} and copper centre, in agreement with the crystal structure of the compound, reported earlier[12]. This indicates that the pyramidal C_{3v} symmetry of the SO_3 group may not be absolutely preserved in this compound[11]. The IR spectrum of $Cu_2SO_3.1/2H_2O$ is straightforward and compares very well with earlier reports[3].

One of the authors (NMB) is thankful to the Principal, Shillong College, Shillong for his permission to carry out the work. The award of a SRF to MD by CSIR is gratefully acknowledged.

References

1 Mellor J W, *Comprehensive treatise on inorganic and theoretical chemistry*, Vol 10 (Longmans, London) 1930, 277.
2 Morgan G T & Burstall F H, *J chem Soc*, (1927) 1259.
3 Dasent W E & Morrison D, *J inorg nucl Chem*, **26** (1964) 1122.
4 Straughan B P, Lam O M & Earnshaw A, *J chem Soc Dalton Trans*, (1987) 97.
5 Vogel A I, *A text book of quantitative inorganic analysis*, (ELBS & Longmans, London) 1978, 379.
6 Ref. 5, P 504.
7 Bhattacharjee M N, Chaudhuri M K & Devi M, *Polyhedron, in press.*
8 *Sneed M C, Maynard J L &Brasted R C, Comprehensive inorganic chemistry*, Vol 2 (Van Nostrand, New York) 1954, 104.
9 Cotton F A & Francis R, *J Am chem Soc*, **82** (1960) 2986.
10 Nyberg B & Larsson R, *Acta chem Scand*, **27** (1973) 63.
11 Nakamoto K, *Infrared and Raman spectra of inorganic and coordination compounds*, (Wiley Interscience, New York) 1977, 247.
12 Kierkegaard P & Nyberg B, *Acta chem Scand*, **19** (1965) 2189.

Indian Journal of Chemistry
Vol. 27A, August 1988, pp. 716-718

Excess Volume of Mixing for Binary Mixtures of Polar Solutes (Methyl Iodide, Ethyl Iodide & *n*-Propyl Iodide) & Non-polar Hydrocarbon Solvents (Cyclohexane, Benzene, *p*-Xylene & Mesitylene)

R R YADAVA*, S S YADAV & S R MAURYA
Chemistry Department, Gorakhpur University, Gorakhpur 273 009

Received 6 *April* 1987; *revised and accepted* 20 *October* 1987

The excess volume of mixing (V^E) for twelve binary mixtures of polar solutes, viz., methyl iodide, ethyl iodide and *n*-propyl iodide with non-polar hydrocarbon solvents, viz., cyclohexane, benzene, *p*-xylene and mesitylene has been measured at 293.15 K for the whole composition range. The V^E values are positive for all the systems throughout the concentration range and have been analysed in terms of molecular interactions. The interactions appear to be dipole-induced dipole type subsceptible to steric effects as indicated by progressive lowering of V^E values with the methylation of aromatic hydrocarbon.

Experimental determination[1-3] of excess volumes for suitably chosen mixtures has provided valuable information regarding the molecular interactions and has also served as a valuable check of different theories of solutions[4,5]. Molecular interaction between the polar molecules, viz., methyl iodide, ethyl iodide and *n*-propyl iodide and the non-polar molecules, viz., cyclohexane, benzene, *p*-xylene and mesitylene, was studied in these laboratories by dielectric constant and refractivity measurements[6]. It was thought worthwhile to study the molecular interactions between the said binary mixtures by excess volume measurements.

The polar solutes (methyl iodide, ethyl iodide and *n*-propyl iodide) (all SISCO reagents) were purified by the method described by Cowley and Partington[7]. The aromatic solvents, benzene (Sarabhai M., spectroscopic grade), *p*-xylene (E. Merck) and mesitylene (E. Merck) were used after distillation. Cyclohexane (Riedel, spectroscopic grade) was used as such.

For each system studied, a series of samples over the whole composition range were prepared gravimetrically. In order to avoid evaporation losses during the preparation of samples, liquids were injected by a syringe into rubber sealed vials. The samples were equilibrated in a thermostatic bath maintained at 293.15 ± 0.1 K. The excess volumes (V^E) have been computed from the densities (determined by Pyknometric method, accurate to ± 0.0001) and the composition of the mixture as,

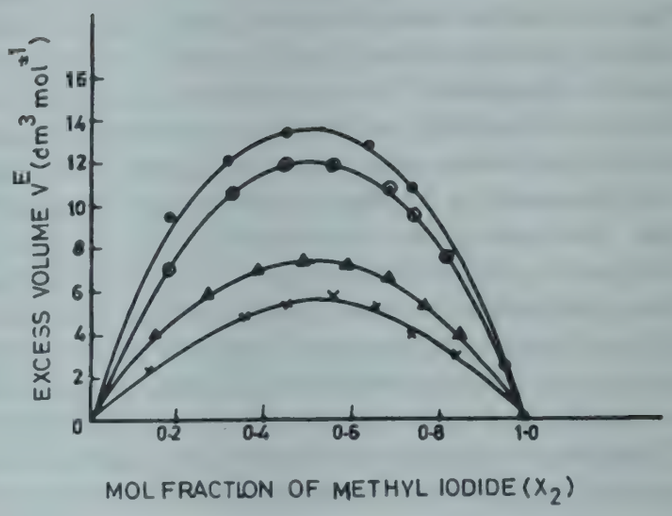

Fig. 1—Variation of excess volume at 293.15 K with mole fraction of methyl iodide [●, methyl iodide-cyclohexane system; ⊙, methyl iodide-benzene system; △, methyl iodide-*p*-xylene system; ×, methyl iodide-mesitylene system]

$$V^E = V_{mixture} - V_{ideal} \quad \ldots (1)$$

$$V_{mixture} = \frac{x_1 M_1 + x_2 M_2}{d_{mixture}} \quad \ldots (2)$$

$$V_{ideal} = x_1 V_1 + x_2 V_2 \quad \ldots (3)$$

where x_1 and x_2 are the mole fractions, M_1 and M_2 the molecular weights and V_1 and V_2 the molar volumes of neat non-polar solvent and polar solute, respectively; $d_{mixture}$ is the density of the mixture at the experimental temperature.

Experimental results for the twelve binary system studied are graphically represented in Figs 1 to 3. The results were fitted using a least square procedure to an equation of the form,

$$V^E = x_1 x_2 [A + B(x_1 - x_2) + C(x_1 - x_2)^2] \quad \ldots (4)$$

A, B and C are constants for each system and are given in Table 1. Standard deviation calculated by Eq. 5,

$$\sigma(V^E)/Cm^3\,mol^{-1} = [\Sigma(\Delta V^E)^2 \times (m-n)^{-1}]^{1/2} \ldots (5)$$

where $\Delta V^E = V^E_{(exp.)} - V^E_{(calc.)}$, m is the number of observations and n is the number of constants used in Eq. (4), are given in Table 1. $V^E_{calc.}$ refers to the value of V^E obtained from Eq. (4) using the constants A, B and C.

Table 1—Parameters of Equation 4 and Standard Deviations

Systems	A ($cm^3\ mol^{-1}$)	B ($cm^3\ mol^{-1}$)	C ($cm^3\ mol^{-1}$)	$\sigma(V^E)$ ($cm^3\ mol^{-1}$)
1 Methyl iodide + cyclohexane	54.5719	3.4051	6.0166	0.3599
2 Methyl iodide + benzene	47.4050	2.8800	4.0676	0.4566
3 Methyl iodide + *p*-xylene	28.9401	0.1797	2.9160	0.1487
4 Methyl iodide + mesitylene	22.3356	0.3913	−3.6798	0.3632
5 Ethyl iodide + cyclohexane	56.3603	1.5587	2.3647	0.1649
6 Ethyl iodide + benzene	48.9813	2.7307	−3.8672	0.1575
7 Ethyl iodide + *p*-xylene	34.4219	−1.9996	3.9987	0.1892
8 Ethyl iodide + mesitylene	28.0269	0.1919	−5.0602	0.3614
9 *n*-Propyl iodide + cyclohexane	63.6082	−3.9497	2.2609	0.4604
10 *n*-Propyl iodide + benzene	54.5109	1.0951	−1.7104	0.1899
11 *n*-Propyl iodide + *p*-xylene	38.8341	−1.3787	0.0711	0.1892
12 *n*-Propyl iodide + mesitylene	31.8223	−1.3123	2.2607	0.1531

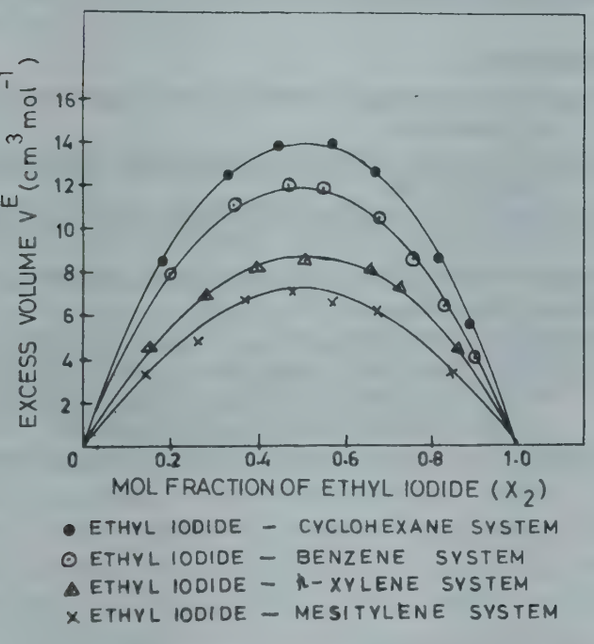

Fig. 2—Variation of excess volume at 293.15 K with mole fraction of ethyl iodide [●, ethyl iodide-cyclohexane system; ⊙, ethyl iodide-benzene system; △, ethyl iodide-*p*-xylene system; ×, ethyl iodide-mesitylene system]

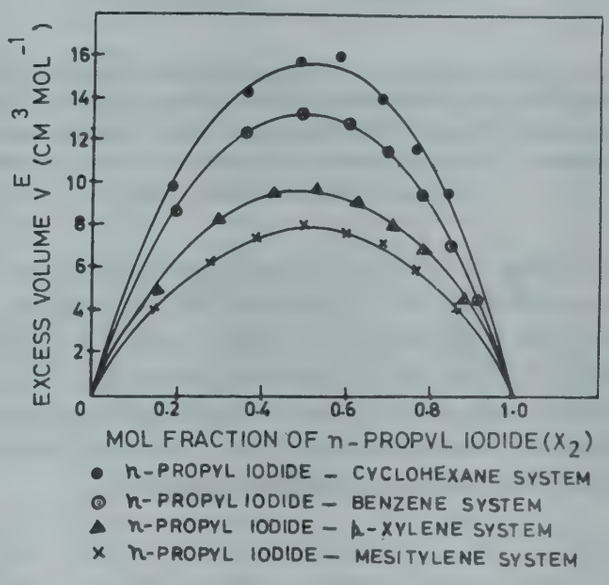

Fig. 3—Variation of excess volume at 293.15 K with mole fraction of *n*-propyl iodide [●, *n*-propyl iodide-cyclohexane system; ⊙, *n*-propyl iodide-benzene system; △, *n*-propyl iodide-*p*-xylene system; ×, *n*-propyl iodide-mesitylene system]

The excess volume of mixing may be used as a qualitative guide to the extent of molecular interactions in binary liquid mixtures of non-electrolytes; V^E is generally large and positive if the unlike interactions within the solutions are weak and the system is tending towards liquid-liquid immiscibility. On the contrary, V^E decreases and eventually becomes negative as the unlike interactions become stronger. Anderson *et al.*[8] measured V^E for nitroethane and a number of hydrocarbons of increasing electron donating power and found that V^E increases with the ionization potential of the hydrocarbon.

In the present study, V^E has been found to be positive for all the mixtures with the maximum lying at the middle of the composition range (Figs 1 to 3), i.e., corresponding to $x_1 = x_2 = 0.5$. V^E values for the equimolar mixtures of all the three polar solutes with different non-polar solvents are in the order: cyclohexane > benzene > *p*-xylene > mesitylene, which is same as the order of their ionization potential values (Fig. 4).

The order of V^E values for equimolar mixtures of a non-polar solvent with different polar solutes is: *n*-propyl iodide > ethyl iodide > methyl iodide.

In view of what has been said just now, it becomes clear that the interactions between unlike molecules of the polar solute and non-polar solvent are far less than the interactions between a pair of solute molecules or a pair of non-polar solvent molecules. However, the gradual lowering of V^E values for any solute from cyclohexane to mesitylene shows that as the ionization potential of the non-polar solvent decreases, the interactions have a tendency to become stronger. This indicates the manifestation of specific

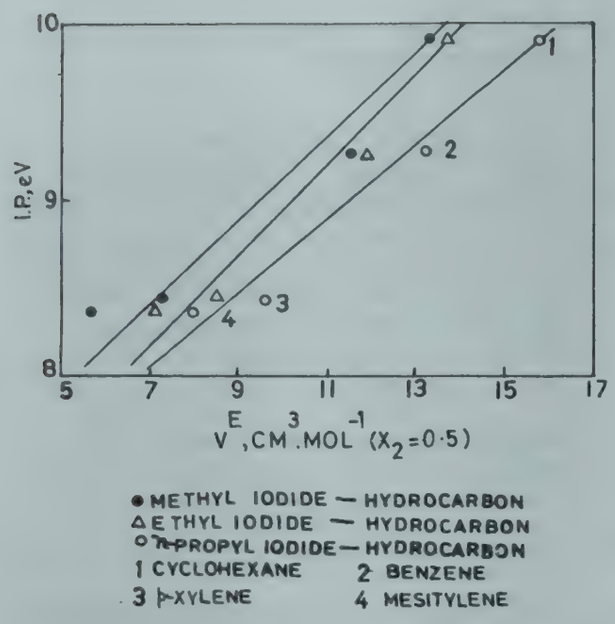

Fig. 4—The correlation of the experimental excess volume of mixing for equimolar solution with the ionisation potential of hydrocarbons [●, methyl iodide-hydrocarbon; △ ethyl iodide-hydrocarbon; ○, *n*-propyl iodide-hydrocarbon (1 cyclohexane, 2 benzene, 3 *p*-xylene, 4 mesitylene)]

interaction of the electron acceptor-donor type. To test whether there is a quantitative relationship between the experimental V^E values and the electron donating power of the non-polar solvent, V^E values for the equimolar mixtures were plotted against the respective ionization potentials. The plot (Fig.4) is linear within limits of experimental error.

In view of the absence of a charge transfer band in the UV spectrum for these systems, it cannot be said unequivocally that the complexing is of charge-transfer type. Even if the interactions are of donor-acceptor type, the strength of such bonding must be extremely weak.

The order of V^E values for any polar solute with different non-polar solvents of increasing polarisability seems to be mainly governed by dipole-induced dipole interactions.

The order of V^E values for any non-polar solvent with the different polar solutes is same as the order of their molar volumes and seems to be governed by the size of the polar solute molecules.

The authors are thankful to the Head, Department of Chemistry, Gorakhpur University, for providing laboratory facilities.

References

1 Duncan W A, Sheridan J P & Swinton F L, *Trans Faraday Soc*, **62** (1966) 1090.
2 Nigam R K, Singh P P, Mishra R & Singh M, *Indian J Chem*, **18A** (1979) 492.
3 Chowdhury M C & Krishnan V R, *Indian J Chem*, **14A** (1976) 377.
4 Nigam R K & Singh P P, *Trans Faraday Soc*, **65** (1966) 1950.
5 Battino Rubin, *Chem Rev*, **71** (1971) 5.
6 Yadav R R & Maurya S R, *Indian J Chem*, **25A** (1986) 460.
7 *Techniques of chemistry-organic solvents*, Vol. II, 3rd Edn, edited by John A Riddick & William B Bunger, Weissberger series (Wiley-Interscience, New York), 1970.
8 Anderson R, Cambio R & Prausnitz J M, *J A I Ch E*, **8** (1962) 66.

Indian Journal of Chemistry
Vol. 27A, August 1988, pp. 719-720

Excess Molar Volumes of Ternary Mixtures of Non-electrolytes

R K NIGAM* & SADHANA AGGARWAL
Department of Chemistry, Maharshi Dayanand University, Rohtak 124 001

Received 27 *July* 1987; *revised* 1 *October* 1987; *accepted* 21 *October* 1987

Excess molar volumes, V^E_{ijk} of the ternary (i+j+k) system, 1,2-dichloroethane (i)+pyridine (j)+α-picoline (k), 1,2-dichloroethane (i)+*n*-heptane (j)+pyridine (k), 1,2-dichloroethane (i)+n-heptane (j)+α-picoline (k), *n*-heptane (i)+pyridine (j)+α-picoline (k), aniline (i)+pyridine (j)+α-picoline (k)+γ-picoline (k) have been measured as a function of composition at 308.15 K.

Since the i-i and j-j contacts in the pure i and j components are replaced by the i-j contacts in the (i+j) mixture, it appears that interactions in a ternary (i+j+k) mixture should be closely dependent on the interactions in (i+j), (j+k), and (i+k) binary mixtures. It was instructive to measure the V^E_{ijk} values of ternary mixtures and correlate them to their corresponding binary mixtures.

1,2-Dichloroethane, pyridine, α- and γ-picolines, aniline and *n*-heptane (all BDH, AR grade) were purified by standard procedure[1] and their purities were checked by measuring their densities at 293.15 ± 0.01 K; these agreed to within ± 0.00005 gm cm^{-3} with the corresponding literature values[2].

Excess molr volumes V^E_{ijk} were determined using a dilatometer[3] similar to that used by Brown and Smith[4], the difference being that there were now three limbs for the three components. The temperature of the water bath was controlled within ± 0.01 K. The change in the level of the liquid in the dilatometer capillary was measured by a cathetometer (accuracy ± 0.001 cm). To ensure complete mixing in the capillary, the dilatometer was placed in a cold bath so that there was a minimum amount of liquid in the capillary. The cold bath was replaced the experimental water bath. This process was repeated two or three times. The uncertainty in the measured V^E_{ijk} values is 0.55%.

The V^E_{ijk} data for the various ternary (i+j+k) mixtures as a fnction of composition at 308.15 K are recorded in Table 1. These data were expressed as

Table 1—Excess Molar Volumes (V^E_{ijk}) for Various Ternary (i+j+k) System at 308.15 K

x_i	x_j	V^E_{ijk} ($cm^3\ mol^{-1}$)	x_i	x_j	V^E_{ijk} ($cm^3\ mol^{-1}$)
(I) 1,2-Dichloroethane(i)+pyridine(j)+α-picoline(k)					
0.1006	0.5066	0.089	0.4074	0.3316	0.203
0.2484	0.1154	0.098	0.4129	0.1683	0.146
0.2533	0.7827	0.147	0.5121	0.4002	0.210
0.2543	0.5711	0.131	0.7647	0.0777	0.122
0.2938	0.2188	0.129			
(II) 1,2-Dichloroethane(i)+*n*-heptane(j)+pyridine(k)					
0.1769	0.1240	0.178	0.4636	0.0326	0.215
0.1942	0.3080	0.336	0.5201	0.3593	0.719
0.1972	0.0789	0.158	0.6601	0.2312	0.539
0.2362	0.5461	0.637	0.8240	0.0960	0.261
0.2863	0.2392	0.315			
(III) 1,2-Dichloroethane(i)+*n*-heptane(j)+α-picoline(k)					
0.0847	0.6642	0.369	0.4724	0.1847	0.335
0.1046	0.0811	0.053	0.4753	0.0581	0.165
0.1260	0.7820	0.420	0.4818	0.3750	0.596
0.1851	0.3933	0.364	0.5275	0.2953	0.554
0.1973	0.0544	0.065	0.6395	0.2102	0.150
(IV) *n*-heptane(i)+pyridine(j)+γ-picoline(k)					
0.0546	0.7268	0.044	0.2998	0.4064	0.122
0.0556	0.5247	0.042	0.3126	0.4928	0.077
0.0772	0.1605	0.033	0.3191	0.3040	0.160
0.0774	0.5112	0.047	0.3612	0.1105	0.124
0.2994	0.3812	0.132	0.6185	0.0643	0.237
(V) Aniline(i)+pyridine(j)+α-picoline(k)					
0.0748	0.8214	−0.153	0.3341	0.3395	−0.479
0.1141	0.0714	−0.287	0.4102	0.3630	−0.499
0.1257	0.7541	−0.241	0.4505	0.1694	−0.473
0.1339	0.1942	−0.290	0.6378	0.1276	−0.382
0.1372	0.1159	−0.312	0.7312	0.0838	−0.291
0.2488	0.6279	−0.362	0.8341	0.0941	−0.174
0.2906	0.4188	−0.451			
(VI) Aniline(i)+pyridine(j)+γ-picoline(j)					
0.0576	0.1212	−0.106	0.2554	0.3372	−0.314
0.0576	0.8186	−0.100	0.2817	0.3965	−0.331
0.1242	0.5739	−0.188	0.4385	0.3486	−0.362
0.1375	0.2168	−0.206	0.5684	0.1368	−0.299
0.1684	0.4867	−0.241	0.6721	0.1421	−0.247
0.2208	0.6941	−0.319	0.7891	0.0799	−0.157

$$V^E_{ijk} = x_i x_j \left[\sum_{n=0}^{2} A^n_{ij}(x_i - x_j)^n\right] + x_j x_k \left[\sum_{n=0}^{2} A^n_{jk}(x_j - x_k)^n\right] + x_i x_k \left[\sum_{n=0}^{2} A^n_{ik}(x_i - x_k)^n\right] + x_i x_j x_k \left[\sum_{n=0}^{2} A^n_{ijk}(x_j - x_k)^n x_i^n\right] \quad \ldots (1)$$

Table 2—Parameters A^0_{ijk}, A^1_{ijk} and A^2_{ijk} of Eq. (1) for Various Ternary (i + j + k) Systems at 308.15 K

System	A^0_{ijk} ($cm^3\ mol^{-1}$)	A^1_{ijk} ($cm^3\ mol^{-1}$)	A^2_{ijk} ($cm^3\ mol^{-1}$)
(I)	0.160	0.262	−41.8224
(II)	−3.5865	22.4	19.833
(III)	−2.000	4.600	−11.700
(IV)	−2.700	−17.100	−200.6
(V)	−2.00	−0.480	114.460
(VI)	−1.340	0.220	21.860

where x_i and x_j are the mole fractions of the i^{th} and the j^{th} components in (i + j + k) mixture, and $A^n (n = 0 - 2)$, etc., are parameters characteristic of the binary (i + j) mixtures. The A^n_{ijk} $(n = 0 - 2)$ parameters (4) in Eq. (1) were evaluated by fitting

$$\left\{V^E_{ijk} - x_i x_j\left[\sum_{n=0}^{2} A^n_{ij}(x_i - x_j)^n\right] - x_j x_k\left[\sum_{n=0}^{2} A^n_{jk}(x_j - x_k)\right] - x_i x_k\left[\sum_{n=0}^{2} A^n_{ik}(x_i - x_k)^n\right]\right\} \Big/ x_i x_j x_k$$

data to Eq. (2)

$$[A^0_{ijk} + A^1_{ijk}(x_j - x_k)x_i + A^2_{ijk}(x_j - x_k)^2 x_i^2] \qquad \ldots (2)$$

by the method of least squares and the values are recorded in Table 2. The parameters A^n_{ij}, A^n_{jk} and A^n_{ik} etc. for the (i + j), (j + k) and (i + k) binary mixtures were taken from literature[2,5]. The standard deviation in V^E_{ijk} values for all the systems is found to be in the vicinity of 0.0002 $cm^3\ mol^{-1}_E$.

There are no literature values of V_{ijk} with which to compare our V^E_{ijk} data. Excess molar volumes for 1,2-dichloroethane (i) + pyridine (j) + α-picoline (k), 1,2-dichloroethane (i) + n-heptane (j) + pyridine (k) and 1,2-dichloroethane (i) + n-heptane (j)-γ-picoline (k) are all positive for all the values of x^i, x^j and x^k. The sign of excess molar volumes V^E_{ijk} is dictated by the values of x_i, x_j and x_k for *n*-heptane (i) + pyridine (j) + α-picoline (k) mixtures. V^E_{ijk} values are all negative for entire range of x_i, x_j and x_k for the mixtures aniline (i) + pyridine (j) + α-picoline (k) and + γ-picoline (k).

One of the authors (S A) thanks the CSIR, New Delhi for the award of a senior research fellowship.

References

1 Vogel A I, *A text book of practical organic chemistry* (ELBS/Longmans, London) 1978.
2 Nigam R K, Singh P P, Aggarwal Sadhana & Sharma S P, *Fluid Phase Equilibria*, **16** (1984) 25.
3 Singh P P & Sharma V K, *Can J Chem*, **61** (1983) 2321-2328.
4 Brown I & Smith F, *Aust J Chem*, **15** (1962).
5 Singh P P, Nigam R K & Sharma S P, *Thermochim Acta*, **63** (1983) 237.

Indian Journal of Chemistry
Vol. 27A, August 1988, pp. 721-724

Thermodynamic Properties of Binary Mixtures of Bromoform with Benzene, Toluene, *p*-Xylene, Nitrobenzene, Acetonitrile & Tetrahydrofuran†

T M AMINABHAVI*, L S MANJESHWAR, S S JOSHI, S B HALLIGUDI & R H BALUNDGI

Department of Chemistry, Karnatak University, Dharwad 580 003

Received 17 *July* 1987; *revised and accepted* 16 *November* 1987

Previously published data on densities and viscosities of binary mixtures of bromoform with benzene, toluene, *p*-xylene, acetonitrile, nitrobenzene and tetrahydrofuran at 298.15, 308.15 and 318.15 K have been used to predict a number of excess thermodynamic quantities such as excess enthalpy, excess entropy, excess Gibb's free energy of flow and excess heat capacity of mixing. A few viscosity models have also been tested to discuss their relative merits.

In continuation of our earlier work[1] on thermodynamic properties of bromoform containing binaries, we now report additional thermodynamic data on the title binaries using density and viscosity results obtained at 298.15, 308.15 and 318.15 K. A few viscosity models have also been tested to discuss their relative merits.

All the solvents used were of either BDH or Fluka AG grade and were purified by standard procedures[2]. The binary mixtures were prepared on volume fraction basis (ϕ). Densities and viscosities of the binaries were measured as described elsewhere[3]. The temperature was maintained constant within ± 0.01 K at 298.15 K and ± 0.05 K at 308.15 and 318.15 K. All computations were done on an HP1000 computer available at CSMRI, Bhavnagar.

The binary contact interaction parameter (A_{12}) and density increment $(\partial\rho/\partial\phi_1)_{P,T}$ were calculated employing Eqs (1) and (2) respectively.

$$A_{12} = (\phi_1\rho_1 + \phi_2\rho_2 - \rho)/\phi_1\phi_2\rho \qquad \ldots (1)$$

and

$$(\partial\rho/\partial\phi_1)_{P,T} = \frac{(\rho_1 - \rho_2) - \rho[A_{12}(\phi_2 - \phi_1) + d A_{12}/d\phi_1(\phi_1\phi_2)]}{(1 + A_{12}\phi_1\phi_2)} \qquad \ldots (2)$$

Details of calculations to compute these parameters have appeared elsewhere[4,5] and the data are presented in Table 1. A_{12} is negative for binaries of bromoform with benzene, toluene, acetonitrile and tetrahydrofuran and positive for those of *p*-xylene and nitrobenzene. Density increments are positive over the entire range of composition for all the mixtures at 298.15, 308.15 and 318.15 K.

Excess molar Gibbs free energies (ΔG^{*E}) of activation as calculated from Eq. (3) from viscosity data were used to calculate excess enthalpy (ΔH^{*E}) (Eq. 4), excess entropy (ΔS^{*E}) (Eq. 5) and excess heat capacity (ΔC_p^{*E}) of activation (Eq. 6) at equimolar concentrations (i.e. $x_1 \approx x_2 \approx 0.5$)

$$\Delta G^{*E} = RT(\ln \eta V - x_1 \ln \eta_1 V_1 - x_2 \ln \eta_2 V_2) \qquad \ldots (3)$$

$$\Delta H^{*E} = -RT^2\left\{\left[\frac{\partial \ln \eta}{\partial T}\right] - x_1\left[\frac{\partial \ln \eta_1}{\partial T}\right] - x_2\left[\frac{\partial \ln \eta_2}{\partial T}\right] + \frac{1}{V}\left[\frac{\partial V}{\partial T}\right] - \frac{x_1}{V_1}\left[\frac{\partial V_1}{\partial T}\right] - \frac{x_2}{V_2}\left[\frac{\partial V_2}{\partial T}\right]\right\} \qquad \ldots (4)$$

$$\Delta S^{*E} = (\Delta H^{*E} - \Delta G^{*E})/T \qquad \ldots (5)$$

$$\Delta C_p^{*E} = -2RT\left\{\left[\frac{\partial \ln \eta}{\partial T}\right] - x_1\left[\frac{\partial \ln \eta_1}{\partial T}\right] - x_2\left[\frac{\partial \ln \eta_2}{\partial T}\right] + \frac{1}{V}\left[\frac{dv}{dT}\right] - \frac{x_1}{V_1}\left[\frac{dV_1}{dT}\right] - \frac{x_2}{V_2}\left[\frac{dV_2}{dT}\right]\right\} - RT^2\left\{\left[\frac{\partial^2 \ln \eta}{\partial T^2}\right] - x_1\left[\frac{\partial^2 \ln \eta_1}{\partial T^2}\right] - x_2\left[\frac{\partial^2 \ln \eta_2}{\partial T^2}\right] + \frac{1}{V}\left[\frac{\partial^2 V}{\partial T^2}\right] - \frac{x_1}{V_1}\left[\frac{\partial^2 V_1}{\delta T^2}\right] - \frac{x_2}{V_2}\left[\frac{\partial^2 V_2}{\partial T^2}\right]\right\} - \left[\frac{1}{V}\frac{\partial V}{\partial T}\right]^2 + x_1\left[\frac{1}{V_1}\frac{\partial V_1}{\partial T}\right]^2 + x_2\left[\frac{1}{V_2}\frac{\partial V_2}{\partial T}\right]^2 \qquad \ldots (6)$$

In Eqs (3-6) the term RT has the conventional meaning; V is molar volume of the mixture; V_1, V_2 and x_1, x_2 are respectively the molar volumes and mol fractions of components 1 and 2; η, η_1, and

†Based on the Ph D thesis of LSM submitted to Karnatak University (1987).

‡Present address: Central Salt & Marine Chemicals Research Institute, Bhavnagar 364 002.

Table 1 – Binary Contact Interaction Parameter and Density Increment of Binaries at 298.15, 308.15 and 318.15 K

ϕ_1	A_{12} (Eq. 1) at			$(\partial\rho/\partial\phi_1)_{P,T}$ (Eq. 2) at		
	298.15	308.15	318.15 K	298.15	308.15	318.15 K
			(I) Bromoform(1)-benzene(2)			
0.15	−0.017	−0.028	−0.034	1.983	1.957	1.843
0.30	−0.016	−0.016	−0.035	1.960	1.936	1.869
0.50	−0.019	−0.025	−0.023	1.935	1.916	1.913
0.65	−0.009	−0.019	−0.021	1.945	1.929	1.926
0.85	0.000	−0.003	−0.033	2.041	2.023	1.864
			(II) Bromoform(1)-toluene(2)			
0.15	−0.025	−0.005	−0.009	1.810	1.979	1.900
0.30	−0.029	−0.005	0.026	1.867	1.957	1.932
0.50	−0.002	−0.006	−0.009	1.959	1.932	1.963
0.65	−0.001	−0.000	−0.010	1.982	1.940	1.952
0.85	−0.028	0.010	−0.014	1.831	2.027	1.832
			(III) Bromoform(1)-p-xylene(2)			
0.15	0.013	0.008	0.007	2.006	1.992	1.971
0.30	0.011	0.007	0.003	1.995	1.971	1.963
0.50	0.010	0.008	0.004	1.979	1.947	1.949
0.65	0.009	0.010	0.002	1.976	1.952	1.945
0.85	0.014	0.020	0.005	2.006	2.030	1.962
			(IV) Bromoform(1)-acetonitrile(2)			
0.30	−0.011	−0.013	−0.013	2.070	2.084	2.070
0.50	−0.017	−0.022	−0.020	2.062	2.062	2.051
0.65	−0.019	−0.027	−0.024	2.048	2.037	2.032
0.85	−0.023	−0.028	−0.025	2.015	2.003	2.012
0.95	−0.027	−0.035	−0.028	1.993	1.992	2.010
			(V) Bromoform(1)-nitrobenzene(2)			
0.15	0.012	0.017	0.013	1.618	1.622	1.674
0.30	0.014	0.016	0.013	1.626	1.620	1.647
0.50	0.010	0.012	0.006	1.629	1.613	1.608
0.65	0.008	0.011	−0.003	1.623	1.605	1.596
0.85	0.005	0.009	0.010	1.589	1.592	1.638
			(VI) Bromoform(1)-tetrahydrofuran(2)			
0.15	−0.044	−0.053	−0.057	1.889	1.844	1.833
0.30	−0.041	−0.044	−0.051	1.884	1.847	1.847
0.50	−0.031	−0.029	−0.038	1.894	1.878	1.885
0.65	−0.023	−0.023	−0.034	1.922	1.918	1.912
0.85	−0.017	−0.013	−0.034	1.988	1.983	1.919

η_2 are viscosities of the mixture and of the components 1 and 2, respectively.

The computed results from Eqs (4-6) at equimolar compositions ($x_1 = x_2 \simeq 0.5$) are given in Table 2. The values of ΔH^{*E} are positive for all the binaries with bromoform(1)-tetrahydrofuran(2) showing the largest and bromoform(1)-benzene(2) showing the smallest ΔH^{*E}. The positive sign for the values of ΔH^{*E} is a clear evidence for the presence of specific interaction and suggests an endothermic interaction. For all the binaries, the ΔH^{*E} values are temperature-dependent. Likewise, the quantity ΔS^{*E}, also varies with temperature; however, it does not follow the same pattern as ΔH^{*E}. It is intriguing to note that ΔC_p^{*E} values do not vary much with temperature. The negative ΔC_p^{*E} for bromoform(1)-toluene(2) system is indicative of specific interaction between the components. For other systems ΔC_p^{*E} values are positive.

The estimated parameters from a least-squares analysis of McAllister[6], Auslaender[7] and Heric[8] viscosity models are given in Table 3. McAllister model gives a good agreement between the observed and back calculated values of the viscosities; the average deviation being less than 0.5% for all mixtures. However, the mathematically less complex Auslaender model gives an error of 0.5-1.0%. The Heric theory gives slightly higher average percentage deviation sometimes exceeding 2%.

The other viscosity models, viz. Tamura-Kurata[9], Hind *et al.*[10] and Grunberg-Nissan[11,12] do not contain adjustable parameters but involve only

Table 2 – Excess Enthalpy, Excess Entropy and Excess Heat Capacity of Activation of Flow for Various Binaries at $x_1 = x_2 \simeq 0.5$

ΔH^{*E} (cal/mol) (Eq. 4) at			ΔS^{*E} (cal/mol) (Eq. 3) at			ΔC_p^{*E} (cal/mol) (Eq. 6) at		
298.15	308.15	318.15K	298.15	308.15	318.15K	298.15	308.15	318.15K
Bromoform(1)-benzene(2)								
−9.844	19.437	52.649	−0.200	−0.105	0.003	2.928	3.125	3.321
Bromoform(1)-toluene(2)								
208.700	192.294	172.314	0.540	0.487	0.422	−1.640	−1.819	−1.998
Bromoform(1)-p-xylene(2)								
36.376	119.147	212.642	−0.002	0.267	0.570	8.281	8.815	9.350
Bromoform(1)-acetonitrile(2)								
138.622	174.050	213.216	−0.138	−0.002	0.104	3.543	3.730	3.917
Bromoform(1)-nitrobenzene(2)								
39.112	130.000	232.618	0.010	0.305	0.637	9.089	9.675	10.262
Bromoform(1)-tetrahydrofuran(2)								
216.001	263.831	316.515	0.252	0.408	0.578	4.783	5.026	5.268

Table 3 – Computer Fittings of Viscosity Models

Temp (K)	McAllister		Auslaender			Heric		
	ν_{12}	ν_{21}	B_{12}	A_{21}	B_{21}	$A.10^2$	$B.10^2$	$C.10^2$
(*I*) *Bromoform(1)-benzene(2)*								
298.15	1.44	1.19	−1.24	−1.62	−0.81	−19.34	12.18	−13.88
308.15	1.28	1.02	0.09	0.16	7.68	−18.67	15.41	−6.63
318.15	1.15	0.89	0.70	1.03	1.13	−17.39	14.36	−7.69
(*II*) *Bromoform(1)-toluene(2)*								
298.15	1-46	1.05	−4.98	−6.92	−0.21	−10.83	13.43	12.37
308.15	1.25	0.90	0.74	1.20	1.08	−12.24	11.23	−1.33
318.15	1.12	0.80	0.20	0.41	3.15	−12.35	10.11	1.58
(*III*) *Bromoform(1)-p-xylene(2)*								
298.15	1.46	1.02	−1.45	−2.06	−0.66	−5.70	11.18	6.41
308.15	1.26	0.88	1.03	1.70	0.76	−8.08	11.44	−0.44
318.15	1.10	0.79	2.58	4.11	0.32	−9.35	7.81	1.63
(*IV*) *Bromoform(1)-acetonitrile(2)*								
298.15	1.52	1.41	1.07	1.50	0.47	−17.07	37.13	−13.24
308.15	1.21	1.44	−0.74	−0.65	−1.32	−17.48	14.93	22.44
318.15	1.13	1.16	0.48	0.65	1.34	−15.72	25.28	−16.47
(*V*) *Bromoform(1)-nitrobenzene(2)*								
298.15	2.12	1.97	6.81	2.41	−1.94	−32.87	23.08	−7.91
308.15	1.78	1.67	1.65	0.92	−1.16	−27.13	15.74	6.50
318.15	1.56	1.45	1.34	0.99	−0.46	−23.14	14.15	−5.05
(*VI*) *Bromoform(1)-tetrahydrofuran(2)*								
298.15	1.61	1.35	0.50	0.59	1.24	12.29	11.67	−10.51
308.15	1.39	1.16	0.49	0.58	1.32	7.91	11.06	−9.48
318.15	1.23	1.03	0.59	0.69	1.11	4.43	10.10	−8.22

one parameter to be evaluated. For mixtures of bromoform with benzene or toluene T_{12} (Tamura-Kurata parameter) and H_{12} (Hind *et al.* parameter) decrease with increase in the concentration of bromoform; the reverse is true for the remaining mixtures. With rise in temperature both T_{12} and H_{12} decrease. This observation is in agreement with the earlier data[13]. The Grunberg-Nissan parameter (G_{12}) increases with increase in bromoform concentration of the mixture. Both positive and negative G_{12} values are observed for the mixtures of bromoform with acetonitrile and tetrahydrofuran, while for the remaining mixtures G_{12} values are always negative. The binaries of bromoform with toluene, *p*-xylene and nitrobenzene show identical pattern in G_{12} values.

References

1 Aminabhavi T M, Manjeshwar L S, Balundgi R H & Halligudi S B, *J chem Engng Data*, in press.

2 Riddick J A & Bunger W B, *Techniques of organic chemistry*, Vol. 2A, edited by Weissberger (Wiley Inter-Science, NY) 1970.

3 Gokavi G S, Raju J R, Aminabhavi T M, Balundgi R H & Muddapur M V, *J chem Engng Data*, **31** (1986) 15.

4 Aminabhavi T M, Manjeshwar L S & Balundgi R H, *Indian J Chem*, **25A** (1986) 820.

5 Aminabhavi T M, Manjeshwar L S, Balundgi R H & Muddapur M V, *Indian J Chem*, **26A** (1987) 106.

6 McAllister R A, *AIChE J*, **6** (1960) 427.

7 Auslaender I G, *Brit Chem Engng*, **9** (1964) 610.

8 Heric E I & Brewer J G, *J Chem Engng Data*, **12** (1967) 574.

9 Tamura M & Kurata M, *Bull chem Soc (Japan)*, **25** (1952) 32.

10 Hind R K, McLaughlin E & Ubbelohde A R, *Trans Faraday Soc*, **56** (1960) 328.

11 Grunberg L & Nissan A H, *Trans Faraday Soc*, **45** (1949) 125.

12 Grunberg L & Nissan A H, *Nature*, **164** (1949) 799.

13 Fort R J & Moore W R, *Trans Faraday Soc*, **62** (1966) 1112.

Indian Journal of Chemistry
Vol. 27A, August 1988, pp. 725-726

Excess Volumes of Binary Mixtures of Acetonitrile with 1,2-Dichloro-, 1,1,1-Trichloro- & 1,1,2,2-Tetrachloroethanes & Trichloro- & Tetrachloro-ethylenes

K N SURENDRA NATH, K RAMANJANEYULU & A KRISHNAIAH*

Chemical Laboratories, College of Engineering, S V University, Tirupati 517 502

Received 7 *September* 1987; *revised* 23 *October* 1987; *accepted* 18 *December* 1987

Excess volumes (V^E) of binary mixtures of acetonitrile with 1,2-dichloroethane, 1,1,1-trichloroethane, 1,1,2,2-tetrachloroethane, trichloroethylene and tetrachloroethylene have been measured at 303.15 K. The negative excess volumes observed for all systems (except acetonitrile + tetrachloroethylene system) are attributed to the existence of specific interactions between components of the binaries.

Molecular interactions in binary mixtures of acetonitrile with chlorinated aliphatic hydrocarbons have been investigated by a number of workers[1-3]. However, no systematic attempt has been made to study the interactions in mixtures of acetonitrile with chlorinated ethanes and ethylenes in terms of excess volumes (V^E), hence the title investigation. This investigation is expected to throw light on the effect of successive chlorination and also unsaturation on V^E.

Acetonitrile (AR, Riedel) was used as such. 1,2-Dichloro-, 1,1,1-trichloro- and 1,1,2,2-tetrachloroethanes (BDH) were purified by the method described elsewhere[4]. Trichloroethylene and tetrachloroethylene (BDH) were purified by the method described by Riddick and Bunger[5]. The measured densities and boiling points of the purified chlorinated hydrocarbons were in good agreement with the literature data[5]. Excess volumes (accuracy ± 0.003 cm^3 mol^{-1}) were measured using the dilatometric method[6].

The V^E-composition profiles for the mixture of acetonitrile with 1,2-dichloro-, 1,1,1-trichloro-, 1,1,2,2-tetrachloroethanes, trichloroethylene and tetrachloroethylene are plotted in Figs 1 and 2. The V^E results were fitted to an empirical equation[7] of the form (1).

$$V^E = X_1(1-X_1)\sum_{i=0}^{2} a_i(2X_1-1)^i \qquad \ldots (1)$$

where X_1 is mol fraction of acetonitrile and a_i's are the parameters which have been estimated by the

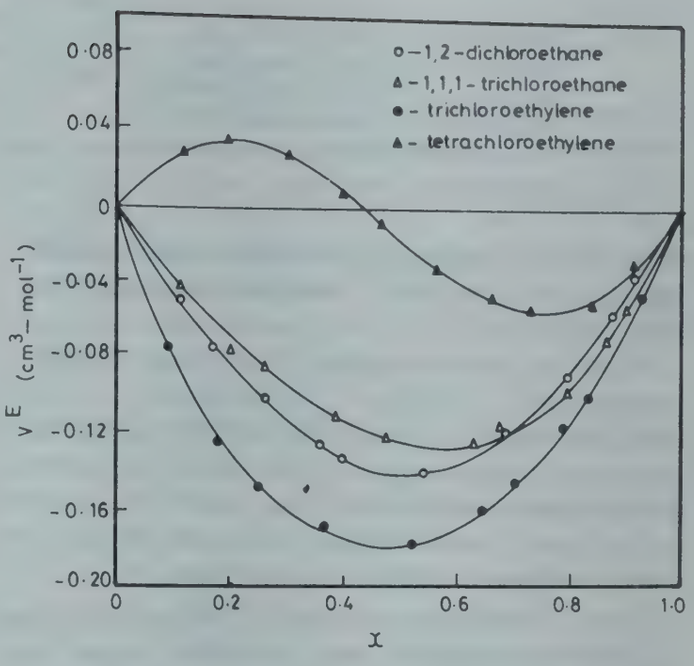

Fig. 1—Excess volumes (V^E) versus mol fraction (X_1) profiles for the binaries of acetonitrile with chloroalkanes and chloroalkenes at 303.15K

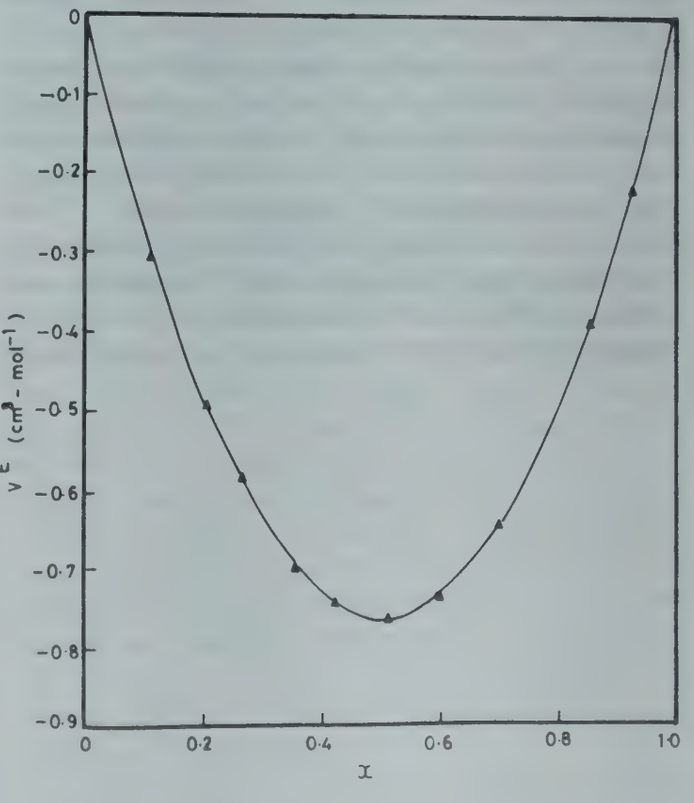

Fig. 2—Excess volume—composition curve for 1,1,2,2-tetrachloroethane with acetonitrile at 303.15K

Table 1—Estimated Parameters of Eq. (1) and Standard Deviation for Binary Mixtures at 303.15 K

System	a_0 ($cm^3\ mol^{-1}$)	a_1 ($cm^3\ mol^{-1}$)	a_2 ($cm^3\ mol^{-1}$)	$\sigma(V^E)$ ($cm^3\ mol^{-1}$)
Acetonitrile + 1,2-dichloroethane	−0.566	−0.018	0.133	0.003
Acetonitrile + 1,1,1-trichloroethane	−0.498	−0.132	−0.016	0.004
Acetonitrile + 1,1,2,2-tetrachloroethane	−3.043	−0.051	−0.075	0.003
Acetonitrile + Trichloroethylene	−0.704	0.104	−0.146	0.003
Acetonitrile + Tetrachloroethylene	−0.052	−0.437	−0.009	0.003

method of least squares. The values of three parameters are given in Table 1, alongwith standard deviations (σ) in V^E.

The V^E values are negative for mixtures of acetonitrile with 1,2-dichloro-, 1,1,1-trichloro-, 1,1,2,2-tetrachloro-ethanes and trichloroethylene. An incipient inversion of sign is observed for the system acetonitrile-tetrachloroethylene, where V^E is positive at lower concentrations of acetonitrile and becomes negative at higher concentrations.

Excess volumes are possibly influenced by (i) loss of dipolar association and difference in size and shape of acetonitrile and chlorinated hydrocarbons, (ii) dipole-dipole, dipole-induced dipole interactions and charge transfer complexation between unlike molecules[8]. The former effect leads to expansion in volume while the latter effect contributes to contraction in volume. The actual V^E value would depend upon the balance between the two opposing contributions. The experimental results suggest that the latter effect is dominant in all mixtures over the entire composition range except at lower mol fraction of acetonitrile in acetonitrile + tetrachloroethylene system. Thermodynamic[1-3] and spectroscopic[9-11] evidences exist for the complex formationbetween acetonitrile and chloroalkanes. The V^E values for acetonitrile + trichloroethylene systems are greater in magnitude than those containing 1,1,1-trichloroethane, probably due to the presence of π-electrons in trichloroethylene. Contrary to this observation the V^E values for acetonitrile + tetrachloroethylene system are less than those of acetonitrile + 1,1,2,2-tetrachloroethane system. This may be ascribed to the shielding of the alkene bond by the four chlorine atoms which prevents it from interacting with acetonitrile. This contention is in line with the observations made by Handa and Benson[12].

The financial assistance from the UGC, New Delhi is gratefully acknowledged.

References

1 Lorimer J W & Jones D E, *Can J Chem*, **55** (1977) 2980.
2 Handa Y P, *J chem Thermodyn*, **9** (1977) 117.
3 Nagata I & Kawamura Y, *Fluid Phase Equilibria*, **3** (1979) 1.
4 Reddy K D, Iloukhani H & Rao M V P, *Fluid Phase Equilibria*, **17** (1984) 123.
5 Riddick J A & Bunger W B, *Techniques of chemistry in organic solvents*, Vol 2 (Wiley-Interscience, New York) 1970.
6 Rao M V P & Naidu P R, *Can J Chem*, **52** (1974) 788.
7 Scatchard G, *Chem Rev*, **44** (1949) 7.
8 Krishnaiah A, Rao D N & Naidu P R, *Polish J Chem*, **55** (1981) 2633.
9 Berkeley P J & Hanna M W, *J phys Chem*, **67** (1963) 846.
10 Howard B B, Jumper C F & Emerson M T, *J molec Spectrosc*, **10** (1963) 117.
11 Lin W & Tsay S, *J phys Chem*, **74** (1970) 1037.
12 Handa Y P & Benson G C, *Fluid Phase Equilibria*, **4** (1980) 269.

Indian Journal of Chemistry
Vol. 27A, August 1988, pp. 727-729

Physico-chemical Studies in Mixed Solvents: Part V – Conductance Behaviour of Tetraethylammonium Bromide & Perchlorate in Dimethyl Sulphoxide-Water Mixtures at 25°C

S P JAUHAR*, P S GURAYA & S P NARULA

Department of Chemistry,
Panjab University, Chandigarh-160014

Received 12 *March* 1987;
revised 8 *October* 1987; *accepted* 21 *December* 1987

The conductances of Et_4NBr and Et_4NClO_4 have been measured at 25°C in dimethyl sulphoxide (DMSO)-water mixtures containing 5.5, 13.3, 25.7, 35.0, 48.0, 67.5, 81.4 and 100 mol% DMSO. The data have been analysed by Fuoss-Hsia equation as expanded by Fernandez-Prini equations, to calculate limiting equivalent conductance (Λ_0) and association constant (K_A). The limiting ionic conductances (λ_0) and relative ionic Walden products (R) of the ions in different DMSO-water mixtures have also been calculated.

In continuation of our earlier studies on the conductances and transport numbers of silver perchlorate[1] and viscosities of a few electrolytes[2] in dimethyl sulphoxide(DMSO)-water mixtures in the entire composition range, conductances of tetraethylammonium perchlorate and bromide have now been measured in DMSO-water mixtures and the results are interpreted in terms of changes in the structure of the solvent system.

The DMSO-water mixtures have been suggested to be highly structured though there is no general agreement on the structural characteristics of these mixtures. Some workers[3-5] have concluded that DMSO behaves as a strong structure maker, while others[6-9] have suggested that DMSO breaks down the water structure.

DMSO (Riedel) was purified as reported[1] (b.p. 68-68.5/7 mm Hg; sp. conductance $2\text{-}5\times10^{-8}$ ohm^{-1} cm^{-1}; density, 1.0956 g ml^{-1}; viscosity, 0.0196 p, all at 25°C). Conductivity water (sp. conductance $4\text{-}6\times10^{-7}$ ohm^{-1} cm^{-1}; density, 0.9970 g ml^{-1}; viscosity, 0.008937 p at 25°C) was obtained as described earlier[1].

Tetraethylammonium perchlorate was prepared in the laboratory, recrystallised from water, dried by heating at about 100°C in a water bath *in vacuo* and cooled in a vacuum desiccator before use. Tetraethylammonium bromide (Fluka AG) was used after drying *in vacuo*.

The preparation of solutions and conductance measurements were carried out by the methods reported before[1]. Conductances were accurate within ± 0.02 ohm^{-1} cm^2 mol^{-1}.

Conductances of tetraethylammonium bromide and perchlorate were measured at 25°C in different DMSO-water mixtures containing 5.5, 13.3, 25.7, 35.0, 48.0, 67.5, 81.4 and 100 mol% DMSO. The conductance data were analysed by the general expressions (Eqs. 1-3) for conductance of symmetrical electrolytes in dilute solutions[10].

$$\Lambda = \gamma[\Lambda_0 - S(C\gamma)^{\frac{1}{2}} + EC\gamma\log C\gamma + JC\gamma + J_{3/2}(C\gamma)^{3/2}] \quad \ldots (1)$$

$$K_A = \frac{1-\gamma}{\gamma^2 C f_{\pm}^2} \quad \ldots (2)$$

$$\ln f_{\pm} = -\frac{A(C\gamma)^{\frac{1}{2}}}{1+BR(C\gamma)^{\frac{1}{2}}} \quad \ldots (3)$$

Equations (1-3) were obtained by expanding[11-13] the Fuoss-Hsia expressions[14]; in these equations the symbols have their usual significance. The distance parameters in Eq. (1), i.e. J and $J_{3/2}$ have been taken to be equal to Bjerrum critical distance, $q = Z^2e^2/2DKT$. The expressions for J and $J^{3/2}$ used here are those given by Fernandez-Prini[11]. The parameters, Λ_0 and K_A were adjusted by least squares method to fit the experimental data and the values, thus obtained are reported in Table 1.

The results of analysis of conductance data by Fuoss-Onsager-Skinner equations[15] used by us in our previous publications are also recorded in Table 1 for comparison. It is clear from Table 1 that the values obtained by the two methods do not differ significantly, though some differences are noticed in K_A values. The K_A values obtained by Fuoss-Hsia and Fernandez-Prini methods are larger than those obtained by Fuoss-Onsager-Skinner method of analysis. These differences may be attributed to the influence of the term $(C\gamma)^{3/2}$, the Bjerrum distance used in J and $J_{3/2}$ and the use of complete Debye-Hückel expression for the activity coefficient in the former method. The similar differences in K_A values have also been noticed in other solvents[12,13,16].

Inspection of Table 1 shows that the limiting equivalent conductances (Λ_0) for both the electrolytes decrease sharply with the increase in DMSO concentration upto 35.0-48.0 mol % and thereaf-

Table 1 – Limiting Equivalent Conductances (Λ_0) and Association Constants (K_A) of Et_4NBr and Et_4NClO_4 in Different DMSO-Water Mixtures at 25°C

Mol % DMSO	Fuoss-Hsia Fernandez-Prini			Fuoss-Onsager-Skinner		
	Λ_0	K_A	$\sigma\Lambda$	Λ_0	K_A	$\sigma\Lambda$
		Et_4NBr				
0.00	110.90*					
5.50	77.71 ± 0.01	22.29 ± 0.03	0.01	77.70 ± 0.01	20.48 ± 0.08	0.01
13.30	44.57 ± 0.02	3.31 ± 0.16	0.02	44.67 ± 0.08	7.40 ± 4.44	0.02
25.70	28.33 ± 0.04	6.28 ± 0.43	0.04	28.35 ± 0.04	—	0.04
35.00	25.12 ± 0.03	9.19 ± 0.48	0.02	25.02 ± 0.02	—	0.02
48.00	27.90 ± 0.02	4.09 ± 0.20	0.02	27.99 ± 0.08	8.64 ± 5.57	0.02
67.50	31.53 ± 0.05	5.97 ± 0.54	0.05	31.86 ± 0.20	25.23 ± 11.70	0.05
100.00	40.29 ± 0.01	3.57 ± 0.12	0.01	40.33 ± 0.03	—	0.03
		Et_4NClO_4				
0.00	100.06*	—				
5.50	62.20 ± 0.02	—	0.02	62.19 ± 0.01		0.02
13.30	37.06 ± 0.01	—	0.01	37.07 ± 0.01		0.01
25.70	23.94 ± 0.01	—	0.01	23.94 ± 0.01		0.01
35.00	22.14 ± 0.01	—	0.01	22.14 ± 0.01		0.01
48.00	24.03 ± 0.01	—	0.02	24.06 ± 0.02		0.03
67.50	30.05 ± 0.02	—	0.03	30.11 ± 0.03		0.04
81.40	34.84 ± 0.01	—	0.02	34.91 ± 0.02		0.04
100.00	40.74 ± 0.01	—	0.01	40.88 ± 0.03		0.04

*Data have been taken from literature (Harned H S & Owen B B, The physical chemistry of electrolytic solutions, Reinhold, New York, 1950.

Table 2 – Limiting Ionic Conductances ($\lambda_0^{\pm}$) and R-Values for Et_4N^+, Br^- and ClO_4^- in DMSO-water Mixtures at 25°C.

Mol % DMSO	λ_0			R		
	Et_4N^+	Br^-	ClO_4^-	Et_4N^+	Br^-	ClO_4^-
0.00	32.60	78.30	68.00			
5.50	21.24	56.46	40.95	1.01	1.11	0.93
13.30	13.28	31.24	23.78	1.02	1.00	0.87
25.70	9.59	18.61	14.35	1.14	0.92	0.82
35.00	9.62	15.40	12.52	1.24	0.83	0.78
48.00	10.92	16.94	13.14	1.29	0.83	0.75
67.50	13.31	18.55	16.79	1.23	0.72	0.75
81.40	15.29	—	19.61	1.21	—	0.74
100.00	17.50	23.60	24.15	1.18	0.66	0.78

ter it gradually increases. The λ_0 of Et_4N^+ ions in different DMSO-water mixtures were calculated from the corresponding Λ_0 values of Et_4NClO_4 and limiting ionic conductances of ClO_4^- ion reported earlier[1], using Kohlrusch law of independent migration of ions: The λ_0 of Et_4N^+ ions are used to calculate λ_0 of Br^- ion in different DMSO-water mixtures. All the results are recorded in Table 2.

The ratio (R) of limiting ionic Walden product of an electrolyte for a solvent mixture and that in pure water, $R = [(\lambda_0^{\pm}\eta_0/(\lambda_0^{\pm}\eta_0)_{H_2O}]$ may provide better understanding[17,18] of the nature of solutions. The R-values of ions in DMSO-water mixtures have been obtained from $\lambda_0^{\pm}$ values of ions calculated in the present study and η_0 values taken from literature[19]. These are recorded in Table 2.

The relative ionic Walden product (R) for Et_4N^+ increases with increase in DMSO concentration and is maximum at 50 mol % DMSO and thereafter it decreases gradually. Et_4N^+ possesses low charge density and, therefore, cannot be considered to interact strongly with solvent molecules. The increase in R for this ion may arise by the hydrophobic dehydration of the ion. The hydrophobic interaction is a specific property of tetraalkyl or tetraaryl ammonium ions in water due to its structure. With increase in concentration of cosolvent, the magnitude of hydrophobic interaction decreases and hence R increases in this region. Similar behaviour has also been shown by this ion in other solvent systems[20]. Beyond the maximum value of R, the ion seems to interact weakly with DMSO molecules and this may be due to more basic nature of DMSO.

The behaviour of Et_4N^+ may be compared with the solvation effects of large Bu_4N^+ inferred from thermochemical data[21]. The Bu_4N^+ undergoes desolvation in the entire solvent composition range, with maximum desolvation occurring at

about 20.2-27.6 mol % DMSO. This solvent composition is very close to $DMSO.2H_2O$, at which aqueous DMSO shows maximum structure. The behaviour of Et_4N^+ exactly goes parallel to this solvation behaviour.

The R-value for Br^- is maximum at about 5.5 mol % DMSO, while for ClO_4^- ion, the R-value decreases with increase in DMSO concentration over the entire range of composition (Table 2). The behaviour of ClO_4^- ion is in agreement with the results of Petrella and coworkers[22,23] in water-rich region of aqueous DMSO mixtures, though no maximum was observed for Br^- ion. The small maximum in case of Br^- ion has also been observed in the case of ethanol-water and *t*-butyl alcohol-water systems[24]. The initial increase in R cannot be attributed mainly to the preferential solvation of ions because DMSO being dipolar aprotic solvent cannot preferentially solvate the anion.

Perchlorate ion, on the other hand, shows fairly good solvation. There is a gradual decrease in R with increase in concentration of DMSO, indicating increasing solvation of anion with increase in DMSO concentration. This is expected since oxianions generally show specific interaction in aqueous mixtures[20,25].

References

1 Narula S P, Guraya P S, Jauhar S P & Delesalle G, *Indian J Chem*, **20A** (1981) 129.

2 Jauhar S P, Guraya P S, Parmar J S & Narula S P, *Z phys Chem (NF)* **146** (1985) 9.

3 Safford G J, Schaffer P C, Leung P S, Doebbler G F, Brady G W & Lyden E F X, *J chem Phys*, **50** (1969) 2140.

4 Rallo F, Rodante F & Silvestroni, *Thermochim Acta*, **1** (1970) 311.

5 Kiyohara O, Perron G & Desnoyers J E, *Can J Chem*, **53** (1975) 3263.

6 Cowie J M G & Taporowski P M, *Can J Chem*, **39** (1961) 2240.

7 Macdonald D D, Smith M D & Hyne J B, *Can J Chem*, **49** (1971) 2817.

8 Kenttamaa J & Lindberg J J, *Suomen Kemi*, **33B** (1960) 98.

9 Parker K J & Tomlinson D J, *Trans Faraday Soc*, **67** (1971) 1302.

10 Justice J C, *Electrochim Acta*, **16** (1970) 701.

11 Fernandez Prini R, *Trans Faraday Soc*, **65** (1969) 3311.

12 Justice J C, Bury R & Treiner C, *J Chem Phys et Biol (France)* **65** (1968) 1708.

13 Justice J C, *J chim Phys et Biol (France)*, **66** (1969) 1193.

14 Fuoss R M & Hsia K L, *Proc Natl Acad Sci (USA)*, **57** (1967) 1550; **58** (1968) 1818.

15 Fuoss R M, Onsager L & Skinner J F, *J phys Chem*, **69** (1965) 2581.

16 Jauhar S P, Guraya P S & Narula S P, *Indian J Chem*, (Communicated).

17 Kay R L, Cunningham G P & Evans D F, *Hydrogen bonded solvent systems*, edited by A Convington & P Jones (Taylor and Francis, London) 1968, 249.

18 Broadwater T L & Kay R L, *J phys Chem*, **74** (1970) 3802.

19 Morel J P, *Bull Soc chim Fr*, **4** (1967) 1405.

20 Kay R L & Broadwater T L, *J Soln Chem*, **5** (1976) 57.

21 Fuchs R & Hagan C P, *J phys Chem*, **77** (1973) 1797.

22 Petrella G & Petrella M, *Electrochim Acta*, **27** (1982) 1733.

23 Petrella G, Petrella M, Castagnolo M, Dell'Atti A & Giglio A D, *J Soln Chem*, **10** (1981) 129.

24 Broadwater T L & Kay R L, *J phys Chem*, **74** (1970) 3802.

25 Kay R L & Broadwater T L, *Electrochim Acta*, **16** (1971) 667.

Indian Journal of Chemistry
Vol. 27A, August 1988, pp. 730-731

Kinetics of Rh(III)-Catalysed Oxidation of Some Alcohols by Diperiodatocuprate(III) in Aqueous Alkaline Medium

K BAL REDDY†, B SETHURAM* & T NAVANEETH RAO
Department of Chemistry, Osmania University, Hyderabad 500 007

Received 1 *October* 1987; *revised* 21 *December* 1987; *accepted* 4 *January* 1988

Rh(III) chloride catalysed oxidation of some alcohols by diperiodatocuprate(III) (DPC) in aqueous alkaline medium has been studied spectrophotometrically at 414 nm. The order in [DPC] is zero and one each in [Rh(III)] and [alcohol]. The rate of oxidation is unaffected by variation in [OH^-]. The effect of added salts on the rate of oxidation is negligible. The stoichiometric studies reveal that one mole of alcohol consumes two moles of DPC, giving the corresponding carbonyl compounds as the reaction products. As in earlier investigation on Ru(III) catalysis in the oxidation of alcohols a direct reaction between Rh(III) and alcohol to give products via hydride ion abstraction by Rh(III) is proposed.

In our previous studies on Os(VIII) and Ru(III) catalysed oxidation of some organic compounds, viz. alcohols and ketones by Cu(III)[1,2] in alkaline medium, a direct reaction between substrate and catalyst in the slow step was postulated. In the case of alcohols, Os(VIII)/Ru(III) were shown to react via hydride ion abstraction from α-carbon atom of the substrate and that Ru(III) was a better hydride ion abstractor than Os(VIII)[2]. Rhodium(III) chloride also reacts with alcohols via hydride ion transfer process[3]. Only sporadic references are available on Rh(III) catalysis in redox reactions[4,5]. No report seems to be available on the use of Rh(III) as a homogeneous catalyst in the oxidation of organic compounds by diperiodatocuprate(III)(DPC) in aqueous alkaline medium, and hence the title investigation.

All the chemicals used were of AR grade and wherever necessary were purified by standard methods. The kinetics was followed in the temperature range of 308 to 325 K by studying the disappearance of diperiodatocuprate(III)(DPC) at regular time intervals spectrophotometrically at 414 nm using Carl-Zeiss spectrocolorimeter. In all kinetic runs blank reactions were also carried out and necessary corrections were made for any self-decomposition of DPC. Stoichiometric studies revealed that one mol of alcohol consumed two mol of DPC. Corresponding carbonyl compounds were identified as products of oxidation and confirmed by preparing their 2,4-dinitrophenylhydrazone derivatives.

Under the conditions [alcohol] ≫ [DPC] the rate of oxidation was independent of initial [DPC] and the plot of absorbance versus time was linear ($r = 0.989$) indicating zero order dependence in [DPC]. The zero order rate constant (k_0) increased with increase in [Rh(III)] and the order in [Rh(III)] was one (Table 1). The k_0 also increased with increase in [alcohol] and the order in [alcohol] was unity (Table 1). The rate of reaction was found to be unaffected by varying [OH^-].

It is known[6-8] that $RhCl_3$ in alkaline solutions exists as $Rh(OH)_3$ and $Rh(OH)_6$. In the present investigation the rate was independent of [OH^-] indicating that the equilibria of any type involving Rh(III) species and OH^- ion may not be operative in the present study. The effect of added salts on the rate of oxidation was negligible. No polymerisation of acrylamide was observed, when added to reaction mixture in N_2 atmosphere, ruling out the possibility of a free radical mechanism. No reaction was observed with *t*-butanol. A clean first order dependence both in [alcohol] and [Rh(III)] and non-dependence in [OH^-] indicated a direct reaction of the substrate either with $Rh(OH)_3$ or $Rh(OH)_6$. Based on the above information a probable mechanism involving hydride ion abstraction from α-carbon of alcohol by Rh(III) to give the product and Rh(III) hydride is proposed,

$$RCH_2OH + Rh(OH)_3 \overset{K}{\rightleftharpoons} RCH_2O - Rh(OH)_2 + H_2O$$

Table 1—Effect of [methanol] and [Rh(III)] on Rate in DPC-methanol Reaction catalysed by Rh(III)

[DPC] = 6.60×10^{-3} mol dm^{-3}; [OH^-] = 0.01 mol dm^{-3}; temp = 308 K

[Methanol] × 10^2 (mol dm^{-3})	[Rh(III)] × 10^4 (mol dm^{-3})	$k_0 \times 10^7$ (mol dm^{-3} s^{-1})
1.00	1.85	2.95
2.00	1.85	5.66
3.00	1.85	8.40
4.00	1.85	11.6
5.00	1.85	14.2
2.00	0.750	2.40
2.00	2.50	7.87
2.00	3.00	9.60
2.00	4.00	12.6

†Present address: Department of Chemistry, P.G. College of Science, Osmania University, Saifabad, Hyderabad 500 004

$$RCH_2O - Rh(OH)_2 \xrightarrow{k} RCHO + RhH(OH)_2$$

Rh(III) hydride thus formed is reoxidized to Rh(III) by Cu(III) in a fast step.

$$(Rh(H)(OH)_2) + 2Cu(III) \xrightarrow[H_2O]{\text{fast}} Rh(OH)_3 + 2Cu(II) + 2H^+$$

The rate law in consonance with the proposed mechanism is given by Eq. (1),

$$-d[DPC]/dt = Kk[Rh(III)][alcohol] \quad \ldots (1)$$

which explains the kinetic data obtained.

The assumption of hydride ion abstraction by Rh(III) from α-carbon atom of alcohol receives support from the previous studies made by Charman[3] and Singh *et al.*[4]

The rate data for the catalysed and uncatalysed reactions, of different alcohols are recorded in Table 2. The rates of oxidation of various alcohols are in the order: methanol < isopropanol < ethanol < *n*-propanol < *n*-butanol < *n*-pentanol < benzyl alcohol. The observed order of reactivity reveals that the rate increases with increase in +I character of alkyl group at α-carbon. This coupled with the fact that there is no reaction with *t*-butanol supports the hydride ion transfer mechanism. But the lower rate of oxidation of isopropanol as compared to that of *n*-propanol may be due to steric effect of alkyl groups overweighing the inductive effect. The higher rate of oxidation of benzyl alcohol may be due to the delocalisation of +ve charge produced at α-carbon during hydride ion abstraction.

The Taft's reaction constant (ρ*) was found to be −0.70 ($r = 0.8276$; $s = 0.1769$). The negative ρ* value indicates that the reaction is facilitated by high electron density at reaction site. This is in conformity with the observed substituent effect at the α-carbon. The negative ρ* value also supports hydride ion abstraction in the slow step. A ρ*-value with such magnitude is not uncommon in the literature[9] for reactions involving hydride ion transfer.

Table 2—Comparison of Rates of Oxidation of Rh(III)-catalysed and Uncatalysed Oxidations of Alcohols by DPC

[DPC] = 6.60×10^{-5} mol dm^{-3}; [OH$^-$] = 0.010 mol dm^{-3}; temp = 308 K

Alcohol	$k \times 10^6$ (s^{-1})*	
	Uncatalysed	Catalysed (Rh(III) = 1.85×10^{-4}) mol dm^{-3}
Methanol	18.0	28.3
Ethanol	28.0	39.0
n-Propanol	30.0	45.8
Isopropanol	16.6	29.1
n-Butanol	43.3	70.8
n-Pentanol	45.2	74.2
Benzylalcohol	55.3	228

*k = Initial rate/[substrate]

References

1 Bal Reddy K, Murthy C P, Sethuram B & Navaneeth Rao T, *Indian J Chem*, **20A** (1981) 272.

2 Bal Reddy K, Sethuram B & Navaneeth Rao T, *Bull Soc Chim Belg*, **90(10)** (1981) 1017.

3 Charman H B, *J chem Soc (B)*, (1967) 629.

4 Singh H S, Singh K K, Singh S M, Singh P & Thakur D, *Indian J Chem*, **21A** (1982) 816.

5 Radhakrishnamurthi P S & Misra S A, *Int J chem Kinet*, **14** (1982) 631.

6 Griffith W P, *The chemistry of rare platinum metals* (Interscience, New York), (1967) pp. 332.

7 Johnson B F G, *A specialist periodic report: Inorganic chemistry of the transition elements* (Chemical Society, London) (1973) pp. 385.

8 Ivanon, Emin B N, Borzoval L D, Egrov A M & Malyuguia S G, *Aust J Chem*, **16** (1974) 1474.

9 Harlan L, Goering & Robert R Jacobson, *J Am chem Soc*, **80** (1958) 3277.

Indian Journal of Chemistry
Vol. 27A, August 1988, pp. 732-733

Chemistry of Unsymmetrical Phosphorus Ligands : Part 2—Synthesis & Spectroscopic Studies of Adducts of Mercury(II) Halides with $Ph_2P(X)(CH_2)_2PPh_2$ & $Ph_2P(S)(CH_2)_nP(Se)Ph_2$ (n = 1,2; X = S,Se)

T S LOBANA* & P K SHARMA

Department of Chemistry, Guru Nanak Dev University, Amritsar-143 005

Received 23 *April* 1987; *revised and accepted* 29 *December* 1987

Reactions of mercury(II) halides with unsymmetrical phosphorus ligands $Ph_2P(X)(CH_2)_2PPh_2$ and $Ph_2P(S)(CH_2)_nP(Se)Ph_2$ (X = S,Se; n = 1,2) in ethanol or ethanol-chloroform mixture give 1:1 and 3:2 (metal:ligand) adducts. The adducts have been characterized by elemental analysis, molar conductance, IR and far IR spectral data. Tetrahedral stereochemistry about mercury(II) has been proposed for all the adducts.

Donor behaviour of mono- and di-tertiary phosphine chalcogenides [I, $R_3P(X)$; II, $R_2P(X)(CH_2)_nP(X)R_2$; R = alkyl or aryl group, X = S, Se, n = 1-4,6] has been extensively studied[1,2]. The unsymmetrical phosphorus ligands [III, $Ph_2P(X)CH_2PR_1R_2$] have been used by Grim *et al.*[3-5] mainly for preparing adducts with group-VI metal carbonyls, while no work has been reported with ligands of the type $Ph_2P(X)(CH_2)_2PPh_2$ (IV) and $Ph_2P(S)(CH_2)_nP(Se)Ph_2$ (n = 1,2) (V). Ligands of types (III-V) are interesting from the point of view of nonequivalent phosphorus atoms. In continuation of our earlier work[6] on the adducts of type III with mercury(II) halides, we report here the complexes of type (IV) and (V) ligands with mercury(II) halides [IV: X = S, 1-(diphenylphosphinoethyl)-2-diphenylphosphine sulphide abbrev. as EDPS; X = Se, 1-(diphenylphosphinoethyl)-2-diphenylphosphine selenide, abbrev. as EDPSe. V: n = 1, (diphenylthiophosphinomethyl)diphenylphosphine selenide; abbrev. as MDSSe; n = 2, 1-(diphenylthiophosphinoethyl)-2-diphenylphosphine selenide, abbrev. as EDSSe].

Mercury(II) halides and solvents were of AR grade and used as such. $Ph_2PCH_2PPh_2$ (MDPP) was procured from M/s Pressure Chemical Company, Pittsburg, U.S.A. $Ph_2P(CH_2)_2PPh_2$ (EDPP) was prepared by a literature method[7]. Type (IV) ligands were obtained by reacting EDPP with stoichiometric amount of sulphur/selenium in an organic solvent. Type (V) ligands were obtained from types (III) and (IV) by reacting them with sulphur/selenium. The melting points (°C) of the ligands are : EDPS, 149-50; EDPSe, 169-70; MDSSe, 179-80 and EDSSe, 204-5.

The methods of preparation of the complexes and the techniques used are the same as described earlier[6].

The analytical data show that the adduct have essentially 1:1 stoichiometry (Table 1). The chloride and bromide adducts are colourless while the iodide adducts are pale yellow in colour. The complexes are insoluble in common organic solvents (ethanol, benzene, chloroform, etc.). However, these are soluble in tetrahydrofuran. The conductivity data reveal their nonionic nature (Table 1). Generally, the melting points of the adducts of MDSSe and EDSSe are higher than those of EDPS and EDPSe.

The characteristic functional group frequencies ν(PS) and ν(PSe) of EDPS and EDPSe occur at 595 m and 535 w cm^{-1}, respectively, and undergo low energy shifts by 7-26 and 7-17 cm^{-1} in the complexes (Table 1). The order of shifts for EDPSe complexes (4-6) is : Cl > Br > I; while for EDPS complexes (1-3), the order is: Br > I > Cl. For MDSSe and EDSSe complexes (7-12), the shifts in ν(PS) vary in the order: Cl > Br > I. However, no regular trend in ν(PSe) is observed for the complexes (7-12).

The decrease in ν(PS)/ν(PSe) is attributed to the weakening of the p_π-d_π bonds between phosphorus and sulphur or selenium after coordination. In complex 7, (PSe) group is bonded to Hg(II) more strongly than (PS) group and this shift is the largest among the selenide ligands used. The magnitude of the shifts in ν(PSe) (compounds 10-12) is small and similar and it shows weak interaction of the selenide ligands. Generally speaking, the shifts in ν(PS) of MDSSe/EDSSe are larger than those in MDPS/EDPS[6]. The difference is attributed to the stronger p_π-d_π bonding in type (V) ligands where both phosphorus atoms are in the pentavalent state as compared to that in type IV ligands, where one phosphorus is trivalent. However, the symmetrical phosphorus ligands, $Ph_2P(S)(CH_2)_nP(S)Ph_2$, show greater shifts (30-70 cm^{-1}) than those shown by type (V) ligands[1,2]. This shows that the p_π-d_π bonding is strongest in the symmetrical phosphorus ligands. The stronger this bonding, the larger is the weakening.

The mercury-halogen stretching frequencies have been assigned in a few cases. In $HgCl_2$(EDPS).$2H_2O$, ν(Hg-Cl) absorbs at 290cm^{-1} while in $HgBr_2$(EDPSe).$2H_2O$, ν(Hg-Br) absorbs at 280cm^{-1}. Other assignments e.g. ν(Hg-S), ν(Hg-Se) and ν(Hg-I) were not possible.

All the 1:1 adducts have been assigned tetrahedral structures with chelating ligands forming six-membered chelate rings in the case of EDPS, EDPSe and MDSSe. EDSSe, however, may form seven-membered rings. The formation of seven-membered rings by the phosphine ligands is well documented[7,8]. Compounds 2 and 3 are probably polymeric.

Table 1—Analytical, Melting Point and IR Data of the Adducts

Sr. No.	Complex (m.p., °C)	Found (Calc.) %			ν(PX)[a,b] (cm^{-1})	$\Delta\nu$(PX) (cm^{-1})
		C	H	Hg		
1	$HgCl_2$(EDPS)[c] (159-60)	41.8 (42.3)	3.2 (3.8)	26.5 (27.2)	588s	7
2	Hg_3Br_3(EDPS)$_2$ (177-78)	33.0 (32.2)	2.6 (2.5)	31.0 (31.0)	569w	26
3	Hg_3I_3(EDPS)$_2$ (194-95)	27.4 (28.1)	2.7 (2.2)	25.9 (26.9)	580w	15
4	$HgCl_2$(EDPSe)[d] (189-90)	38.1 (38.9)	2.9 (3.7)	24.2 (25.0)	518m	17
5	$HgBr_2$(EDPSe)[c] (204-05)	35.5 (35.8)	2.6 (3.2)	22.0 (22.9)	520m	15
6	HgI_2(EDPSe)[d] (217-18)	32.2 (31.6)	2.9 (3.0)	20.7 (20.4)	528m	7
7	$HgCl_2$(MDSSe) (239-40)	40.0 (39.1)	2.9 (2.9)	26.5 (26.2)	562m (510w)	38(18)
8	$HgBr_2$(MDSSe) (249-50)	35.8 (35.1)	2.6 (2.6)	22.8 (23.4)	570m (520w)	30(8)
9	HgI_2(MDSSe) (217-18)	32.4 (31.6)	2.3 (2.3)	20.3 (21.1)	580w (500w)	20(28)
10	$HgCl_2$(EDSSe)[c] (234-35)	38.1 (38.2)	3.0 (3.4)	23.2 (24.6)	570w (519m)	30(11)
11	$HgBr_2$(EDSSe)[d] (244-45)	33.8 (33.8)	2.6 (3.2)	20.7 (21.7)	578w (521w)	22(9)
12	HgI_2(EDSSe) (224-25)	32.0 (32.4)	2.4 (2.5)	20.7 (20.8)	589m (520m)	11(10)

[a]For 7-12, values in parenthesis belong to ν(PSe). [b]Free ligand values: EDPS, 595m; EDPSe, 535w; MDSSe, 600w (528m), EDSSe, 600w(530s).
[c]$2H_2O$. [d]$3H_2O$(as lattice water).

One of us (PKS) is thankful to the Guru Nanak Dev University, Amritsar for the research facilities. We are thankful to RSIC, Panjab University, Chandigarh for elemental analysis.

References

1 Lobana T S & Sandhu S S, *J chem Sci* (Guru Nanak Dev University), **4** (1978) 37; *Chem Abstr*, **91** (1979) 67636 j.
2 Lobana T S, *Progr Inorg Chem* (accepted).
3 Grim S O & Mitchell J D, *Inorg Chem*, **16** (1977) 1762.
4 Grim S O & Walten E D, *Inorg Chem*, **19** (1980) 1982.
5 Grim S O & Matienzo L J, *Inorg Chem*, **14** (1975) 1014.
6 Lobana T S & Sharma P K, *Indian J Chem*, **26A** (1987) 784.
7 Anderson M P & Pignolet L H, *Inorg Chem*, **20** (1981) 9101.
8 Harrison P G, Sharpe N W, Pelizzi C, Pelizzi G & Tarasconi P, *J chem Soc Dalton Trans*, (1983) 1687.

Indian Journal of Chemistry
Vol. 27A, August 1988, pp. 734-736

Synthesis & Characterisation of Organotellurium Compounds of Phenacyl Bromide

SURENDRA SRIVASTAVA* & AJAY SINGH
Chemistry Division, Crop Research Centre, Bahraich 271 801

and

Y D KULKARNI
Department of Chemistry, University of Lucknow, Lucknow 226 007

Received 24 *August* 1987; *revised and accepted* 4 *January* 1988

Diphenacyltellurium dihalides, dipseudohalides, dioximes, aniline/piperidine dithiocarbamate derivatives and adducts with some nitrogen donors have been synthesised and characterised. The tetracoordinated organotellurium compounds exhibit keto-enol tautomerism with enol form being present to the extent of (~ 50%) while the hexacoordinated tellurium adducts exist in the keto form. The proton of the enol form and hydroxyl proton of oximino derivative seem to be attached to the lone pair of tellurium atom forming novel Te-H bonds.

In continuation of our earlier studies[1–6], we now report the synthesis and characterisation of some novel organotellurium dihalides, dipseudohalides, dioximes and adducts with some nitrogen donors. Dibenzyltellurium compounds[7] have been found to be less stable under the experimental conditions while the diphenacyl tellurium derivatives were found to be highly stable, probably due to the presence of the carbonyl group adjacent to the methylene group.

The compounds prepared in the present study are summarised in Table 1.

Diphenacyltellurium dibromide (I) and diiodide (II)

A mixture of phenacylbromide (3.98 g; 0.02 mol) and tellurium metal powder (1.276, 0.01 g. atom) for (I) and sodium iodide (3.00 g; 0.02 mol) for II was heated on a water bath for 14 - 18 hr. The residue was repeatedly extracted with chloroform/acetone and the compounds were recrystallized from chloroform/acetone-pet. ether (1:1).

Diphenacyltellurium derivatives (III-XIII)

Pseudohalides (III,IV) and aniline/piperidine dithiocarbamate derivatives (V,VI) were prepared by taking a mixture of II (0.619 g; 0.001 mol) and freshly prepared silver salt of thiocyanate/cyanate or ammonium salt of aniline/piperidine (0.002 mol) and stirring for ~ 10 hr/refluxing in dry toluene (25 ml) for 10-14 hr. The precipitated salts were filtered off and the residues were recrystallised from acetone/benzene-pet.ether. Diphenacyltelluride (VII) was prepared by

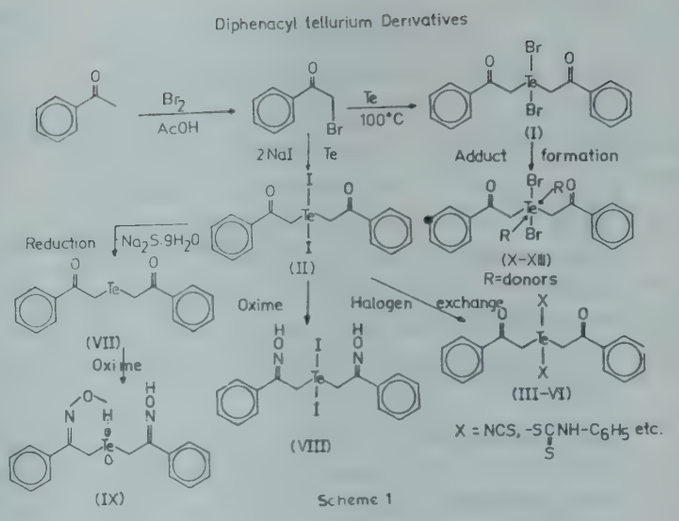

stirring a mixture of II (6.19 g; 0.01 mol) and $Na_2S.9H_2O$ (3.6 g; 0.15 mol) at 100°C for ~ 14 hr. The mixture was cooled, poured over crushed ice and extracted with ether. The extract was dried and concentrated *in vacuo*. For preparing diphenacyltellurium dioximes (VIII, IX), a solution of compound II/VII (0.001 mol) in absolute ethanol (50 ml) was added to hydroxylamine hydrochloride (0.13 g; 0.001 mol). Ethanoic sodium acetate (0.164 g; 0.002 mol) was added dropwise over a period of ~ 3 hr and contents were further heated for ~ 10 hr. The compounds were recrystallised from ethanol.

The adducts (X-XIII) were synthesised by refluxing a mixture of (I) (0.525 g; 0.001 mol) with the appropriate amine (0.002 mol) (pyrrolidine, pyridine, etc.) in dry dichloromethane for ~ 6 hr. The separated product was recrystallised from chloroform-pet.ether.

The characterisation data of the compounds are given in Table 1. All the melting points are uncorrected. The IR spectra were recorded in CsI on a Perkin Elmer 577 instrument. The ^1H NMR spectra were recorded in $CDCl_3$ on a Varian EM 360L instrument using TMS as an internal reference (chemical shifts are given in τ scale). Silica gel G (GLAXO) was used for TLC.

The IR spectra of compounds (I-XIII) (Table 1) showed characteristic peaks at 1740-1680 cm^{-1} ($\nu C=O$). Compound IV showed a peak at 2230 cm^{-1} due to the $\nu C \equiv N$ frequency, indicating that the cyano group was covalently bonded to the tellurium metal[8]. The IR spectrum of dithiocyanato compound (III) showed peaks at 2110, 760 and 465 cm^{-1}, characteristic of nitrogen bonded[9] NCS group with the tellurium metal. In the diphenacyl tellurium dianilinodithiocarbamate (V) and the corresponding piperidino

Table 1—Characterisation Data of Diphenyltellurium Derivatives

Compd.	Mol. formula	m.p. °C	Colour (% yield)	Found(Calc.)%				νTe-H	νC=O	νTe-C	νTe-N νTe-S*
				Te	C	H	N				
I	$C_{16}H_{14}O_2TeBr_2$	130(d)	Brown (65)	24.19 (24.27)	36.48 (36.52)	2.63 (2.66)	—	2310	1680	520	—
II	$C_{16}H_{14}O_2TeI_2$	160(d)	Violet (60)	20.50 (20.59)	30.92 (30.98)	2.23 (2.25)	—	2315	1700	515	—
III	$C_{18}H_{14}O_2N_2TeS_2$	115	White (45)	26.42 (26.49)	44.83 (44.85)	2.86 (2.90)	5.78 (5.81)	2300	1690	530	415
IV	$C_{18}H_{14}O_2N_2Te$	127	White (50	30.50 (30.55)	51.65 (51.72)	3.22 (3.35)	6.64 (6.70)	2320	1710	535	—
V	$C_{30}H_{26}O_2N_2TeS_4$	148	Dark yellow (55)	18.14 (18.18)	51.28 (51.31)	3.65 (3.70)	3.92 (3.99)	2310	1685	510	270*
VI	$C_{28}H_{34}O_2N_2TeS_4$	130	Yellow (60)	16.58 (18.61)	49.07 (49.00)	4.92 (4.95)	4.00 (4.08)	2315	1690	515	280*
VII	$C_{16}H_{14}O_2Te$	110	Light brown (45)	34.86 (34.90)	52.45 (52.51)	3.80 (3.82)	—	2300	1710	525	—
VIII	$C_{16}H_{16}O_2N_2TeI_2$	148	Cream (50)	19.60 (19.64)	29.48 (29.65)	2.39 (2.46)	4.30 (4.31)	—	—	535	—
IX	$C_{16}H_{16}O_2N_2Te$	134	White (55)	32.19 (32.25)	48.50 (48.53)	4.01 (4.04)	7.00 (7.07)	2330	—	520	—
X	$C_{24}H_{32}O_2N_2TeBr_2$	184	Choco-late brown (65)	19.06 (19.11)	43.11 (43.13)	4.72 (4.79)	4.14 (4.19)	—	1710	510	415
XI	$C_{26}H_{24}O_2N_2TeBr_2$	172	Brown (70)	18.72 (18.66)	45.59 (45.64)	3.46 (3.51)	4.04 (4.09)	—	1740	525	425
XII	$C_{26}H_{36}O_2N_2TeBr_2$	204	Light brown (60)	18.28 (18.34)	44.79 (44.85)	5.12 (5.17)	3.96 (4.02)	—	1690	515	415
XIII	$C_{24}H_{32}O_4N_2TeBr_2$	163	Dark brown (55)	18.17 (18.23)	41.10 (41.16)	4.54 (4.57)	3.91 (4.00)	—	1680	530	420

compound (VI), a single peak at 960 and 980 cm^{-1} respectively due to νCSS indicated their monodentate nature[10]. The IR spectra of halides (I,II), pseudohalides (III,IV) and telluride (VII) exhibited bands at 1710-1680 cm^{-1} (νC=O), tertiary C-H bending at 1350-1310 cm^{-1}, νOH at 3490-3410 cm^{-1} and OH bending vibrations (1390-1370) indicating the partial conversion of keto form into enol (~ 50%). The appearance of a new band around 2300 cm^{-1} is due to Te-H (enolic) bond[5,11]. The intensity ratio between the peaks originating from the C=O and OH groups seems to depend also on the nature of the anion attached to tellurium atom.

The IR spectra of oximino derivatives (VIII, IX) showed νC=N (oxime) at 1650 cm^{-1} and νOH (bonded) at 3310 cm^{-1} indicating the presence of oxime function in the compounds. A new peak occurring in (IX) at 2330 cm^{-1} is assigned to νTe-H[6] (oximino OH) mode. The IR spectra of adducts (X-XIII) showed strong bands due to νC=O and νC-H whereas νOH bands were completely absent indicating presence of purely keto function. The donor molecules, viz., pyrrolidine, pyridine, piperidine and morpholine exhibited bands in the range 3400-3170 cm^{-1}, attributable to νNH mode.The spectra of adducts showed, in general, an appreciable lowering of the characteristic peaks due to the coordination with tellurium atom, but in the case of adduct with pyridine there was a positive shift in the pyridine ring stretching vibrations[12] which was indicative of back bonding from tellurium atom to pyridine through the formation of an extensive π bonding. In the far IR region, bands due to νTe-C[13], νTe-N[14] and νTe-S[15] appeared at 535-510, 425-410 and 280-270 cm^{-1}, respectively.

In the ^1H NMR spectra of compounds (I—VII), aromatic protons appeared as multiplets in the region τ 3.2-1.6, while in the adducts (X-XIII) these were deshielded (τ 1.2-0.6) probably due to the steric hindrance by the donor molecules around the tellurium atom. The OH proton of the enol form (~ 50%) attached to the lone pair of tellurium atom, forming a

novel Te-H bond[16,17], gave a singlet between τ 10 and 9.2. The methylene protons appeared in the regions τ 7.9-7.3 and τ 7.1-6.6; probably the drift in the electron density around tellurium atom changes the electronic environment of the adjacent methylene groups. The spectra of adducts showed only one signal for two methylene protons and no signal was observed for Te-H bond.

The ^{1}H NMR spectrum of oximino derivatives (VIII) showed aromatic multiplets between τ 2.8 and 2.2 and broad singlet at τ 3.8 due to OH proton whereas the oximino derivative (IX) from telluride, in which the bulky iodine atoms had been removed, showed phenyl protons as multiplets between τ 2.8 and 1.8 and two singlets, one at τ 3.1 due to OH proton and another at τ 8.9 due to Te-H proton. The steric hindrance exhibited by the bulky iodine atoms prevented the formation of Te-H bond[6] in derivative (VIII).

Thanks are due to Dr R S Kapil, CDRI, Lucknow for providing spectral facilities and Dr Mohd. Athar, ITRC, Lucknow, for helpful discussions.

References

1 Kulkarni Y D & Srivastava S, *Indian J Chem*, **24A** (1985) 65.
2 Kulkarni Y D & Srivastava S, *Indian J Chem*, **24A** (1985) 429.
3 Kulkarni Y D, Srivastava S, Abdi S H R & Athar M, *Synth React inorg met-org Chem*, **15** (1985) 1043.
4 Kulkarni Y D & Srivastava S, *Indian J Chem*, **24A** (1985) 710.
5 Kulkarni Y D, Srivastava S & Athar M, *Indian J Chem*, **24A** (1985) 1069.
6 Kulkarni Y D, Srivastava S & Athar M, *Indian J Chem*, **25A** (1986) 57.
7 Spencer H K & Cava M P, *J org Chem*, **42** (1977) 2937.
8 Rao C N R, *Chemical applications of infrared spectroscopy* (Academic Press, New York) 1963, 343.
9 Bailey R A, Kozak S L, Michelsen T W & Mills W N, *Coord Chem Rev*, **6** (1971) 407.
10 Srivastava T N, Srivastava R C & Bhargava A, *Indian J Chem*, **18A** (1979) 236.
11 Rossmann K & Straaley J W, *J chem Phys*, **24** (1956) 1276.
12 Wilmhurst J K & Bermstein H J, *Can J Chem*, **35** (1957) 1183.
13 Smith K N & Thayer J S, *Inorg Chem*, **13** (1974) 3021.
14 Srivastava T N, Srivastava R C & Singh M, *Inorg chim Acta*, **33** (1979) 149.
15 Clark E R, Collect A J & Naik D G, *J chem Soc, Dalton Trans*, (1973) 1961.
16 Frischleder H, Klose G & Ranft J, *Z Karl-Marx Univ*, **14** (1965) 863.
17 Anderson S J, Barnes J R, Goggin P L & Goodfellow R J, *J chem Res*, (1979) 286.

Indian Journal of Chemistry
Vol. 27A, August 1988, pp. 737-738

Halo & Nitrato Complexes of Cobalt(II), Nickel(II) & Copper(II) with Glutamine

R SHANTHI, K S NAGARAJA & M R UDUPA*
Department of Chemistry, Indian Institute of Technology, Madras 600 036

Received 14 *September* 1987; *revised* 26 *October* 1987; *accepted* 4 *January* 1988

Metal complexes of glutamine (HGln), having the composition, $M(Gln)X(H_2O)_2$ [M = Co(II), Ni(II) or Cu(II); X = Cl, Br or NO_3] have been prepared and characterized. The magnetic moments for cobalt(II) (4.8 B.M.), nickel(II) (2.9 B.M.) and copper(II) (1.9 B.M.) complexes and the UV-visible spectral data suggest an octahedral geometry around the metal atoms. The IR spectral data of the complexes indicate coordination through amino and carboxylate groups of glutamine. The EPR spectra of Cu(II) complexes at room temperature and liquid nitrogen temperature have also been recorded and discussed.

Glutamine and its metal complexes play a significant role in cancer therapy[1,2]. Eventhough a number of 1:2 complexes of glutamine were isolated in the solid state[3-5], no reports are available on complexes with 1:1 composition. Herein we report the isolation and characterization of 1:1 halo and nitrato complexes of cobalt(II), nickel(II) and copper(II) with glutamine.

L-Glutamine was obtained from Loba Chemie (Germany) and the metal salts were of laboratory grade and used as such.

The complexes (**1-7**; Table 1) were prepared by the following general procedure:

A methanolic solution of metal(II) salt (0.02 mol, 20 ml) was added to an aqueous solution of glutamine (0.02 mol, 20 ml) and the reaction mixture was heated over a water-bath for 15 min and cooled. Slow evaporation of the solvent led to precipitation of the complex which was filtered, washed with MeOH and dried in a vacuum desiccator over fused calcium chloride. The nitrato complexes of Co(II) and Ni(II) could not be isolated in solid state.

Thermogravimetric analysis was performed in air using Stanton recording thermobalance at a heating rate of 6°C min^{-1}. The magnetic susceptibilities of the complexes were measured at room temperature on a Guoy balance using $[Hg(SCN)_4Co]$ as the calibrant. The magnetic moments were calculated applying Pascal's constants. UV-visible spectra of the complexes were recorded in nujol on a Carl-Zeiss DMR-21 spectrophotometer. IR and far IR spectra were recorded in KBr and polythene pellets on Perkin-Elmer-257 and Fourier Polytech IR-30 spectrophotometers. The EPR spectra were recorded at room temperature and liquid nitrogen temperature on a Varian E-4 X-band spectrometer employing DPPH as the calibrant.

The halo and nitrato complexes of Mn(II) (d^5), Zn(II) (d^{10}) and Cd(II) (d^{10}) with glutamine could not be prepared as the bisglutaminates separated out[5]. The difficulty in isolating 1:1 complexes may be attributed to very low crystal field stabilization energy of these metal ions.

The isolated complexes are insoluble in acetone and methanol. The analytical data of the complexes, given in Table 1, are suggestive of 1:1 composition. The complexes were found to decompose in the temperature ranges of 120-200° and 200-600°C. The mass loss in the first stage corresponded to the removal of water molecules and as these were lost comparatively at higher temperatures. It is inferred that the water molecules are coordinated to the metal ions. The mass loss, chemical analyses and X-ray diffraction data indicated that the end residues were Co_3O_4, NiO and CuO respectively.

The magnetic moments of Co(II) (4.8 B.M.) and

Table 1—Analytical, Magnetic and Electronic Spectral Data of Metal(II) Glutaminate Complexes

Sl No.	Complex	Found (calc) %			μ_{eff} (B.M.)
		N	Halide	M	
1	$Co(Gln)Cl(H_2O)_2$[a]	10.3(10.2)	12.7(12.8)	20.8(21.4)	4.76
2	$Co(Gln)Br(H_2O)_2$	8.0(8.7)	24.4(24.9)	20.3(18.4)	4.65
3	$Ni(Gln)Cl(H_2O)_2$[b]	10.0(10.2)	12.6(12.8)	21.1(21.3)	2.90
4	$Ni(Gln)Br(H_2O)_2$	6.2(7.7)	25.4(25.0)	16.3(18.3)	2.89
5	$Cu(Gln)Cl(H_2O)_2$	10.3(10.3)	12.5(12.6)	22.5(22.7)	1.89
6	$Cu(Gln)Br(H_2O)_2$	8.0(8.6)	24.3(24.6)	20.5(19.5)	1.90
7	$Cu(Gln)(NO_3)(H_2O)_2$	13.5(13.7)	—	20.4(20.6)	1.93

a) % C, 20.5(21.8); % H, 3.9(4.0); (b) % C, 20.5(21.8); % H, 4.1(4.0).

Ni(II) (2.9 B.M.) complexes are indicative[6] of octahedral ligand field environment around central metal ion. The μ_{eff} values for copper(II) complexes (1.9 B.M.) are as expected for tetragonal complexes.

The electronic spectra of the Co(II) complexes exhibited bands around 8, 16 and 19 kK which have been attributed to $^4T_{1g}(F) \rightarrow {}^4T_{2g}$, $^4T_{1g} \rightarrow {}^4A_{2g}$ and $^4T_{1g} \rightarrow {}^4T_{1g}(P)$, respectively[7,8] corresponding to octahedral Co(II). The appearance of a shoulder at high energy region (~ 20.8 kK) may be due to splitting of $^4T_{1g}(P)$ state, because of spin-orbit coupling. The adsorption maxima around 9.5 [$^3A_{2g} \rightarrow {}^3T_{2g}$], 16 [$^3A_{2g} \rightarrow {}^3T_{1g}(F)$] and 26 kK [$^3A_{2g} \rightarrow {}^3T_{1g}(P)$] suggest nickel(II) in an octahedral environment. The transitions around 14 kK due to $^2E_g \rightarrow {}^2T_g$ indicated six-coordination of Cu(II) in its comploexes. The calculated crystal field parameters D_q (cm^{-1}), B(cm^{-1}) and β are: for **1** (860, 863, 0.89); **2** (828, 857, 0.89), **3** (961, 833, 0.79) and **4** (943, 872, 0.82). The D_q values for **5, 6** and **7** are 1379, 1370 and 1492 cm^{-1}, respectively. These values are in agreement with the positions of the halo-ligands in their spectrochemical and nephelauxetic series.

The disappearance of the free ligand $\nu(NH_3^+)$ (at 3150 cm^{-1}) and the appearance of a new band at 3340 cm^{-1} in the IR spectra of the complexes suggest coordination of the amine group of glutamine to the metal ion. The free ligand bands at 1670 (amide-I), 1620 (amide-II), 1585 ($\nu_{as}COO^-$) and 1405 ($\nu_s COO^-$) cm^{-1} are shifted in the IR spectra of the complexes. The difference ($\nu_{as} - \nu_s$) of 200 cm^{-1} in the νCOO^- modes indicated monodentate nature of the carboxyl group[9]. The bands in the IR spectrum of the nitrato complex at 780, 1410 and 1280 cm^{-1} indicated the monodentate[10] nature of the nitrato group. The IR bands observed in the region 400-425, 300-370, 250 and 220 cm^{-1} have been assigned to $\nu(M-N)$, $\nu(M-O)$, $\nu(M-Cl)$ and $\nu(M-Br)$ respectively.

A qualitative discussion on the molecular and solid state structures of copper(II) complexes is provided in the light of EPR spectral studies. The EPR spectrum of bis(glutaminato)copper(II) was recorded for comparison. The g_{iso} values at room temperature of **5, 6** and **7** are 2.12, 2.15 and 2.13 respectively. The $g_{\|}$ and $g_{\perp}$ values of **7** are 2.14 and 2.12 respectively. However the spectra of **5** and **6** show slight anisotropy at liquid nitrogen temperature. The spectrum of **5** at 77 K in a mixture of H_2O and EtOH exhibited four hyperfine lines due to Cu(II), and $g_{\|}$ (2.36) > $g_{\perp}$ (2.10) indicated axial symmetry. The absence of anisotropic spectrum for **5** or **6** at room temperature may be attributed to the dipolar interaction between the two copper centres favoured by the bridging characteristic of the chloro or bromo ligand. This is not observed in the nitrato complex. It may be deduced qualitatively from the nature of the EPR spectra that the intermolecular distances in the complexes follow the order: $Cu(glu)_2 > 7 > 5 \sim 6$. The calculated covalency factors, k_0^2 for **5** (0.46), **6** (0.60) and **7** (0.57) suggest[11] that the covalent bond characters follow the order Cu-Br > Cu-ONO_2 > Cu-Cl as the other ligands around copper are the same.

Thus, the glycinyl moiety of the glutamine coordinates to the metal forming five-membered chelate ring. Further, the amide oxygen of the glutamine may be involved in bonding with the neighbouring metal and thereby effectively forming tridentate ligand as observed in the 1:2 complexes.

References

1 Charlson A J, Banner R J, Gale R P, McArdie N T, Trainer K E & Walton E C, *J clin hematol Ontol*, **7** (1977) 293.
2 Charlson A J, Banner R J, Gale R P, McArdle N T, Trainer K E & Walton E C, *Cancer treat Rep*, **61** (1977) 469.
3 Albert A, *Biochem J*, **47** (1905) 531.
4 Kirson B & Barsily I, *Bull Chim Soc Fr*, (1959) 90.
5 Tiwari R C & Srivastava M N, *J inorg nucl Chem*, **35** (1973) 3044.
6 Figgis B N & Lewis J, *Modern coordination chemistry*, edited by J Lewis & R G Wilkins (Interscience, New York) 1960, pp. 403.
7 Lever A B P, *Inorganic electronic spectroscopy* (Elsevier, Amsterdam) 1984, pp. 479, 507 & 553.
8 Jorgensen C K, *Acta chem Scand*, **10** (1956) 887.
9 Nakamoto K, Morimoto Y & Martell A E, *J Am chem Soc*, **88** (1961) 4528.
10 Nakamoto K, *J phys Chem*, **64** (1960) 1420.
11 Yokoi A, Sai M, Isobe T & Oshwawa S, *Bull chem Soc Japan*, **45** (1972) 2189.

Indian Journal of Chemistry
Vol. 27A, August 1988, pp. 739-741

Complexes of *o*-Vanillin Oxime with La(III), Ce(III), Pr(III), Nd(III), Sm(III), Gd(III), Tb(III), Dy(III), Ho(III) & Yb(III)

M L DHAR*, V K GUPTA & ONKAR SINGH
Department of Chemistry, Jammu University (New Campus), Jammu 180 004

Received 9 *February* 1987; *revised* 2 *July* 1987; *rerevised and accepted* 18 *January* 1988

Ten complexes of lanthanides with *o*-vanillin oxime have been synthesised and characterised. The composition of the complexes as determined by elemental and thermal analyses infrared electronic spectral and magnetic moment studies is $[Ln(C_8H_8NO_3)_3.XH_2O]$, where X = 2 when Ln = La, Ce, Pr, Nd, Sm and X = 3 when Ln = Gd, Dy, Tb, Ho, Yb; $C_8H_8NO_3^-$ represents the the anion of the ligand.

o-Vanillin oxime has been reported to give colour reactions with a number of metal ions[1]. We report here the results of our systematic study on the nature and compositions of some lanthanide complexes of *o*-vanillin oxime (I), isolated in the solid state.

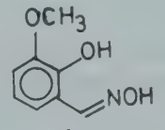

(I)

o-Vanillin oxime was prepared by the known method[2] and recrystallized from water, m.p. 123° (lit. 123°). The Lanthanide (III) complexes were prepared by mixing the metal ion solution (in doubly distilled water) and ligand solution (in 95% ethanol) in the molar ratio of 1:10 (metal:ligand). The precipitated complexes were washed free of the excess of ligand by ethanol and dried *in vacuo* over anhydrous calcium chloride. Carbon, hydrogen and metal contents were estimated by standard methods while IR (4000-200 cm^{-1}), DRS (50,000-10,000 cm^{-1}) and thermal studies were carried out using Perkin-Elmer-377 grating IR spectrophotometer, VSU2P (Carl-Zeiss) spectrophotometer and Paulik-Paulik Erdy MOM derivatograph respectively. Magnetic measurements were done by the Gouy method.

The elemental analysis results (Table 1) for C, H and metal (M) suggest the composition of the metal complexes to be $[Ln(C_8H_8NO_3)_3.XH_2O]$, where X = 2 when Ln = La, Ce, Pr, Nd, Sm and X = 3 when Ln = Gd, Dy, Tb, Ho, Yb; $C_8H_8NO_3^-$ represents the anion of the ligand. This composition is further supported by the IR spectral studies of the ligand and the complexes. The ligand spectrum shows a band at 3350 cm^{-1} due to hydrogen bonded ν(OH) mode. This band disappears in the spectra of complexes indicating coordination through hydroxyl oxygen

Table 1—Elemental Analysis (%) of the Complexes

Sl No.	Complexes	Colour	Found (Calc.), %			
			C	H	N	M
1	$[La(C_8H_8NO_3)_3.2H_2O]$	Grey	42.46 (42.79)	4.41 (4.16)	6.46 (6.24)	20.92 (20.64)
2	$[Ce(C_8H_8NO_3)_3.2H_2O]$	Dark grey	43.06 (42.72)	4.32 (4.15)	6.61 (6.23)	20.17 (20.73)
3	$[Pr(C_8H_8NO_3)_3.2H_2O]$	Light grey	42.45 (42.67)	4.38 (4.14)	6.59 (6.22)	21.10 (20.87)
4	$[Nd(C_8H_8NO_3)_3.2H_2O]$	Dark grey	42.79 (42.46)	4.40 (4.12)	6.38 (6.19)	21.52 (21.26)
5	$[Sm(C_8H_8NO_3)_3.2H_2O]$	Grey	42.45 (42.08)	4.38 (4.09)	6.27 (6.13)	22.25 (21.96)
6	$[Gd(C_8H_8NO_3)_3.3H_2O]$	Grey	40.95 (40.60)	4.55 (4.22)	6.20 (5.92)	22.44 (22.17)
7	$[Tb(C_8H_8NO_3)_3.3H_2O]$	Dark green	40.24 (40.51)	4.62 (4.21)	6.39 (5.90)	22.66 (23.35)
8	$[Dy(C_8H_8NO_3)_3.3H_2O]$	Grey	40.79 (40.30)	4.32 (4.19)	6.08 (5.87)	22.43 (22.74)
9	$[Ho(C_8H_8NO_3)_3.3H_2O]$	Dark grey	40.49 (40.17)	4.38 (4.18)	6.15 (5.85)	22.77 (23.00)
10	$[Yb(C_8H_8NO_3)_3.3H_2O]$	Grey	40.15 (39.72)	4.39 (4.13)	8.04 (5.79)	23.59 (23.86)

after deprotonation. This is corroborated by appearance of new bands in the spectra of complexes in the region 650-415 cm^{-1} due to $\nu(M-O)$ mode. The ligand shows a band at 1625 cm^{-1} which has been assigned to $\nu(C=N+C\cdots C)$ mode. Its lowering by 10-45 cm^{-1} in the complexes shows coordination through oxime nitrogen. The complexes also show bands in the region 3780-3700 cm^{-1} due to coordinated water molecules.

The magnetic susceptibility values and electronic absorption spectra (DRS) further corroborate the nature of the complexes. The La(III) complex is diamagnetic while the others are paramagnetic. The values are little different from those reported by

Table 2—Diffuse Reflectance Spectral and Magnetic Moment Data of the Complexes

Sl No.*	$\mu_{eff.}$ (B.M.)	Observed bands (cm^{-1})	Probable assignment of some bands (cm^{-1})	
1	0.00	40000, 29411, 25000, 22727, 17857	17857	Intra-ligand charge transfer
2	0.42	40816, 31461, 31250, 28571, 19230	40816	$^2D_{5/2} \leftarrow {}^2F_{5/2}$
			31250	$^2D_{3/2} \leftarrow$
3	3.46	42553, 37735, 23809, 16666	2380[Ω]	$^3P_2 \leftarrow {}^3H_4$
			16666	$^1D_2 \leftarrow$
4	3.54	38461, 28571, 22222, 18518	28571	$^2P_{1/2} \leftarrow {}^4I_{9/4}$
			22222	$^2G_{9/2} \leftarrow$
			18518	$^4G_{7/2} \leftarrow$
5	0.88	38461, 29411, 14705, 11111	14705	$^6D_{7/2} \leftarrow {}^6H_{5/2}$
			11111	$^6F_{7/2} \leftarrow$
6	7.83	39215, 26315, 21739, 16129	26315	$^6P_{7/2} \leftarrow {}^8S_{7/2}$
7	4.40	42553, 28571, 21739, 15262	15262	$^6H_{3/2} \leftarrow {}^6H_{5/2}$
8	10.40	40816, 26315, 23255, 15125	26315	$^5D_3 \leftarrow {}^7F_6$
			15125	$^5D_2 \leftarrow$
9	10.32	42553, 26315, 19230, 15625	26315	$^5G_4 \leftarrow {}^5I_8$
			19230	$^5F_4 \leftarrow$
			15625	$^5F_5 \leftarrow$
10	4.43	41666, 28571, 20833, 13513	20833	$4f \leftarrow 5P$
			13513	$^2F_{5/2} \leftarrow$

*Numbers same as in Table 1.

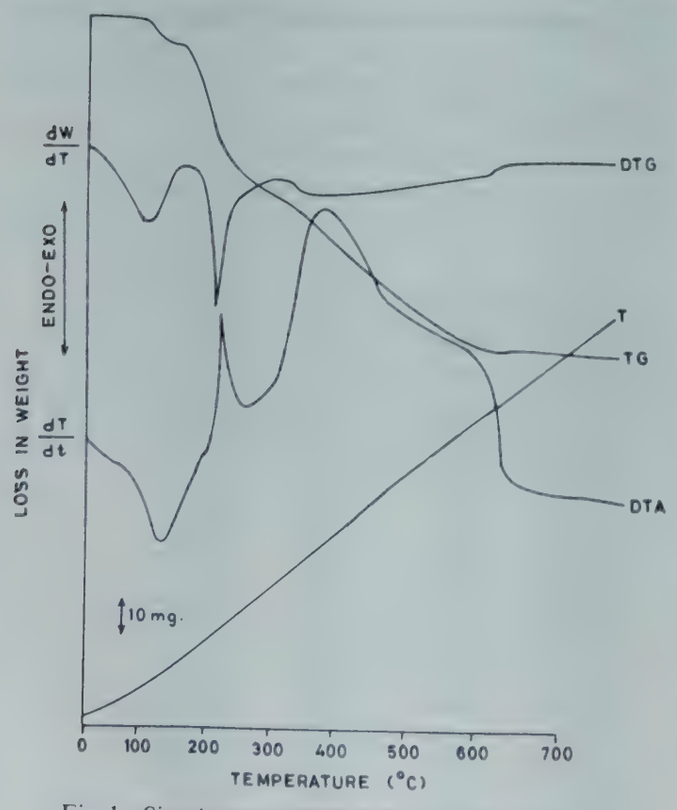

Fig. 1—Simultaneous DTG, DTA and TG curves of $[La(C_8H_8NO_3)_3.2H_2O]$

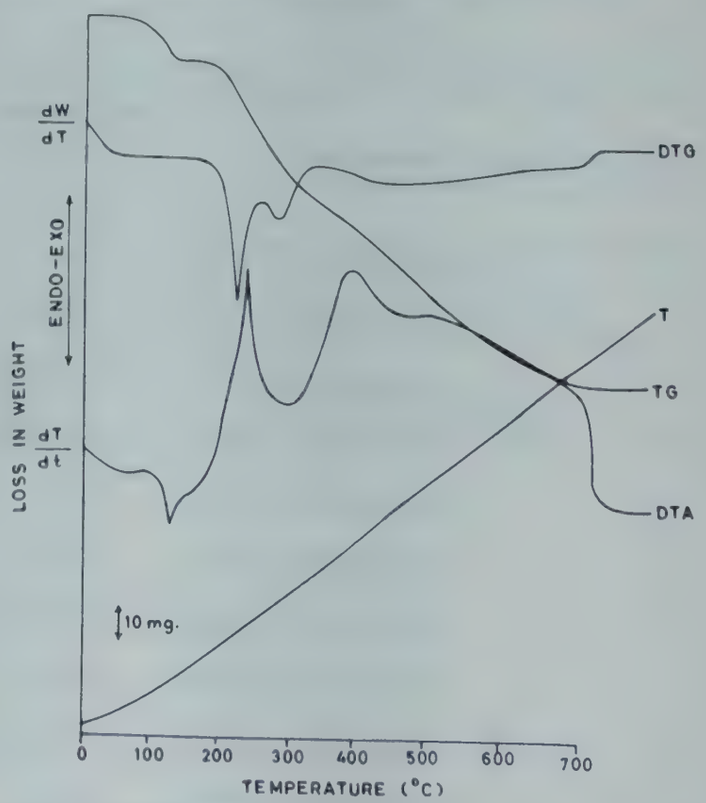

Fig. 2—Simultaneous DTG, DTA and TG curves of $[Yb(C_8H_8NO_3)_3.3H_2O]$

Hund and Van Vleck for free ions[3]. This behaviour is in agreement with similar literature reports[4,5]. The electronic absorption spectra and the assignment of bands are based on the available data on the absorption spectra of free lanthanide ions, the hypersensitive transitions in lanthanides and the absorption spectra of lanthanide ions in crystals and in solutions. The qualitative assignments[6-12] of the bands are given in Table 2. The other unassigned bands are electron transfer bands of the $5d \leftarrow 4f$ type, charge transfer bands and intra-ligand transitions. Based on observed data, square antiprismatic geometries[13,14] for La(III), Ce(III), Pr(III), Nd(III) and Sm(III) complexes and tricapped trigonalbipyramidal configurations[15,16] for Gd(III), Dy(III), Tb(III), Ho(III) and Yb(III) complexes are suggested.

Figures 1 and 2 show the simultaneous DTA, DTG and TG curves of La(III) and Yb(III) complexes at the heating rate of 10° per minute. The DTA curve of La(III) complex shows one sharp endothermic peak at 140°C and one broad at 390°C, whereas the DTA curve of Yb(III) complex shows one sharp endotherm at 130°C and two exotherms (one sharp at 250°C and one broad at 390°). There are corresponding peaks in DTG curves, but at slightly lower temperatures. The first arrest in TG curves of these complexes shows mass loss of 5.73% for La(III) complex (calc. 5.43%) and 7.27% for Yb(III) complex (calc. 7.44%) corresponding to the elimination of water molecules. After complete decomposition, the mass loss shown by TG curves is 75.40% for La(III) complex (calc. 75.79%) and 72.72% for Yb(III) complex (calc. 72.82°). The oxides formed on the pyrolysis of these complexes are La_2O_3 and Yb_2O_3, respectively. It is inferred from spectral, magnetic and thermal studies that water molecules are coordinated to the metal ions.

From the above discussion it is concluded that *o*-vanillin oxime behaves as a bidentate ligand coordinating through oxygen and nitrogen to the metal ions and forms 8 or 9 coordinated complexes.

References

1 Raina R K, Ph.D. Thesis, Jammu University, 1979.
2 Vogel A I, *A text book of quantitative organic analysis* (Longman Green, London), 1962.
3 Spedding F H & Danne A H, *Rare earths* (Interscience Publishers, New York), 1963, 13.
4 Agarwala R C & Gupta S P, *Curr Sci*, **43** (1974) 3263.
5 Srivastava A K & Rana V B, *J inorg nucl Chem*, **37** (1975) 723.
6 Moeller T, *Rec Chem Progr*, **14** (1953) 69.
7 Dike G H, *Spectra and energy levels of rare earth ionsin crystals* (Wiley, New York), 1968.
8 Sinha S P, *Complexes of rare earths* (Pergamon Press, New York), 1966.
9 Karraker D G, *Inorg Chem*, **7** (1968) 473; **6** (1967) 1863; *J inorg nucl Chem*, **31** (1969) 2815.
10 Judd B R, *Phys Rev*, **127** (1962) 750.
11 Vickery R C, *J chem Soc*, (1952) 421.
12 Fisher R D & Fisher H, *J org Chem*, **27** (1965) 273.
13 Cunninghan J A, Sands D E & Wagner W F, *Inorg Chem*, **6** (1967) 499.
14 Phillips I I T, Sands D E & Wagner W F, *Inorg Chem*, **7** (1968) 2295.
15 Helmoholz L, *J Am chem Soc*, **61** (1939) 1544.
16 Fitzwater D R & Rundle R E, *Z Kristallog*, **112** (1959) 632.

Indian Journal of Chemistry
Vol. 27A, August 1988, pp. 742-744

Metal Chelates as Fungicides: Part IV† – Metal(II) Complexes of 4-Chloro-5,6,7,8-tetrahydrobenzothieno[2,3-*d*]pyrimidine

LALLAN MISHRA*, L B TIWARI‡,
H N PANDEY & V UPADHYAY
Department of Chemistry, SCPG College, Ballia 277 001
and
U C AGARWALA*
Department of Chemistry, Indian Institute of Technology, Kanpur 208 016

Received 14 *August* 1987; *revised* 6 *October* 1987; *accepted* 27 *November* 1987

The complexing behaviour of 4-chloro-5,6,7,8-tetrahydrobenzothieno[2,3-*d*]pyrimidine (L) with Mn(II), Co(II), Ni(II), Cu(II), Zn(II), Cd(II) and Hg(II) salts has been studied. The complexes have been characterized by elemental analyses, magnetic measurements, IR and photoacoustic spectral studies. The ligand and metal complexes have also been tested for their fungicidal activity.

Pyrimidine derivatives are well known for exhibiting a variety of biological activites[1-5]. In exhibiting these properties, metal ions sometimes play very important roles. Herein we report the metal complexes of 4-chloro-5,6,7,8-tetrahydrobenzothieno[2,3-*d*]pyrimidine (I) with Mn(II), Co(II), Ni(II), Cu(II), Zn(II), Cd(II) and Hg(II). The complexes have also been screened for their fungicidal activity against *helminthosporium oryzae* and *Trichophyton grophytes* by the method described earlier[6]. However, none of the complexes, except those of Mn(II) and Cu(II) was found to be active against these fungi.

All the chemicals were either chemically pure or of AR grade. The ligand 4-chloro-5,6,7,8-tetrahydrobenzothieno[2,3-*d*]pyrimidine I was synthesised by literature method[7].

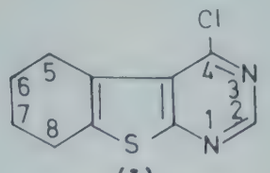

(I)

All the complexes were prepared by the following general method:

Equimolar amounts of $CuCl_2.2H_2O$ (1 mmol) and the ligand (1.1 mmol) were dissolved in boiling ethanol (50 ml). To this were added a few drops of NaOH (8% w/v) when a greenish precipitate was obtained. (The addition of base is essential for the better precipitation of the complexes). After cooling the precipitates were filtered, washed successively with water, ethanol and dried in open atmosphere, m.p. > 300°C. Analytical data of the complexes are recorded in Table 1.

IR Spectra of the samples were recorded in KBr on a Perkin-Elmer 621 spectrophotometer and the photoacoustic spectra of the powdered samples on a locally fabricated single beam photacoustic spectrometer[9] in the wavelength region 400-750 nm. All the spectra were normalized by the photoacoustic spectrum of carbon black recorded in the same wavelength region. Magnetic susceptibilities were determined on a Cahn electrobalance using $Hg[Co(NCS)_4]$ as the calibrant. The diamagnetic corrections were estimated from Pascals constant[10].

All the complexes listed in Table 1 are insoluble in aqueous and nonaqueous solvents. The IR spectra of the complexes exhibited a broad band around 3500 cm^{-1} assignable to νOH mode of water molecules. The ligand band at 1620 cm^{-1}, which has contributions from ν(C=C), ν(C=N) and δ(CH) was shifted to around 1600 cm^{-1} in the complexes. Since the formation of π-complexes with aromatic part of the molecule is not expected, the bonding of the ligand is presumed through one of the nitrogen atoms of the pyrimidine moiety, particularly N-1 because of steric reasons. The positions of the remaining characteristic ligand bands remained unchanged in the IR spectra of the complexes. In the IR spectra of Mn(II) and Cd(II) complexes, the coordinated nature of the acetate group was ascertained by shift ($\Delta\nu = 20$ cm^{-1}) of ν_{as} (COO) and ν_s(COO) modes of the acetate group around 1590 and 1450 respectively to lower wavenumbers. The presence of coordinated SO_4^{2-} group in Ni(II) and Zn(II) complexes was confirmed by the characteristic SO_4^{2-} bands[11]. Owing to too many bands in the lower far IR region, it was difficult to make unambiguous assignment to ν(M–Cl) in the spectra of Co, Cu and Hg complexes.

The number of water molecules of crystallization and coordinated water molecules present in

† Part III: *Synth React Inorg Met-org;* **16** (1986) 831.
‡ Department of Physics, SC College, Ballia 277 001.

Table 1 – Analytical Data, Photoacoustic Spectral Data (PAS), Magnetic Moments of the Ligand and Complexes

Compounds (colour)	Found (calc) %				PAS				μ_{eff} (BM)
	N	S*	Cl*	Metal*	T←S (nm)	M→L CT (nm)	*d-d* Transition		
							λ_{max} (nm)	Assignment	
Ligand (L)	11.9 (12.4)	13.8 (14.2)	15.1 (15.8)	—	430	—	—	—	—
$[Mn(CH_3COO)_2L.H_2O].2H_2O$	6.8 (6.2)	7.9 (7.0)	8.1 (7.8)	13.1 (12.16)	430	460	650 590	 $^6S \rightarrow {}^4G$	6.1
$[CoLCl_2.H_2O].2H_2O$ (pink)	6.1 (6.8)	7.2 (7.8)	25.2 (26.0)	13.2 (14.4)	420	470	730 570 530	$^4A'_2(F) \rightarrow {}^4E'(F)$ $^4A_2(F) \rightarrow {}^4A'_2(P)$ $^4A_2(F) \rightarrow {}^4E''(P)$	4.2
$[NiLSO_4.2H_2O].H_2O$ (green)	6.5 (6.4)	14.6 (14.7)	7.8 (8.1)	14.8 (13.5)	420	465	660	$^3A_{2g}(F) \rightarrow {}^3T_{2g}(F)$	2.9
$[CuLCl_2.H_2O].2H_2O$ (green)	6.9 (6.8)	7.8 (7.8)	27.1 (25.6)	15.2 (15.4)	420	460	700	$^2E \rightarrow {}^2T_2$	2.2
$[ZnLSO_4.H_2O].2H_2O$ (white)	6.5 (6.3)	14.8 (14.5)	7.9 (8.0)	15.1 (14.9)	420	—	—		DM
$[CdL(CH_3COO)_2.H_2O].2H_2O$ (white)	5.9 (5.5)	7.3 (6.3)	7.1 (6.9)	23.5 (22.1)	430	—	—		DM
$[HgLCl_2].2H_2O$ (white)	5.4 (5.2)	7.1 (6.0)	20.9 (20.0)	38.9 (37.8)	430	—	—		DM

DM = diamagnetic
*Estimated by literature method (see ref. 8).

the complexes were determined by the literature method[12]. In this determinations a fixed amount of complex was first heated at 100-120°C and then subsequently at 180°C. From the loss in mass in these two heatings, the number of water molecules of crystallization and coordinated water molecules were calculated.

The photoacoustic spectrum (PAS) of benzothienopyrimidine (I) displayed a band at 430 nm which was also observed in the PAS of all metal complexes. In the parent pyrimidine the longest wavelength band due to S→T transition[13] appeared at 345 nm which should have shifted towards higher wavelength region in the spectrum of PAS I because of higher degree of conjugation of π-electrons in the latter. Therefore 430 nm band present in I PAS and complex spectra has been assigned to S→T transition.

The position of the other bands in the PAS of Mn(II), Co(II), Ni(II) and Cu(II) complexes alongwith their possible assignments are given in Table 1. Since the structures of the complexes do not correspond to O_h symmetry, the bands generally found in the PAS of the octahedral complexes are expected to split into two or more bands. The assignments given in Table 1 are thus purely tentative. Besides these bands, the PAS of the complexes exhibited one relatively intense band around 460 nm. The order (energywise) of shifts in the position of 460 nm band is Cu > Ni > Co which is the same order as that of oxidizability of the metal ion[14]. It suggests the charge transfer nature of the band (M→L). Since the ligand (L) has empty π-orbitals we assign this band to M→π*(L) CT type. It is interesting to note that this band is not observed in the PAS of Zn(II), Cd(II) and Hg(II) complexes. This behaviour is quite normal because of the very high energy needed to oxidize these metal ions. This further substantiates our assignment.

The PAS of Mn(II) complex exhibited a number of very weak bands. As a matter of fact the whole spectrum showed a wavy pattern which is expected because of the unsymmetrical nature of the complex which is expected to result in splitting of all the energy levels found in octahedral complexes and hence a number of transitions. The band at 460 nm is assigned to M→L CT type. The position of this band should have been on longer wavelength side compared to that in Co(II) complex (470 nm). One of the many possible reasons for its appearance towards higher energy side could be the higher oxidizability of Mn(II) because all of its electrons are unpaired. This explanation is purely tentative.

The PAS of Zn(II), Cd(II) and Hg(II) complexes were found to be very similar to that of the ligand and the lack of *d-d* transitions seems to be quite normal because of their closed shell electronic configuration (d^{10}).

The magnetic moment data of the complexes suggested the complexes to be high spin octahedral ones[10].

Based on the preferred geometries[15] which the metal ions will have in their complexes and because of their insolubility in all the solvents, the polymeric octahedral structures were tentatively proposed for all complexes, except Hg(II) complex which is proposed to be polymeric tetrahedral.

One of the authors (LM) is thankful to the UGC New Delhi for financial assistance.

References

1 Schmidt P, Eichemberger K & Schweizer E, *Chem Abstr*, **72** (1970) 319374.
2 Eichemberger K, Schweizer E & Schmidt P, *Chem Abstr*, **74** (1971) 88638W.
3 Burger A, *Medicinal chemistry* (Wiley-Interscience, New York) 1970 pp. 72, 544 & 719.
4 Manhas M S, Amin S G, Sharma S D, Daya B & Bose A K, *J heterocyclic chem*, **16** (1977) 371.
5 Sauter F, *Chem Abstr*, **77** (1972) 16475 m.
6 Mishra Lallan, Ram V J & Mishra Saraswati, *J Agric Biol Chem (Japan)*, **46** (1982) 2147.
7 Ram V J, *Arch pharm (Weinheim)*, **312** (1972) 19.
8 Vogel A I, *Quantitative inorganic analysis* (Longmans, New York) 1978 pp. 460, 462, 488, 494, 504.
9 Tiwari L B & Thakur S N, *J Optics*, **12** (1983) 74.
10 Lewis J & Wilkins R G, *Modern coordination chemistry* (Interscience, New York) 1960 pp. 403.
11 Nakamoto K, *Infrared and Raman spectra of inorganic and coordination compounds* (John Wiley, New York) 1978, pp. 142.
12 Fabretti A C, Franchini C G, Preti C & Tosi G, *Can J Chem*, **55** (1977) 344.
13 Krishna V G & Goodman L, *J chem Phys*, **36** (1962) 2217.
14 Cotton F A & Wilkinson G, *Advanced inorganic chemistry* (John Wiley, New York) 1980, 691.
15 Cotton F A & Wilkinson G, *Advanced inorganic chemistry* (John Wiley, New York), 1980 pp. 740, 769, 786, 811, 590.

Indian Journal of Chemistry
Vol. 27A, August 1988, pp. 745-746

Ion-exchange Chromatographic Separations of Some Anions on Hydrated Stannic Oxide Impregnated Paper

S K DABRAL*, K P SINGH MUKTAWAT & J P RAWAT†
Department of Chemistry, Govt. Post-graduate College, Uttarkashi 249 193

Received 25 *August* 1987;
revised and accepted 18 *December* 1987

A comparative study of the chromatographic behaviour of a few common anions on untreated Whatman no 1 paper and paper impregnated with hydrated stannic oxide has been made by employing identical aqueous, non-aqueous and mixed solvent systems. Sharp, compact and distinct spots are obtained with impregnated papers. Various analytically important binary and ternary separations are reported.

The chromatography of anions on plain paper has been studied by various workers[1-3]. Kocjan *et al.*[4-6] reported the behaviour of various anions on paper strips impregnated with salts of trioctylamine. The importance and potentialities of inorganic ion-exchanger papers have been explored extensively for the separation of metal ions. However, the chromatography of inorganic anions on these papers has not been reported in detail except for a few reports[7,8]. In this note is reported the use of stannic oxide impregnated paper in the separation of some common anions.

Development of the chromatograms was carried out in glass chromatographic jars (30 × 5 cm) using the ascending method on 20 × 3 cm Whatman no 1 impregnated paper strips. Stannic chloride ($SnCl_4.5H_2O$) and other chemicals and solvent systems were of A.R. grade.

Aqueous solutions (nearly 1 mg/ml) of inorganic anions in doubly distilled water (mainly in the form of sodium or potassium salts) were used.

Preparation of impregnated papers

Paper strips (20 × 3 cm) were dipped in 0.1 *M* stannic chloride solution for 10-15 sec, excess reagent was drained off and the strips were dried over the filter paper sheets at room temperature. The dried strips were then dipped in 0.2 *M* sodium hydroxide solution for 20 sec and, after drying, the strips were washed with distilled water to remove excess of the reagent. The strips were finally dried and used as such for the chromatographic studies.

The spots of iodide and thiocyanate were detected with 5% ferric nitrate solution in 0.5 *N* HNO_3, of chromate, dichromate and vanadate with 1% diphenylcarbazide, of sulphide and phosphate with 5% ammonium molybdate, of thiosulphate with 1% aq. $AgNO_3$, of arsenite with tollen's reagent and of ferricyanide and ferrocyanide with 5% hydrous $FeCl_3$ solution containing 2 ml conc hydrochloric acid.

Procedure

The test solutions were spotted with the aid of a micropipette or a fine capillary tube and dried at room temperature by evaporation. For binary and ternary separations the previous spots were dried completely before another application to the same spot was made. After conditioning, the strips were developed by allowing the solvent to move upto 16 cm in each case. The detection of the spots was carried out either by spraying or by drawing the chromatographs through the solution of the detectors. The R_f values were calculated as usual. The same procedure was applied to study the chromatographic behaviour of anions on untreated paper strips using identical solvent systems.

The movement of 11 common inorganic anions was studied in 14 aqueous, non-aqueous and mixed solvent systems (A—N). The R_f values are presented in Table 1. The results reveal that solvents which have no donor properties, like carbon tetrachloride, benzene and acetone, fail to induce migration; weakly polar solvents like ethanol and *n*-butanol also fail to bring about any movement of anions without the presence of a proton donor[9,10].

With untreated papers, the spots are generally wide and diffused and in most of the cases R_f values are comparatively higher, resulting in poor separations, whereas with stannic oxide impregnated paper spots are sharp, compact and distinct and reduced R_f values have been observed, resulting in good and clearcut separations.

It is also observed that with almost all the solvent systems the R_f values of phosphate, vanadate and arsenite are high with untreated papers, but these are remarkably reduced on using stannic oxide impregnated paper (Table 1). This may be due to strong adsorption of these ions on impregnated papers or by the formation of insoluble salts[7]. The selectivity of stannic oxide impregnated paper towards phosphate, vanadate and arsenite offers an opportunity of separating these ions from other anions.

† Department of Chemistry, Aligarh Muslim University, Aligarh 202 001

Table 1—R_f Values of Anions on Stannic Oxide Impregnated & Untreated Papers*

Anions		Solvent Systems									
		A	B	C	G	I	J	K	L	M	N
Iodide	I.P.	0.67	0.82	0.83	0.57	0.58	0.71	0.71	0.80	0.56	0.80
	P.P.	0.75	0.94	0.91	0.64	0.69	0.77	0.80	0.80	0.60	0.84
Thiocyanate	I.P.	0.80	0.81	0.72	0.60	0.68	0.75	0.76	0.83	0.67	0.81
	P.P.	0.92	0.93	0.88	0.77	–	0.83	0.81	0.87	0.70	0.85
Sulphide	I.P.	0.48	0.56	0.80	0.00	0.12	0.65	0.69	0.68	0.12	0.84
	P.P.	0.81	0.72	0.91	0.24	0.46	0.77	0.83	0.73	0.13	0.89
Phosphate	I.P.	0.29	0.34	0.36	0.16	0.06	0.02	0.31	0.23	0.02	0.16
	P.P.	0.64	0.61	0.68	0.30	0.58	0.70	0.80	0.65	0.06	0.30
Dichromate	I.P.	0.81	0.73	0.72	0.08	0.08	0.29	0.23	0.08	0.09	0.77
	P.P.	0.96	0.89	—	0.36	0.28	0.73	0.75	0.67	0.09	0.82
Chromate	I.P.	0.81	0.77	0.76	0.00	0.00	0.38	0.28	0.06	0.08	0.72
	P.P.	1.00	0.86	0.89	0.21	0.36	0.77	0.74	0.62	0.09	0.85
Vanadate	I.P.	0.09	0.09	0.10	0.00	0.00	0.03	0.08	0.00	0.00	0.17
	P.P.	0.73	0.64	0.58	0.18	0.22	0.60	0.55	0.39	0.04	0.70
Thiosulphate	I.P.	0.71	0.87	0.80	0.00	0.13	0.60	0.61	0.62	0.09	0.80
	P.P.	0.82	0.94	0.92	0.27	0.22	0.77	0.78	0.73	0.10	0.90
Arsenite	I.P.	0.13	0.11	—	0.06	0.08	0.18	0.13	0.10	0.06	0.12
	P.P.	0.82	0.68	0.28	0.26	0.21	0.58	0.61	0.50	0.15	0.67
Ferricyanide	I.P.	0.85	0.93	0.87	0.00	0.14	0.66	0.69	0.76	0.12	0.84
	P.P.	1.00	0.99	1.00	0.20	0.31	0.86	0.87	0.90	0.17	0.91
Ferrocyanide	I.P.	0.73	0.70	0.70	0.00	0.00	0.31	0.20	0.70	0.02	0.73
	P.P.	1.00	0.81	0.84	0.32	0.41	0.80	0.77	0.84	0.04	0.94

* Anions did not move in solvents D,E,F and H. I.P. = impregnated paper; P.P. = plain paper.
Solvents: A = distilled water, B = 0.1 *M* sodium nitrate solution, C = 0.1 *M* sodium acetate solution, D = carbon tetrachloride, E = benzene, F = *n*-butanol, G = ethanol, H = acetone, I = isopropanol, J = ethanol:water (1:1), K = isopropanol:water (1:1), L = acetone:water (1:1), M = ethanol:acetic acid:water (2:1:2) and N = *n*-butanol:acetic acid:water (2:1:2).

On the basis of appreciable differences in the R_f values of anions, numerous analytically important binary and ternary separations in different systems have been achieved. Important separations achieved are: separation of vanadate (0.04) from ferrocyanide (0.33), chromate (0.38), sulphide (0.66), ferricyanide (0.67), iodide (0.71) and thiocyanate (0.75); phosphate (0.03) from chromate (0.38), sulphide (0.66), iodide (0.71) and thiocyanate (0.75); and ferrocyanide (0.33) from ferricyanide (0.67) and thiocyanate (0.75) in ethanol:water (1:1). Iodide (0.55) and thiocyanate (0.67) could be separated from vanadate (0.00), phosphate (0.02), ferrocyanide (0.02), arsenite (0.06), chromate (0.09), dichromate (0.08), thiosulphate (0.09), sulphide (0.12) and ferricyanide (0.12) in ethanol:acetic acid:water (2:1:2) as binary separations. Other separations achieved are vanadate (0.09) from phosphate (0.30) and thiocyanate (0.75), phosphate (0.30) and iodide (0.70), arsenite (0.12) from chromate (0.29) and sulphide (0.69) and chromate (0.29) and thiocyanate (0.75) in isoproponol:water (1:1); chromate (0.08), dichromate (0.09), sulphide (0.13), ferrocyanide (0.02) and ferricyanide (0.12) from iodide (0.56) and thiocyanate (0.66) in ethanol:acetic acid:water (2:1:2) and phosphate (0.16) from chromate (0.71) and sulphide (0.83) and ferrocyanide (0.72) and sulphide (0.83) in *n*-butanol:acetic acid:water (2:1:2) as ternary separations.

References

1 Okumara T & Nishikawa Y, *Bunscki Kagaku*, **25(7)** (1976) 419.
2 Okumara T & Nishikawa Y, *Bunscki Kagaku*, **26(9)** (1977) 582.
3 Ferrer N & Perez J J, *J environ anal Chem*, **27(4)** (1986) 273.
4 Przeszlakowski S & Kocjan R, *Chromatographia*, **10(7)** (1977) 358.
5 Kocjan R & Przeszlakowski S, *Chromatographia*, **11(2)** (1978) 96.
6 Przeszlakowski S & Kocjan R, *Chromatographia*, **12(9)** (1979) 587.
7 Ghatuary R K & Sen A K, *J Indian chem Soc*, **55(4)** (1978) 337.
8 Rajput R P S & Agarwal S, *Anal Lett*, **18** (A14) (1985) 1783.
9 Burma D P, *Anal Chem*, **25 A** (1953) 549.
10 Bhatnagar R P & Bhatnagar N P, *Indian J Chem*, **15A** (1977) 1089.

THE WEALTH OF INDIA

An Encyclopaedia of Indian Raw Materials and Industrial Products, published in two series :

(i) Raw Materials, and **(ii) Industrial Products.**

RAW MATERIALS

The articles deal with Animal Products, Dyes & Tans, Essential Oils, Fats & Oils, Fibres & Pulps, Foods & Fodders, Drugs, Minerals, Spices & Flavourings, and Timbers and other Forest products. Names in Indian languages, and trade names are provided.

For important crops, their origin, distribution, evolution of cultivated types and methods of cultivation, harvesting and storage are mentioned in detail. Data regarding area and yield and import and export are provided. Regarding minerals, their occurrence and distribution in the country and modes of exploitation and utilization are given. The articles are well illustrated. Adequate literature references are provided.

Eleven volumes of the series covering letters A–Z have been published.

Vol. I : A (Revised) Rs. 300.00; Vol. I (A-B) Rs. 120.00; Vol. II (C) Rs. 143.00; Vol. III (D-E) with index to Vols. I-III Rs. 158.00; Vol. IV (F-G) Rs. 150.00; Vol. IV Suppl. Fish & Fisheries Rs. 84.00; Vol. V (H-K) Rs. 171.00; Vol. VI (L-M) Rs. 135.00; Vol. VI : Suppl. on Livestock including poultry Rs. 153.00; Vol. VII (N-Pe) Rs. 150.00; Vol. VIII (Ph-Re) Rs. 129.00; Vol. IX (Rh-Sc) Rs. 200.00; Vol. X (Sp-W) Rs. 338.00; Vol. XI (X-Z) with Cumulative Index to Vols. I-XI Rs. 223.00.

INDUSTRIAL PRODUCTS

Includes articles giving a comprehensive account of various large, medium and small scale industries. Some of the major industries included are : Acids, Carriages, Diesel Engines, Fertilizers, Insecticides & Pesticides, Iron & Steel, Paints & Varnishes, Petroleum Refining, Pharmaceuticals, Plastics, Ship & Boatbuilding, Rubber, Silk, etc.

The articles include an account of the raw materials and their availability, manufacturing processes, and uses of products, and industrial potentialities. Specifications of raw materials as well as finished products and statistical data regarding production, demand, exports, imports, prices, etc. are provided. The articles are suitably illustrated. References to the sources of information are provided.

Nine volumes of the series covering letters A–Z have been published.

Part I (A-B) Rs. 87.00; Part II (C) Rs. 111.00; Part III (D-E) with Index to Parts I-III Rs. 150.00; Part IV (F-H) Rs. 189.00; Part V (I-L) Rs. 135.00; Part VI (M-Pi) Rs. 42.00; Part VII (Pl-Sh) Rs. 90.00; Part VIII (Sl-Tl) Rs. 99.00; Part IX (To-Z) with Index to Parts I-IX Rs. 120.00.

HINDI EDITION : BHARAT KI SAMPADA—PRAKRITIK PADARTH

Vols. I to VII and two supplements of Wealth of India—Raw Materials series in Hindi already published.

Published Volumes :

Vol. I (अ-औ) Rs. 57.00; Vol. II (क) Rs. 54.00; Vol. III (ख-न) Rs. 54.00; Vol. IV (प) Rs. 125.00; Vol. V (फ-मेरे) Rs. 90.00; Vol. VI (मेल-रू) Rs. 120.00; Vol. VII (रे-वाटा) Rs. 203.00; Vol. VIII (वाय-सीसे) Rs. 300.00.

Supplements :

Fish & Fisheries (Matsya & Matsyaki) Rs. 74.00;
Livestock (Pashudhan aur Kukkut Palan) Rs. 51.00

Vols. IX to XI under publication.

Please contact :

SENIOR SALES AND DISTRIBUTION OFFICER

PUBLICATIONS & INFORMATION DIRECTORATE, CSIR

Hillside Road, New Delhi 110 012

RN 7090/63

CSIR PUBLICATIONS

WEALTH OF INDIA

An encyclopaedia of the economic products and Industrial resources of India issued in two series

RAW MATERIALS SERIES – Contains articles on plant, animal and mineral resources.

	Rs.	$	£
Vol. I(A) (Revised)	300.00	94.00	74.00
Vol. I (A-B)	120.00	60.00	26.00
Vol. II (C)	143.00	66.00	34.00
Vol. III (D-E)	158.00	64.00	40.00
Vol. IV (F-G)	98.00	54.00	24.00
Supplement (Fish & Fisheries)	84.00	32.00	21.00
Vol. V (H-K)	171.00	68.00	42.00
Vol. VI (L-M)	135.00	68.00	30.00
Supplement (Livestock including Poultry)	153.00	68.00	39.00
Vol. VII (N-Pe)	150.00	60.00	38.00
Vol. VIII (Ph-Re)	129.00	64.00	28.00
Vol. IX (Rh-Se)	156.00	70.00	38.00
Vol. X (Sp-W)	338.00	150.00	85.00
Vol. XI (X-Z)	223.00	77.00	44.00

INDUSTRIAL PRODUCTS SERIES – Deals with major, Small-Scale and Cottage Industries

Part I (A-B)	87.00	40.00	22.00
Part II (C)	111.00	48.00	28.00
Part III (D-E)	150.00	67.00	39.00
Part IV (F-H)	189.00	84.00	48.00
Part V (I-L)	135.00	46.00	34.00
Part VI (M-Pi)	42.00	16.00	5.60
Part VII (Pl-Sh)	90.00	36.00	12.00
Part VIII (Si-Ti)	99.00	54.00	20.00
Part IX (To-Z)	120.00	68.00	24.00

BHARAT KI SAMPADA (Hindi Edition of Wealth of India, Raw Materials):

Vol. I (अ-औ)	57.00	32.00	13.00
Vol. II (क)	54.00	30.00	12.00
Vol. III (ख-न)	54.00	30.00	12.00
Vol. IV (प)	125.00	68.00	32.00
Vol. V (फ-मेरे)	90.00	44.00	20.00
Vol. VI (मेल-रू)	120.00	54.00	26.00
Vol. VII (रे-वाटा)	203.00	80.00	50.00
Vol. VIII (वाय-सीसे)	300.00	80.00	50.00
Livestock (Kukkut Palan)	51.00	30.00	12.00
Fish & Fisheries (Matsya aur Matsyaki)	74.00	42.00	10.00
A Dictionary of Generic & Specific Names of Plants & Animals Useful to Man	45.00	22.00	10.00

Please Contact :

SENIOR SALES & DISTRIBUTION OFFICER
PUBLICATIONS & INFORMATION DIRECTORATE, CSIR
HILLSIDE ROAD, NEW DELHI - 110012

OTHER PUBLICATIONS

	Rs.	$	£
The Useful Plants of India	192.00	64.00	48.00
A Dictionary of the Flowering Plants in India by H. Santapau & A.N. Henry	63.00	28.00	16.00
Glossary of Indian Medicinal plants by R.N. Chopra, S.L. Nayar & I.C. Chopra	93.00	32.00	20.00
Supplement to Glossary of Indian Medicinal Plants by R.N. Chopra, I.C. Chopra & B.S. Verma	51.00	18.00	12.00
The Flora of Delhi by J.K. Maheshwari	42.00	16.00	5.50
Illustrations to the Flora of Delhi by J.K. Maheshwari	105.00	44.00	26.00
Herbaceous Flora of Dehra Dun by C.R. Babu	216.00	120.00	44.00
Gnetum by P. Maheshwari & Vimla Vasil	30.00	12.00	4.00
Marsilea by K.M. Gupta	62.00	27.00	16.00
Aquatic Angiosperms	30.00	12.00	4.00
Indian Fossil Pteridophytes by K.R. Surange	99.00	44.00	25.00
Cedrus by P. Maheshwari & Chhaya Biswas	63.00	28.00	16.00
Proteaceae by C. Venkata Rao	108.00	48.00	27.00
Pinus by P. Maheshwari & R.N. Konar	45.00	22.00	16.00
Loranthaceae by B.M. Johri & S.P. Bhatnagar	83.00	37.00	21.00
Abies & Picea by K.A. Chowdhury	21.00	12.00	4.20
Indian Thysanoptera by T.N. Ananthakrishnan	39.00	16.00	5.20
The Millipede Thyropygus by G. Krishnan	18.00	7.00	2.40
Indian Sardines by R.V. Nair	33.00	14.00	4.40
Drug Addiction with special Reference to India by R.N. Chopra & I.C. Chopra	19.00	7.00	2.40
Diosgenin & other Steroid Drug Precursors by L.V. Asolkar & Y.R. Chandha	54.00	26.00	12.00
Cholera Bacteriophages by Dr. Sachimohan Mukerjee	45.00	20.00	12.00
Cottonseed Chemistry & Technology by K.S. Murti & K.T. Achaya	116.00	64.00	26.00
Corrosion Map of India	27.00		3.60
Rural Development and Technology: A Status Report-cum-Bibliography by PR Bose and V.N. Vashist	150.00	76.00	34.00
Termite Problems in India	14.00	6.00	1.80
Research & Development Management	38.00	20.00	
Proceedings of the Seminar on Primary Communications in Science & Technology in India by R.N. Sharma & S. Seetharama	78.00	35.00	68.00

Packing and Postage Extra

Printed & Published by Shri S.S. Saksena, Editor, Publications & Information Directorate (PID) Hillside Road, New Delhi 110012, at PID Photocomposition-cum-Printing Unit

Regd No. D(C)-1018